Cardiovascular biomechanics

Leif Rune Hellevik

Oct 9, 2018

(Download as PDF)

Contents

Chapter 1

Nomenclature

symbol	definition
m	Mass [kg]
ρ	Mass density $[kg/m^3]$
$\mathbf{P}$	Linear momentum $[kg\,m/s]$
$\mathbf{v}$	Velocity or specific linear momentum [m/s]
K	Kinetic energy $[kg\,m^2/s^2]$
$\mathbf{v}\cdot\mathbf{v}/2$	Specific kinetic energy $[m^2/s^2]$
B	Generic extensive property
β	Generic specific intensive property per mass unit
$\mathbf{n}$	Outward unit normal for the surface $A(t)$
$\mathbf{e}_i$	Orthogonal unit vectors
T_{ik}	Coordinate stresses [Pa]
T	Stress matrix
T_{iI}	Normal stresses
T_{ij}	Shear stresses, when $i \neq k$
$\mathbf{T}$	Stress tensor [Pa]
γ	Shear strain []
ϵ_v	Volumetric strain []
η	Modulus of elasticity [Pa]
ν	Poisson's ratio []
$\varepsilon_v = E_{ii}$	Voumetric strain
w	Stress work per unit volume
$\boldsymbol{T}_0$	The first Piola-Kirchhoff stress tensor
PKS	Piola-Kirchhoff stress tensor
$\boldsymbol{S}$	The second Piola-Kirchhoff stress tensor
p	Thermodynamical pressure
R	Gas constant for a particular gas
α	Womersley parameter
pp	Pulse pressure [mmHg]
CO	Cardiac output [ml/min]
$\tau = RC$	Relaxation time s
$\dot{V}$	Rate of change in volume
Q_i	Flow rate into a volume
Q_o	Flow rate out of a volume
Q	Volumetric flow rate.
δ	Nonlinear velocity profile correction factor
δ	Correction factor

Chapter 2

Dynamics

In physics, dynamics is a branch of classical mechanics, that is concerned with the effect of forces on the motion of objects or bodies. The incorporation of forces distinguishes dynamics from kinematics, while motion distinguishes it from statics. Dynamics is normally subdivided into kinematics, forces, and deformation.

Kinematics (Greek: kinein, to move) describes the motion of objects without the consideration of the forces that bring about the motion. In kinematics the position of a body is represented as a function of time. The position is represented with a set of coordinates in a reference frame. Velocity is the rate of change of position. Acceleration is the rate of change of velocity. Velocity and acceleration are the two principal quantities in kinematics which describe how position changes.

The forces encountered in this book are constrained to surface and body forces. A convenient representation of the forces are stresses (i.e., force per unit area), and a mathematical representation of the internal forces in a continuum is provided in section 2.3.1. The generic Cauchy equations of motion, valid for both solids and fluid, are presented in section 2.4. A separate chapter 3 is devoted to deformation analysis. And further, separate chapters (4,refchap:fluid) are devoted to constitutive equations which relate stresses to deformation. A constitutive equation is a relation between stress and strains (often represented by tensors), specific to a material or body, and does not follow directly from a physical law. By substitution of the constitutive equation into the Cauchy equations, the dynamics of the material may be solved when appropriate boundary conditions are imposed.

2.1 Kinematics

At the outset we define a restricted volume of the continuum as a *body* (see Figure 2.1). A *particle* denotes a material point in the body. The body contains the same particles at any time and contains per definition the same mass at any time. However, the volume V(t) and surface area A(t) of the body are functions of time. A reference frame, denoted by *Rf*, with an associated coordinate system *Ox*, is needed to represent the position, velocity, and acceleration of the particles. A position in space may then be represented by the position vector $\mathbf{r}$ from the origin of O of the coordinate system, or equivalently by the coordinate components of $\mathbf{r}$ denoted x_1, x_2 and x_3. Whenever appropriate or convenient we will use the equivalent representations for positions:

$$\mathbf{r} = [x_1, x_2, x_3] \qquad \text{and} \qquad (x_1, x_2, x_3) = x_i = x \tag{2.1}$$

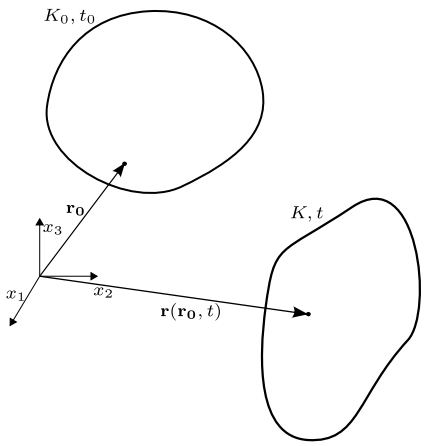

Figure 2.1: A body in current the configuration K and the reference configuration K_0.

The *current configuration* K denotes the current set of positions of the body, whereas the *reference configuration* K_0 refers the set of positions of the body at time t_0. A particular position in $\mathbf{r}_0$ in K_0, will be referred to as *particle* X_i. At the current time t the particle X will be at position x or $\mathbf{r}$. A functional relationship is the assumed betwesen $\mathbf{r}_0$ and $\mathbf{r}$:

$$\mathbf{r} = \mathbf{r}(\mathbf{r}_0, t) \tag{2.2}$$

$$x_i = x_i(X_1, X_2, X_3, t) = x_i(X, t) \Leftrightarrow x = x(X, t) \tag{2.3}$$

Due to the impermeability of matter (2.3) represents a one-to-one mapping between the set of positions in K_0 and K. The functions $x_i(X,t)$ and $\mathbf{r}(\mathbf{r}_0,t)$ are mathematical representations of the motion or kinematics of the body. The displacement vector $\mathbf{u}$ is another useful quantity representing the motion relative to the reference configuration:

$$\mathbf{u} = \mathbf{u}(X,t) = \mathbf{u}(\mathbf{r}_0,t) = \mathbf{r}(\mathbf{r}_0,t) - \mathbf{r}_0 \tag{2.4}$$

The motion of the body from K_0 to K will in general lead to deformation (i.e., change of shape and size) of the body. The deformation is illustrated in Figure 2.1 by material lines parallel with the coordinate lines in K_0. In the current configuration K these material lines represent a curvilinear coordinate system. Such coordinate systems will not be pursued further here, however, the interested reader may find a presentation and analysis of this subject in [16].

2.1.1 Extensive and intensive properties

Physical quantities may be divided into extensiveand intensive properties. An extensive property is a physical property that is a function of the volume or mass of a body. By contrast, an intensive property is a physical property independent of the body mass or volume, but given in every particle of the body. An intensive property may represent the intensive property of an extensive property. Further, an intensive property that is given per unit volume is normally called a density, whereas a property defined per unit mass is denoted as a specific property. With this formalism the mass m of a body:

$$m = \int_V \rho \, dV \tag{2.5}$$

is an example of an extensive property, whereas ρ is an intensive property which may be called mass density or density for short. The riddle "what weighs more, a pound of feathers or a pound of lead?" is an example showing that it may be easy to confuse the intensive and extensive quantities.

Other examples of extensive properties with corresponding intensive properties are listed below. Extensive linear momentum $\mathbf{P}$:

$$\mathbf{P} = \int_V \mathbf{v} \, \rho \, dV \tag{2.6}$$

with a corresponding intensive specific linear momentum $\mathbf{v}$, the velocity. Kinetic energy K is also an extensive property

$$K = \int_V \frac{\mathbf{v} \cdot \mathbf{v}}{2} \, \rho \, dV \tag{2.7}$$

with a corresponding specific kinetic energy $\mathbf{v} \cdot \mathbf{v}/2$.

A general form of an *extensive quantity* is

$$B(t) = \int_{V(t)} \beta \, \rho \, dV = \int_{V(t)} b \, dV \tag{2.8}$$

where β and b represent a generic specific intensive property and a generic (intensive) density, respectively.

2.1.2 Notation and conventions

An arbitrary intensive physical property (either scalar or vector) may be represented by a particle function $f(X, t)$. For a particular choice of position or particle X, the function is connected to this particle at all times t. The material derivative of the particle function f is then defined as the rate of change of f per unit time. In mathematical terms this may be expressed:

$$\dot{f} = \left.\frac{df}{dt}\right|_{X=\text{const}} = \frac{\partial f(X,t)}{\partial t} \equiv \partial_t f(X,t) \tag{2.9}$$

In the literature this quantity may also be denoted the substantial derivative, the particle derivative, and the individual derivative.

The velocity $\mathbf{v}$ and the acceleration $\mathbf{a}$ of the particle X are defined in a natural manner:

$$\mathbf{v}(X,t) = \dot{\mathbf{r}} = \partial_t \mathbf{r}(X,t) \tag{2.10}$$

$$\mathbf{a}(X,t) = \dot{\mathbf{v}} = \ddot{\mathbf{r}} = \partial_t^2 \mathbf{r}(X,t) \tag{2.11}$$

Alternatively, these quantities may be expressed by the displacement vector $\mathbf{u}$ by using the definition in (2.4):

$$\mathbf{v}(X,t) = \dot{\mathbf{u}} = \partial_t \mathbf{u}(X,t) \tag{2.12}$$

$$\mathbf{a}(X,t) = \ddot{\mathbf{u}} = \partial_t^2 \mathbf{u}(X, \tag{2.13}$$

The components of the velocity vector and the acceleration vector in the coordinate system Ox are:

$$v_i = \dot{x}_i = \partial_t x_i(X,t) = \dot{u}_i = \partial_t u_i(X,t) \tag{2.14}$$

$$a_i = \dot{v}_i = \ddot{x}_i = \partial_t^2 x_i(X,t) = \ddot{u}_i \tag{2.15}$$

Similarly, let the *position* function $f(x,t)$ also represent an intensive physical property. The rate of change of f per unit time for a fixed *position* in space has the mathematical representation:

$$\frac{\partial f(x,t)}{\partial t} \equiv \left.\frac{df}{dt}\right|_{x=\text{const}} \equiv \partial_t f(x,t) \tag{2.16}$$

To express the material derivative of the position function f, we attach the function to the particle X which has the position x at time t:

$$f = f(x,t) = f(x(X,t),t) \tag{2.17}$$

Then by using of the definitions (2.9) and (2.11) and the chain rule we get:

$$\dot{f} = \left.\frac{df}{dt}\right|_{X=\text{const}} = \frac{\partial f(x,t)}{\partial t} + \sum_{i=1}^{3} \frac{\partial f(x,t)}{\partial x_i}\frac{\partial x_i(X,t)}{\partial t} = \frac{\partial f(x,t)}{\partial t} + \sum_{i=1}^{3} \frac{\partial f(x,t)}{\partial x_i} v_i \tag{2.18}$$

To simplify the expressions we introduce a common notation in mathematical physics, namely the comma notation for spatial, partial derivatives, and an alternative expression for partial derivative with respect to time:

$$\frac{\partial f}{\partial x_i} \equiv f_{,i}, \qquad \frac{\partial f}{\partial x_i \partial x_j} \equiv f_{,ij}, \qquad \frac{\partial f}{\partial t} = \partial_t f \tag{2.19}$$

Additionally, we make use of Einstein's summation convention:

Einstein's summation convention: Summation is implied when an index repeated once and only once. Roman indices imply summation from 1 to 3, whereas Greek indices implies summation from 1 to 2. An index that is summed over is called a *dummy index*; whereas one that is not summed out is called a *free index*.

By making use of these conventions, the expression in (2.18) for the material derivative reduces to:

$$\dot{f} = \partial_t f + v_i\, f_{,i} \tag{2.20}$$

In a Cartesian coordinate system with basis-vectors $\mathbf{e}_i$, the del-operator ∇ is defined as:

$$\nabla = \mathbf{e}_i \frac{\partial}{\partial x_i} \tag{2.21}$$

A new scalar operator may then be introduced:

$$\mathbf{v} \cdot \nabla = v_i \frac{\partial}{\partial x_i} \tag{2.22}$$

A vector representation of the material derivative may then be obtained by substitution of (2.22) into (2.20):

$$\dot{f} = \partial_t f + (\mathbf{v} \cdot \nabla) f \tag{2.23}$$

The acceleration of a particle may then be computed from the velocity field $\mathbf{v}(x,t)$ by making use of (2.11) and (2.20)eq:20:

$$a_i = \dot{v}_i = \partial_t v_i + v_k v_{i,k} \tag{2.24}$$
$$\mathbf{a} = \dot{\mathbf{v}} = \partial_t \mathbf{v} + (\mathbf{v} \cdot \nabla) \mathbf{v} \tag{2.25}$$

The particle acceleration has two terms: the local acceleration $\partial_t \mathbf{v}$ and the convective acceleration $(\mathbf{v} \cdot \nabla) \mathbf{v}$.

2.1.3 Reynolds transport theorem of a moving control volume

The fundamental conservation laws (conservation of mass and energy, and balance of linear momentum) are normally formulated for bodies (i.e., systems of particles) in motion. However, in fluid mechanics it is more convenient to work with a control volume, i.e., a volume independent of time or which does not follow the system of particles for which the conservation law is formulated . The Eulerian description is usually preferred over the Lagrangian description for the same reason. Therefore, we need to transform the conservation laws from a system to a control volume. This is accomplished with the Reynolds Transport theorem (RTT).

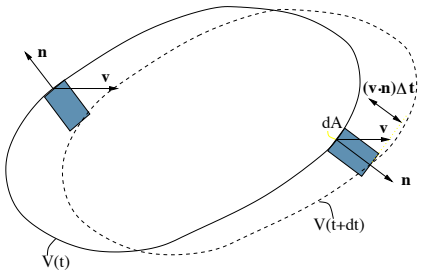

Figure 2.2: Control volume at time t and $t + \Delta t$.

The fundamental conservation laws (mass, momentum, energy) contain material derivatives of both intensive and extensive properties. In the following the RTT will be derived.

For convenience we introduce the density $b = \rho\beta$ of an extensive property B with a corresponding body of volume V(t) and surface area A(t) (Figure 2.2):

$$B(t) = \int_{V(t)} b(\mathbf{r}, t)\, dV \tag{2.26}$$

The volume $V(t)$ may be thought of as the volume of the system or the system of particles, which at a given point in time has the extensive property B. The outset for the derivation, is the canonical definition of a derivative:

$$\dot{B} \equiv \frac{dB}{dt} = \lim_{\Delta t \to 0} \frac{B(t + \Delta t) - B(t)}{\Delta t} \tag{2.27}$$

Further, $B(t + \Delta t)$ must be expanded:

$$\begin{aligned} B(t + \Delta t) &= \int_{V(t+\Delta t)} b(\mathbf{r}, t + \Delta t)\, dV \\ &= \int_{V(t)} b(\mathbf{r}, t + \Delta t)\, dV + \int_{\Delta V} b(\mathbf{r}, t + \Delta t)\, dV \end{aligned}$$

The last integral may be expressed by a surface integral:

$$\int_{\Delta V} b(\mathbf{r}, t + \Delta t)\, dV = \int_{A(t)} b(\mathbf{r}, t + \Delta t)\, (\mathbf{v} \cdot \mathbf{n}\, \Delta t)\, dA \tag{2.28}$$

Here, $\mathbf{v}$ is the velocity of the moving body and $\mathbf{n}$ is the outward unit normal.

By collection terms:

$$\frac{B(t + \Delta t) - B(t)}{\Delta t} = \int_{V(t)} \frac{b(\mathbf{r}, t + \Delta t) - b(\mathbf{r}, t)}{\Delta t}\, dV + \int_{A(t)} b(\mathbf{r}, t + \Delta t)\, (\mathbf{v} \cdot \mathbf{n})\, dA \tag{2.29}$$

By letting $\Delta t \to 0$ the Reyonlds transport theorem is obtained:

Theorem 2.1.1. Reynolds transport theorem

$$\dot{B} = \int_{V(t)} \frac{\partial b}{\partial t}\, dV + \int_{A(t)} b\, (\mathbf{v} \cdot \mathbf{n})\, dA \tag{2.30}$$

The expression in equation (2.30) is also frequently referred to as *Leibniz's rule for 3D integrals* (see equation (45)).

In some applications, in particular fluid-structure interaction applications, the governing equations have to be formulated on grids which are deforming, but at a different velocity than the fluid/structure. In such cases it is beneficial

to introduce a *control volume* $V_c(t)$ which deforms at a velocity $\boldsymbol{v}_c(t)$. An extensive property $B_c(t)$ may then be introduced in the natural manner:

$$B_c(t) = \int\limits_{V_c(t)} b(\mathbf{r}, t)\, dV \tag{2.31}$$

Note, that B_c is not related to the system (or system of particles), but rather to the control volume V_c. In general we have $B_c(t) \neq B(t)$ whenever $V_c(t) \neq V(t)$, and thus B_c is normally not the quantity of interest whenever governing equations for physical phenomena are to be developed. However, we may compute the time derivative of B_c by using the Reynolds transport theorem in equation (2.30) and note that in this particular instance velocity with which the surface is deforming is $\boldsymbol{v}_c$, i.e., the velocity of the control volume surface:

$$\dot{B}_c = \frac{dB_c}{dt} = \int\limits_{V_c(t)} \frac{\partial b}{\partial t}\, dV + \int\limits_{A_c(t)} b\,(\mathbf{v}_c \cdot \mathbf{n})\, dA \tag{2.32}$$

By subtracting equation (2.32) from equation (2.30), rearranging and introducing the definition of B_c, we obtain a version of the Reynolds transport theorem for a moving control volume V_c:

Theorem 2.1.2. RTT for a moving control volume

$$\dot{B} = \frac{d}{dt} \int\limits_{V_c(t)} b\, dV + \int\limits_{A_c(t)} b\,(\mathbf{v} - \mathbf{v}_c) \cdot \mathbf{n})\, dA \tag{2.33}$$

Note, that we tacitly assume that $V_c(t) = V(t)$ at time t to derive equation (2.33).

2.1.4 The material derivative of an extensive property

Based on conservation of mass (i.e., $\dot{\rho J} = 0$) it may be shown that for a generic specific intensive property [17, Theorem C.11] that:

$$\dot{B} = \frac{d}{dt} \int\limits_{V(t)} \beta\, \rho\, dV = \int\limits_{V(t)} \dot{\beta}\, \rho\, dV \tag{2.34}$$

2.2 Conservation of mass

A body of continuous matter with volume V(t) and surface area A(t) (Figure 2.2) has, according to the *principle of conservation of mass*, the same mass

at any time. The mass m may be expressed by the integral: mathematical terms may be expressed by:

$$m = \int_{V(t)} \rho(\mathbf{r}, t)\, dV \tag{2.35}$$

and consequently due to the above mentioned principle:

$$\frac{dm}{dt} = \dot{m} = \frac{d}{dt} \int_{V(t)} \rho(\mathbf{r}, t)\, dV = 0 \tag{2.36}$$

The conservation of mass equation is obtained by setting $b = \rho$ in Reynolds transport theorem (2.30)

$$\dot{m} = \frac{d}{dt} \int_{V(t)} \rho(\mathbf{r}, t)\, dV = \int_{V} \frac{\partial \rho}{\partial t}\, dV + \int_{A} \rho\, (\mathbf{v} \cdot \mathbf{n})\, dA = 0 \tag{2.37}$$

Note that $V(t)$ denote the time-varying volume of the body at a given time t, whereas V and A are the fixed volume and surface area of a control volume, respectively. The control volume $V = V(t)$ at time t.

By using the Gauss theorem the surface integral in (2.37) is transformed to a volume integral and the two integrals in (2.37) collapse to one:

$$\dot{m} = \int_{V} \frac{\partial \rho}{\partial t} + \nabla \cdot (\rho \mathbf{v})\, dV = 0 \tag{2.38}$$

As (2.38) must be valid for arbitrary volumes V the integrand must be zero and a differential form for mass conservation is obtained:

$$\frac{\partial \rho}{\partial t} + \nabla \cdot (\rho \mathbf{v}) = 0 \tag{2.39}$$

This is an differential equation which represents mass conservation in an Eulerian reference frame. The importance of the reference frame will become clearer in chapter 3, where the concepts of deformation are introduced.

An equivalent presentation of the mass conservation on component form reads:

$$\frac{\partial \rho}{\partial t} + (\rho v_i)_{,i} = 0 \tag{2.40}$$

For incompressible fluid the mass density ρ is constant and (2.40) reduces to:

$$\nabla \cdot \mathbf{v} = 0 \quad \Leftrightarrow \quad v_{i,i} = 0 \tag{2.41}$$

2.3 Equations of motion

As Newton's laws for the motion of mass particles cannot be transferred directly to a body of continuously distributed matter, Euler's two axioms are postulated in Continuum Mechanics: Law of balance of linear momentum and Law of balance of angular momentum. The axioms will be presented in mathematical terms in this section, and based on these axioms the equations of motion will be derived. We will also show that, based on the two axioms, the equations of motion for the *center of mass* (to be defined) of a body is identical with Newton's second law. One may also show that Newton's third law of action and reaction also follow from the two axioms (see section 3.2.2 [17]).

Axiom 2.3.1. Law of balance of linear momentum

Euler's first axiom may be stated: *The rate of change of the linear momentum for a continuum volume equals the resultant force.* The linear momentum is an extensive property given in (2.6) and by letting $\mathbf{f}$ denote the resultant force, the axiom has the mathematical representation:

$$\dot{\mathbf{P}} \equiv \int_V \dot{\mathbf{v}} \rho \, dV = \mathbf{f} \tag{2.42}$$

Note that the relation in (2.42), between the rate of change of the extensive linear momentum $\dot{\mathbf{P}}$, and the integral of the rate of change of the intensive specific linear momentum $\dot{\mathbf{v}}$, follow from (2.34).

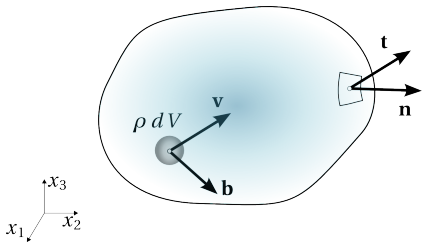

Figure 2.3: Body forces $\mathbf{b}$ and surface forces $\mathbf{t}$ on a volume V with surface area A.

As we in applications of continuum mechanics are concerned with how strains and stresses are distributed throughout the body of interest, the forces of (2.42) must be represented as intensive quantities too. This is due to that we will present the final governing equations as differential equations rather than integral equations. The body of interest (see Figure 2.3) is assumed to be acted upon by two types of forces: body force $\mathbf{b}$ per unit mass, and

contact force $\mathbf{t}$ per unit area. Consequently, the extensive resultant force is related with its intensive components by:

$$\mathbf{f} = \int_A \mathbf{t}\, dA + \int_V \mathbf{b}\, \rho\, dV \tag{2.43}$$

By substitution of (2.43) in (2.42) an integrated representation of the the law of balance of linear momentum may be found:

Law of balance of linear momentum integral formulation

$$\int_V \dot{\mathbf{v}} \rho\, dV = \int_A \mathbf{t}\, dA + \int_V \mathbf{b}\, \rho\, dV \tag{2.44}$$

Balance of linear momentum and Newton's second law To see how (2.42) is related with Newton's second law, we introduce the center of mass:

$$\mathbf{r}_C = \frac{1}{m} \int_V \mathbf{r}\, \rho\, dV \tag{2.45}$$

Further, the velocity and acceleration of the center of mass is defined in a logical manner:

$$\mathbf{v}_C = \frac{1}{m} \int_V \mathbf{v}\, \rho\, dV = \frac{1}{m} \int_V \dot{\mathbf{r}}\, \rho\, dV = \dot{\mathbf{r}}_C \tag{2.46}$$

$$\mathbf{a}_C = \dot{\mathbf{v}}_C = \frac{1}{m} \int_V \dot{\mathbf{v}}\, \rho\, dV = \ddot{\mathbf{r}}_C = \frac{1}{m} \int_V \mathbf{a}\, \rho\, dV \tag{2.47}$$

Substitution of (2.47) in (2.42) yields:

$$\mathbf{f} = m\mathbf{a}_C \tag{2.48}$$

which is Newton's second law for the center of mass and an extensive representation of (2.44).

Axiom 2.3.2. Law of balance of angular momentum

Euler's second axiom: *The rate of change of the angular momentum for a continuum volume equals the resultant moment.*

$$\dot{\mathbf{l}}_0 = \mathbf{m}_0 \tag{2.49}$$

To express this axiom in a more useful way mathematically, we must find the intensive expressions for its constituents. The resultant moment $\mathbf{m}_0$ has contributions both from surface forces and body forces:

$$\mathbf{m}_0 = \int_A \mathbf{r} \times \mathbf{t}\, dA + \int_V \mathbf{r} \times \mathbf{b}\, \rho\, dV \tag{2.50}$$

The angular momentum is given by:

$$\mathbf{l}_0 = \int_V \mathbf{r} \times \mathbf{v}\rho \, dV \tag{2.51}$$

and the rate of change of the angular momentum may be show to be:

$$\dot{\mathbf{l}}_0 = \int_V \mathbf{r} \times \dot{\mathbf{v}}\rho \, dV \tag{2.52}$$

The result in (2.52) follow from (2.34) and from by the expansion:

$$\mathbf{r} \dot{\times} \mathbf{v} = \dot{\mathbf{r}} \times \mathbf{v} + \mathbf{r} \times \dot{\mathbf{v}} \tag{2.53}$$

The first term in (2.53) vanishes due to:

$$\dot{\mathbf{r}} = \mathbf{v} \quad \text{and} \quad \mathbf{v} \times \mathbf{v} = 0 \tag{2.54}$$

An equivalent representation of the law of balance of angular momentum is then found by substitution of Eqs. (2.52) and (2.50) in (2.49):

Law of balance of angular momentum integral formulation

$$\int_V \mathbf{r} \times \dot{\mathbf{v}}\rho \, dV = \int_A \mathbf{r} \times \mathbf{t} \, dA + \int_V \mathbf{r} \times \mathbf{b} \, \rho \, dV \tag{2.55}$$

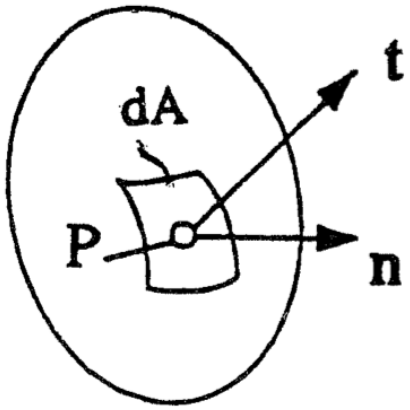

Figure 2.4: Surface stress $\mathbf{t}$ on surface with normal vector $\mathbf{n}$.

2.3.1 Coordinate stresses

In Figure 2.4 the stress vector $\mathbf{t}$ is shown on a surface with orientation $\mathbf{n}$ in a particle (or point) P. This surface may either be the physical surface or an arbitrary oriented surface within a body of interest. In an orthogonal

coordinate system Ox with orthogonal unit vectors $\mathbf{e}_i$, the vectors $\mathbf{t}$ and $\mathbf{n}$ are expressed as a sum their *components* t_i and n_i, respectively (remember Einsteins's summation convention):

$$\mathbf{t} = t_i\ \mathbf{e}_i \qquad \text{and} \qquad \mathbf{n} = n_k\ \mathbf{e}_k \tag{2.56}$$

Now, let us consider the situation illustrated in Figure 2.5, in which we have oriented three orthogonal planes through the point P, with unit normals $\mathbf{e}_k$. On each of the planes $\mathbf{e}_k$, a stress vector $\mathbf{t}_k$ acts, with $k = 1 \ldots 3$.

In the same way as in (2.56), the three $\mathbf{t}_k$ vectors may be expressed by their components,

$$\mathbf{t}_k = T_{ik}\mathbf{e}_i \quad \Leftrightarrow \quad \mathbf{e}_i \cdot \mathbf{t}_k = T_{ik} \tag{2.57}$$

for an arbitrary k, where we have introduced T_{ik} which denotes the coordinate stresses in the particle P. The coordinate stresses T_{ik} are elements of the *stress matrix* T. in P with respect to the coordinate system Ox. And as T_{ik}, represents, the components in Ox of the three $\mathbf{t}_k$ on three orthogonal surfaces, it T_{ik} represents the complete stress situation in the particle P.

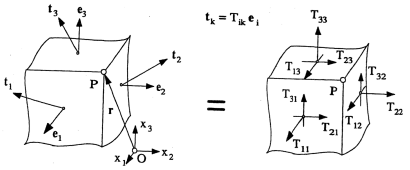

Figure 2.5: Stresses and coordinate stresses on three orthogonal surfaces.

The coordinate stresses T_{11}, T_{22}, T_{33}, are denoted *normal stresses*, whereas T_{ik}, when $i \neq k$, are denoted *shear stresses*. In this presentation, first index i refers to the direction of the of the stress, while the second index k refers to the face, with normal vector $\mathbf{e}_k$, on which the stress T_{ik} acts. The order or meaning of the indices are often reversed in the literature. However, the laws of balance of angular/linear momentum will later be used be used to show that the stress matrix is symmetric when only body forces $\mathbf{b}$ and contact forces $\mathbf{t}$ are considered (see (2.93).

$$T_{ij} = T_{ji} \quad \Leftrightarrow \quad \mathbf{T}^T = \mathbf{T} \tag{2.58}$$

Thus, the order of the indices is normally not important, and one may use the mnemonic: "First Face Second Stress" to remember the meaning of the indices.

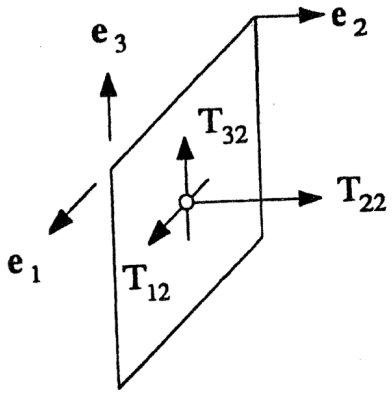

Figure 2.6: Coordinate stresses on a surface parallel with $\mathbf{e}_2$.

Sign convention for coordinate stresses A positive coordinate stress acts in the direction of the positive coordinate axis on that side of the surface facing the positive direction of a coordinate axis (see Figure 2.6).

Positive and negative normal stresses are denoted *tensile stresses* and *compressive stresses*, respectively.

A variety of symbols for coordinate stresses may be found in other texts:

$$T_{ik} = \sigma_{ik} = \tau_{ik} \tag{2.59}$$

Additionally, when xyz-coordinates are used, common ways of referring to normall stresses are, σ_x or σ_{xx} etc., and the shear stresses by τ_{xy} or σ_{xy}. Thus, equivalent representations of the stress matrix T are:

$$T = \begin{bmatrix} T_{11} & T_{12} & T_{13} \\ T_{21} & T_{22} & T_{23} \\ T_{31} & T_{32} & T_{33} \end{bmatrix} \equiv \begin{bmatrix} \sigma_x & \tau_{xy} & \tau_{xz} \\ \tau_{yx} & \sigma_y & \tau_{yz} \\ \tau_{zx} & \tau_{zy} & \sigma_z \end{bmatrix} \equiv \begin{bmatrix} \sigma_{xx} & \tau_{xy} & \tau_{xz} \\ \tau_{yx} & \sigma_{yy} & \tau_{yz} \\ \tau_{zx} & \tau_{zy} & \sigma_{zz} \end{bmatrix} \tag{2.60}$$

In other orthogonal coordinate systems like cylindrical (r, θ, z) and spherical (r, θ, ϕ), the stress matrix have a natural representation:

$$T = \begin{bmatrix} \sigma_r & \tau_{r\theta} & \tau_{rz} \\ \tau_{\theta r} & \sigma_\theta & \tau_{\theta z} \\ \tau_{zr} & \tau_{z\theta} & \sigma_z \end{bmatrix}, \qquad T = \begin{bmatrix} \sigma_r & \tau_{r\theta} & \tau_{r\phi} \\ \tau_{\theta r} & \sigma_\theta & \tau_{\theta\phi} \\ \tau_{\phi r} & \tau_{\phi\theta} & \sigma_\phi \end{bmatrix} \tag{2.61}$$

Below, some examples are presented to familiarize the reader with the stress concept and coordinate stresses.

Example 2.3.1. *Uniaxial state of stress.*

Consider at straight rod with cross-sectional area A, subjected to an axial force N and orient an orthogonal coordinate system with the x_1-axis along the direction of the axial force. The corresponding state of stress for the rod is given by the stress matrix:

$$T = \begin{bmatrix} \sigma & 0 & 0 \\ 0 & 0 & 0 \\ 0 & 0 & 0 \end{bmatrix}, \qquad \sigma = \frac{N}{A} \tag{2.62}$$

The cross-section A is the subjected to a normal stress σ. The cross-section is free of shear, i.e., $T_{12} = T_{13} = 0$, and sections parallell to the axis of the rod are stress free, *i.e.* $T_{2i} = T_{3i} = 0$, with $i = 1 \ldots 3$. Such a state of stress is denoted a uniaxial state of stress.

Example 2.3.2. *Pure shear stress state.*

y

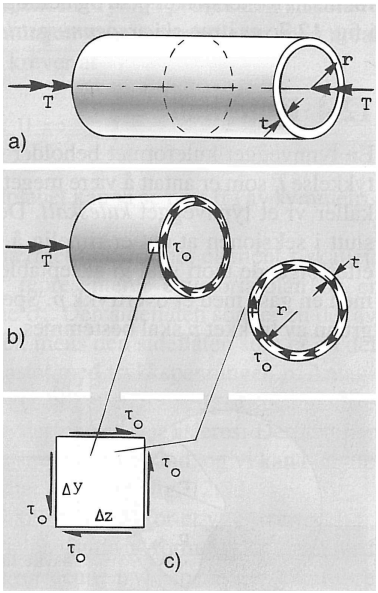

Figure 2.7: Torsion of thin-walled cylinder.

A thin-walled (i.e., $t \ll r$) cylinder with mean radius r and wall thickness t is subjected to a torsion moment, or *torque*, T (see Figure 2.7). A tangential shear stress $\tau_0 = \tau_{z\theta}$ constitutes a moment $\tau_0 r$, with respect to the cylinder axis. This is the moment per cross-sectional area, and a first order approximation to the cylindrical cross-sectional area is $A = 2\pi rt$. The moment must

balance the imposed torque, and thus we find an expression for the shear stress in the cylinder wall:

$$\tau_0 = \tau_{z\theta} = \frac{T}{2\pi r^2 t} \tag{2.63}$$

In Figure 2.7 c) the state of stress in an element of the tube wall is illustrated. We have already found $\tau_{z\theta}$ and may argue the two force couples must balance for the element to be in equilibrium, and thus: $\tau_{\theta z} = \tau_{z\theta} = \tau_0$. We might also have argued that the stress matrix is symmetric, which in fact is based on momentum balance. Thus, the state of state in a wall element of the cylinder may be expressed by:

$$T = \begin{bmatrix} 0 & 0 & 0 \\ 0 & 0 & \tau_0 \\ 0 & \tau_0 & 0 \end{bmatrix}, \qquad \tau_0 = \frac{T}{2\pi r^2 t} \tag{2.64}$$

2.3.2 Cauchy's stress theorem and the Cauchy stress tensor

An important theorem, the Cauchy's stress theorem (CST), will prove useful in the derivation of Cauchy's equations of motion in section 2.4 and the derivation of principal stresses in section 2.5.1:

Theorem 2.3.3. Cauchy's stress theorem and the stress tensor

Consider an arbitrary plane through P with normal vector $\mathbf{n} = n_k \mathbf{e}_k$. The stress vector $\mathbf{t} = t_i \mathbf{e}_i$ on this plane is the related to the coordinate stresses T_{ik} by

$$t_i = T_{ik} n_k \Leftrightarrow \mathbf{t} = \mathbf{T} \cdot \mathbf{n} \tag{2.65}$$

Proof. Consider a tetrahedron as illustrated in Figure 2.8, with a surface made up of triangles (such a tetrahedron is often referred to as a Cauchy tetrahedron). Three of these triangles are parallell to the orthogonal coordinate planes, intersect the point P and have areas A_k. The orientation of the fourth triangular plane with surface A, is given by its normal vector $\mathbf{n}$ and has a distane h from the point P.

The tetrahedron is subjected to a body force $\mathbf{b}$, the stress vectors $-\mathbf{t}_k$ on the coordinate planes, and the stress vector $\mathbf{t}$ on the last triangle. By claiming balance of linear momentum from (2.44) we get for this tetrahedron:

$$\sum_{k=1}^{3} \int_{A_k} -\mathbf{t}_k \, dA + \int_A \mathbf{t} \, dA + \int_V \mathbf{b}\rho \, dV = \int_V \mathbf{a}\rho \, dV \tag{2.66}$$

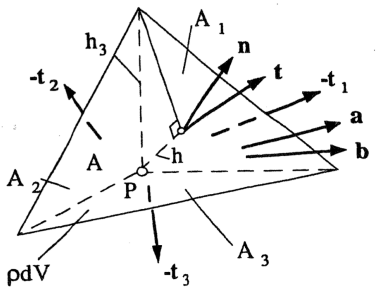

Figure 2.8: Cauchy's tetrahedron with forces

If we let $\mathbf{t}_k$, $\mathbf{t}$, $\mathbf{b}\rho$ and $\mathbf{a}\rho$ represent mean values on the surfaces and in the volume, the equation of motion in (2.66) simplifies to:

$$-\mathbf{t}_k A_k + \mathbf{t}A + \mathbf{b}\rho V = \mathbf{a}\rho V \tag{2.67}$$

Further, let h_k denote edges parallel to the base vectors $\mathbf{e}_k$, and since $\mathbf{n}$ is a unit vector:

$$n_k = \frac{h}{h_k} \tag{2.68}$$

To see this, consider the vector $\boldsymbol{s}_{21}$ from the end of h_2 to h_1 which has the components:

$$\boldsymbol{s}_{21} = (h_1, -h_2, 0) \tag{2.69}$$

and correspondingly the vector $\boldsymbol{s}_{23}$ from the end of h_2 to h_3 with components:

$$\boldsymbol{s}_{23} = (0, -h_2, h_3) \tag{2.70}$$

The area A is then given by the absolute value of the cross-product:

$$A = |\boldsymbol{s}_{21} \times \boldsymbol{s}_{23}| = \frac{1}{2}\sqrt{{h_2}^2{h_3}^2 + {h_1}^2{h_3}^2 + {h_1}^2{h_2}^2} \tag{2.71}$$

The volume V may be expressed in four different ways:

$$V = \frac{1}{3}Ah = \frac{1}{3}A_1h_1 = \frac{1}{3}A_2h_2 = \frac{1}{3}A_3h_3, \quad \text{or} \quad V = \frac{1}{3}A_kh_k \quad \text{no summation} \tag{2.72}$$

and as e.g., $A_3 = h_2h_3/2$ the volume may be expressed by the edges only as:

$$V = \frac{1}{6}\,h_1h_2h_3 \tag{2.73}$$

By combination of equations (2.71), (3.32), and (2.73) we get an expression for h:

$$h = \frac{h_1 h_2 h_3}{\sqrt{{h_2}^2{h_3}^2 + {h_1}^2{h_3}^2 + {h_1}^2{h_2}^2}} = \frac{h_1 h_2 h_3}{2\,A} \tag{2.74}$$

An expression for a unit normal vector to A may be found by:

$$\boldsymbol{n} = \pm\frac{\boldsymbol{s}_{21} \times \boldsymbol{s}_{23}}{|\boldsymbol{s}_{21} \times \boldsymbol{s}_{23}|} = \pm\frac{\boldsymbol{s}_{21} \times \boldsymbol{s}_{23}}{2\,A} \tag{2.75}$$

we choose the version with positive components for convenience:

$$\boldsymbol{n} = \frac{(h_2 h_3, h_1 h_3, h_1 h_2)}{2A} = h\left(\frac{1}{h_1}, \frac{1}{h_2}, \frac{1}{h_3}\right) \tag{2.76}$$

where the latter equality of equation (2.76) follows from equation (2.74). Thus, we have derived a convenient expression for the normal vector, which is given on component for in equation (2.68).

By combination of (2.68) and (2.72) we get:

$$A_k = An_k \quad \text{and} \qquad V = \frac{1}{3}Ah \tag{2.77}$$

And subsequently, by substitution of the geometric relations in (2.77) into (2.67) we obtain:

$$-\mathbf{t}_k n_k + \mathbf{t} + \mathbf{b}\rho\frac{h}{3} = \mathbf{a}\rho\frac{h}{3} \tag{2.78}$$

By letting $h \to 0$ in (2.78), the only terms left are the ones pertaining to surface stresses, which yields:

$$\mathbf{t} = \mathbf{t}_k n_k \tag{2.79}$$

From the definition of coordinate stresses ((2.57)) we have $\mathbf{t}_k = T_{ik}\mathbf{e}_i$ which by substitution into (2.79) yields

$$\mathbf{t} = T_{ik} n_k \mathbf{e}_i \Leftrightarrow t_i = T_{ik} n_k \tag{2.80}$$

and thus completes the proof of Cauchy's stress theorem.

The CST express how the coordinate stresses T_{ik} completely determines the state of stress in a particle. Both the stress vector $\mathbf{t}$ and the unit normal $\mathbf{n}$ are coordinate invariant particle properties(i.e., independent of choice of coordinate system), which implies that (2.65) has a coordinate invariant character. In this presentation we simply state that the stress vector $\mathbf{t}$ may be expressed by the vector $\mathbf{n}$, by an operator $\mathbf{T}$. We denote this operator the

stress tensor $\mathbf{T}$, which in a given coordinate system Ox is represented by the matrix T. The stress tensor $\mathbf{T}$ is a coordinate invariant, intensive quantity that in any Cartesian coordinate system is represented by the corresponding stress matrix T (in the same manner as for vectors). The coordinate stresses T_{ik} are the components of the stress tensor in a particular coordinate system.

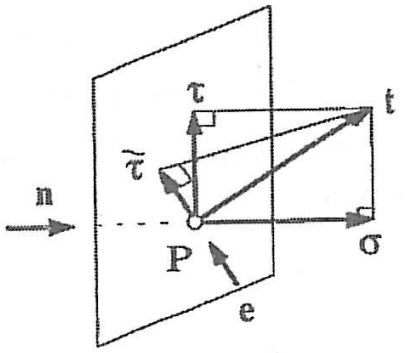

Figure 2.9: Decomposition of the stress vector $\mathbf{t}$.

Based on the CST, we may now find expressions for the normal stress component and the shear stress component of the stress vector $\mathbf{t}$. The *normal stress* σ, is the component of $\mathbf{t}$, acting in the direction of the surface normal $\mathbf{n}$, and is thus found by the scalar product between the two vectors:

$$\sigma = \mathbf{n} \cdot \mathbf{t} = \mathbf{n} \cdot \mathbf{T} \cdot \mathbf{n} = n_i T_{ik} n_k \tag{2.81}$$

The component of $\mathbf{t}$, remaining after subtraction of the normal stress, is denoted the *shear stress vector* $\boldsymbol{\tau}$ and is orthogonal to $\mathbf{n}$ and aligned with the surface:

$$\boldsymbol{\tau} = \mathbf{t} - \sigma \mathbf{n}, \qquad \boldsymbol{\tau} \cdot \mathbf{n} = 0 \tag{2.82}$$

The magnitude of the shear stress vector is simply denoted *shear stress* τ, and may be expressed:

$$\tau = \sqrt{\tau_i \tau_i} = \sqrt{t_i^2 - 2\sigma t_i n_i + \sigma^2 n_i^2} = \sqrt{\mathbf{t} \cdot \mathbf{t} - \sigma^2} \tag{2.83}$$

by the use of (2.81).

Further, the component $\tau_e$of the stress vector $\mathbf{t}$ acting on the surface with orientation $\mathbf{n}$, in an arbitrary direction $\mathbf{e}$ by:

$$\tau_e = \mathbf{e} \cdot \mathbf{t} = \mathbf{e} \cdot \mathbf{T} \cdot \mathbf{n} = e_i T_{ik} n_k \tag{2.84}$$

By selecting $\mathbf{e}$ and $\mathbf{n}$ as the base vectors $\mathbf{e}_i$ and $\mathbf{e}_k$, respectively, in a general Cartesian coordinate system Ox, the coordinate stresses (or components) of the stress tensor $\mathbf{T}$ may be expressed as:

$$T_{ik} = \mathbf{e}_i \cdot \mathbf{T} \cdot \mathbf{e}_k \tag{2.85}$$

Example 2.3.3. *Example: Fluid at rest: Isotropic state of stress.*

In section 5.1 we define a fluid as a material that deforms continuously when subjected to an *anisotropic* state of stress. Conversely, no deformation implies an *isotropic* state of stress, i.e., all material surfaces through a fluid particle transmits the same normal stress. This normal stress is what conventionally is denoted the pressure p, and the shear stresses on the surfaces are zero. The stress matrix in *any* Cartesian coordinate system Ox is therefore for a fluid at rest:

$$\mathbf{T} = \begin{bmatrix} -p & 0 & 0 \\ 0 & -p & 0 \\ 0 & 0 & -p \end{bmatrix} = -p\mathbf{I} \tag{2.86}$$

2.4 Cauchy's equations of motion

We have previously presented the integral formulations of Euler's axioms in (2.44) and (2.55), respectively. In the current section we will present these laws as more suitable field equations or differential equations, valid in each point/particle in a continuum.

2.4.1 Derivation of Cauchy's equations of motion

On component form, the balance of linear momentum in (2.44) may be presented:

$$\int_V \dot{v}_i \rho \, dV = \int_A t_i \, dA + \int_V b_i \, \rho \, dV \tag{2.87}$$

and we observe that in (2.87) there are two volume integrals and one surface integral. A common way to transform integral equations like (2.87) to a differential equation, is to put all terms in a common integral in some way, and then claim that the integrand must vanish. For (2.87), a common integral may be obtained by transforming the surface integral to a volume integral. From Cauchy's stress theorem (2.65) and the divergence theorem in (31) we have:

$$\int_A t_i \, dA = \int_A T_{ik} n_k \, dA = \int_V T_{ik,k} \, dV \tag{2.88}$$

Note that for the latter equality in (2.88) to hold, we let $a_k = T_{ik}$ in the divergence theorem, which may be done as T_{ik} are scalars. Cauchy's equations of motion are finally obtained by substitution of (2.88) into (2.87) and claiming that the integrand must vanish for an arbitrary V:

Cauchy's equations of motion

$$\rho\,\dot{v}_i = T_{ik,k} + \rho b_i \tag{2.89}$$

(2.89) is the fundamental equation motion in continuum mechanics, valid for the motion of any continuum, both fluids and solids. In solid mechanics the equations are normally formulated in Lagrangian coordinates in which the material derivative (see (2.24) and (2.25)) on the left hand side will reduce to a normal time derivative. In fluid mechanics (2.89) is normally rendered in Eulerian coordinates and consequently convective terms will appear on the right hand side. If a system is in equilibrium, the left hand side will vanish are there is no acceleration and consequently no change in linear momentum with respect to time.

By means of the permutation symbol e_{ijk} and the representation of vector products in (12), the law of balance of angular momentum (2.55) has the following component form:

$$e_{ijk}\left(\int_A x_i\,t_j\;dA + \int_V x_i\,(b_j - \dot{v}_j)\,\rho\;dV\right) = 0 \tag{2.90}$$

Proceeding in the same manner as for the balance of linear momentum, the surface integral may be transformed to a volume integral by employing the divergence theorem in (31), the chain rule, and the Cauchy's stress theorem (2.65):

$$\int_A x_i\,t_j\;dA = \int_A x_i\,T_{jl}n_l\;dA = \int_V x_{i,l}\,T_{jl} + x_i\,T_{jl,l}\;dV = \int_V T_{ji} + x_i\,T_{jl,l}\;dV \tag{2.91}$$

where the latter identity follow by realizing that: $x_{i,l} = \delta_{il}$ and $x_{i,l}\,T_{jl} = \delta_{il}\,T_{jl} = T_{ji}$. Substitution of (2.91) into (2.90) yields:

$$e_{ijk}\int_V x_i\,(T_{jl,l} + \rho b_j - \rho\dot{v}_j)\,dV + \int_V e_{ijk}\,T_{jk}\;dV = 0 \tag{2.92}$$

Now, the first integral vanish due to balance of linear momentum as expressed in Cauchy's equations of motion (2.89), and consequently the integrand of the latter integral must vanish too:

$$e_{ijk}\,T_{ji} = 0 \Leftrightarrow T_{ji} - T_{ij} = 0 \Rightarrow T_{ji} = T_{ij} \tag{2.93}$$

The stress tensor is symmetric
The balance of angular momentum implies that the stress matrix is symmetric, $\mathbf{T} = \mathbf{T}^T$.

Example 2.4.1. *The hydrostatic pressure distribution.*

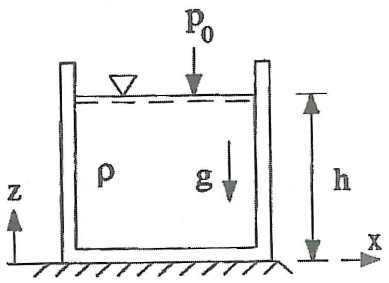

Figure 2.10: Fluid at rest in a container.

Consider a cylinder with a homogenous liquid at rest of constant density ρ (Figure 2.10). The only force acting is the constant gravitational force g in the negative z-direction.

The state of stress in the fluid is given by (2.86), which only contains the pressure p. The pressure may in general vary in space, i.e., as a function of the spatial coordinates x, y, and z. In this situation the left hand side of the Cauchy equations (2.89) vanishes and the balance of linear momentum reduce to:

$$0 = (-p\delta_{ik})_{,k} + \rho\, b_i \tag{2.94}$$

which yields:

$$-p_{,i} + \rho\, b_i = 0 \qquad \Leftrightarrow \qquad -\nabla p + \rho \mathbf{b} = 0 \tag{2.95}$$

on component and vector form, respectively. In this example with a constant gravitational force g in the negative z-direction, we have: $b_1 = b_x = b_2 = b_y = 0$ and $b_3 = b_z = -g$. Consequently, (2.95) reduce to:

$$\frac{\partial p}{\partial x} = 0, \quad \frac{\partial p}{\partial y} = 0, \quad \frac{\partial p}{\partial z} = -\rho g \tag{2.96}$$

From the first two equations in (2.96) we realize that the pressure is a function of z only, i.e., $p = p(z)$. Further, we orient the coordinate system so that $z = 0$ at the cylinder bottom and $z = h$ at the liquid surface, where $p(z) = p_0$,

i.e., atmospheric pressure at the liquid surface. By integration of the last equation in (2.96) we get:

$$p(z) = p_0 + \rho g(h - z) \tag{2.97}$$

(2.97) is a *hydrostatic pressure distribution*, which is valid for all fluids at rest of constant density ρ, regardless of e.g., their viscous properties.

Example 2.4.2. *Cauchy equations in cylindrical coordinates.*

The challenge to express the Cauchy equations (2.89) in cylindrical coordinates, is to present the divergence of the stress tensor $\mathbf{T}$. In this example we will first find expressions for the unit base vectors in a cylindrical coordinate system and their derivatives before we apply the generic expression for the divergence of a second order tensor derived in section .3.1.

Consider the position vector $\mathbf{r}$ on a cylinder with radius r, at an angle θ with the x_1-axis, and at height z. In a Cartesian coordinate system the position $\mathbf{r}$ has the representation:

$$\mathbf{r} = r\cos\theta\mathbf{e}_1 + r\sin\theta\mathbf{e}_2 + z\mathbf{e}_3 \tag{2.98}$$

For convenience we introduce cylindrical coordinates $(y_1, y_2, y_3) = (r, \theta, z)$ and from the equation (13) we find expressions or the base vectors and base unit vectors, corresponding to the cylindrical directions. For simplicity we drop the y-superscript for the base unit vectors (i.e., $\mathbf{e}_1^y = \mathbf{e}_r$ and so on). In the r-direction we find:

$$\mathbf{g}_r = \frac{\partial \mathbf{r}}{\partial r} = \cos\theta\mathbf{e}_1 + \sin\theta\mathbf{e}_2 = \mathbf{e}_r \quad \Leftarrow \quad h_r^2 = \mathbf{g}_r \cdot \mathbf{g}_r = 1 \tag{2.99}$$

and in the z-direction:

$$\mathbf{g}_z = \frac{\partial \mathbf{r}}{\partial z} = \mathbf{e}_3 = \mathbf{e}_z, \quad \Rightarrow \quad h_z^2 = \mathbf{g}_z \cdot \mathbf{g}_z = 1 \tag{2.100}$$

Only in the θ-direction we find a base vector with length greater than unity:

$$\mathbf{g}_\theta = \frac{\partial \mathbf{r}}{\partial \theta} = -r\sin\theta\mathbf{e}_1 + r\cos\theta\mathbf{e}_2 \quad \Rightarrow \quad h_\theta^2 = r^2 \tag{2.101}$$

and thus the unit base vector in the θ-direction become:

$$\mathbf{e}_\theta = \frac{\mathbf{g}_\theta}{h_\theta} = -\sin\theta\mathbf{e}_1 + \cos\theta\mathbf{e}_2 \tag{2.102}$$

Now, from equation (2.98) and (2.99) we find two equivalent expressions for the position vector $\mathbf{r}$:

$$\mathbf{r} = r\cos\theta\mathbf{e}_1 + r\sin\theta\mathbf{e}_2 + z\mathbf{e}_3 = r\mathbf{e}_r + z\mathbf{e}_z \tag{2.103}$$

Further, we also find from equation (2.99) and (2.102):

$$\frac{\partial \mathbf{e}_r}{\partial\theta} = \mathbf{e}_\theta \quad \text{and} \quad \frac{\partial \mathbf{e}_\theta}{\partial\theta} = -\mathbf{e}_r \tag{2.104}$$

With the relations in equation (2.104) we may use the expression derived in equation (29) to present the divergence of the stress tensor $\mathbf{T}$ in cylindrical coordinates. Note that we for convenience use subscripts (r, θ, z) for the components rather than $(1, 2, 3)$.

$$\operatorname{div}\mathbf{T} = \sum_i \left(\frac{1}{h_i}\frac{\partial T_{ri}}{\partial y_i}\,\mathbf{e}_r + \frac{1}{h_i}\frac{\partial T_{\theta i}}{\partial y_i}\,\mathbf{e}_\theta + \frac{1}{h_i}\frac{\partial T_{zi}}{\partial y_i}\,\mathbf{e}_z \right) \tag{2.105}$$

$$+ \frac{1}{h_\theta} T_{r\theta}\frac{\partial \mathbf{e}_r}{\partial\theta} + \frac{1}{h_\theta} T_{\theta\theta}\frac{\partial \mathbf{e}_\theta}{\partial\theta} \tag{2.106}$$

$$+ \frac{1}{h_\theta} T_{kl}\,\mathbf{e}_k \otimes \frac{\partial \mathbf{e}_l}{\partial\theta}\cdot\mathbf{e}_\theta \tag{2.107}$$

The expression in equation (2.107) may be simplified by taking into account the relations in equation (2.104):

$$\operatorname{div}\mathbf{T} = \sum_i \left(\frac{1}{h_i}\frac{\partial T_{ri}}{\partial y_i}\,\mathbf{e}_r + \frac{1}{h_i}\frac{\partial T_{\theta i}}{\partial y_i}\,\mathbf{e}_\theta + \frac{1}{h_i}\frac{\partial T_{zi}}{\partial y_i}\,\mathbf{e}_z \right) \tag{2.108}$$

$$+ \frac{1}{h_\theta} T_{r\theta}\,\mathbf{e}_\theta - \frac{1}{h_\theta} T_{\theta\theta}\,\mathbf{e}_r \tag{2.109}$$

$$+ \frac{1}{h_\theta} T_{kr}\,\mathbf{e}_k \tag{2.110}$$

By introducing the common engineering notation introduced in equation (2.60) and collecting terms in each of the cylindrical directions in equation (2.110), results in the following representation of the the Cauchy equations (2.89) in cylindrical coordinates:

$$\rho a_r = \frac{\partial\sigma_r}{\partial r} + \frac{\sigma_r - \sigma_\theta}{r} + \frac{1}{r}\frac{\partial\tau_{r\theta}}{\partial\theta} + \frac{\partial\tau_{rz}}{\partial z} + \rho b_r \tag{2.111}$$

$$\rho a_\theta = \frac{\partial}{\partial r}\left(r^2\tau_{r\theta}\right) + \frac{1}{r}\frac{\partial\sigma_\theta}{\partial\theta} + \frac{\partial\tau_{\theta z}}{\partial z} + \rho b_\theta \tag{2.112}$$

$$\rho a_z = \frac{1}{r}\frac{\partial}{\partial r}\left(r\tau_{zr}\right) + \frac{1}{r}\frac{\partial\tau_{z\theta}}{\partial\theta} + \frac{\partial\sigma_z}{\partial z} + \rho b_z \tag{2.113}$$

This formulation of the Cauchy equation will turn out to be useful e.g., when we later will study wave propagation phenomena in compliant vessels.

2.5 Stress analysis

From Cauchy's stress theorem ((2.65)) we may compute a stress vector, normal stress, and shear stress on an arbitrary plane with normal $\mathbf{n}$ in a point/particle P, whenever the stress tensor in known. Below we will simply state without proof a theorem, which will prove useful to identify maximum stresses and planes without shear stress, for generic stress state.

2.5.1 Principal stresses

Theorem 2.5.1. Principal stress theorem

For any state of stress in a particle there are three orthogonal planes free of shear stress. (2.114)

The shear stress free planes are referred to as *principal planes*, with corresponding *principal directions* $\mathbf{n}$, and *principal stresses* σ. As the principal planes are shear stress free, the stress vector on a principal plane may be expressed by $\mathbf{t} = \sigma\mathbf{n}$, i.e., the stress vector is parallel with the normal vector on the principal plane. By substitution of $\mathbf{t} = \sigma\mathbf{n}$ into (2.65)), the identification of principal stresses and principal directions is reduced to the eigenvalue problem:

$$\mathbf{T} \cdot \mathbf{n} = \sigma\mathbf{n} \tag{2.115}$$

where the stress-matrix $\mathbf{T}$ real and symmetric $\mathbf{T} = \mathbf{T}^T$ (see (2.93). Equivalent representations of the eigenvalue problems in (2.115) are:

$$(\sigma\mathbf{I} - \mathbf{T}) \cdot \mathbf{n} = 0 \qquad \Leftrightarrow (\sigma\delta_{ik} - T_{ik})\ n_k \tag{2.116}$$

where the latter component form follows is perhaps most easily realized as $\sigma n_i = \sigma\delta_{ik}n_k$ and δ_{ik} are the components of the unit matrix $\mathbf{I}$. For a given principal stress σ, (2.116) form a set of three linear, homogenous equations for the three components n_k of the corresponding principal direction. The

condition that (2.116) has a solution, is that the determinant of the coefficient matrix is equal to zero:

$$|\sigma\delta_{ik} - T_{ik}| = 0 \Rightarrow \begin{vmatrix} \sigma - T_{11} & -T_{12} & -T_{13} \\ -T_{21} & \sigma - T_{22} & -T_{23} \\ -T_{31} & -T_{32} & \sigma - T_{33} \end{vmatrix} = \sigma^3 - I_1\sigma^2 + I_2\sigma - I_3 = 0 \tag{2.117}$$

According to conventions, we have introduced the *principal invariants of the stress tensor*:

$$I_1 = T_{kk} = \mathrm{tr}\mathbf{T} \tag{2.118}$$

$$I_2 = \frac{1}{2}\left(T_{ii}T_{kk} - T_{ik}T_{ik}\right) = \frac{1}{2}\left[(\mathrm{tr}\mathbf{T})^2 - \|\mathbf{T}\|^2\right] \tag{2.119}$$

$$I_3 = \det \mathbf{T} \tag{2.120}$$

The cubic (2.117) is called *the characteristic equation of the stress tensor*. As $\mathbf{T}$ is real and symmetric, it follows from basic linear algebra that the three principal stresses $\sigma_1 \ldots \sigma_3$ (eigenvalues) , are real, and when distinct, the corresponding principal planes (eigenvectors) are orthogonal. For convenience, the principal stresses may be ordered by their numerical values such that:

$$\sigma_3 \leq \sigma_2 \leq \sigma_1 \tag{2.121}$$

The fact that any cubic equation with real coefficients, such as (2.117), has a least one real root, may be realized by the following. Let $f(\sigma)$ denote the left hand side of (2.117). Then, $f(\sigma) \to -\infty$ when $\sigma \to -\infty$ and $f(\sigma) \to \infty$ when $\sigma \to \infty$. Thus, there is a least one $\sigma = \sigma_3$ for which $f(\sigma = \sigma_3) = 0$. For principal stress $\sigma = \sigma_3$ the corresponding principal direction $\mathbf{n}_3$ may be found from (2.116). Now, for convenience, select a coordinate system such that $\mathbf{e}_3 = \mathbf{n}_3$. In this coordinate system the corresponding stress vector $\mathbf{t}_3 = \sigma_3\,\mathbf{n}_3$ and $T_{\alpha 3} = 0$, and the stress matrix is:

$$\mathbf{T} = \begin{bmatrix} T_{11} & T_{12} & 0 \\ T_{21} & T_{22} & 0 \\ 0 & 0 & \sigma_3 \end{bmatrix} \tag{2.122}$$

For this choice of coordinate system, (2.116), simplifies to (note that n_3 denotes the component in the $\mathbf{e}_3$-direction, for all principal directions $\mathbf{n}_1$, $\mathbf{n}_2$, and $\mathbf{n}_3$.) :

$$\left(\sigma\delta_{\alpha\beta} - T_{\alpha\beta}\right) n_\alpha = 0, \qquad (\sigma - \sigma_3)\, n_3 = 0 \tag{2.123}$$

By initially assuming that $\sigma \neq \sigma_3$ we get from (2.123) that $n_3 = 0$, i.e., the principal directions $\mathbf{n}_1$ and $\mathbf{n}_2$, will be parallel to the x_1x_2-plane, and normal to $\mathbf{n}_3$. The first two equations in (2.123) may be represented in matrix form as:

$$\begin{bmatrix} \sigma - T_{11} & -T_{12} \\ -T_{21} & \sigma - T_{22} \end{bmatrix} \begin{bmatrix} n_1 \\ n_2 \end{bmatrix} = 0 \tag{2.124}$$

the corresponding determinant has to be zero for (2.124) to hold for all choices of n_1 and n_2:

$$(\sigma - T_{11})(\sigma - T_{22}) - T_{12}T_{21} = \sigma^2 - (T_{11} + T_{22})\sigma + T_{11}T_{22} + T_{12}^2 = 0 \tag{2.125}$$

where the latter equality follow from the symmetry of $\mathbf{T}$, i.e., $T_{12} = T_{21}$. The solution of the quadratic equation for the determinant is given by:

$$\sigma_{1,2} = \frac{1}{2}(T_{11} + T_{22}) \pm \sqrt{\left(\frac{T_{11} - T_{22}}{2}\right)^2 + T_{12}^2} \tag{2.126}$$

The two solutions σ_1 and σ_2 will always be real as the radicand of (2.126) never will be negative. Subject to the condition that the $\mathbf{e}_3$-direction is aligned with the third principal direction $\mathbf{n}_3$, (2.126) offers a simple formula to compute the principal stresses. This is very useful for planar states of stress (section 2.5.3).

If we let ϕ denote the angle between a normal vector $\mathbf{n}$ and the x_1-axis, we can express the components of $\mathbf{n}$ as:

$$\mathbf{n} = [\cos\phi, \sin\phi, 0] \tag{2.127}$$

The corresponding principal direction to the eigenvalue σ_α, may be found by substitution of (2.127) into (2.124), an operations which yields two equations out of which the first one reads:

$$(\sigma_\alpha - T_{11})\cos\phi_\alpha - T_{12}\sin\phi_\alpha = 0 \tag{2.128}$$

and thus the corresponding principal direction to σ_α is given by:

$$\tan\phi_\alpha = \frac{\sigma_\alpha - T_{11}}{T_{12}} \tag{2.129}$$

For a coordinate system aligned with the principal directions, which we denote a *principal coordinate system*, the stress matrix $\mathbf{T}$ takes the form,:

$$\mathbf{T} = \begin{bmatrix} \sigma_1 & 0 & 0 \\ 0 & \sigma_2 & 0 \\ 0 & 0 & \sigma_3 \end{bmatrix} \quad \Leftrightarrow \quad T_{ik} = \sigma_i \delta_{ik} \quad \text{no sum over i} \tag{2.130}$$

and then an equivalent, but simpler representation of the principal invariants may be found as:

$$I_1 = \sigma_1 + \sigma_2 + \sigma_3 \tag{2.131}$$
$$I_2 = \sigma_1\sigma_2 + \sigma_2\sigma_3 + \sigma_3\sigma_1 \tag{2.132}$$
$$I_3 = \sigma_1\sigma_2\sigma_3 \tag{2.133}$$

Thus, in (2.131) and (2.133), the principal invariants are expressed by the principal stresses, whereas in (2.118) - (2.120) they are expressed by the coordinate stresses.

For a principal coordinate system, the normal stress σ on a plane with unit normal $\mathbf{n}$ is given by:

$$\sigma = \mathbf{n} \cdot \mathbf{T} \cdot \mathbf{n} = \sum_{i,k} n_i \sigma_i \delta_{ik} n_k = \sigma_1 n_1^2 + \sigma_2 n_2^2 + \sigma_3 n_3^2 \tag{2.134}$$

From (2.134), the ordering in (2.121) and the property of a unit normal vector $\mathbf{n} \cdot \mathbf{n} = n_1^2 + n_2^2 + n_3^2 = 1$, one may find that:

$$\sigma_3 \left(n_1^2 + n_2^2 + n_3^2\right) \leq \sigma \leq \sigma_1 \left(n_1^2 + n_2^2 + n_3^2\right) \quad \Rightarrow \quad \sigma_3 \leq \sigma \leq \sigma_1 \tag{2.135}$$

Thus, as (2.135) must hold for any $\mathbf{n}$, the extremal normal stresses $(\sigma_{\max}, \sigma_{\min})$ are given by:

$$\sigma_{\max} = \sigma_1, \qquad \sigma_{\min} = \sigma_3 \tag{2.136}$$

The largest principal stress σ_1, is therefore the maximum normal stress on any planes at a given location/particle. Correspondingly, σ_3 is the minimum normal stress on any planes at a given location/particle, whereas σ_2 is called the intermediate principal stress.

Extremal normal stresses The extremal normal stresses are given by the principal stresses σ_1 and σ_3.

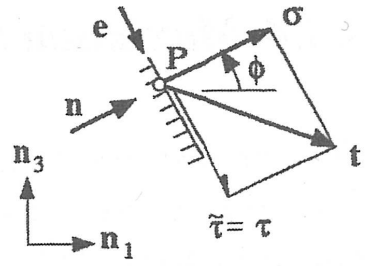

Figure 2.11: Shear stress τ and normal stress σ in planes parallel to $\mathbf{n}_2$.

2.5.2 Maximum shear stress

The component τ in an arbitrary direction $\mathbf{e}$ of the stress vector $\mathbf{t}$ acting on a surface with orientation $\mathbf{n}$ is given by (2.84):

$$\tau = \mathbf{e} \cdot \mathbf{t} = e_i T_{ik} n_k = \sum_{i,k} e_i \sigma_i \delta_{ik} n_k = \sigma_1 e_1 n_1 + \sigma_2 e_2 n_2 + \sigma_3 e_3 n_3 \qquad (2.137)$$

The latter expression in (2.137), follow by assuming a principal coordinate system with a stress matrix given by (2.130). Now, by choosing $\mathbf{e}$ to be orthogonal to $\mathbf{n}$, i.e., computing the shear stress which is the component of the stress vector $\mathbf{t}$ in the plane which has $\mathbf{n}$ as normal vector:

$$\mathbf{e} \cdot \mathbf{n} = e_i \, n_i = 0 \qquad \Rightarrow \qquad e_2 n_2 = -e_1 n_1 - e_3 n_3 \qquad (2.138)$$

Substituting (2.138) into (2.137) we get:

$$\tau = (\sigma_1 - \sigma_2) \, e_1 n_1 - (\sigma_2 - \sigma_3) \, e_3 n_3 \qquad (2.139)$$

Due to the ordering in (2.121), the expressions in the parenthesis of (2.139) will always be positive. Thus, in order to maximize τ, the expressions $e_1 n_1$ and $-e_3 n_3$ must be taken as large as possible. The absolute of e_1, n_1, e_3, and n_3 become largest if $e_2 = n_2 = 0$, as $\mathbf{e}$ and $\mathbf{n}$ are orthogonal unit vectors. In other words, to find the maximum shear stress we should choose $\mathbf{e}$ and $\mathbf{n}$ in a plane parallel to the plane spanned by the principal directions $\mathbf{n}_1$ and $\mathbf{n}_3$. Equivalently, the plane with orientation $\mathbf{n}$, should be parallel to the $\mathbf{n}_2$ principal direction (Figure 2.11). Note that since $\mathbf{n}_2$ is a principal direction, the stress vector $\mathbf{t}$ in Figure 2.11 has no component in the $\mathbf{n}_2$-direction. Letting ϕ denoting the angle in the counter clockwise direction with respect to the first principal direction $\mathbf{n}_1$, we may deduce from Figure 2.11:

$$n_1 = \cos\phi = -e_3 \qquad \text{and} \qquad e_1 = \sin\phi = n_3 \qquad (2.140)$$

By substituting (2.140) into (2.139), we realize that the σ_2-terms cancel and that the shear stress may be represented:

$$\tau = (\sigma_1 - \sigma_3)\cos\phi\sin\phi = \frac{1}{2}(\sigma_1 - \sigma_3)\sin 2\phi \tag{2.141}$$

the latter relation follow from the trigonometric formula (2).

Thus, the shear stress has its maximum value $\tau_{\max}$, for $\phi = \pi/4$, and

$$\tau_{\max} = \frac{1}{2}(\sigma_{\max} - \sigma_{\min}) \tag{2.142}$$

which is a generic important result:

The maximum shear stress

The maximum shear stress acts on planes that are inclined 45° with respect to the principal directions of the maximum and minimum principal stresses.

This result may also be obtained by considering a cube is aligned with the principal directions (Figure 2.12, upper panel). Consider a cross-section parallel with $\mathbf{n}_2$, tilted with an angle ϕ with respect to the $\mathbf{n}_3$-direction (Figure 2.12, lower panel).

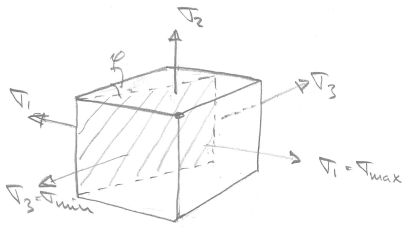

Figure 2.12: A cube aligned with the principal directions.

On such a surface there will be a normal stress σ and shear stress τ, to satisfy equilibrium (balance of linear momentum). Without loss of generality, the length of the tilted edge in Figure 2.13 (lower panel), is taken to be unity.

We then find an expression for the shear stress by balancing the forces in the τ-direction:

$$\tau + \sigma_3\cos\phi\sin\phi - \sigma_1\sin\phi\cos\phi = 0 \tag{2.143}$$

which provides an expression for the shear stress τ:

$$\tau = (\sigma_1 - \sigma_3)\sin\phi\cos\phi = \frac{1}{2}\sin 2\phi\,(\sigma_1 - \sigma_3) \tag{2.144}$$

which is identical to (2.141) and leads to (2.142).

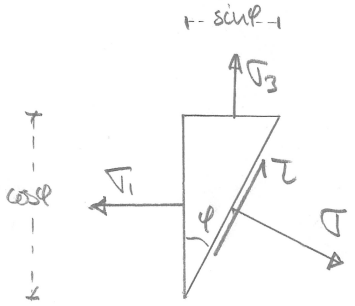

Figure 2.13: Max shear stress illustration.

The corresponding normal stress σ may be found by fulfillment of the equilibrium criterion in the normal direction:

$$\sigma - \sigma_1 \cos^2 \phi - \sigma_3 \sin^2 \phi = 0 \tag{2.145}$$

which at $\phi = \pi/4$ yields:

$$\sigma = \frac{1}{2}(\sigma_1 + \sigma_3) \tag{2.146}$$

2.5.3 Planar stress

If there is a stress free plane for a given stress state, we say that the structure/particle is in a *state of plane stress* or equivalently *a state of biaxial stress*. In particular for extreme loads, this is often the case in engineering/bioengineering application. Even when the surface is loaded, a planar stress assumption may serve as a good first approach, as will be seen for thin-walled spheres and cylinders in example 2.5.1.

For a planar stress situation, we may select a coordinate system such that the z-axis is orthogonal to the stress free plane. Consequently, all stress components in the z-direction will be zero: $\sigma_z = \tau_{xz} = \tau_{yz} = 0$. Therefore, the xy-plane is a principal plane with corresponding principle stress $\sigma_3 = \sigma_z = 0$, and the stress matrix in (2.60) reduces to:

$$\mathbf{T} = \begin{bmatrix} \sigma_x & \tau_{xy} \\ \tau_{xy} & \sigma_y \end{bmatrix} \tag{2.147}$$

In the following we will present two ways to derive the expressions for the stresses σ and τ on a plane parallel to the z-axis, for an arbitrary plane with

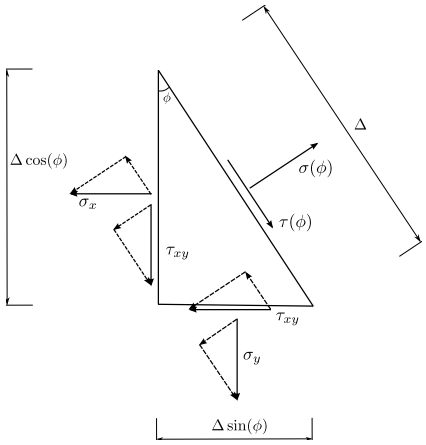

Figure 2.14: Planar stress situation.

a unit normal $\mathbf{n}$ at angle ϕ with respect to the x-axis. First, we will use the generic expressions for σ and τ as presented in Eqs. (2.134) and (2.137).

A generic planar stress situation is illustrated in Figure 2.14 and the unit normal and the unit tangent vectors may be expressed by:

$$\mathbf{n} = [\cos\phi, \sin\phi] \tag{2.148}$$
$$\mathbf{e} = [\sin\phi, -\cos\phi] \tag{2.149}$$

From CST in (2.65) we get:

$$t_\alpha = T_{\alpha\beta} n_\beta \tag{2.150}$$

and by use of the stress matrix in (2.147) we get:

$$t_1 = \sigma_x \cos\phi + \tau_{xy} \sin\phi \tag{2.151}$$
$$t_2 = \tau_{xy} \cos\phi + \sigma_y \sin\phi \tag{2.152}$$

Now, the normal stress σ an the shear stress τ are found from Eqs. (2.134) and (2.137):

$$\sigma = \mathbf{n} \cdot \mathbf{t} = n_\alpha t_\alpha = \sigma_x \cos^2\phi + \sigma_y \sin^2\phi + 2\tau_{xy} \sin\phi \cos\phi \tag{2.153}$$
$$\tau = \mathbf{e} \cdot \mathbf{t} = e_\alpha t_\alpha = (\sigma_x - \sigma_y) \sin\phi \cos\phi - \tau_{xy} \left(\cos^2\phi - \sin^2\phi\right) \tag{2.154}$$

Now, by making use of the trigonometric relations in (2), the expressions for the normal and shear stress at an arbitrary plane given by (2.153) and (2.154) may be simplified to:

$$\sigma(\phi) = \frac{\sigma_x + \sigma_y}{2} + \frac{\sigma_x - \sigma_y}{2}\cos 2\phi + \tau_{xy}\sin 2\phi \tag{2.155}$$

$$\tau(\phi) = \frac{\sigma_x - \sigma_y}{2}\sin 2\phi - \tau_{xy}\cos 2\phi \tag{2.156}$$

The second way of derving the expressions in (2.155) and (2.156), for the normal stress σ and the shear stress τ, is to formulate expressions which meet the requirement of force equilibrium in two perpendicular directions. The expression for the normal stress σ is obtained from the requirement of force equilibrium in the $\mathbf{n}$-direction (Figure 2.14):

$$\sigma(\phi)\cdot 1 - \sigma_x\cos^2\phi - \sigma_y\sin^2\phi - \tau_{xy}\sin\phi\cos\phi - \tau_{xy}\cos\phi\sin\phi = 0 \tag{2.157}$$

which may be reorganized to the previously derived expressions for the normal stress $\sigma(\phi)$ as given by Eqs. (2.153), (2.154), (2.155), and (2.156). Similarly, an expression for the shear stress τ is obtained from the requirement of force equilibrium in the τ-direction:

$$\tau(\phi)\cdot 1 - \sigma_x\sin\phi\cos\phi + \sigma_y\cos\phi\sin\phi + \tau_{xy}\cos^2\phi - \tau_{xy}\sin^2\phi = 0 \tag{2.158}$$

which also may be reorganized to the previously derived expressions for the shear stress as given by Eqs. (2.153), (2.154) and (2.156).

For a planar state of stress, one may orient a coordinate system with the x_3-direction perpendicular to the stress free plane. Thus, $\mathbf{e}_3$ is a principal direction, with a *known* principal stress $\sigma_3 = 0$. We may then use the perviously derived, generic expressions for the principal stresses in Eqs. (2.126) and (2.129), for the normal stress values in a planar state of stress. We repeat them here, using engineering notation:

$$\sigma_{1,2} = \frac{1}{2}(\sigma_x + \sigma_y) \pm \sqrt{\left(\frac{\sigma_x - \sigma_y}{2}\right)^2 + \tau_{xy}^2} \tag{2.159}$$

$$\tan\phi_\alpha = \frac{\sigma_\alpha - \sigma_x}{\tau_{xy}} \tag{2.160}$$

Note that σ_1 and σ_2 may both be positive, or both be negative, or have different signs. Thus, the conventional ordering of $\sigma_3 \leq \sigma_2 \leq \sigma_1$, is *not* adopted for planar states of stress, as $\sigma_3 = 0$ is tacitly assumed while employing (2.159). Keeping this in mind, (2.142) is still valid for the calculation of the maximum shear stress for a planar state of stress:

$$\tau_{\max} = \frac{1}{2}\left(\sigma_{\max} - \sigma_{\min}\right) \tag{2.161}$$

where:

$$\sigma_{\max} = \max(0, \sigma_1), \qquad \sigma_{\min} = \min(0, \sigma_2) \tag{2.162}$$

Example 2.5.1. *Biaxial state of stress for thin-walled structures.*

In this example we will consider two typical planar or biaxial states of stress, resulting from a thin-walled assumption. As we will see, this assumption has the convenient consequence, that one of the normal stress components is much smaller than the two others.

First we consider a thin-walled spherical shell (Figure 2.15) subjected to an internal pressure p. The mid wall radius of the shell is r, and the wall thickness is $t \ll r$. We conveniently select a spherical coordinate system (r, θ, ϕ), which is also a principal coordinate system for the current state of stress.

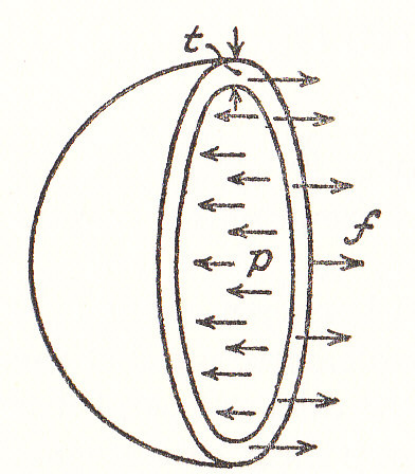

Figure 2.15: A free-body diagram of a hemisphere.

To meet the requirement of equilibrium of forces for two perpendicular cross-sections at the equator, with orientation $\mathbf{e}_\phi$ and $\mathbf{e}_\theta$, respectively, the following equations must be satisfied:

$$p\pi r^2 = \sigma_\theta 2\pi r t = \sigma_\phi 2\pi r t \tag{2.163}$$

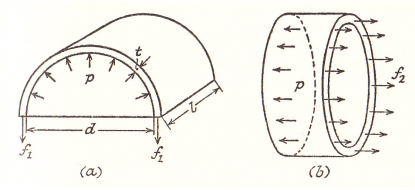

Figure 2.16: A free-body diagram of a circular cylinder.

from which the expressions for the average wall stresses σ_ϕ and σ_θ, may be derived:

$$\sigma_\phi = \sigma_\theta = \frac{1}{2}\frac{r}{t}p \tag{2.164}$$

The Eqs. (2.164) are commonly referred to as the *Laplace equations*. The remaining stress σ_r in the r-direction must be in the range $[-p, 0]$ to meet the requirement of equilibrium. Thus from the thin-walled assumption ($t \ll r$) and Eqs. (2.164) we find that $\sigma_r \ll \sigma_\phi = \sigma_\theta$. Consequently, σ_r may be disregarded for the stress analysis of a thin-walled spherical shell. The stress state may be regarded as planar or biaxial with the following the stress matrix:

$$\mathbf{T} = \begin{bmatrix} 0 & 0 & 0 \\ 0 & 1 & 0 \\ 0 & 0 & 1 \end{bmatrix} \frac{1}{2}\frac{r}{t}p \tag{2.165}$$

in a spherical coordinate system, which is seen to be a principal coordinate system, as there are no shear stresses present in the stress matrix of (2.165). We observe the common property of thin-walled structures, namely, that two stress components scale with r/t and p, *i.e.*

$$\sigma_{\phi,\theta} \propto \frac{r}{t}\, p \tag{2.166}$$

whereas the third stress component σ_r, scales with p only, and may consequently be disregarded.

Further, any direction parallel to the shell surface is a principal direction, since the stresses in the ϕ- and the θ-directions are equal. The state of stress for the thin-walled spherical shell may therefore be referred to as biaxial and plane-isotropic.

The second thin-walled structure we consider in this example, is a circular cylinder loaded with an internal pressure p (see Figure 2.16). The mid wall radius of the cylinder is r, and the wall thickness is $t \ll r$. Analogous to the

spherical shell, we conveniently select a cylindrical coordinate system (r, θ, z), which is also a principal coordinate system for the current state of stress.

To meet the requirement of equilibrium of forces for a perpendicular cross-sections at the equator, with orientation $\mathbf{e}_r$ the following equations must be satisfied:

$$2\,\sigma_\theta \Delta z\, t = p\, 2r\Delta z \tag{2.167}$$

and an expression for σ_θ, commonly referred to as the *hoop stress*, is obtained:

$$\sigma_\theta = \frac{r}{t}\, p \tag{2.168}$$

For a cross-section with orientation $\mathbf{e}_z$, the requirement of force equilibrium yields the same value as for the sphere in (2.163):

$$\sigma_z = \frac{1}{2}\frac{r}{t} p \tag{2.169}$$

Again, as for the thin-walled sphere, the remaining stress σ_r in the r-direction must be in the range $[-p, 0]$ to meet the requirement of equilibrium. From the thin-walled assumption ($t \ll r$) and Eqs. (2.168) and (2.169) we find that $\sigma_r \ll \sigma_\phi = 2\,\sigma_z$. We observe that the stresses for a thin-walled cylinder conform to the generic stress state of a thin-walled structure in (2.166). Consequently, σ_r may be disregarded for the stress analysis of a thin-walled circular cylinder and the stress state may be regarded as planar or biaxial with the following the stress matrix in a cylindrical, principal coordinate system:

$$\mathbf{T} = \begin{bmatrix} 0 & 0 & 0 \\ 0 & 2 & 0 \\ 0 & 0 & 1 \end{bmatrix} \frac{1}{2}\frac{r}{t} p \tag{2.170}$$

Observe, that the thin-walled circular cylinder is *statically determinate*, i.e., the stress state may be found from equilibrium analysis alone. On the contrary, a thick-walled cylinder is *statically indeterminate*, which has the consequence that the material properties of the wall has to be accounted for to determine the state of stress.

Chapter 3

Deformation

Strain is the term introduced in continuum mechanics for local deformation in a material, i.e., deformation in the neighborhood of a particle. Such local deformation is normally represented by changes in material lines, angles and volume. Correspondingly, three primary measures of strain is introduced; longitudinal strain ϵ, shear strain γ, and volumetric strain ϵ_v.

3.1 Measures of strain

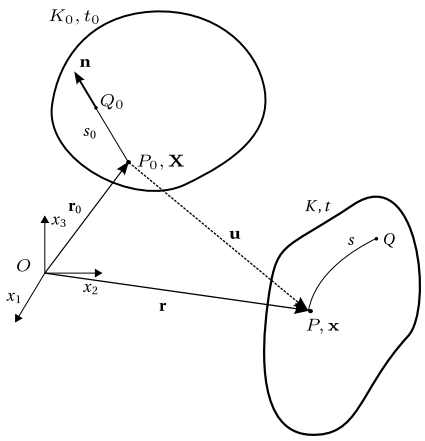

Figure 3.1: Deformation of a body by relating the current configuration (K, t) to the reference configuration$(K_0, t_0$.

In Figure 3.1 a body is represented in the current configuration K at time t and in the reference configuration K_0 at time t_0. The position of an arbitrary particle, denoted P, in the body in the current configuration K is given by $\boldsymbol{r}(\boldsymbol{r}_0, t)$, where $\boldsymbol{r}_0$ is the location of the same particle, denoted P_0, in

the reference configuration K_0. The set of coordinates of $\boldsymbol{r}_0$ is conventionally denoted X with corresponding spatial components X_1, X_2, X_3. The terms location and particle are used interchangeably for convenience, and thus we may refer to the *particle* $\boldsymbol{r}_0$ or the *particle* X.

The vector $\boldsymbol{r}(\boldsymbol{r}_0, t)$ is a function which represents the motion of an arbitrary particle in the body, which originally had the position $\boldsymbol{r}_0$. It may also be thought of as a map between the reference and current configuration. The motion may be represented as vector valued function or by its components:

$$\boldsymbol{r} = \boldsymbol{r}(\boldsymbol{r}_0, t) \Leftrightarrow x_i = x_i(X, t) \tag{3.1}$$

The displacement vector $\boldsymbol{u}(\boldsymbol{r}_0, t)$ (see Figure 3.1) is also a function which represents motion relative to the original location:

$$\boldsymbol{u}(\boldsymbol{r}_0, t) = \boldsymbol{r}(\boldsymbol{r}_0, t) - \boldsymbol{r}_0 \tag{3.2}$$

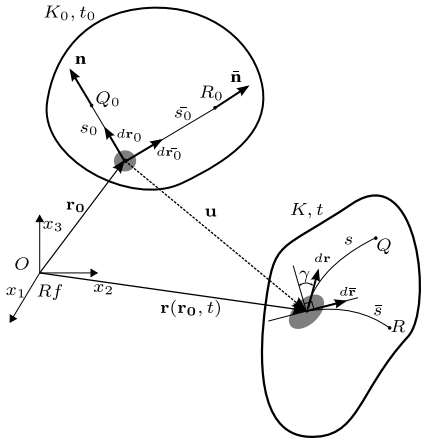

Figure 3.2: Deformation of a body from the current configuration (K, t) to the reference configuration$(K_0, t_0$.

Let P_0 denote the point with coordinates $\mathbf{r_0}$ inK_0 Let $s_0 = P_0Q_0$ denote the length the straight line from P_0 to Q_0 in the reference configuration K_0 from $\mathbf{r_0}$ in the direction of $\boldsymbol{n}$. In general this line will change both form and length in the current configuration K, where its length is represented by $s = PQ$. Definitions of the three measures strain may then be formulated:

Longitudinal strain ϵ The longitudinal strain ϵ in the direction $\boldsymbol{n}$ in a particle $\boldsymbol{r}_0$ is defined by:

$$\epsilon = \lim_{s_0 \to 0} \frac{s - s_0}{s_0} = \frac{ds - ds_0}{ds_0} = \frac{ds}{ds_0} - 1 \tag{3.3}$$

The longitudinal strain ϵ represents the change of length per unit length in the direction of $\boldsymbol{n}$ in particle $\boldsymbol{r}_0$.

Figure 3.2 illustrates the same situation as in Figure 3.1, albeit with some more details, allowing for the definition of shear strain:

Shear strain γ The angular deviation (in radians) from $\pi/2$ between two material lines in K which originally were perpendicular in K_0. The shear strain γ, is taken to be positive when the angle is reduced.

In Figure 3.2, the shear strain γ is illustrated at the location $\mathbf{r}_0$, as the angular deviation from $\pi/2$ between $\mathbf{n}$ and $\bar{\mathbf{n}}$, two perpendicular material line elements in the reference configuration K_0.

Volumetric strain ϵ_v

$$\epsilon_v = \lim_{\Delta V_0 \to 0} \frac{\Delta V - \Delta V_0}{\Delta V_0} \tag{3.4}$$

The volumetric strain ϵ_v represents change in a differential volume per unit undeformed differential volume around the particle $\boldsymbol{r}_0$.

In the following, commonly used expressions for the primary measures of strain will be introduced.

3.2 The Green strain tensor

The objective in this section is to express the three primary measures of strain ϵ, γ, and ϵ_v (see definitions in the previous section) by means of the Green strain tensor $\boldsymbol{E}$, which will be defined below. Before ending up with the Green strain tensor, other commonly used tensors will also be introduced, such as the deformation gradient tensor $\mathbf{F}$, Green's deformation tensor $\mathbf{C}$, the displacement gradient tensor $\mathbf{H}$.

The length s_0 of the material line P_0Q_0 in direction $\boldsymbol{n}$, will now be used to parameterize the length s in the current configuration K, i.e., $s(s_0)$ is a function of s_0. The coordinates of the endpoints Q_0 and Q are $X_i + s_0 n_i$ and $x_i\left(X + s_0\boldsymbol{n}, t\right)$, respectively. Here the directional unit vector is expressed by its components $\mathbf{n} = \mathbf{n_i e_i}$. The length s calculated with s_0 as curve parameter by the arc length formula:

$$s = \int_0^{s_0} \sqrt{\frac{\partial x_i}{\partial s_0}\frac{\partial x_i}{\partial s_0}}\, ds_0 \tag{3.5}$$

which yields

$$ds^2 = \left(\frac{\partial x_i}{\partial s_0}\frac{\partial x_i}{\partial s_0}\right) ds_0^2 \tag{3.6}$$

Let ds_0 be the length of $d\mathbf{r}_0$ in direction of $\boldsymbol{n}$ in K_0 (Fig. 3.2). Then it follows that:

$$d\boldsymbol{r}_0 = \boldsymbol{n}\, ds_0 = dX_k \boldsymbol{e}_k \tag{3.7}$$

which yields:

$$|d\mathbf{r_0}| = ds_0, \quad dX_k = n_k ds_0 \Leftrightarrow n_k = \frac{dX_k}{ds_0} \tag{3.8}$$

The expression for the components of the directional unit vector n_k in (3.8), will be useful, in the following derivation. Similarly, let $d\mathbf{r}$ be a line element from P in K, which due to our parameterization may be expressed:

$$d\mathbf{r} = \frac{\partial \mathbf{r}}{\partial s_0}\, ds_0 \quad \Leftrightarrow \quad dx_i = \frac{\partial x_i}{\partial s_0} ds_0 \tag{3.9}$$

From (3.6), we see that ds is the length of $d\mathbf{r}$. As the current position $\boldsymbol{r}$ is a function of the reference position $\boldsymbol{r}_0$, the relation between $d\mathbf{r}$ in K and its corresponding representation $d\mathbf{r_0}$ in K_0 may be presented:

$$d\mathbf{r} = \frac{\partial \mathbf{r}}{\partial \mathbf{r}_0} \cdot\, d\mathbf{r}_0 = \mathbf{F} \cdot\, d\mathbf{r}_0 \quad \Leftrightarrow \quad dx_i = \frac{\partial x_i}{\partial X_k} dX_k = F_{ik} dX_k \tag{3.10}$$

where the deformation gradient $\mathbf{F}$ has been introduced:

$$\mathbf{F} = \frac{\partial \mathbf{r}}{\partial \mathbf{r}_0} \quad \Leftrightarrow \quad F_{ik} = \frac{\partial x_i}{\partial X_k} \tag{3.11}$$

Loosely speaking, one may say that the deformation gradient holds information about the difference in the current locations of neighboring particles in K_0, which is unity when they are displaced equally i.e., for no deformation.

Now, consider an expression for the directional derivative $\partial x_i / \partial s_0$ of the components of $\boldsymbol{r}$ in direction of $\boldsymbol{n}$:

$$\left.\frac{\partial x_i \left(X + s_0 \boldsymbol{n}, t\right)}{\partial s_0}\right|_{s_0=0} = \frac{\partial x_i \left(X, t\right)}{\partial X_k} \left.\frac{d \left(X_k + s_0 n_k, t\right)}{ds_0}\right|_{s_0=0} \tag{3.12}$$

which may be simplified by substitution of (3.8):

$$\frac{\partial x_i}{\partial s_0} = F_{ik} \frac{dX_k}{ds_0} = F_{ik} n_k \tag{3.13}$$

The result in (3.13) may be substituted into (3.6) to yield:

$$\left(\frac{ds}{ds_0}\right)^2 = \frac{\partial x_i}{\partial s_0}\frac{\partial x_i}{\partial s_0} = F_{ij}n_jF_{ik}n_k = \boldsymbol{n}\cdot\left(\boldsymbol{F}^T\boldsymbol{F}\right)\cdot\boldsymbol{n} = \boldsymbol{n}\cdot\boldsymbol{C}\cdot\boldsymbol{n} \tag{3.14}$$

where the Green deformation tensor is introduced as a second order symmetric tensor:

$$\boldsymbol{C} = \boldsymbol{F}^T\boldsymbol{F} \quad \Leftrightarrow \quad C_{ij} = F_{ki}F_{kj} \tag{3.15}$$

This tensor is also commonly called the Left Green deformation tensor as the transpose $\boldsymbol{F}^T$ occurs on the left hand side of equation (3.15), as opposed to its equivalent Right Green deformation tensor:

$$\boldsymbol{B} = \boldsymbol{F}\boldsymbol{F}^T \quad \Leftrightarrow \quad B_{ij} = F_{ik}F_{jk} \tag{3.16}$$

which plays an important role the modelling of isotropic materials (see e.g., 4.3.2).

Longitudinal strain ϵ

From (3.3) and (3.14) an expression for the longitudinal strain ϵ in the direction $\boldsymbol{n}$ may be presented:

$$\epsilon = \sqrt{\boldsymbol{n}\cdot\boldsymbol{C}\cdot\boldsymbol{n}} - 1 \tag{3.17}$$

However, in (3.15) $\boldsymbol{C}$ is implicitly related to the deformation gradient $\boldsymbol{F}$, which in some applications is not a preferable way of representing deformation, as it is based on the current location $\mathbf{r}$ and not the displacement $\mathbf{u}(\mathbf{r}_0, t)$. From Eq. (3.2) and Figure 3.1, we see that

$$\mathbf{r} = \mathbf{r}_0 + \mathbf{u}(\mathbf{r}_0, t) \qquad \Leftrightarrow \qquad x_i(X,t) = X_i + u_i(X,t) \tag{3.18}$$

Thus, to obtain strain tensors based on displacement rather than the current location, the displacement gradient $\boldsymbol{H}$ is commonly introduced:

$$H_{ik} = \frac{\partial u_i}{\partial X_k} \quad \Leftrightarrow \quad \mathbf{H} = \frac{\partial \mathbf{u}}{\partial \mathbf{r}_0} \tag{3.19}$$

A relation between the displacement gradient $\boldsymbol{H}$ and the deformation gradient $\boldsymbol{F}$ by combining Eqs. (3.2), (3.11), and (3.19):

$$F_{ik} = \delta_{ik} + H_{ik} \quad \Leftrightarrow \quad \mathbf{F} = \mathbf{1} + \mathbf{H} \tag{3.20}$$

as:

$$\frac{\partial x_i}{\partial X_k} = \delta_{ik} + \frac{\partial u_i}{\partial X_k} \tag{3.21}$$

Thus, from (3.15) and (3.20) an alternative representation of the Green deformation tensor is found based on displacements:

$$\boldsymbol{C} = \boldsymbol{F}^T\boldsymbol{F} = \left(\mathbf{1} + \boldsymbol{H}^T\right)(\mathbf{1} + \boldsymbol{H}) = \mathbf{1} + \boldsymbol{H} + \boldsymbol{H}^T + \boldsymbol{H}^T\boldsymbol{H} \tag{3.22}$$

The expression for $\boldsymbol{C}$ in (3.22) may be simplified further by introducing the definition of the Green strain tensor:

$$\boldsymbol{E} = \frac{1}{2}\left(\boldsymbol{H} + \boldsymbol{H}^T + \mathbf{H}^T\boldsymbol{H}\right) \Leftrightarrow E_{kl} = \frac{1}{2}\left(\frac{\partial u_k}{\partial X_l} + \frac{\partial u_l}{\partial X_k} + \frac{\partial u_i}{\partial X_k}\frac{\partial u_i}{\partial X_l}\right) \tag{3.23}$$

such that by substitution of (3.23) into (3.22) the expression for the Green deformation tensor reduces to:

$$\boldsymbol{C} = \mathbf{1} + 2\boldsymbol{E} \tag{3.24}$$

An expression for the longitudinal strain ϵ based on the Green strain tensor is then obtained by substitution of (3.24) into (3.17):

$$\epsilon = \sqrt{1 + 2\,\boldsymbol{n}\cdot\boldsymbol{E}\cdot\boldsymbol{n}} - 1 \tag{3.25}$$

Shear strain γ

An expression for the shear strain γ may be found by considering two differential material elements, which were perpendicular in K_0, in the current configuration K:

$$d\mathbf{r} = \boldsymbol{F}\cdot d\mathbf{r}_0 = (\mathbf{1} + \boldsymbol{H})\cdot\boldsymbol{n}\,ds_0 \tag{3.26}$$

$$d\bar{\boldsymbol{r}} = \boldsymbol{F}\cdot d\bar{\boldsymbol{r}}_0 = (\mathbf{1} + \boldsymbol{H})\cdot\bar{\boldsymbol{n}}\,d\bar{s}_0 \tag{3.27}$$

The scalar product between the two vectors in (3.26) and (3.27) takes the form:

$$d\mathbf{r}\cdot d\bar{\boldsymbol{r}} = d\bar{s}_0\bar{\boldsymbol{n}}\cdot(\mathbf{1} + \boldsymbol{H}^T)(\mathbf{1} + \boldsymbol{H})\cdot\boldsymbol{n}ds_0 = \bar{\boldsymbol{n}}\cdot\boldsymbol{C}\cdot\boldsymbol{n}\,d\bar{s}_0 ds_0 \tag{3.28}$$

From (3.14) the length of the two differential vectors are found to be:

$$|d\mathbf{r}| = ds = \sqrt{\boldsymbol{n}\cdot\boldsymbol{C}\cdot\boldsymbol{n}}\,ds_0, \quad |d\bar{\boldsymbol{r}}| = d\bar{s} = \sqrt{\bar{\boldsymbol{n}}\cdot\boldsymbol{C}\cdot\bar{\boldsymbol{n}}}\,d\bar{s}_0 \tag{3.29}$$

The definition of a scalar product along with (3.28) and (3.29) may then be used to find an expression for the shear strain:

$$\sin\gamma = \frac{\bar{\boldsymbol{n}}\cdot\boldsymbol{C}\cdot\boldsymbol{n}}{\sqrt{\boldsymbol{n}\cdot\boldsymbol{C}\cdot\boldsymbol{n}}\,\sqrt{\bar{\boldsymbol{n}}\cdot\boldsymbol{C}\cdot\bar{\boldsymbol{n}}}} = \frac{\bar{\boldsymbol{n}}\cdot\boldsymbol{C}\cdot\boldsymbol{n}}{(1+\epsilon)\,(1+\bar{\epsilon})} \tag{3.30}$$

As $\bar{\boldsymbol{n}}$ and $\boldsymbol{n}$ are orthogonal, an expression for the shear strain based on the Green strain tensor is obtained from (3.24) and (3.30):

$$\sin\gamma = \frac{\bar{\boldsymbol{n}}\cdot\boldsymbol{C}\cdot\boldsymbol{n}}{(1+\epsilon)\,(1+\bar{\epsilon})} = \frac{2\,\bar{\boldsymbol{n}}\cdot\boldsymbol{E}\cdot\boldsymbol{n}}{(1+\epsilon)\,(1+\bar{\epsilon})} \tag{3.31}$$

Volumetric strain ϵ_v

The volume of a differential volume element dV_0 in K_0 is:

$$dV_0 = dX_1\,dX_2\,dX_3 \tag{3.32}$$

the corresponding deformed volume dV in K by the volume spanned by the the three vectors $d\mathbf{r}_i$:

$$d\mathbf{r}_1 = \frac{\partial\boldsymbol{r}}{\partial X_1}\,dX_1 = \frac{\partial x_i}{\partial X_1}\,\boldsymbol{e}_i\,dX_1, \quad d\mathbf{r}_2 = \frac{\partial x_j}{\partial X_2}\,\boldsymbol{e}_j\,dX_2, \quad d\mathbf{r}_3 = \frac{\partial x_k}{\partial X_3}\,\boldsymbol{e}_k\,dX_3 \tag{3.33}$$

which may be expressed by the box product (see (7.11)) of the vectors in (3.33):

$$dV = [d\mathbf{r}_1\,d\mathbf{r}_2\,d\mathbf{r}_3] = (d\mathbf{r}_1\times d\mathbf{r}_2)\cdot d\mathbf{r}_3 = e_{ijk}\,\frac{\partial x_j}{\partial X_1}\,dX_1\frac{\partial x_j}{\partial X_2}\,dX_2\,\frac{\partial x_j}{\partial X_3}\,dX_3 \tag{3.34}$$

In the latter expression of (3.34), the determinant (see (7.12)) of the deformation gradient is identified, and thus (3.34) may be represented:

$$dV = \det\boldsymbol{F}\,dV_0 = \det(\mathbf{1}+\boldsymbol{H})\;dV_0 = \sqrt{\det\boldsymbol{C}}\,dV_0 \tag{3.35}$$

the latter equalities follow from (3.20) and (3.22) and determinants of products. Various expressions for the volumetric strain ϵ_v may then be found from (3.32) and (3.35):

$$\epsilon_v = \frac{dV-dV_0}{dV_0} = \det\boldsymbol{F}-1 = \det(\mathbf{1}+\boldsymbol{H})-1 = \sqrt{\det\boldsymbol{C}}-1 = \sqrt{\det\mathbf{1}+2\boldsymbol{E}}-1 \tag{3.36}$$

In this section, all measures of strain, $\epsilon,\ \gamma,\ \epsilon_v$, have been expressed by the Green strain tensor $\boldsymbol{E}$ and the Green deformation tensor $\boldsymbol{C}$, which in turn are related to the deformation gradient $\boldsymbol{F}$ or the displacement gradient $\boldsymbol{H}$. In the following chapters it will be shown that material models relevant for biomechanical applications are mostly defined by relations between a stress tensor ($\boldsymbol{T}$ or other appropriate stresses) and the Green strain tensor $\boldsymbol{E}$ or the Green deformation tensor $\boldsymbol{C}$.

3.3 Small strains and small deformations

For a wide range of loading conditions on typical structural materials (e.g., steel, aluminum, concrete, wood) the resulting strains are small. A state for which the absolute value of the longitudinal strains are less than 1%, will be referred to as a state of *small strains* . In biomechanical applications however, small strains are the exception rather than the rule. Still, an exposition of the strain measures subject to the state of small strain is provided below, as they are simpler and thus more understandable than their large strain counterparts.

3.3.1 Small strains

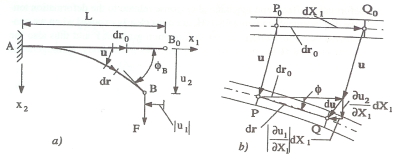

Figure 3.3: Illustrations of small strains and large deformations.

Note that small strains do not necessarily imply that either displacements or rotations of a line element are small (see Figure 3.3 adapted from fig 5.3.1 in [17,]).

Longitudinal strain We assume a state of small strains, i.e., $\epsilon < 1\%$. Then the generic expression for ϵ in (3.17) may be reformulated:

$$(1+\epsilon)^2 = 1 + 2\epsilon + \epsilon^2 = \boldsymbol{n}\cdot\boldsymbol{C}\cdot\boldsymbol{n} = \boldsymbol{1} + 2\,\boldsymbol{n}\cdot\boldsymbol{E}\cdot\boldsymbol{n} \tag{3.37}$$

From (3.37) an expression for ϵ valid for small strains is obtained by dropping higher order terms in ϵ

$$\epsilon = \boldsymbol{n}\cdot\boldsymbol{E}\cdot\boldsymbol{n} = n_i E_{ij} n_j \tag{3.38}$$

Similarly, an expression for the shear strain for small strains is obtained from (3.30), by setting $\gamma \approx \sin\gamma$ and the denominator to 1:

$$\gamma = 2\,\bar{\boldsymbol{n}} \cdot \boldsymbol{E} \cdot \boldsymbol{n} = 2\,\bar{n}_i E_{ij} n_j = \bar{\boldsymbol{n}} \cdot \boldsymbol{C} \cdot \boldsymbol{n} = \bar{n}_i C_{ij} n_j \tag{3.39}$$

Coordinate strains

may then naturally be introduced whenever material line elements in K_0 are parallel to the reference coordinate system:

$$\epsilon_{ii} = E_{ii} \quad \text{no summation}, \quad \gamma_{ij} = 2\,E_{ij} \quad i \neq j \tag{3.40}$$

Further, rearrangement of (3.36) for the volumetric strain ϵ_v yields:

$$1 + 2\epsilon_v + \epsilon_v^2 = \det(\mathbf{1} + 2\boldsymbol{E}) = 1 + 2\,E_{kk} + \mathcal{O}(E_{ik}\,E_{lm}) \tag{3.41}$$

which by neglection of higher order terms (i.e., ϵ_v^2 and $\mathcal{O}(E_{ik}\,E_{lm})$) yields and expression for the volumetric strain ϵ_v valid for small strains:

$$\epsilon_v = \mathrm{tr}(\boldsymbol{E}) \tag{3.42}$$

3.3.2 Small deformations

To relate the concept of small deformations to the elements in the displacement gradient tensor $\mathbf{H}$, consider the deformation of a line element PQ along the beam AB in Figure 3.3 a), where P_0Q_0 denote PQ in the reference configuration or in the undeformed case (Figure 3.3 b)). Small deformations will conventionally imply both a small angle of rotation ϕ, and small strain, which from Figure 3.3 b), is seen to be satisfied when:

$$\left|\frac{\partial u_2}{\partial X_1}\right| \equiv |H_{21}| \ll 1 \qquad \text{and} \qquad \left|\frac{\partial u_1}{\partial X_1}\right| \equiv |H_{11}| \ll 1 \tag{3.43}$$

Small deformations In the general case, the condition of small deformations is defined by the requirement that all components of the displacement gradient tensor H_{ik} must be small

$$|H_{ij}| = \left|\frac{\partial u_i}{\partial X_j}\right| \ll 1 \quad \Leftrightarrow \quad norm\,(\boldsymbol{H}) \ll 1 \tag{3.44}$$

Small deformations imply both small strains and small rotations. Occasionally *infinitesimal deformations* is used as a synonym in the literature for small deformations.

Now, the assumption of small deformations has implications for how one may interpret gradients and derivatives. For example for an arbitrary field $f(\mathbf{r},t) = f(\mathbf{r}(\mathbf{r}_0,t),t)$, one may obtain by using Eq. (3.18)

$$\frac{\partial f}{\partial X_j} = \frac{\partial f}{\partial x_k}\frac{\partial x_k}{\partial X_j} = \frac{\partial f}{\partial x_k}\left(\delta_{ki} + \frac{\partial u_k}{\partial X_i}\right) \approx \frac{\partial f}{\partial x_i} \equiv f_{,i} \tag{3.45}$$

which means that the spatial gradient in the current and in the reference configuration are the same.

Normally, small deformations imply small displacements, and we may replace the particle reference $\mathbf{r}_0$ by the position vector $\mathbf{r}$, and consequently use the position coordinates x_i as particle coordinates, rather than X_i. For the same reason we will also have for small displacements/deformations:

$$\dot{f}(\mathbf{r},t) = \dot{f}(x,t) = \partial_t f(\mathbf{r},t) \equiv \frac{\partial f(\mathbf{r},t)}{\partial t} \tag{3.46}$$

which means that the particle derivative and the partial derivative with respect to time are equivalent subject to the small displacements assumption.

Further, the displacement gradient are also simplified for small displacements (compare Eq. (3.19)):

$$H_{ij} = u_{i,j} \qquad \Leftrightarrow \qquad \mathbf{H} = *grad * \mathbf{u} \tag{3.47}$$

and the Green strain tensor Equation (3.23) reduce to:

$$\mathbf{E} = \frac{1}{2}\left(\mathbf{H} + \mathbf{H}^T\right) \quad \Leftrightarrow \quad E_{ij} = \frac{1}{2}\left(u_{i,j} + u_{j,i}\right) \tag{3.48}$$

From Eq. (3.48) we may infer that the expressions for the coordinate strains reduce to:

$$\epsilon_{11} = E_{11} = u_{1,1}, \qquad \gamma_{12} = 2E_{12} = u_{1,2} + u_{2,1}, \qquad \text{etc.} \tag{3.49}$$

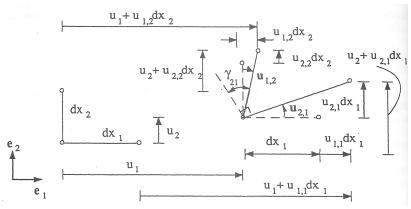

Figure 3.4: Two-dimensional illustration of coordinate strains.

The expressions for coordinate strains in Eq. (3.49) are illustrated in Figure 3.4 in the two-dimensional case.

As for small strains the volumetric strain ϵ_v for small displacements reduces to:

$$\epsilon_v = \text{tr}\mathbf{E} = E_{kk} = u_{k,k} = \div\mathbf{u} \tag{3.50}$$

From Eq. (3.50) we realize that the divergence of the displacement vector is an expression for the *change of volume per unit volume*, when the material in question has been transformed from the undeformed reference configuration K_0 to the deformed current configuration K.

3.3.3 Principal strains

In section 3.3.1 expressions were derived for longitudinal strain ϵ and shear strain γ (see (3.38) and (3.39)), valid for states of small strain:

$$\epsilon = \boldsymbol{n} \cdot \boldsymbol{E} \cdot \boldsymbol{n} = n_i E_{ij} n_j, \quad \gamma = 2\,\bar{\boldsymbol{n}} \cdot \boldsymbol{E} \cdot \boldsymbol{n} = 2\,\bar{n}_i E_{ij} n_j \tag{3.51}$$

As the Green strain tensor is symmetric by construction (see (3.23)), three orthogonal principal strain directions with corresponding principal strain values may be found. This result is the strain equivalent to the principal stress theorem (2.114). However, we do not have a Cauchy stress theorem (2.65) equivalent for strains, as no vector for strains have been introduced. Rather, for any direction $\boldsymbol{n}$ in K_0 we define a vector $\boldsymbol{E} \cdot \boldsymbol{n}$. The longitudinal strain in the direction of $\boldsymbol{n}$ is then the projection of the vector $\boldsymbol{E} \cdot \boldsymbol{n}$ in the direction of $\boldsymbol{n}$:

$$\epsilon = \boldsymbol{n} \cdot (\boldsymbol{E} \cdot \boldsymbol{n}) = n_i E_{ij} n_j, \tag{3.52}$$

Similarly, the shear strain is equal to twice the component of $\boldsymbol{E} \cdot \boldsymbol{n}$ in the direction of $\bar{\boldsymbol{n}}$:

$$\gamma = 2\,\bar{\boldsymbol{n}} \cdot (\boldsymbol{E} \cdot \boldsymbol{n}) = 2\,\bar{n}_i E_{ij} n_j \tag{3.53}$$

The conditions for the principal strains ϵ_i and the corresponding principal directions $\boldsymbol{n}_i$ forms an eigenvalue problem[1]:

$$\boldsymbol{E} \cdot \boldsymbol{n} = \epsilon \boldsymbol{n} \Leftrightarrow (\epsilon \mathbf{1} - \boldsymbol{E}) \cdot \boldsymbol{n} = 0 \Leftrightarrow (\epsilon \delta_{ij} - E_{ij})\, n_j = 0 \tag{3.54}$$

with corresponding characteristic equation for the small strain tensor $\boldsymbol{E}$:

$$\epsilon^3 - I\epsilon^2 + II\epsilon - III = 0 \tag{3.55}$$

[1] Indices are dropped for clarity.

and where the principal invariants

I, II, and III of the strain tensor $\boldsymbol{E}$ are given by:

$$I = \mathrm{tr}\boldsymbol{E} = E_{kk} \tag{3.56}$$

$$II = \frac{1}{2}\left[(\mathrm{tr}\boldsymbol{E})^2 - \|\boldsymbol{E}\|^2\right] = \frac{1}{2}\left[E_{ii}E_{jj} - E_{ij}E_{ij}\right] \tag{3.57}$$

$$III = \det \boldsymbol{E} = e_{ijk}E_{i1}E_{j2}E_{k3} \tag{3.58}$$

The characteristic equation (3.55) has three real solutions, the principal strains ϵ_i. Their corresponding principal directions $\boldsymbol{n}_i$ are orthogonal, subject to the condition that all principal strains are different. In general three orthogonal directions may always be specified. From (3.54) and (3.53), the shear strains related to principal directions are seen to be zero. From the above we formulate the following theorem:

Theorem 3.3.1. Principal strain theorem

Through every particle there exist three orthogonal material line elements which remain orthogonal after deformation.

The principal strains in a particle represent extremal values of longitudinal strains. By ordering the longitudinal strains such that: $\epsilon_3 < \epsilon_2 < \epsilon_1$, we get:

$$\epsilon_{\max} = \epsilon_1, \quad \epsilon_{\min} = \epsilon_3 \tag{3.59}$$

Further, the *maximum shear strain* is given by:

$$\gamma_{\max} = \epsilon_{\max} - \epsilon_{\min} \tag{3.60}$$

for the directions:

$$\boldsymbol{n} = \frac{\boldsymbol{n}_1 + \boldsymbol{n}_3}{\sqrt{2}}, \quad \bar{\boldsymbol{n}} = \frac{\boldsymbol{n}_1 - \boldsymbol{n}_3}{\sqrt{2}} \tag{3.61}$$

3.3.4 Small strains in a surface

Measurements of strains or deformation are generally easier to perform, than measurements of stresses or forces. Additionally, given an appropriate material model, stresses may be derived for measured strains. Strain measurements are often performed by using strain rosettes. In the following we shall analyze the state of strain in a surface in a surface and introduce a coordinate system with its x_3-axis normal to the tangent plane of the surface.

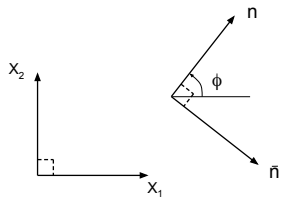

Figure 3.5: Orthogonal unit vectors $\mathbf{n}$ and $\bar{\mathbf{n}}$ in a material surface.

The two other axes will then be tangent plane to the surface in which the strains are located. Two orthogonal unit vectors in the tangent plane $\boldsymbol{n}$ and $\bar{\boldsymbol{n}}$ may then be expressed by their angle with respect to x_1-axis (see Fig. 3.5).

$$\boldsymbol{n} = [\cos\phi, \sin\phi, 0], \quad \bar{\boldsymbol{n}} = [\sin\phi, -\cos\phi, 0] \tag{3.62}$$

The longitudinal strain in the $\boldsymbol{n}$-direction and the shear strain with respect to $\boldsymbol{n}$ and $\bar{\boldsymbol{n}}$ is given by (3.38) and (3.39):

$$\epsilon = \epsilon(\phi) = \boldsymbol{n} \cdot \boldsymbol{E} \cdot \boldsymbol{n} = n_\alpha E_{\alpha\beta} n_\beta = E_{11}\cos^2\phi + E_{22}\sin^2\phi + 2E_{12}\cos\phi\sin\phi \tag{3.63}$$

$$\begin{aligned}\gamma = \gamma(\phi) &= 2\,\bar{\boldsymbol{n}} \cdot \boldsymbol{E} \cdot \boldsymbol{n} = 2\bar{n}_\alpha E_{\alpha\beta} n_\beta \\ &= 2\left[E_{11}\sin\phi\cos\phi - E_{22}\cos\phi\sin\phi - E_{12}(\cos^2\phi - \sin^2\phi)\right]\end{aligned} \tag{3.64}$$

The conventional notation for coordinate strains is then introduced:

$$\epsilon_x = E_{11}, \quad \epsilon_y = E_{22}, \quad \gamma_{xy} = 2E_{12} \tag{3.65}$$

Then, by employing the trigonometric formulas for $\sin 2\phi$ and $\cos 2\phi$ in (2)) and (3.65), the expressions for strains in (3.63) and (3.64) may be transformed to:

$$\epsilon(\phi) = \frac{\epsilon_x + \epsilon_y}{2} + \frac{\epsilon_x - \epsilon_y}{2}\cos 2\phi + \frac{1}{2}\sin 2\phi \tag{3.66}$$

$$\gamma(\phi) = (\epsilon_x + \epsilon_y)\sin 2\phi - \gamma_{xy}\cos 2\phi \tag{3.67}$$

These formulas are equivalent to those derived for plane stress in section 2.5.3, and the formulas for principal strains in the surface ϵ_1 and ϵ_2, and the angle ϕ_1 for the principle direction, follow directly from the corresponding formulas for plane stress (see Eqs. (2.159) and (2.160)):

$$\epsilon_{1,2} = \frac{\epsilon_x + \epsilon_y}{2} \pm \sqrt{\left(\frac{\epsilon_x - \epsilon_y}{2}\right)^2 + \left(\frac{\gamma_{xy}}{2}\right)^2} \tag{3.68}$$

$$\phi_1 = \arctan 2\frac{\epsilon_x - \epsilon_y}{\gamma_{xy}} \tag{3.69}$$

Note that the x_3-direction need not necessarily be a principal direction, and consequently the expressions in (3.68) are not necessarily principal strains for the general state of strain. However, this will be the case in many situations, e.g., for a thin-walled isotropic geometry.

Similarly, the expression for the maximum shear strain in the surface are equivalent to the shear stress expressions (Eq. (2.161)), and may be presented:

$$\gamma_{\max} = |\epsilon_1 - \epsilon_2| = 2\sqrt{\left(\frac{\epsilon_x - \epsilon_y}{2}\right)^2 + \left(\frac{\gamma_{xy}}{2}\right)^2} \tag{3.70}$$

Thus, from Eq. (3.70) we see that $\gamma_{\max}$ may be computed either form the principal strains or from the coordinate strains.

Example 3.3.1. *Strain rosettes.*

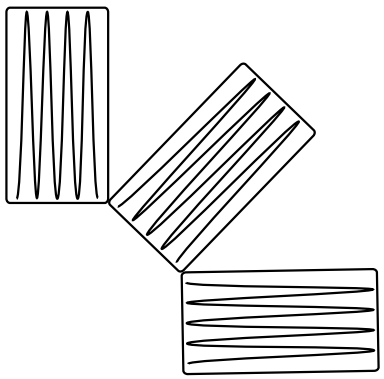

Figure 3.6: $0° - 45° - 90°$ rectangular strain rosette.

As previously stated in the beginning of section 3.3.4, measurements of strains or deformation are generally easier to perform, than measurements of stresses or forces. In this example we show the principal strains may be calculated based on measurements from a 0°-45°-90° rectangular strain rosette (Figure 3.6).

Note that if the material in question is well characterized, one may deduce the principal stresses from the principal strains.

From the previous expressions for small strains in a surface (3.66) and (3.67) we have:

$$\epsilon_{45} \equiv \epsilon(\phi = 45^\circ) = \frac{\epsilon_x + \epsilon_y}{2} + \frac{1}{2}\,\gamma_{xy} \quad \Rightarrow \quad \gamma_{xy} = 2\epsilon_{45} - \epsilon_x - \epsilon_y \tag{3.71}$$

Note that (3.66) and (3.67) also yield $\epsilon_0 \equiv \epsilon(\phi = 0) = \epsilon_x$ and $\epsilon_{90} \equiv \epsilon(\phi = 90^\circ) = \epsilon_y$. With the expression for γ_{xy} at hand we may readily compute the principal strains by substitution into (3.68):

$$\epsilon_{1,2} = \frac{\epsilon_x + \epsilon_y}{2} \pm \sqrt{\frac{1}{2}\left(\epsilon_x^2 + \epsilon_y^2\right) + \epsilon_{45}\left(\epsilon_{45} - \epsilon_x - \epsilon_y\right)} \tag{3.72}$$

$$\phi_1 = \arctan \frac{2\,\epsilon_{45} - \epsilon_x - \epsilon_y}{2\left(\epsilon_1 - \epsilon_y\right)} \tag{3.73}$$

Thus, we see that the principal strains ϵ_1 and ϵ_2 are determined completely by the measurements of ϵ_{45}, ϵ_x, ϵ_y.

3.4 Strain rates and rates of rotation

Eulerian coordinates and the current configuration K are commonly used to represent mathematically the motion and deformation of fluids, and sometimes solids with fluid like behavior.

The particles are in such a scenario denoted by the position vector $\mathbf{r}$ in K, rather than the original position $\mathbf{r}_0$ or X. We then consider a particle P at location $\mathbf{r}$ at time t, with the velocity $\mathbf{v}(\mathbf{r}, t)$. During a short time increment dt the particle P is subjected to the displacement $d\mathbf{u} = \mathbf{v}dt$, and associated small deformations given by the displacement tensor $d\mathbf{H}$:

$$dH_{ik} = \frac{\partial v_i}{\partial x_k}\,dt \equiv v_{i,k}\,dt \tag{3.74}$$

and accordingly a small strain tensor $d\mathbf{E}$ (compare with Eq. (3.48) for small displacements) and a rotation tensor for small deformations $d\tilde{\mathbf{R}}$:

$$d\mathbf{E} = \frac{1}{2}\left(d\mathbf{H} + d\mathbf{H}^T\right), \qquad d\tilde{\mathbf{R}} = \frac{1}{2}\left(d\mathbf{H} - d\mathbf{H}^T\right) \tag{3.75}$$

As the velocity has entered the expressions in Eq. (3.74) and (3.75), three new tensors are defined as a consequence: the *velocity gradient tensor* $\mathbf{L}$, the symmetric *rate of deformation tensor* $\mathbf{D}$, and the antisymmetric *rate of rotation tensor* $\mathbf{W}$:

$$\mathbf{L} = \frac{\partial \mathbf{v}}{\partial \mathbf{r}} \qquad \Leftrightarrow L_{ik} = v_{i,k} \tag{3.76}$$

$$\mathbf{D} = \frac{1}{2}\left(\mathbf{L} + \mathbf{L}^T\right) \qquad \Leftrightarrow D_{ik} = \frac{1}{2}\left(v_{i,k} + v_{k,i}\right) \tag{3.77}$$

$$\mathbf{W} = \frac{1}{2}\left(\mathbf{L} - \mathbf{L}^T\right) \qquad \Leftrightarrow W_{ik} = \frac{1}{2}\left(v_{i,k} - v_{k,i}\right) \tag{3.78}$$

The new definitions lead to:

$$d\mathbf{H} = \mathbf{L}dt, \qquad d\mathbf{E} = \mathbf{D}dt, \qquad d\tilde{\mathbf{R}} = \mathbf{W}dt, \qquad \dot{\mathbf{E}} = \mathbf{D}, \qquad \dot{\tilde{\mathbf{R}}} = \mathbf{W} \tag{3.79}$$

Note that $\dot{\mathbf{E}}$ is the material derivative of the small strain tensor from Eq. (3.48) for small deformations. In the general case relation between the material derivative om the general Green strain tensor $\mathbf{E}$ as defined by Eq. (3.23) and the rate of deformation tensor $\mathbf{D}$ is more complex.

The change of length of a material line per unit length and per unit time is denoted the *rate of longitudinal strain* or for short *rate of strain* . By arguing in the same manner as in section 3.3.1, it follows that the rate of strain in the direction $\mathbf{n}$ is:

$$\dot{\epsilon} = \mathbf{n} \cdot \mathbf{D} \cdot \mathbf{n} \tag{3.80}$$

In the coordinate directions $\mathbf{e}_i$, we get the *coordinate rates of strain* :

$$\dot{\epsilon}_{ii} = D_{ii} = v_{i,i}, \qquad *nosummation* \tag{3.81}$$

and similarly the *rate of shear strain* or the *shear rate* with respect to two orthogonal lines $\mathbf{n}$ and $\bar{\mathbf{n}}$:

$$\dot{\gamma} = 2\bar{\mathbf{n}} \cdot \mathbf{D} \cdot \mathbf{n} \tag{3.82}$$

whereas the *coordinate shear rate* for the direction $\mathbf{e}_1$ and $\mathbf{e}_2$ are given by:

$$\dot{\gamma}_{21} = 2D_{21} = v_{2,1} + v_{1,2} \tag{3.83}$$

Finally, based on Eq. (3.50) one may obtain the expression for the *rate of volumetric strain*:

$$\dot{\epsilon}_v = D_{kk} = tr\mathbf{D} = div\mathbf{v} = v_{k,k} \tag{3.84}$$

and consequently, the divergence of the velocity field $\mathbf{v}(\mathbf{r}, t)$, represents the rate of change of the volume per unit volume for the particle in question.

The antisymmetric rate of rotation tensor $\mathbf{W}$ has only three distinct elements:

$$W = \begin{bmatrix} 0 & -w_3 & w_2 \\ w_3 & 0 & -w_1 \\ -w_2 & w_1 & 0 \end{bmatrix} \tag{3.85}$$

and may therefore conveniently be represented by its dual *angular velocity vector*

p.98 [17,]:

$$\mathbf{w} = -\frac{1}{2}\mathbf{P} : \mathbf{W} = \frac{1}{2}\text{rot}\mathbf{v} \Leftrightarrow w_i = \frac{1}{2}e_{ijk}W_{kj} = \frac{1}{2}e_{ijk}v_{k,j} \tag{3.86}$$

or with less complexity:

$$w_1 = W_{32}, \qquad w_2 = W_{13}, \qquad w_3 = W_{21} \tag{3.87}$$

The concept *vorticity* is normally introduced in fluid dynamics as:

$$\mathbf{c} \equiv \nabla \times \mathbf{v} = 2\mathbf{w} \tag{3.88}$$

and will discussed further in section 5.1.1. Further, one may show (p. 153 [17,]):

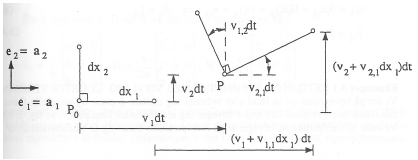

Figure 3.7: Rotation about an axis parallel to the x_3-direction

The rate of rotation tensor $\mathbf{W}$ represents the instantaneous angular velocity of the three orthogonal material line elements that are oriented in the principal directions of the rate of deformations tensor $\mathbf{D}$.

To illustrate this, the coordinate system of Figure 3.7 is aligned with axes parallel to the principal directions $\mathbf{a}_i$ of the rate of strain tensor $\mathbf{D}$, which therefore as the components:

$$D_{ik} = \dot{\epsilon}\,\delta_{ik} \tag{3.89}$$

As consequence of this alignment $D_{12} = v_{1,2} + v_{2,1} = 0$ and thus $v_{1,2} = -v_{2,1}$, and finally from Eqs. (3.86), (3.86), and (3.77) and (3.78) we get:

$$w_3 = W_{21} = v_{2,1} \tag{3.90}$$

From Figure 3.7, $w_3 dt = v_{2,1} dt$, is seen to be the angle of rotation about an axis parallel to the x_3-axis on a material line element in the time interval dt. The quantity w_3 represents the angular velocity of the line element about the x_3-axis.

Example 3.4.1. *Simple shear flow. Rectilinear rotational flow.*

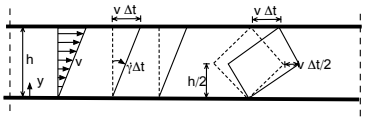

Figure 3.8: Simple shear flow with curl.

Consider fully developed fluid flow between two parallel planes, of which the lower plane is at rest, whereas the upper plane is moving with a constant velocity v parallel to the planes (see Figure 3.8). Assume further that the fluid particles move in straight parallel lines, and that the velocity field may be presented:

$$v_x = \frac{v}{h}\,y, \qquad v_y = v_z = 0 \tag{3.91}$$

Thus, the velocity field satisfy the *no slip* boundary conditions, which is used frequently in fluid dynamics. Intuitively, there might not be much in such a flow regime, normally called *simple shear flow*, which allude to concepts such as rotation and vorticity. However, investigation of Eq. (3.91), reveal that one component of the rate of deformation tensor $\mathbf{D}$ is different from zero, a fact which yield a nonzero shear rate (see Eq. (3.83)):

$$\dot{\gamma}_{xy} = 2D_{xy} = \frac{v}{h}, \qquad W_{xy} = \frac{v}{2h} \tag{3.92}$$

and then from Eq. (3.87) we get:

$$w_z \equiv \omega_z = -\frac{v}{2h} \tag{3.93}$$

In Figure 3.8, the deformation from time t to time $t + \Delta t$ of two different fluid elements is illustrated. Fluid element 1 has been deformed with the shear rate $\dot{\gamma}_{xy}$. Fluid element 2, was oriented with edges parallel to the principal directions of the rate of deformation tensor $\mathbf{D}$. Fluid element 2, does not reveal the shear rates so clearly but rather show rotation with angular velocity w_z. Note that the $\epsilon_v = \text{div}\mathbf{v} = 0$, and therefor the flow is *isochoric* or volume persevering. The matrices for the velocity gradient tensor $\mathbf{L}$, the rate of deformation tensor $\mathbf{D}$, and the rate of rotation tensor $\mathbf{W}$ are for this simple shear flow:

$$\mathbf{L} = \frac{v}{h}\begin{bmatrix} 0 & 1 & 0 \\ 0 & 0 & 0 \\ 0 & 0 & 0 \end{bmatrix}, \quad \mathbf{D} = \frac{v}{2h}\begin{bmatrix} 0 & 1 & 0 \\ 1 & 0 & 0 \\ 0 & 0 & 0 \end{bmatrix}, \quad \mathbf{W} = \frac{v}{2h}\begin{bmatrix} 0 & 1 & 0 \\ -1 & 0 & 0 \\ 0 & 0 & 0 \end{bmatrix} \tag{3.94}$$

Simple shear flow is also commonly called *Couette flow*, after M. Couette (1890). This flow regime may be found in many applications e.g., in the flow between two cylinders with large diameter/gap ratio, of which the outer cylinder is rotating, whereas the inner cylinder is at rest.

Chapter 4

Elasticity

A material is (Cauchy) elastic if the stresses are functions of the deformations and position only:

$$\boldsymbol{T} = \boldsymbol{T}(\boldsymbol{E}, \boldsymbol{r}) \tag{4.1}$$

An equation, like (4.1), which expresses the relation between the stresses and strains for a material is normally referred to as a *constitutive* equation or a *material* equation. The relation in equation (4.1) may be linear or nonlinear, and is expressed by some material parameters which defines a given material. The constitutive equation is referred to as homogeneous if the elastic properties are the same *in every particle* or position. For a homogeneous material there is no explicit dependency of the position and equation (4.1) reduces to:

$$\boldsymbol{T} = \boldsymbol{T}(\boldsymbol{E}) \tag{4.2}$$

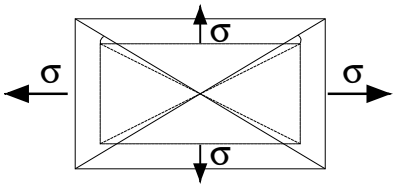

Figure 4.1: Coaxial stresses and strains.

If the material properties are the same in every direction through a particle, the material is *isotropic*. For an isotropic material the principal directions for the stress and strain tensors are co-axial, i.e., the principal stresses and principal strains have the same orientation. To see this, consider a box element

with edges oriented parallel to the principal stress directions. The box element is illustrated in figure 4.1, in both an undeformed state (corresponding to the unloaded situation) and a deformed state. The deformations are highly exaggerated for illustrative purposes. The diagonal planes P_1 and P_2 will be equally stretched due to the symmetry in the stresses and the isotropic elastic properties. Consequently, the normal angels betwen the edges of the box element will be maintained after deformation,and concequently the principal directions for the stresses and strains will be co-axial.

Finally, the constitutive model is referred to as *linear elastic* if the stress is a linear function of strain. For the linear case the six elements of the stress tensor T_{ij}, are linear functions of the six elements of the strain tensor E_{ij}. For a fully anisotropic material, this corresponds to $6 \times 6 = 36$ material parameters, which normally are denoted elasticities or stiffnesses. These elasticities are constants for a homogenous material.

4.0.1 Fundamental properties of elastic materials

In this section some prominent features of elastic materials (meaning materials which stress-strain relation is represented by equation (4.1))are noted.

The first feature of *reversibility* follows due to the assumption that the stress is a function of the strain only, and not of the rate of strain (or stress), the stress (or strain) level, or the stress (or strain) history. Many materials (in particular biomaterials) exhibits such effects, and may consequently not be denoted elastic. Reversibility means that strain curves (which may be both linear and nonlinear as seen in figures 4.2 and 4.3) are identical during loading and unloading, and independent of stress/strain levels and history.

An elastic material is also non-dissipative, as no net work is performed from an external actor for a closed loading-unloading loop (see figures 4.2 and 4.3), and thus the deformation energy may be recovered upon unloading.

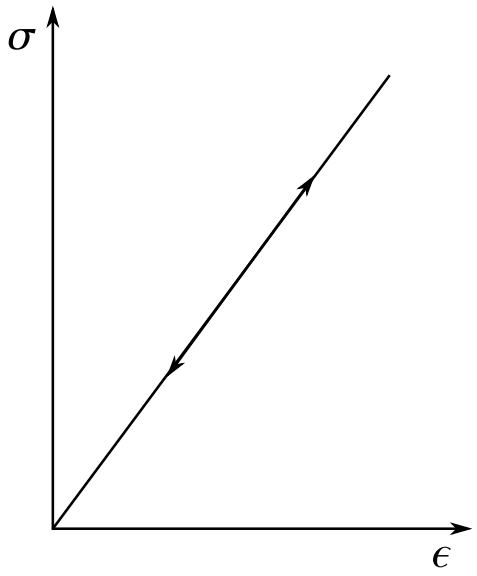

Figure 4.2: Uniaxial behaviour of linear elastic materials.

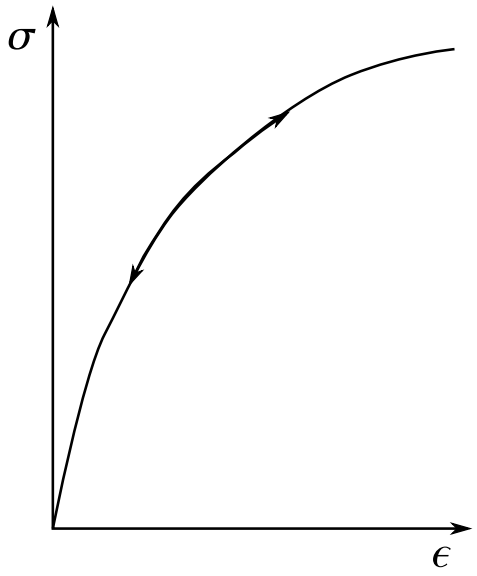

Figure 4.3: Uniaxial behaviour of linear elastic materials elasticity

4.1 Isotropic and linearly elastic materials

One may show [17] that an isotropic, linearly elastic material is completely characterized by only two independent material parameters or elasticities. Such a material is normally referred to as a *Hookean material* or a *Hookean*

solid. In the following section we will derive the constitutive equations for a Hookean solid.

4.1.1 The Hookean solid

To derive the constitutive equations for a Hookean solid, consider a test beam exposed to a load of uniaxial stress, i.e., $\sigma_1 \neq 0, \sigma_2 = \sigma_3 = 0$. For this load the strains may be measured as:

$$\epsilon_1 = \frac{\sigma_1}{\eta}, \quad \epsilon_2 = \epsilon_3 = -\nu\frac{\sigma_1}{\eta} \tag{4.3}$$

where η is the modulus of elasticity (commonly also referred to as the E-modulus) and ν the Poisson's ratio. Now as the stress-strain relation is assumed to be linear and isotropic, the solutions of equation (4.3) may be superimposed. Consequently, a generic state of stress with three principal stresses different from zero will result in the following principal strains:

$$\epsilon_1 = \frac{\sigma_1}{\eta} - \frac{\nu}{\eta}(\sigma_2 + \sigma_3) = \frac{1+\nu}{\eta}\sigma_1 - \frac{\nu}{\eta}(\sigma_1 + \sigma_2 + \sigma_3) \qquad \text{etc for } \epsilon_2 \text{ and } \epsilon_3 \tag{4.4}$$

the expression in equation (4.4) may be generalized to:

$$\epsilon_i = \frac{1+\nu}{\eta}\sigma_i - \frac{\nu}{\eta}(\sigma_1 + \sigma_2 + \sigma_3) = \frac{1+\nu}{\eta}\sigma_i - \frac{\nu}{\eta}\mathrm{tr}\boldsymbol{T} \tag{4.5}$$

where the we have introduced the invariant $\mathrm{tr}\boldsymbol{T} = T_{kk} = \sigma_1 + \sigma_2 + \sigma_3$ of the stress tensor. Further, in an Ox-system with base vectors parallel to the principal directions, equation (4.5) has the matrix representation :

$$\epsilon_i\,\delta_{ij} = \frac{1+\nu}{\eta}\sigma_i\,\delta_{ij} - \frac{\nu}{\eta}\mathrm{tr}\boldsymbol{T}\,\delta_{ij} \tag{4.6}$$

We may interpret equation (4.6) as a matrix representation of a tensor equation in the Ox-system with base vectors parallel to the principal directions. For an an arbitrary Ox-system, the tensor equation has the matrix representation:

$$E_{ij} = \frac{1+\nu}{\eta}T_{ij} - \frac{\nu}{\eta}T_{kk}\,\delta_{ij} \tag{4.7}$$

The coordinate invariant tensor equation may be written:

$$\boldsymbol{E} = \frac{1+\nu}{\eta}\boldsymbol{T} - \frac{\nu}{\eta}\mathrm{tr}\boldsymbol{T}\,\boldsymbol{1} \tag{4.8}$$

The equations (4.7) and (4.8) are normally denoted the generalized Hooke's law and represent the constitutive equations for a Hookean material, i.e., an isotropic, linearly elastic material. Equivalent representations of the generalized Hooke's law, may be formulated with stress on the left hand side of the equations:

$$T_{ij} = \frac{\eta}{1+\nu}\left(E_{ij} + \frac{\nu}{1-2\nu}\,E_{kk}\,\delta_{ij}\right) \tag{4.9}$$

$$\boldsymbol{T} = \frac{\eta}{1+\nu}\left(\boldsymbol{E} + \frac{\nu}{1-2\nu}\,E_{kk}\,\mathbf{1}\right) \tag{4.10}$$

Keep in mind that a Hookean material is completely characterized by two material parameters (η and ν). Observe from equations (4.7) and (4.9) and (4.10) that normal stresses (*i.e.* T_{ii} with no summation) only result in longitudinal strains (*i.e.* E_{ii} with no summation), and vice versa. Similarly, shear stresses (T_{ij}) only produce shear strains (E_{ij}). These relations are not valid in general for anisotropic materials.

For shear stresses and shear strains (i.e., when $i \neq j$), the last term of equation (4.9) drops out and one may write:

$$T_{ij} = 2\mu E_{ij} = \mu\gamma_{ij}, \quad i \neq j \tag{4.11}$$

where we have introduced the *shear modulus* as:

$$\mu = \frac{\eta}{2(1+\nu)} \tag{4.12}$$

The shear modulus may thus be thought of as an E-modulus for shear stress/strain conditions, such as torsion of a cylinder.

A relation between the volumetric ε_v strain and the stresses may be found by computing the trace of equation (4.7):

$$\varepsilon_v = E_{ii} = \frac{1+\nu}{\eta}\,T_{ii} - \frac{\nu}{\eta}\,T_{kk}\,\delta_{ii} = \frac{1-2\nu}{\eta}T_{ii} \tag{4.13}$$

By introducing the *bulk modulus* κ:

$$\kappa = \frac{\eta}{3\,(1-2\nu)} \tag{4.14}$$

and the mean stress as:

$$\sigma^0 = \frac{1}{3}T_{ii} \tag{4.15}$$

equation (4.13) may be presented in the more compact form:

$$\sigma^0 = \frac{1}{\kappa}\varepsilon_v \tag{4.16}$$

Fluids are generally considered to be linearly elastic materials when sound wave propagation is to be analyzed. The bulk modulus for water is $\kappa = 2.1\,GPa$, for mercury $\kappa = 27\,GPa$, and for alcohol $\kappa = 0.91\,GPa$. From equation (4.14), we see that $\nu > 1/2$, would give unphysical values for the bulk modulus $\kappa < 0$, as in such a situation the volume of a material would increase when being exposed to an isotropic pressure. Further, the Poissons ratio is expected to be positive $\nu \leq 0$, as $\nu < 0$ corresponds to a material which expand in the direction perpendiualr to the stress direction, in the case of uniaxial stretch. Thus, we expect:

$$0 \leq \nu \leq 0.5 \tag{4.17}$$

Among real materials, rubber is considered to be almost incompressible with $\nu = 0.49$, whereas cork represents the other extreme with $\nu \approx 0$. This property for cork is indeed a desired property whenever one is trying to cork a bottle.

A simple form for Hooke's law may be obtained by splitting the stress and strain tensors in isotropic and deviatoric parts:

$$T_{ij} = T^0_{ij} + T'_{ij} \quad \text{and} \quad E_{ij} = E^0_{ij} + E'_{ij} \tag{4.18}$$

where 0-superscripts denote the isotropic tensors:

$$T^0_{ij} = \sigma^0\,\delta_{ij} \quad \text{and} \quad E^0_{ij} = \frac{1}{3}\varepsilon_v\,\delta_{ij} = \frac{1}{3}E_{kk}\,\delta_{ij} \tag{4.19}$$

Substitution of equation (4.19) into equation (4.7) or (4.9) the yields the simple forms for isotropic or deviatoric loads repsectively:

$$T^0_{ij} = 3\kappa E^0_{ij} \quad \text{and} \quad T'_{ij} = 2\mu E'_{ij} \tag{4.20}$$

By summation of the two equations in (4.20) we get:

$$T_{ij} = T'_{ij} + T^0_{ij} = 2\mu E'_{ij} + 3\kappa E^0_{ij} \tag{4.21}$$

$$= 2\mu(E_{ij} - E^0_{ij}) + \kappa E_{kk}\delta_{ij} \tag{4.22}$$

where we use the trace of the strain tensor E_{kk} in equation (4.19) to eliminate expressions with the isotropic strain tensor E^0. A final elimination of E^0 yields yet another formulation of a Hookean material:

$$T_{ij} = 2\mu E_{ij} + \left(\kappa - \frac{2\mu}{3}\right) E_{kk}\delta_{ij} \tag{4.23}$$

For an incompressible Hookean material the volume does not change (*i.e.* $\varepsilon_v = 0$), and the mean stress $\sigma^0 = T_{kk}/3$ can not be determined from Hooke's law. For such materials the constitutive equation (4.9) is normally reformulated as:

$$\boldsymbol{T} = -p\,\mathbf{1} + 2\mu\,\boldsymbol{E} \tag{4.24}$$

which on component form has the representation:

$$T_{ij} = -p\,\delta_{ij} + 2\mu E_{ij} \tag{4.25}$$

where $p = p(\boldsymbol{r}, t)$ is an unknown pressure (or positive normal stress) which can only be determined from the equations of motion and the boundary conditions.

4.1.2 Navier equations

In this section we use the Cauchy equations (2.89) and the constitutive equations for a Hookean material (4.7), to derive the governing Navier equations for a Hookean material.

For convenience we introduce the shear modulus:

$$\mu = \frac{\eta}{2(1+\nu)} \tag{4.26}$$

and multiply (4.7) with $\frac{2(1+\nu)}{\eta} = 1/\mu$, and differentiate with respect to x_k to obtain an expression for the divergence of the stress tensor:

$$\frac{1}{\mu} T_{ik,k} = u_{i,kk} + \underbrace{u_{k,ik}}_{=u_{k,ki}} + \frac{2\nu}{1-2\nu} \underbrace{u_{l,lk}\delta_{ik}}_{=u_{l,li}=u_{k,ki}} \tag{4.27}$$

$$= u_{i,kk} + \left(1 + \frac{2\nu}{1-2\nu}\right) u_{k,ki} \tag{4.28}$$

$$\frac{1}{\mu} T_{ik,k} = u_{i,kk} + \frac{1}{1-2\nu} u_{k,ki} \tag{4.29}$$

The expression for the divergence of the stress tensor (4.29) may the be substituted into Cauchy equations (2.89) to give the:

Navier equations:

$$u_{i,kk} + \frac{1}{1-2\nu} u_{k,ki} + \frac{\rho}{\mu}(b_i - \ddot{u}_i) = 0 \tag{4.30}$$

which constitute a system of partial differential equations which may be solved along with appropriate boundary conditions.

4.1.3 2D theory of elasticity

The general equations for Hookean materials have solutions only in a few special and simple cases. However, in many problems of practical interest we may introduce simplifications, either with respect to the state of stress or the state of strain, in such a way that useful solutions may be found analytically.

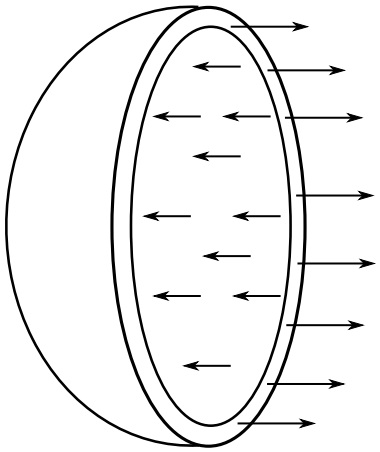

Figure 4.4: A thin walled spherical shell of steel.

Plane stress. For a plane stress assumption to be valid, we normally consider a thin structure of some kind such as a thin plate or a thin sphere (see figure 4.4) loaded by body forces $\boldsymbol{b}$ and contact forces $\boldsymbol{t}$ on the surface A of the structure such that:

$$b_\alpha = b_\alpha(x_1, x_2, t), \qquad b_3 = 0 \tag{4.31}$$

$$t_\alpha = t_\alpha(x_1, x_2, t), \qquad t_3 = 0 \tag{4.32}$$

In such a situation one may approximate the state of stress as a state of plane stress, which may be represented mathematically:

$$T_{i3} = 0 \qquad \text{and} \qquad T_{\alpha\beta} = T_{\alpha\beta}(x_1, x_2, t) \tag{4.33}$$

The validity of the plane stress assumption will normally rest on the condition that the wall thickness h of the structure is much smaller than the a characteristic dimension, such as the diameter, of the structure.

The govering equations for a thin walled structure in plane stress are Cauchy's equations of motion (see (2.89))[1]

$$\rho\ddot{\boldsymbol{u}} = \nabla \cdot \boldsymbol{T} + \rho\boldsymbol{b} \Leftrightarrow \rho\ddot{u}_\alpha = T_{\alpha\beta,\beta} + \rho b_\alpha \tag{4.34}$$

Note that we have used the second material derivative of the displacement for the acceleration, which in turn will be represented by the second partial derivative of **u** with respect to time, while assumping small deformations:

$$\ddot{u}_\alpha = \frac{\partial^2 u_\alpha}{\partial t^2} \tag{4.35}$$

Further, we assume that the material may be represented with Hooke's law for plane stress (see Exercise 1):

$$T_{\alpha\beta} = 2\mu\left(E_{\alpha\beta} + \frac{\nu}{1-\nu}E_{\rho\rho}\delta_{\alpha\beta}\right), \quad 2\mu = \frac{\eta}{1+\nu} \tag{4.36}$$

where the *shear modulus* μ has been introduced conventionally.

As for the generic Hookean law the plane stress version may be written with the strains on the right hand side:

$$E_{\alpha\beta} = \frac{1}{2\mu}\left(T_{\alpha\beta} - \frac{\nu}{1+\nu}T_{\rho\rho}\delta_{\alpha\beta}\right), \qquad E_{33} = -\frac{\nu}{\eta}T_{\rho\rho} \tag{4.37}$$

Note that the strain has three components even though the stress is planar, due to the conservation of mass.

For small displacements (see equation (3.48)) the Green strain tensor reduce to:

$$E_{\alpha\beta} = \frac{1}{2}\left(u_{\alpha,\beta} + u_{\beta,\alpha}\right) \tag{4.38}$$

which explicitly relates the strain tensor to displacements. Together, the equations (4.34), (4.36), and (4.38) constitute 8 equations (2+3+3), for what may be regarded as 8 unknown fuctions $T_{\alpha\beta}$ (3 components), $E_{\alpha\beta}$ (3 components), and u_α (2 components). Thus, these equations represent a

[1]Repeated Greek indices imples sum from 1 to 2.

closed system of partial differential equations. As there is a linear relation between stresses and strains (displacements), one may choose either stresses or displacements as the primary function when representing the resulting partial differential equations.

By substitution of the plane stress version of Hooke's law as given by equation (4.36), and equation (4.38), into the Cauchy equations (4.34) (see Exercise 1) we get a displacement version of the:

Navier equations for plane stress:

$$u_{\alpha,\beta\beta} + \frac{1+\nu}{1-\nu}\, u_{\beta,\beta\alpha} + \frac{\rho}{\mu}\,(b_\alpha - \ddot{u}_\alpha) = 0 \tag{4.39}$$

With these substitutions, both stresses and strains have been eliminated, while the displacements remain as the only two unknowns in the two equations of motion in (4.39).

To complete the solution to the problem, boundary conditions must be provided. Normally, one assume that contact forces, or stresses/tractions, are imposed on a part A_σ of the surface of the structure, while displacements are imposed on the remaining part $A_u = A - A_\sigma$, which may be represented mathematically:

$$t_\alpha = t^*_\alpha, \quad \text{on } A_\sigma \tag{4.40}$$

$$u_\alpha = u^*_\alpha, \quad \text{on } A_u \tag{4.41}$$

Having found the solution of the Navier equations (4.39), typically by means of some numerical method, for the imposed boundary conditions (4.40) and (4.41), one may compute the stresses for the constitutive relation in equation (4.36).

Example 4.1.1. *Spherical shell of steel.*

We consider a thin walled spherical shell of steel with diameter $d_0 = 2000$ mm (Figure 4.4) and wall thickness $t_0 = 5$ mm at zero transmural pressure. The sphere is then inflated with a transmural pressure of $p = 1.5$ MPa. We want to find the change in diameter and wall thickness due to the imposed load.

From the stress analysis in example 2.5.1 we get expressions for the wall stresses in the θ- and ϕ-directions, which are principal stress directions[2], from (2.164):

$$\sigma_\phi = \sigma_\theta = \sigma = \frac{1}{2}\frac{r}{t}p = \frac{1}{2\,(5\cdot 10^{-3})}\,1.5\cdot 10^6 = 150 \text{ MPa} \tag{4.42}$$

[2]Engineering notation is used as stresses are principal stresses.

The stress in the radial direction must be in the order of p, *i.e.* $\sigma_r \propto p \ll \sigma \Rightarrow \sigma_r \approx 0$. Steel is assumed to be a Hookean material with $\eta = 210$ GPa and $\nu = 0.3$ and strains resulting from the imposed stresses may either be calculated from Hooke's law in (4.7) or from the tailor made version of Hooke's law for plane stress in equation (4.37). In the azimuthal direction, we denote the coordinate strain by ε_θ and get from (4.7):

$$\begin{aligned}\varepsilon_\theta = E_{11} &= \frac{1+\nu}{\eta}\sigma_\theta - \frac{\nu}{\eta}(\sigma_\theta + \sigma_\phi) = \frac{1-\nu}{\eta}\,\sigma \\ &= \frac{1-0.3}{210\cdot 10^9}\cdot 150\cdot 10^6 = 0.5\cdot 10^{-3}\end{aligned} \tag{4.43}$$

From the Hooke's law for plane stress in equation (4.37) we get the same expression as in equation (4.43):

$$\varepsilon_\theta = \frac{1+\nu}{\eta}\left(\sigma_\theta - \frac{\nu}{1+\nu}(\sigma_\theta + \sigma_\phi)\right) = \frac{1-\nu}{\eta}\,\sigma \tag{4.44}$$

The azimuthal strain ε_θ is related with changes in the diameter in the following manner:

$$\varepsilon_\theta = \frac{\pi d - \pi d_0}{\pi d_0} = \frac{d-d_0}{d_0} = \frac{\Delta d}{d_0} \tag{4.45}$$

Thus, the change in diameter due to the imposed pressure load is:

$$\Delta d = \varepsilon_\theta\, d_0 = 0.5\cdot 10^{-3}\, 2000 = 1\,\text{mm} \tag{4.46}$$

The strain in the radial direction ε_r is also readily obtained from (4.7) or from the planar stress version in equation (4.37):

$$\begin{aligned}\varepsilon_r = E_{33} &= -\frac{\nu}{\eta}(\sigma_\theta + \sigma_\phi) = \frac{-2\nu}{\eta}\,\sigma \\ &= \frac{-0.6}{210\cdot 10^9}\cdot 150\cdot 10^6 = -\frac{3}{7}\cdot 10^{-3}\end{aligned} \tag{4.47}$$

and is related with changes in wall thickness:

$$\varepsilon_r = \frac{t-t_0}{t_0} = \frac{\Delta t}{t_0} \tag{4.48}$$

Consequently, the change in wall thickness is negative and given by:

$$\Delta t = \varepsilon_r t_0 = -\frac{3}{7}\cdot 10^{-3} \approx -2.1\cdot 10^{-3}\text{mm} \tag{4.49}$$

4.1.4 Plane displacement

For plane displacements we assume that the displacement vector have only to components which in tur are functions of the two coordinate direction in which the displacements are taking place :

$$u_\alpha = u_\alpha(x_1, x_2, t), \quad u_3 = 0 \tag{4.50}$$

Consequently, we have $E_{i3} = 1/2(u_{i,3} + u_{3,i}) = 0$ and the strain tensor reduces to:

$$E_{\alpha\beta} = \frac{1}{2}\left(u_{\alpha,\beta} + u_{\beta,\alpha}\right), \quad E_{i3} = 0 \tag{4.51}$$

One may show that in the case of plane displacements given by (4.51) the generic Navier equations (4.30) reduce to:

$$u_{\alpha,\beta\beta} + \frac{1}{1-2\mu}\, u_{\beta,\alpha\beta} + \frac{\rho}{\mu}(b_\alpha - \ddot{u}_\alpha) = 0 \tag{4.52}$$

i.e., the only diffenrences from equations (4.30) are that the sums are trucanted to constitute only two elements.

Further, we assume that the displacements are axisymmetric, which in mathematical terms means:

$$u_r = u_r(r), \quad u_\theta = u_\theta(r) \tag{4.53}$$

and consequently:

$$u_{\beta,\beta\alpha} = u_{\alpha,\beta\beta} = \begin{cases} 0 & \alpha = \theta \\ \dfrac{\partial^2 u_r}{\partial r^2} & \alpha = r \end{cases} \tag{4.54}$$

Substitution of (4.54) into (4.52) yields:

$$\frac{2\,(1-\mu)}{1-2\mu}\, u_{\beta,\beta\alpha} + \frac{\rho}{\mu}(b_\alpha - \ddot{u}_\alpha) = 0 \tag{4.55}$$

For longitudinal strains and axisymmetric displacements:

$$\begin{aligned} \epsilon_r &= \frac{du}{dr}, \qquad \epsilon_\theta = \frac{l - l_0}{l_0} = \frac{2\pi(r+u) - 2\pi r}{2\pi r} = \frac{u}{r} \\ \epsilon_A &= \epsilon_r + \epsilon_\theta = \frac{du}{dr} + \frac{u}{r} = \frac{1}{r}\frac{d(ur)}{dr} \end{aligned} \tag{4.56}$$

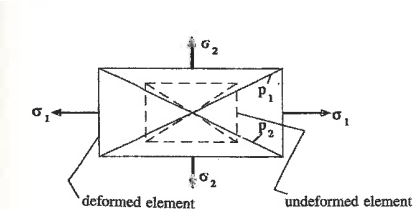

Figure 4.5: Radial and cicumferential strains for plane displacement.

By differentiation of (4.56) we get:

$$\epsilon_{A,\alpha} = u_{\beta,\beta\alpha} \Rightarrow \epsilon_{A,r} = \frac{d}{dr}\left(\frac{1}{r}\frac{d(ur)}{dr}\right) \tag{4.57}$$

If we neglect body forces and intertia, we get by substitution of (4.57) into (4.55):

$$\frac{d}{dr}\left(\frac{1}{r}\frac{d(ur)}{dr}\right) = 0 \tag{4.58}$$

Thick walled cylinder with internal and external pressures

$$u(r) = \frac{1}{2\eta}\frac{a}{1-(a/b)^2}\left[\left(\frac{a}{r} + (1-2\nu)\left(\frac{a}{b}\right)^2\frac{r}{a}\right)p - \left(\frac{a}{r} + (1-2\nu)\frac{r}{a}\right)q\right] \tag{4.59}$$

$$\sigma_r(r) = \frac{2\mu}{1-\nu}\left(\frac{du}{dr} + \nu\frac{u}{r}\right) \tag{4.60}$$

$$\sigma_\theta(r) = \frac{2\mu}{1-\nu}\left(\frac{u}{r} + \nu\frac{du}{dr}\right) \tag{4.61}$$

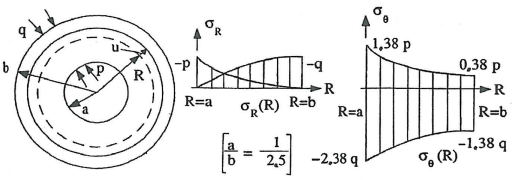

Figure 4.6: Solutions for thick walled cylinder with internal and external pressures

Example 4.1.2. *Plane displacements for a thick walled cylinder.*

The assumption of plane displacements may be expressed mathematically as:

$$u_\alpha = u_\alpha(x_1, x_2, t), \quad u_3 = 0 \tag{4.62}$$

The Green deformation tensor for small deformations (see Equation (3.48)) reduce to:

$$E_{\alpha\,\beta} = \frac{1}{2}\left(u_{\alpha,\beta} + u_{\beta,\alpha}\right), \quad E_{i3} = 0 \tag{4.63}$$

The components of the stress tensor for a Hookean material Equation (4.9) corresponding to the directions of non-zero displacements may the be represented:

based on Equation (4.63) and by using the shear modulus in Equation (4.26).

4.2 Mechanical energy balance

For a system of particles and for rigid bodies the work W done by external forces on the system is equal to the change in the kinetic energy ΔK of the system:

$$W = \Delta K \qquad \text{for rigid bodies} \tag{4.64}$$

The *rigid body work-energy equation* (4.64) is a special result of the more generic mechanical energy balance to be derived in the following. The special rigid body form follow as there are no *internal* deformations for a rigid body exposed to external forces.

Consider a body of volume V and surface area A, which is subjected to body forces $\mathbf{b}$ and surface forces $\mathbf{t}$. These forces exert work on the body, which per unit time is expressed by:

$$P = \int_V \boldsymbol{b} \cdot \boldsymbol{v}\, \rho\, dV + \int_A \boldsymbol{t} \cdot \boldsymbol{v}\, dA \tag{4.65}$$

Further, we define the *kinetic energy* for the body in a natural manner as:

$$K = \int_V \frac{1}{2}\rho \mathbf{v} \cdot \mathbf{v}\, dV \tag{4.66}$$

and from equation (2.34) we get that the rate of change of the kinetic energy for the body is given by:

$$\dot{K} = \int_V \dot{\boldsymbol{v}} \cdot \boldsymbol{v} \rho\, dV \tag{4.67}$$

Now, from the integral form of Cauchy's stress theorem (see equation (2.65) one may express:

$$\int_A \mathbf{v}\cdot\mathbf{t}\,dA = \int_A \mathbf{v}\cdot\mathbf{T}\cdot\mathbf{n}\,dA = \int_A (\mathbf{v}\cdot\mathbf{T})\cdot\mathbf{n}\,dA = \int_V \mathrm{div}(\mathbf{v}\cdot\mathbf{T})\,dV \quad (4.68)$$

The latter expression of equation (4.68) need some consideration:

$$\mathrm{div}(\mathbf{v}\cdot\mathbf{T}) = (v_i T_{ik})_{,k} = v_{i,k}T_{ik} + v_i T_{ik,k} = T_{ik}D_{ik} + v_i T_{ik,k} \quad (4.69)$$

where we have introduced the strain rate tensor $\mathbf{D}$ as defined in Eqs. (3.77) and (3.78). The expressions in equation (4.69) have the coordinate invariant representation:

$$\mathrm{div}(\mathbf{v}\cdot\mathbf{T}) = \mathbf{T}:\mathbf{D} + \mathbf{v}\cdot\mathrm{div}\mathbf{T} = \mathbf{T}:\mathbf{D} + \mathbf{v}\cdot(\rho\dot{\mathbf{v}} - \rho\mathbf{b}) \quad (4.70)$$

where the latter equality follow from Cauchy's equations of motion (2.89). Further, if we define the *stress power* P_d as:

$$P_d = \int_V \mathbf{T}:\mathbf{D}\,dV \quad (4.71)$$

the equations (4.71), (4.70), and (4.68) may be substutited into equation (4.65) to give:

The mechanical energy balance equation:

$$P = \dot{K} + P_d \quad (4.72)$$

One may show (see e.g. p.185 [17]) that the stress power P_d represents the deformation work done in the body per unit time. The stress power results in a change in the internal energy, which in part may be recovarable elastic energy, and partly may be represented by an increase in the temperature of the body, and in heat conducted to the surroundings of the body.

4.3 Hyperelastic materials and strain energy

The deformation work per unit time or stress power for short, is given in in the previous section by equation (4.71), where T_{ij} and D_{ij}, represent the

stress tensor and is the rate of deformation tensor, respectively. The stress power per unit volume ω, may then naturally be introduced as:

$$\omega = T_{ij} D_{ij} \tag{4.73}$$

which readily allows for the introduction of the stress work per unit volume W as:

$$w = \int_{t_0}^{t} \omega \, dt \tag{4.74}$$

For small deformations we have the relation:

$$\boldsymbol{D} = \dot{\boldsymbol{E}} \tag{4.75}$$

and then the stress work per unit volume may be computed as:

$$w = \int_{t_0}^{t} \omega \, dt = \int_{t_0}^{t} T_{ij} \, \dot{E}_{ij} \, dt = \int_{\boldsymbol{E}_0}^{\boldsymbol{E}} T_{ij} \, dE_{ij} \tag{4.76}$$

i.e., the relation in equation (4.75) allows for a variable substitution on the computation of the stress work per unit volume such that the integral in equation (4.76) may be computed as an integral between the tqo strain states $\mathbf{E}_0$ and $\mathbf{E}$.

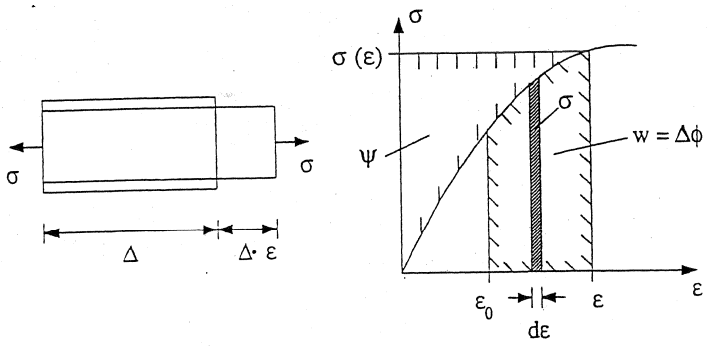

Figure 4.7: Stress work per unit volume w and elastic energy ϕ for a uniaxial stress situation.

Now, to simplify, consider a case of uniaxial stress (see figure 4.7), where the principal stress σ is co-axial with the principal strain ε, and they are both functions of time. The stress power per unit volume is the given as $\omega = \sigma \cdot \dot{\varepsilon}$. The stress work per unit volume can then be computed as:

$$w = \int_{t_0}^{t} \omega \, dt = \int_{t_0}^{t} \sigma \dot{\epsilon} \, dt = \int_{\epsilon_0}^{\epsilon} \sigma \, d\epsilon \tag{4.77}$$

A material is classified as *hyperelastic* if ω and w may derived from a scalar valued potential $\phi(\boldsymbol{E})$ such that:

$$\omega = \dot{\phi} = \frac{\partial \phi}{\partial E_{ij}} \dot{E_{ij}} \qquad \text{and} \qquad \phi = \phi(\boldsymbol{E}) \tag{4.78}$$

Mathematically, this has the beneficial consequense that the stress work per unit volume for a hyperealstic material may be computed simply as:

$$w = \int_{t_0}^{t} \omega \, dt = \phi|_{t_0}^{t} = \phi(\boldsymbol{E}) - \phi(\boldsymbol{E}_0) \tag{4.79}$$

i.e., as the difference of the potential ϕ evaluated at the current and reference strain state. The potential $\phi(\boldsymbol{E})$ is commonly denoted the *elastic energy* or *strain energy* per unit volume.

Now, from the definition of the stress power per unit volume given in equation (4.73) and from the definition of the hyperelastic potential in equation (4.78) we have to expressions for the stress power per unit volme:

$$\omega = T_{ij} \dot{E}_{ij} = \frac{\partial \phi}{\partial E_{ij}} \dot{E}_{ij} \tag{4.80}$$

As the hyperelastic potential per definition is a function of strain only (i.e., $\phi(\boldsymbol{E})$) and not the strain rate $\dot{E}_{ij}$, we get:

$$T_{ij} = \frac{\partial \phi}{\partial E_{ij}} \tag{4.81}$$

Therefore, is the hyperelastic potential ϕ is is given for a material, one may compute all the stress components from equation (4.81) for given strains E_{ij}. From equations (4.78) and (4.81) we deduce that $\boldsymbol{T} = \boldsymbol{T}(\boldsymbol{E})$, and according to equation (4.1), the assumption of a hyperelastic material implies that the material is elastic too (i.e., hyperelasticity $\Rightarrow$ elasticity). Note that the converse is not necessarily true.

4.3.1 Hyperelasticity for large derformations

For large deformations it is customary to introduce the elastic energy (or hyperelastic potential) per *mass unit* $\psi(\boldsymbol{C})$ rather than per volume unit $\phi(\boldsymbol{E})$, and further to express the energy as a function of the Green's deformations tensor $\boldsymbol{C}$ rather than the Green strain tensor (see previous section 4.3 for small deformations) . The stress power $\omega \, dV$ for a differential volume dV may be derived from the potential $\psi \, \rho \, dV$ in the following manner:

$$\omega \, dV = \frac{d}{dt} \left(\psi \rho \, dV \right) = \dot{\psi} \, \rho dV \tag{4.82}$$

Consequently, the stress power per unit volume an the elastic energy per unit mass are related by:

$$\omega = \rho\dot{\psi} = \rho\frac{\partial\psi}{\partial C_{ij}}\dot{C}_{ij} \qquad \text{and} \qquad \psi = \psi(\boldsymbol{C}) \tag{4.83}$$

In order to relate the potential to the stress as given in equation (4.73), we need to establish a relation between $\dot{\boldsymbol{C}}$ and $\boldsymbol{D}$. From the definition of Green's deformation tensor in equation (3.15) we get:

$$\dot{\boldsymbol{C}} = \dot{\boldsymbol{F}}^T \cdot \boldsymbol{F} + \boldsymbol{F}^T \cdot \dot{\boldsymbol{F}} \tag{4.84}$$

Further, from equations (3.11), (3.77), and (3.78), the rate of deformation gradient tensor, the velocity gradient tensor, and the strain rate tensor are given by:

$$F_{ik} = \frac{\partial x_i}{\partial X_k} \quad \text{and} \quad L_{il} = v_{i,l} \quad \text{and} \quad D_{ik} = \frac{1}{2}(v_{i,k} + v_{k,i}) \tag{4.85}$$

Now, the expression for $\dot{\boldsymbol{F}}$ may be computed from equation (4.85) as:

$$\dot{F_{ik}} = \frac{\partial^2 x_i}{\partial t \partial X_k} = \frac{\partial}{\partial X_k}\left(\frac{\partial x_i}{\partial t}\right) = \frac{\partial}{\partial X_k} v_i = \frac{\partial v_i}{\partial x_l}\frac{\partial x_l}{\partial X_k}$$

which yields in tensor notation has the representtion:

$$\dot{\boldsymbol{F}} = \boldsymbol{L} \cdot \boldsymbol{F} \quad \text{and} \quad \dot{\boldsymbol{F}^T} = \boldsymbol{F}^T \cdot \boldsymbol{L}^T \tag{4.86}$$

And finally, from equation (4.86), (4.85), and (4.84) we get the wanted relation $\dot{\boldsymbol{C}}$ and $\boldsymbol{D}$:

$$\begin{aligned} \dot{\boldsymbol{C}} &= \dot{\boldsymbol{F}}^T \cdot \boldsymbol{F} + \boldsymbol{F}^T \cdot \dot{\boldsymbol{F}} \\ &= 2\,\boldsymbol{F}^T \cdot \boldsymbol{D} \cdot \boldsymbol{F} \end{aligned} \tag{4.87}$$

By substitution of the expression for $\dot{C}_{ij}$ in equation (4.87) in to equation (4.83) we get:

$$\dot{\psi} = \frac{\psi}{C_{ij}}\dot{C}_{ij} = \frac{\psi}{C_{ij}}\left(2F_{ki}D_{kl}F_{lj}\right) = 2\left(\boldsymbol{F}\frac{\boldsymbol{\partial\psi}}{\boldsymbol{\partial C}}\boldsymbol{F}^T\right) : \boldsymbol{D} \tag{4.88}$$

Having proceeded in the same way as in derivation of hyperelasticity for small deformations (see equation (4.80)), we now have two expressions for the stress power which must hold, namely the definition of stress power in

equation (4.73) and the propery for hyperelasticity in equation (4.83) which yields:

$$\omega = T_{ij} D_{ij} = \rho \dot{\psi} = \rho \frac{\partial \psi}{\partial C_{ij}} \dot{C}_{ij} \tag{4.89}$$

and by employing the expression for $\dot{\psi}$ in equation (4.88) we get:

$$\omega = \boldsymbol{T} : \boldsymbol{D} = \left(2\,\rho \boldsymbol{F} \frac{\boldsymbol{\partial \psi}}{\boldsymbol{\partial C}} \boldsymbol{F}^T \right) : \boldsymbol{D} \tag{4.90}$$

and finally as the hyperelastic potential ψ per definition is independent of $\boldsymbol{D}$, we find how the Cauchy stress tensor $\boldsymbol{T}$ may be derived from the hyperelastic potential ψ per mass unit for large deformations:

$$\boldsymbol{T} = 2\,\rho \boldsymbol{F} \frac{\boldsymbol{\partial \psi}}{\boldsymbol{\partial C}} \boldsymbol{F}^T \tag{4.91}$$

From equations (3.15) and (3.24) we know that the deformation tensors $\boldsymbol{F}$, $\boldsymbol{C}$, and $\boldsymbol{E}$, are functionally related. Thus, from the expression for the Cauchy stress for a hyperelastic material in equation (4.91), we may conclude that $\boldsymbol{T} = \boldsymbol{T}(\boldsymbol{E})$, and that an assumption of hyperelasticity for large deformations also implies elasticity. Note that we already came to the same conclusion for small deformations in section 4.3.

4.3.2 Stress tensors for large deformations

The governing equations are often formulated in K_0 for large deformations, i.e., (X, t) and conservation of mass implies $\rho\, dV = \rho_0\, dV_0$ and consequently the volume integrals in Cauchy's equations (2.87) are easily represented in the reference frame by:

$$\int_V \boldsymbol{b}\,\rho\, dV = \int_{V_0} \boldsymbol{b}\,\rho_0\, dV_0, \quad \int_V \boldsymbol{a}\,\rho\, dV = \int_{V_0} \boldsymbol{a}\,\rho_0\, dV_0 \tag{4.92}$$

However, the challenge is how to represent the surface integrals of the $\int_A \boldsymbol{t}\, dA$. To approach this issue we define a stress vector $\boldsymbol{t}_0$ in K_0 by:

$$\boldsymbol{t}_0\, dA_0 = \boldsymbol{t}\, dA \quad \Leftrightarrow \quad \int_{A_0} \boldsymbol{t}_0\, dA_0 = \int_A \boldsymbol{t}\, dA \tag{4.93}$$

which yields:

$$\boldsymbol{t}_0 = \frac{dA}{dA_0}\, \boldsymbol{t} \tag{4.94}$$

where $\boldsymbol{t}_0$ represents forces in K. Note that $\boldsymbol{t}_0$ has same direction as $\boldsymbol{t}$ but not with the same magnitude. With the definition in equation (4.94) we may now formulate the balance of linear monemntu based on Euler's first axiom in the reference frame K_0 (or in Lagrangian coordinates):

$$\int_{V_0} \boldsymbol{a}\,\rho_0\,dV_0 = \int_{A_0} \boldsymbol{t}_0\,dA_0 + \int_{V_0} \boldsymbol{b}\,\rho_0\,dV_0 \tag{4.95}$$

Albeit formulated in the reference configuration, this equation has both volume and surface integrals and is therefore not transferable to a partial differential equation form. Therefore, the first Piola-Kirchhoff stress tensor (PKS) $\boldsymbol{T}_0$ is introduced in analogy with the Cauchy stress theorem (see equation (2.65)):

$$\boldsymbol{t}_0 = \boldsymbol{T}_0 \cdot \boldsymbol{n}_0 \tag{4.96}$$

Equation (4.96) is an invariant linear tensor equation and $\boldsymbol{n}_0$ is a unit normal on dA_0 in the reference configuration K_0. The first PKS $\boldsymbol{T}_0$ is related with the Cauchy stress tensor $\boldsymbol{T}$ by:

$$\boldsymbol{T}_0 = J\boldsymbol{T}\boldsymbol{F}^{-T}, \qquad \text{where} \quad J = \det \boldsymbol{F} \tag{4.97}$$

As can be seen from equation (4.97), the first PKS $\boldsymbol{T}_0$ is not symmetric, and represents what is commonly called engineering or nominal stress.(**CHECK: footnote** at end of sentence placed in parenthesis) (i.e., Force in the current configuration divided by the area in the reference configuration.)

The second PKS $\boldsymbol{S}$ is conventionally defined by:

$$\boldsymbol{S} = \boldsymbol{F}^{-1}\boldsymbol{T}_0 = J\boldsymbol{F}^{-1}\boldsymbol{T}\boldsymbol{F}^{-T} \tag{4.98}$$

and one may easily show that $\boldsymbol{S} = \boldsymbol{S}^T$.

By introducing these stress tensors one may derive the Cauchy's equations of motions in the reference configuration K_0 (see p. 178 [17]).

In the previous section 4.3.1 the relation between the Cauchy stress tensor $\boldsymbol{T}$ and a hyperelastic potential per mass unit ψ was derived in equation (4.91). An expression for the the second PKS $\boldsymbol{S}$ from ψ may be obtained by combining equation (4.98) and (4.91):

$$\boldsymbol{S} = 2J\rho\frac{\partial\psi}{\partial\boldsymbol{C}} = 2\rho_0\frac{\partial\psi}{\partial\boldsymbol{C}}, \qquad \text{where} \quad \rho J = \rho_0 \tag{4.99}$$

We state without proof that $\boldsymbol{S}$ also may be express by a hyperelastic potential per unit volume $\phi = \rho_0\psi$ by:

$$\boldsymbol{S} = 2\frac{\partial\phi}{\partial\boldsymbol{C}} \tag{4.100}$$

which is indeed a simpler expression than the one relating the Cauchy stress tensor $\boldsymbol{T}$ and the hyperelastic potential in equation (4.100).

4.3.3 Isotropic hyperelastic materials

For isotropic materials, the hyperelastic potential per unit volume ϕ is commonly expressed as a function of the invariants of the Green deformation tensor $\boldsymbol{C}$, which we denote $I_1, \ldots, I_3$, i.e., $\phi = \phi(I_1, I_2, I_3)$. The motivation for such a formulation is that the mathematical representation will be independent of the particular coorindate system, and thus ensure that the mathematical representation is isostropic. The invariants of a second order tensor are well defined an given by e.g., equations (3.56) to (3.58):

$$\begin{aligned} I_1 &= \mathrm{tr}(\boldsymbol{C}) \\ I_2 &= \frac{1}{2}((\mathrm{tr}\boldsymbol{C})^2 - \|\boldsymbol{C}\|^2 \\ I_3 &= \det(\boldsymbol{C}) = \det(\boldsymbol{F}^2) = J^2 \end{aligned} \tag{4.101}$$

For such a formulation the second PKS $\boldsymbol{S}$ may be derived from the general relation given in equation (4.100) by empolying the chain rule for differentiation:

$$\boldsymbol{S} = 2\frac{\partial \phi}{\partial \boldsymbol{C}} = 2\sum_{k=1}^{3} \frac{\partial \phi}{\partial I_k} \frac{\partial I_k}{\partial \boldsymbol{C}} \tag{4.102}$$

One may show (see Exercise 2):

$$\frac{\partial I_1}{\partial \boldsymbol{C}} = \boldsymbol{1}, \quad \frac{\partial I_2}{\partial \boldsymbol{C}} = I_1 \boldsymbol{1} - \boldsymbol{C}, \quad \frac{\partial I_3}{\partial \boldsymbol{C}} = I_3 \boldsymbol{C}^{-1} \tag{4.103}$$

Note that the partial derivatives of the invariants are quantities which are computed once and for all, and thus one may establish a more practical representation for how the $\boldsymbol{S}$ may be computed from ϕ, by substitution of equation (4.103) into equation (4.102):

$$\boldsymbol{S} = 2\left(\frac{\partial \phi}{\partial I_1} + I_1 \frac{\partial \phi}{\partial I_2}\right) \boldsymbol{1} - 2\frac{\partial \phi}{\partial I_2} \boldsymbol{C} + 2I_3 \frac{\partial \phi}{\partial I_3} \boldsymbol{C}^{-1} \tag{4.104}$$

For incompressible materials we have that $\det \boldsymbol{F} = J = 1$ which from equation (4.101) is equivalent to $I_3 = 1$. For the incompressible materials it is thefore customary to introduce a modified strain energy function:

$$\bar{\phi} = \phi(\boldsymbol{C}) + p(J - 1) \tag{4.105}$$

where p denote an undetermined Lagrange multiplier which has to be determined from boundary conditions. As for incompressible fluids, only gradients of pressure determine the solutions of the governing equations for incompressiblesolids, and the level of the pressure (stresses) must be determined from the boundary conditions.

The second PKS may the be found by:

$$\boldsymbol{S} = 2\,\frac{\partial \bar{\phi}}{\partial \boldsymbol{C}} = 2\frac{\partial \phi(\boldsymbol{C})}{\partial \boldsymbol{C}} + pJ\boldsymbol{C}^{-1} \tag{4.106}$$

as:

$$\frac{\partial J}{\partial \boldsymbol{C}} = \frac{\partial J}{\partial I_3}\,\frac{\partial I_3}{\partial \boldsymbol{C}} = \frac{\partial \sqrt{I_3}}{\partial I_3}\,I_3\boldsymbol{C}^{-1} = \frac{J}{2}\,\boldsymbol{C}^{-1} \tag{4.107}$$

Example 4.3.1. *Thin sheet of incompressible material.*

For a thin sheet of incompressible material (i.e., with $I_3 = 1$) we have $\phi = \phi(I_1, I_2)$. Furthermore, due to the thin sheet we orient our coordinate system in such a way that we may assume zeero stress in direction orthogonal to the sheet plane. From equation (4.106) we get for the S_{33} component:

$$S_{33} = 2\left(\frac{\partial \phi}{\partial I_1} + I_1\frac{\partial \phi}{\partial I_2}\right) - 2\frac{\partial \phi}{\partial I_2}C_{33} + p\,\boldsymbol{C}_{33}^{-1} = 0 \tag{4.108}$$

Thus, an expression for the Lagrangian multiplier may be found from equation (4.108) :

$$p = 2\frac{\partial \phi}{\partial I_2}C_{33}^2 + 2\left(\frac{\partial \phi}{\partial I_1} + I_1\frac{\partial \phi}{\partial I_2}\right)C_{33} \tag{4.109}$$

Example 4.3.2. *The Mooney-Rivlin material.*

For isotropic materials one may express the hyperelastic potential per unit mass ψ as a function of the invariants of the left deformation tensor $\boldsymbol{B}$ (see equation (3.16)). The hyperelastic potential is formulated accordingly as:

$$\psi = \psi(I_B, II_B, III_B) \tag{4.110}$$

where I_B, II_B, and III_B denote the principal invariants of $\boldsymbol{B}$. By proceeding the same way as for the formulation the left Green deformation tensor $\boldsymbol{C}$ in equation (4.83), we differentiate the potential with respect to time to get:

$$\dot{\psi} = \frac{\partial \psi}{\partial \boldsymbol{B}} : \dot{\boldsymbol{B}} \tag{4.111}$$

The expresson for $\dot{\boldsymbol{B}}$ may be found to be (see Exercise 2):

$$\dot{\boldsymbol{B}} = \boldsymbol{L}\boldsymbol{B} + \boldsymbol{B}\boldsymbol{L}^T \tag{4.112}$$

Substitution of equation (4.112) in equation (4.111):

$$\dot{\psi} = \frac{\partial \psi}{\partial \boldsymbol{B}} : \dot{\boldsymbol{B}} = \frac{\partial \psi}{\partial B_{ij}} \dot{B}_{ij} = \frac{\partial \psi}{\partial B_{ij}} \left(L_{ik} B_{kj} + B_{ik} L_{jk} \right) = \left(2 \frac{\partial \psi}{\partial \boldsymbol{B}} \boldsymbol{B} \right) : \boldsymbol{L} \tag{4.113}$$

where the latter equality comes from the symmetric property of $\boldsymbol{B}$. From equation (4.89) and (4.113) on may obtain:

$$\omega = \boldsymbol{T} : \boldsymbol{D} = \boldsymbol{T} : \boldsymbol{L} = \rho \dot{\psi} = \left(2\rho \frac{\partial \psi}{\partial \boldsymbol{B}} \boldsymbol{B} \right) : \boldsymbol{L} \tag{4.114}$$

and as $\boldsymbol{L}$ may be chosen arbitrarily, we find that the Cauchy stress tensor can be derived from the strain energy potential as:

$$\boldsymbol{T} = \left(2\rho \frac{\partial \psi}{\partial \boldsymbol{B}} \boldsymbol{B} \right) \tag{4.115}$$

In particular, the Mooney-Rivlin material is an example of a material models which has been used to model rubber, which is considered to be isotropic and incompressible, and easily subject to large deformations for typical loading conditions. The Mooney-Rivlin material is defined by the specific elastic energy:

$$\psi = \frac{1}{2} \frac{\mu}{\rho} \left(\frac{1}{2} + \alpha \right) \left(I_B - 3 \right) + \frac{1}{2} \frac{\mu}{\rho} \left(\frac{1}{2} - \alpha \right) \left(II_B - 3 \right) \tag{4.116}$$

where α and μ are material parameters (elasticities). The Cauchy stress tensor may for the Mooney-Rivlin material be obatained from equation (4.116) and (4.115):

$$\boldsymbol{T} = \mu \left(\frac{1}{2} + \alpha \right) \boldsymbol{B} - \mu \left(\frac{1}{2} - \alpha \right) \boldsymbol{B}^{-1} - p\boldsymbol{I} \tag{4.117}$$

As the Mooney-Rivlin material is incompressible, an isotropic stress $-p\boldsymbol{I}$, has to be added to the stress tensor. A so-called neo-Hookean material is obtained for $\alpha = 1/2$ in equation (4.117).

4.4 Anisotropic Materials

Notation for anisotropic materials. Angular momentum $\Rightarrow \boldsymbol{T} = \boldsymbol{T}^T$. Green's strain $\boldsymbol{E} \equiv \boldsymbol{E}^T \Leftarrow \boldsymbol{E} \equiv \boldsymbol{H} + \boldsymbol{H^T} + \boldsymbol{H^T H}$. Only 6 distinct values for $\boldsymbol{T}$ and $\boldsymbol{E}$. Special notation for coordinate stresses and strains

$$T = \begin{bmatrix} T_1 & T_6 & T_5 \\ \vdots & T_2 & T_4 \\ \vdots & \vdots & T_3 \end{bmatrix} \qquad E = \begin{bmatrix} E_1 & E_6 & E_5 \\ \vdots & E_2 & E_4 \\ \vdots & \vdots & E_3 \end{bmatrix} \tag{4.118}$$

Anisotropic constitutive equation A fully anisotropic, linearly elastic constitutive equation

$$T_\alpha = S_{\alpha\,\beta} E_\beta, \qquad \{\alpha, \beta\} \in \{1 \ldots 6\} \tag{4.119}$$

T_α and E_β are 6×1 vector matrices, whereas $S_{\alpha\,\beta}$ is a 6×6 *elasticity* or *stiffness* matrix. We will show $S = S^T$ for a hyperelastic material, i.e., only 21 independent stiffnesses for full anisotropy.

Alternative formulation

$$E_\alpha = K_{\alpha\,\beta} T_\beta, \qquad K = S^{-1} \tag{4.120}$$

$K_{\alpha\,\beta}$ is a 6×6 *compliance* or *flexibility* matrix

Stiffness matrix for Hookean materials.

Isotropic, linearly elastic material

$$S = \frac{\eta}{2(1+\nu)(1-2\nu)} \begin{bmatrix} 2(1-\nu) & 2\nu & 2\nu & 0 & 0 & 0 \\ 2\nu & 2(1-\nu) & 2\nu & 0 & 0 & 0 \\ 2\nu & 2\nu & 2(1-\nu) & 0 & 0 & 0 \\ 0 & 0 & 0 & (1-2\nu) & 0 & 0 \\ 0 & 0 & 0 & 0 & (1-2\nu) & 0 \\ 0 & 0 & 0 & 0 & 0 & (1-2\nu) \end{bmatrix} \tag{4.121}$$

Note: $S = S^T$

Symmetry of stiffness matrix. Hyperelastic anisotropic materials

Hyperelastic material

$$\boldsymbol{T} = \frac{\partial \phi}{\partial \boldsymbol{E}} \Leftrightarrow T_{ij} = \frac{\partial \phi}{\partial E_{ij}} \tag{4.122}$$

$$\Leftrightarrow T_\alpha = \frac{\partial \phi}{\partial E_\alpha} \tag{4.123}$$

The stress tensor $\boldsymbol{T}$. Elastic energy ϕ per unit volume.

Linearly anisotropic material

$$T_\alpha = S_{\alpha\beta} E_\beta \tag{4.124}$$

Hyperelastic linearly anisotropic material

$$\frac{\partial T_\alpha}{\partial E_\beta} = S_{\alpha\beta} = \frac{\partial^2 \phi}{\partial E_\alpha \partial E_\beta} \equiv \frac{\partial^2 \phi}{\partial E_\beta \partial E_\alpha} = S_{\beta\alpha} \tag{4.125}$$

$$\Rightarrow S_{\alpha\beta} = S_{\beta\alpha} \Leftrightarrow S = S^T \tag{4.126}$$

$$\Rightarrow S_{\alpha\beta} = S_{\beta\alpha} \Leftrightarrow S = S^T \tag{4.127}$$

Independent stiffnesses reduces from 36 to 21.

Materials with one plane of symmetry:

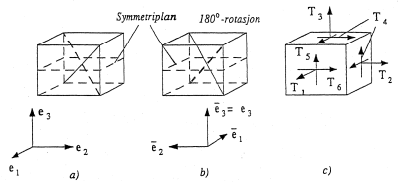

Figure 4.8: Materials with one plane of symmetry.

Structure symmetric with respect to a plane through the particle. The mirror image of the structure is identical to the structure itself. The number of stiffnesses is reduced from 21 to 13.

The fig a) shows a plane of symmetry normal to $\boldsymbol{e}_3$. The fig b) shows 180° rotation about the $\boldsymbol{e}_3$-axis A state of strain E will produce the $\Rightarrow \bar{S} = S$ The number of stiffnesses is reduced from 21 to 13.

π-rotation about the $\boldsymbol{e}_3$-axis

$$T = \begin{bmatrix} T_1 & T_6 & T_5 \\ \vdots & T_2 & T_4 \\ \vdots & \vdots & T_3 \end{bmatrix} \qquad E = \begin{bmatrix} E_1 & E_6 & E_5 \\ \vdots & E_2 & E_4 \\ \vdots & \vdots & E_3 \end{bmatrix} \tag{4.128}$$

Transformation matrix

$$Q = \begin{bmatrix} \cos\theta & \sin\theta & 0 \\ -\sin\theta & \cos\theta & 0 \\ 0 & 0 & 1 \end{bmatrix}, \quad Q_\pi \begin{bmatrix} -1 & 0 & 0 \\ 0 & -1 & 0 \\ 0 & 0 & 1 \end{bmatrix} \tag{4.129}$$

$$\bar{T} = Q^T T Q = \begin{bmatrix} T_1 & T_6 & -T_5 \\ \vdots & T_2 & -T_4 \\ \vdots & \vdots & T_3 \end{bmatrix}, \quad \bar{E} = Q^T E Q = \begin{bmatrix} E_1 & E_6 & -E_5 \\ \vdots & E_2 & -E_4 \\ \vdots & \vdots & E_3 \end{bmatrix} \tag{4.130}$$

Plane symmetric anisotropic constitutive equations

$$T_\alpha = S_{\alpha\,\beta} E_\beta, \qquad \bar{T}_\alpha = \bar{S}_{\alpha\,\beta} \bar{E}_\beta \tag{4.131}$$

Plane symmetry $\Rightarrow \bar{S}_{\alpha\,\beta} = S_{\alpha\,\beta}$. Notation: λ= 4 and 5, and $\rho,\ \gamma = 1 \ldots 3$ and 6. From the constitutive equations

$$T_\lambda = S_{\lambda\rho} E_\rho + S_{\lambda 4} E_4 + S_{\lambda 5} E_5 \tag{4.132}$$
$$-T_\lambda = S_{\lambda\rho} E_\rho + S_{\lambda 4}(-E_4) + S_{\lambda 5}(-E_5) \tag{4.133}$$
$$T_\gamma = S_{\gamma\rho} E_\rho + S_{\gamma 4} E_4 + S_{\gamma 5} E_5 \tag{4.134}$$
$$T_\gamma = S_{\gamma\rho} E_\rho + S_{\gamma 4}(-E_4) + S_{\gamma 5}(-E_5) \tag{4.135}$$

By comparison $S_{\lambda\,\rho} = 0$ and $S_{\gamma\lambda} = 0$.

4.5 Waves in elastic materials

4.5.1 Plane elastic waves

To analyse plane elastic waves we consider an infinite body of isotropic elastic material, which is subjected to a mechanical disturbance so small that it may be rendered as a point source e.g., a displacement point source. This displacement disturbance will propagate in the undisturbed material as a displacement wave. In the subsequent analysis, we assume that sufficiently far away from the point source, the displacements propagate as plane waves (see figure 4.9), which in mathematical terms means:

$$\mathbf{u} = \mathbf{u}(x_3, t) \quad \text{and} \quad u_i(x_3, t) \tag{4.136}$$

The three displacement components u_i, thus propagate in the x_3-direction as planes defined by their unit normal $\boldsymbol{e}_3$. The waves are given names according to how the displacement is oriented relative to the direction of propagation: $u_3(x_3, t)$ is *the longitudinal wave*, while $u_1(x_3, t)$ and $u_2(x_3, t)$ are *transverse waves*.

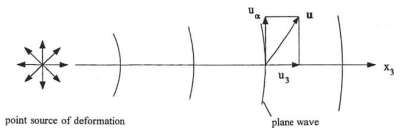

Figure 4.9: Plane wave propagation of displacements from a distant point source.

Now, if we assume that the material may be considered as a Hookean material, the Navier equations (4.30) are the relevant equations of motion. Further, if body forces are neglected the Navier equations take the form:

$$u_{i,kk} + \frac{1}{1-2\nu} u_{k,ki} = \frac{\rho}{\mu} \ddot{u}_i \tag{4.137}$$

when bodyforces have been neglected.

In the following, we will show that the (4.137) reduce to wave equations in the longitudinal and the transverse directions, albeit with different wave velocities in the two directions. The wave speed c_l in the longitudinal direction will be shown to be:

$$c_l = \sqrt{\frac{2\,(1-\nu)}{(1-2\nu)}\,\frac{\mu}{\rho}} = \sqrt{\frac{1-\nu}{(1-2\nu)(1+\nu)}\,\frac{\eta}{\rho}} \tag{4.138}$$

whereas in the transverse direction the wave speed c_t may be represented:

$$c_t = \sqrt{\frac{\mu}{\rho}} = \sqrt{\frac{1}{2(1+\nu)}\frac{\eta}{\rho}} \tag{4.139}$$

$$c = \sqrt{\frac{\eta}{\rho}} \tag{4.140}$$

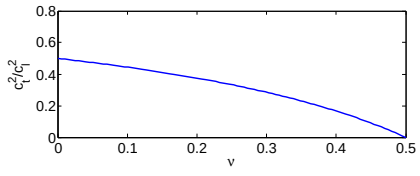

Figure 4.10: Wave speed ratio squared as a function of Poisson's ratio.

First we focus on the longitudinal direction of the Navier-equation without body forces (4.137), i.e., for component $i = 3$. We note that the first term in (4.137) for $i = 3$ is $u_{i,kk} = u_{3,33}$ due to the assumption of a planar wave in Eq. (4.136). Similarly we note that $u_{k,ki} = u_{3,33}$ for the same reason. Thus, the Navier-equation Eq. (4.137) in the longitudinal direction reduce to:

$$u_{3,33}\left(1 + \frac{1}{1-2\nu}\right) = \frac{\rho}{\mu}\,\ddot{u}_3 \tag{4.141}$$

which may be presented in the form of a canonical wave equation:

$$\frac{\partial^2 u_3}{\partial t^2} = c_l^2\,\frac{\partial^2 u_3}{\partial {x_3}^2} \tag{4.142}$$

with c_l as defined in (4.138).

For the transverse directions, we use Greek indices to refer to the first two spatial directions only $\alpha = (1, 2)$. The Navier-equations (4.137) in the tranverse directions have a generic representation which also may be simplified due to the planar wave assumption in Eq. (4.136):

$$\underbrace{u_{\alpha,kk}}_{=u_{\alpha,33}} + \left(\frac{1}{1-2\nu}\right)\underbrace{u_{k,k\alpha}}_{=u_{k,3\alpha}=0} = \frac{\rho}{\mu}\,\ddot{u}_\alpha \tag{4.143}$$

which is also a wave equation of the form as in (4.142):

$$\frac{\partial^2 u_\alpha}{\partial t^2} = c_t^2\frac{\partial^2 u_\alpha}{\partial {x_3}^2} \tag{4.144}$$

with a wave speed given by (4.139). From (4.138) and (4.139) the ratio of the squared wave speeds may be expressed as:

$$\frac{c_t^2}{c_l^2} = \frac{1-2\nu}{2\,(1-\nu)} \tag{4.145}$$

and further for c_l to be real we see that $0 < \nu < 0.5$. The ratio of the squared wave speeds is plotted in Figure 4.10, and we see $c_t < c_l$ for real c_l.

Typically, steel have the material paramteters $\nu = 0.3$, $\eta = 210\,GPa$, and $\rho = 7.83 \cdot 10^3\,kg/m^3$ which corresponds to a transverse wave speed of $c_t = 3212\,m/s$, a longitudinal wave speed of $c_l = 6009\,m/s$, whereas the cylindrical bar assumption given by equation (4.140) gives $c = 5179\,m/s$.

A longitudinal wave induces volume changes as $\varepsilon_v = u_{3,3} = E_{33}$, and for that reason the wave is called a *dilatational wave* or a *volumetric wave*.

The stresses associated with the longitudinal waves are given by Hooke's law in equation (4.9):

$$T_{33} = \frac{2(1-\nu)\mu}{1-2\nu}\, u_{3,3}, \qquad \text{and} \qquad T_{11} = T_{22} = \frac{\nu}{1-\nu}\, T_{33} \tag{4.146}$$

The transverse waves are denoted isochoric, i.e., $\varepsilon_v = 0$, and for this reason also called *dilatation free waves* or *equivoluminal waves*. The corresonding stresses are found from Hooke's law as for the longitudinal waves:

$$T_{13} = \mu u_{1,3}, \qquad \text{and} \qquad T_{23} = \mu u_{2,3} \tag{4.147}$$

From equation (4.147) we see that the transverse waves also has associated shear stresses on planes orthogonal to the direction of propagation, and for that reason they are also called *shear waves*.

Exercise 1: The generalized Hooke's law

a) Show that:

$$E_{ij} = \frac{1+\nu}{\eta}\, T_{ij} - \frac{\nu}{\eta}\, T_{kk}\, \delta_{ij} \tag{4.148}$$

and

$$T_{ij} = \frac{\eta}{1+\nu}\left(E_{ij} + \frac{\nu}{1-2\nu}\, E_{kk}\, \delta_{ij}\right) \tag{4.149}$$

are equivalent representations of the constitutive equation for an isotropic, linearly elastic material.

b) Derive Hooke's law for plane stress as given by the equations (4.36) and (4.37) from the general Hookean law represented by equations (4.7) and (4.9).

Exercise 2: Invariants

a) Show that that the time derivative of the right Green deformation tensor is given by:

$$\dot{\boldsymbol{B}} = \boldsymbol{L}\boldsymbol{B} + \boldsymbol{B}\boldsymbol{L}^T \tag{4.150}$$

Exercise 3: Shear modulus

Add a standard exercise for thin walled cylinder loaded with torsion from e.g. TKT 4123

Chapter 5

Fluid mechanics

5.1 Introduction

In a continuum mechanical setting, it is convenient to define a fluid based on the macro mechanical conditions which are the most prominent for a fluid or gass compared to a solid. Thus, we have chosen the
following definition:

Theorem 5.1.1. Fluid
A fluid is a material that deforms continuously when subjected to anisotropic stress.

For an anisotropic stress condition, one may always find planes with shear stress. A fluid will therefore deform contiuously while exposed to shear stress. Conversely, the fluid may be at rest for only isotropic stress states, and the constitutive equation for any fluid at rest (relative to a reference) may be expressed by the simple relation:

$$\boldsymbol{T} = -p\,\mathbf{1}, \qquad p = p(\rho, \theta) \tag{5.1}$$

where p is the *thermodynamical pressure* which is a function of the density ρ and the temperature θ. The expression for p on the right hand side of equation (5.1), is often referred to as an equation of state. A familiar example of the latter, is the equation of state for the *ideal gas*:

$$p = R\rho\theta \tag{5.2}$$

where R is the gas constant for the gas, and θ is the absolute temperature (in degrees Kelvin). Note that, this equation of state is a model for an ideal gas, but may be used as a good approximation for many real gases, for example air.

Small fluid elements, or fluid particles, are in general exposed to large displacements and chaotic motions and it is impossible to follow the motion of the individual particles. A fixed position in space therefore normally used for the observation and mathematical representation of the velocity, pressure, and physical properties of fluids in motion.

Eulerian coordinates due to large displacements and chaotic motion of the individual fluid particles. The velocity vector $\boldsymbol{v}(\boldsymbol{r}, t)$ is the primary kinetic property

5.1.1 Fundamental concepts in fluid mechanics

Stream lines Vector lines to the velocity field. Changes with time for non-steady flow $\boldsymbol{v} = \boldsymbol{v}(\boldsymbol{r}, t)$. Coincide with particle trajectories (path lines) for *steady flow* ($\boldsymbol{v} = \boldsymbol{v}(\boldsymbol{r})$). Differential vector parallel with velocity vector implies: $d\boldsymbol{r} \times \boldsymbol{v}(\boldsymbol{r}, t) = 0$.

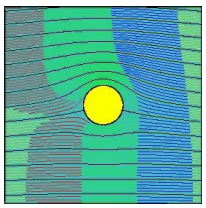

Figure 5.1: Illustration of streamlines.

Path lines (particle trajectories):

$$\dot{\boldsymbol{r}} = \boldsymbol{v}(\boldsymbol{r}, t) \tag{5.3}$$

Vorticity field:

$$\boldsymbol{c} = \nabla \times \boldsymbol{v} \tag{5.4}$$

Potential flow

$$\boldsymbol{v} = \nabla\phi, \quad \phi = \phi(\boldsymbol{r}, t) \quad \Leftarrow \nabla \times \boldsymbol{v} = 0 \tag{5.5}$$

The Reynolds number: Solutions to the governing equations may not be unique. Increasing velocities in a pipe will eventually produce chaotic unsteady flow. The Reynolds number predicts transition from *laminar* to *turbulent* flow.

$$\Re = \frac{\rho\bar{v}d}{\mu}, \quad \bar{v} = \frac{Q}{A} \tag{5.6}$$

ρ density, μ viscosity, d pipe diameter, Q flow rate $[m^3/s]$, A pipe cross section

Turbulent flow when $\Re > 2000$.

5.2 Conservation of mass

Derived with $b = \rho$ in Reynolds Transport Theorem Eq. (2.33)

$$\dot{m} = \frac{d}{dt}\int\limits_{V(t)} \rho(\boldsymbol{r}, t)\, dV = \int\limits_{V} \frac{\partial\rho}{\partial t}\, dV + \int\limits_{A} \rho\,(\boldsymbol{v}\cdot\boldsymbol{n})\, dA = 0 \tag{5.7}$$

Field equation

$$\frac{\partial\rho}{\partial t} + \nabla\cdot(\rho\boldsymbol{v}) = 0 \tag{5.8}$$

$$\frac{\partial\rho}{\partial t} + (\rho v_i)_{,i} = 0 \tag{5.9}$$

Equivalent presentations of conservation of mass.

Conservative formulation:

$$\frac{\partial\rho}{\partial t} + (\rho v_i)_{,i} = 0 \quad \Leftrightarrow \quad \frac{\partial\rho}{\partial t} + \nabla\cdot(\rho\boldsymbol{v}) = 0 \tag{5.10}$$

Non-conservative formulation

$$\frac{\partial\rho}{\partial t} + \rho_{,i}v_i + \rho v_{i,i} = 0 \quad \Leftrightarrow \quad \dot{\rho} + \rho\nabla\cdot\boldsymbol{v} = 0 \tag{5.11}$$

where we have introduced the material derivative of ρ is defined in Eq. (2.20).

Mass conservation for incompressible flow (ρ = constant)

$$\frac{\partial \rho}{\partial t} + \nabla \cdot (\rho \boldsymbol{v}) = 0 \tag{5.12}$$

$$\nabla \cdot \boldsymbol{v} = 0 \quad \Leftrightarrow \quad v_{i,i} = 0 \tag{5.13}$$

5.3 Inviscid fluids

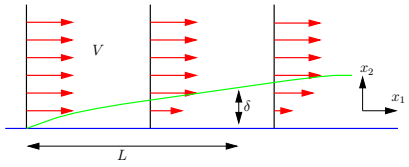

Figure 5.2: Uniform flow and development of a viscous boundary layer near a solid surface [40].

Eulerian fluid = perfect fluid

Shear stresses due to a viscous fluid may be neglected in many situations. Boundary layer (BL) analysis near the solid surfaces may be sufficient. Outside the BL, the fluid may be taken as inviscid. Constitutive equation (material)

$$\boldsymbol{T} = -p\,\mathbf{1}, \quad T_{ij} = -p\,\delta_{ij} \tag{5.14}$$

where $p = p(\rho, \theta)$, $\rho(\boldsymbol{r}, t)$ is the fluid density $\theta(\boldsymbol{r}, t)$ is the fluid temperature. Thermoelastic material as $p = p(\rho, \theta)$

Incompressible Eulerian fluids

Compressibility may often be disregarded. Liquids are rarely considered compressible. Gases may also often be rendered incompressible ($v < c/3$). The pressure is no longer a state variable: $p = p(\boldsymbol{r}, t)$ and must be found from boundary conditions.

Linear momentum with Reynolds and Gauss

$$\frac{d}{dt}\int_V v_i\rho\, dV = \int_V \frac{\partial \rho v_i}{\partial t} + \frac{\partial}{\partial x_k}(\rho v_i v_k)\, dV \tag{5.15}$$

$$= \int_V \rho\frac{\partial v_i}{\partial t} + v_i\frac{\partial \rho}{\partial t} + v_i\frac{\partial}{\partial x_k}(\rho v_k) + \rho v_k\frac{\partial v_i}{\partial x_k} \tag{5.16}$$

$$= \int_V \rho \underbrace{\left(\frac{\partial v_i}{\partial t} + v_k\frac{\partial v_i}{\partial x_k}\right)}_{\dot{v}_i} + v_i \underbrace{\left(\frac{\partial \rho}{\partial t} + \frac{\partial}{\partial x_k}(\rho v_k)\right)}_{=0 \Leftarrow \text{ mass conservation}} dV \tag{5.17}$$

$$= \int_V \dot{v}_i\, \rho dV \tag{5.18}$$

and consequently:

$$\frac{d}{dt}\int_V \boldsymbol{v}\rho\, dV = \int_V \dot{\boldsymbol{v}}\rho\, dV \tag{5.19}$$

Equations of motion for Eulerian fluids. From Cauchy's equations of motion:

$$\frac{d}{dt}\int_V \boldsymbol{v}\rho\, dV = \int_V \dot{\boldsymbol{v}}\rho\, dV = \int_V \nabla\cdot\boldsymbol{T} + \boldsymbol{b}\rho\; dV \tag{5.20}$$

General field equations:

$$\dot{\boldsymbol{v}} = \frac{\partial \boldsymbol{v}}{\partial t} + (\boldsymbol{v}\cdot\nabla)\boldsymbol{v} = \frac{1}{\rho}\nabla\cdot\boldsymbol{T} + \boldsymbol{b} \tag{5.21}$$

The constitutive equation for a perfect fluid $T_{ij} = -p\delta ij$

$$T_{ik,k} = -\frac{\partial p\delta_{ik}}{\partial x_k} = -\frac{\partial p}{\partial x_k}\delta_{ik} = -p_{,i} \tag{5.22}$$

The Euler equations

$$\frac{\partial \boldsymbol{v}}{\partial t} + (\boldsymbol{v}\cdot\nabla)\boldsymbol{v} = -\frac{1}{\rho}\nabla p + \boldsymbol{b} \tag{5.23}$$

The governing equations for Eulerian fluids The Euler equations (momentum equations)

$$\frac{\partial \boldsymbol{v}}{\partial t} + (\boldsymbol{v}\cdot\nabla)\boldsymbol{v} = -\frac{1}{\rho}\nabla p + \boldsymbol{b} \tag{5.24}$$

Conservation of mass (continuity):

$$\frac{\partial \rho}{\partial t} + \nabla\cdot(\rho\boldsymbol{v}) = 0 \tag{5.25}$$

Together, (5.24) and (5.25) form 4 equations with 6 unknowns $\boldsymbol{v}, p, \rho, \theta$. Thus in order to close equation system, an energy equation and a state equation $p = p(\rho, \theta)$, are called for.

Equations of state

Ideal gas $p = R\rho\theta$ Polytropic process

$$p = p_0 \left(\frac{\rho}{\rho_0} \right)^{\alpha} \tag{5.26}$$

where α is constant and p_0 and ρ_0 are reference values.

Various processes

- Isobaric process $\Leftrightarrow$ constant pressure ($\alpha = 0$)
- Isothermal process $\Leftrightarrow$ constant temperature ($\alpha = 1$)
- Isentropic process $\Leftrightarrow$ constant entropy ($\alpha = \kappa = c_p/c_\mu$)
- Isochoric process $\Leftrightarrow$ constant volume $\nabla \cdot \boldsymbol{v} = 0$ and ($\alpha = \infty$)

Example 5.3.1. *Sound waves.*

Audible sound consists of minute variations or perturbations of pressure which propagate as waves. One way to quantify sound, is to state the amount of pressure variation relative to atmospheric pressure. The threshold of hearing is generally reported as: $p_h = 2 \cdot 10^{-5}$ Pa, which is extremely small compared to the atmospheric pressure $p_o = 1.01 \cdot 10^5$ Pa. The standard threshold of hearing can be stated in terms of pressure and the sound intensity in decibels can be expressed in terms of the sound pressure:

$$I = 10 \log_{10} \left[\frac{I}{I_0} \right] = 10 \log_{10} \left[\frac{p^2}{p_h^2} \right] = 20 \log_{10} \left[\frac{p}{p_h} \right] \tag{5.27}$$

In the following we will show that sound waves propagate as elastic waves. The elastic waves correspond to small variations in pressure. We assume that sound propagation is an isentropic process governed by the Euler Eqs. (5.23), the mass conservation equation Eq. (5.8), and a constitutive equation $p = p(\rho)$. A fluid is called barotropic if $p = p(\rho)$ and $\rho = \rho(p)$ are one-to-one relations. Further, the fluid is denoted an elastic fluid if it is both barotropic and inviscid. An elastic fluid is hyperelastic.

The atmospheric pressure p_0 and the ρ_0 represent together an equilibrium stationary state of the Euler Eqs. (5.23):

$$0 = -\frac{1}{\rho_0} \nabla p_0 = \boldsymbol{b} \tag{5.28}$$

Now, we introduce sound waves as perturbations in pressure ($\tilde{p}$) and density ($\tilde{\rho}$):

$$\rho = \rho_0 + \tilde{\rho}, \qquad p = p_0 + \tilde{p} = p_0 + c^2\,\tilde{\rho} \tag{5.29}$$

where the pressure perturbation was be eliminated by employing the constitutive equation to find:

$$c^2 = \left.\frac{dp}{d\rho}\right|_{\rho=\rho_0} \tag{5.30}$$

and thus $\tilde{p} = c^2\,\tilde{\rho}$. Substitution of Eq. (5.29) into the linearized form of the Euler Eqs. (5.23) and subtraction of the stationary state in Eq. (5.28) yields the following system of equations:

$$\frac{\partial \tilde{\rho}}{\partial t} = -\rho_0 \tag{5.31}$$

$$\frac{\partial \boldsymbol{v}}{\partial t} = -\frac{1}{\rho_0}\nabla\tilde{p} = -\frac{c^2}{\rho_0}\nabla\tilde{\rho} \tag{5.32}$$

The mass Eq. (5.31) may be differentiated with respect to time yield:

$$\frac{\partial^2 \tilde{\rho}}{\partial t^2} = -\rho_0 \frac{\partial}{\partial t}\left(\nabla \cdot \boldsymbol{v}\right) = -\rho_0 \nabla \cdot \frac{\partial \boldsymbol{v}}{\partial t} = \rho_0 \nabla \cdot \frac{c^2}{\rho_0}\nabla\tilde{\rho} \tag{5.33}$$

where the latter equality follow from (5.32). The canonical linear wave equation results from (5.33):

$$\frac{\partial^2 \tilde{\rho}}{\partial t^2} = c^2 \nabla^2 \tilde{\rho} \tag{5.34}$$

and we observe that c corresponds to the wave speed, which in this case is the velociy of sound, and may be found from the particular constitutive equation, e.g., Eq. (5.26).

For refence the speed of sound in air is $c = 340$ m/s, and in water it is $c = 1460$ m/s.

5.4 Linear viscous fluids

Viscous fluids Fluid particles are slowed down in the vicinity of a solid wall (see Figure 5.2). Shear stresses are present wherever there are velocity gradients. The influence of (wall) shear stresses (WSS) are most prominent in the vicinity of solid walls.

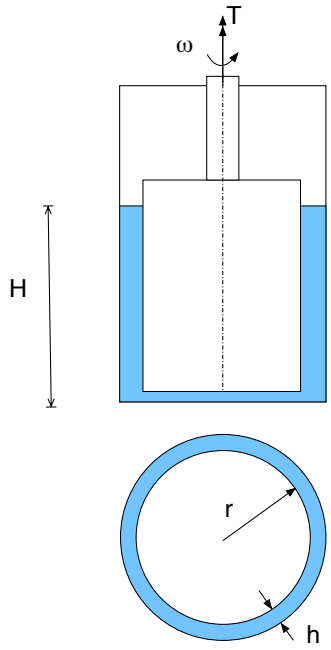

Figure 5.3: Cylindrical viscometer.

Flow around rigid bodies. External flow field modeled as a perfect fluid. BL flow near the rigid surface with asymptotic external flow.

The velocity field for simple shear flow

$$v_1 = \frac{v}{h}x_2, v_2 = v_3 = 0 \tag{5.35}$$

Strain rate

$$\dot{\gamma} = 2D_{12} = \frac{dv_1}{dx_2} = \frac{v}{h} = \frac{\omega r}{h} \tag{5.36}$$

Shear stress from torque T

$$(\tau r)(2\pi r H) = T \tag{5.37}$$

$$\tau = \frac{T}{2\pi r^2 H} \tag{5.38}$$

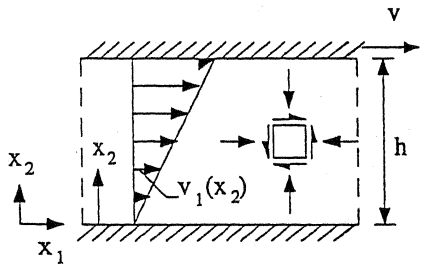

Figure 5.4: Illustration of simple shear flow between two parallel planes.

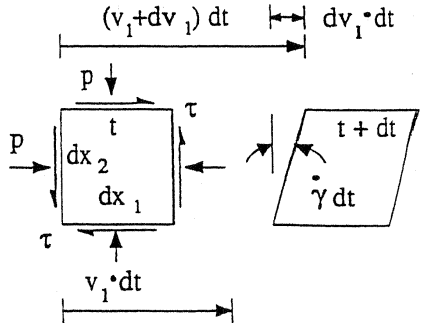

Figure 5.5: Illustration of the shear rate for a small fluid element in a simple shear flow.

5.4.1 Simple shear flow

The velocity field

$$v_1 = \frac{v}{h} x_2, v_2 = v_3 = 0 \tag{5.39}$$

The rate of deformation

$$\boldsymbol{D} = \begin{bmatrix} 0 & 1 & 0 \\ 1 & 0 & 0 \\ 0 & 0 & 0 \end{bmatrix} \frac{\dot{\gamma}}{2} \tag{5.40}$$

where:

$$\dot{\gamma} = \dot{\gamma}_{12} = \boldsymbol{e}_1 \cdot \boldsymbol{D} \cdot \boldsymbol{e}_2 = 2D_{12} = \frac{dv_1}{dx_2} = \frac{v}{h} \tag{5.41}$$

From experiments:

$$\tau = \mu \dot{\gamma} \tag{5.42}$$

Generalization from simple shear flow From experiments:

$$\tau = \mu \dot{\gamma} = 2\mu D_{12} \tag{5.43}$$

Newton's law of fluid friction:

$$T_{ij} = 2\mu D_{ij} = \mu(v_{i,j} + v_{j,i}) \quad \text{for} \quad i \neq j \tag{5.44}$$

Stokes' criteria for stress/velocity relation in viscous fluids

- $\boldsymbol{T}$ is a continuous function of $\boldsymbol{D}$
- Homogeneous, i.e., $\boldsymbol{T}$ independent of particle coordinates
- $\boldsymbol{T} = -p(\rho, \theta)\mathbf{1}$ when $\boldsymbol{D} = 0$
- Viscosity is an isotropic property (redundant)

Newtonian fluid

The Stokes criteria imply a constitutive equation for a Stokes fluid of the form

$$\boldsymbol{T} = \boldsymbol{T}[\boldsymbol{D}, \rho, \theta], \quad \boldsymbol{T}[\mathbf{0}, \rho, \theta] = -p(\rho, \theta)\mathbf{1} \tag{5.45}$$

Linear viscous fluid (Newtonian)

- Linear viscous isotropic properties implies that $\boldsymbol{T}$ and $\boldsymbol{D}$ are co-axial
- The constitutive equation may be shown to be:

$$\boldsymbol{T} = -p(\rho, \theta)\mathbf{1} + 2\mu\boldsymbol{D} + (\kappa - \frac{2\mu}{3})\,(\mathrm{tr}\boldsymbol{D})\,\mathbf{1} \tag{5.46}$$

$$T_{ij} = -p(\rho, \theta)\delta_{ij} + 2\mu D_{ij} + (\kappa - \frac{2\mu}{3})\,D_{kk}\,\delta_{ij} \tag{5.47}$$

The properties of the Newtonian fluid. Dynamic shear viscosity

- $\mu = \mu(\theta)$ (rarely pressure dependent)
- Relatively simple to determine experimentally
- $\mu = 1.8 \cdot 10^{-3}$ Ns/m^2 at 0° C
- $\mu = 1.0 \cdot 10^{-3}$ Ns/m^2 at 20° C
- $\mu = 1.7 \cdot 10^{-5}$ Ns/m^2 at 0° C
- $\mu = 1.8 \cdot 10^{-5}$ Ns/m^2 at 20° C

Bulk viscosity κ

- Difficult to measure experimentally
- Resistance toward rapid volume changes
- Incompressible Newtonian fluid

$$\boldsymbol{T} = -p(\rho, \theta)\mathbf{1} + 2\mu\boldsymbol{D} \tag{5.48}$$

5.4.2 The Navier-Stokes equations

The Navier-Stokes equations

Equations of motion for Newtonian fluids may be derived from Cauchy's equations of motion

$$\dot{\boldsymbol{v}} = \frac{\partial \boldsymbol{v}}{\partial t} + (\boldsymbol{v} \cdot \nabla)\boldsymbol{v} = \frac{1}{\rho}\nabla \cdot \boldsymbol{T} + \boldsymbol{b} \tag{5.49}$$

and employihg the constitutive equations for a Newtonian fluid:

$$\boldsymbol{T} = -p(\rho, \theta)\mathbf{1} + 2\mu\boldsymbol{D} + (\kappa - \frac{2\mu}{3})\,(\mathrm{tr}\boldsymbol{D})\,\mathbf{1} \tag{5.50}$$

The Navier-Stokes (NS) equations are obtained by substitution

$$\frac{\partial \boldsymbol{v}}{\partial t} + (\boldsymbol{v} \cdot \nabla)\boldsymbol{v} = -\frac{1}{\rho}\nabla p + \frac{\mu}{\rho}\,\nabla^2\boldsymbol{v} + \frac{1}{\rho}(\kappa + \frac{\mu}{3})\nabla(\nabla \cdot \boldsymbol{v}) + \boldsymbol{b} \tag{5.51}$$

The NS equations for incompressible fluids

$$\frac{\partial \boldsymbol{v}}{\partial t} + (\boldsymbol{v} \cdot \nabla)\boldsymbol{v} = -\frac{1}{\rho}\nabla p + \frac{\mu}{\rho}\,\nabla^2\boldsymbol{v} + \boldsymbol{b} \tag{5.52}$$

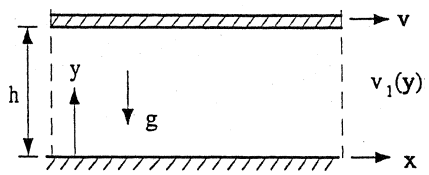

Figure 5.6: Flow between parallel planes

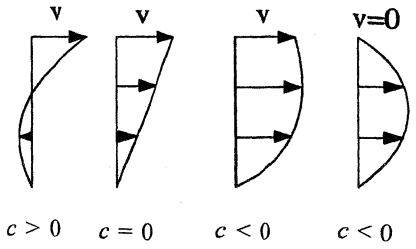

Figure 5.7: Solutions forvarious pressure gradients and upper plane velocities.

5.4.3 About the NS equations

After Claude-Louis Navier and George Gabriel Stokes. The most important equations for viscous fluids. Analytical solutions require major simplifications due to the complexity Models for weather forecasts, ocean currents, pollution, stars in galaxies, aircraft and car design, blood flow. Coupled with Maxwell's equations to model and study magnetohydrodynamics. Coupled with Cauchy's equations for solid materials to study fluid structure interaction problems, e.g., blood and vessel wall. All but the simplest problems must be solved with Computational Fluid Dynamics (CFD) codes

Example 5.4.1. *Flow between parallel planes.*

Saint-Venant's semi-inverse method: Unknown functions are partly assumed known. Employ the governing equations and BCs to determine completely.

Assume steady state and velocity field:

$$v_1 = v_1(y), v_2 = v_3 = 0 \tag{5.53}$$

Incompressibility $\nabla \cdot \boldsymbol{v} = 0$. The constitutive equation yields:

$$T_{11} = T_{22} = T_{33} = -p, \quad T_{12} = \mu v_{1,2} \tag{5.54}$$

Both pressure gradient and upper plate are driving forces for the flow. For convenience $-p_{,1} = c$.

By substitution of the stress field in Cauchy's equation

$$0 = c + \mu v_{1,22} \tag{5.55}$$
$$0 = -p_{,2} - \rho g \tag{5.56}$$
$$0 = -p_{,3} \tag{5.57}$$

By integration

$$p = -\rho g y - cx \tag{5.58}$$

$$v_1 = -\frac{c}{2\mu} y^2 + By + C \tag{5.59}$$

where B and C are constants. BCs $v_1 = 0$ at $y = 0$ and $v_1 = v$ at $y = h$ to find constants. The velocity field:

$$v_1(y) = \frac{ch^2}{2\mu} \left[\frac{y}{h} - \left(\frac{y}{h} \right)^2 \right] + v \frac{y}{h} \tag{5.60}$$

Example 5.4.2. *Laminar pipe flow.*

Incompressible Newtonian flow. Pipe with diameter d. Flow driven by pressure gradient in z-direction. Laminar, steady flow field

$$v_z = v(R), \quad v_R = v_\theta = 0 \tag{5.61}$$

NS in cylindrical coordinates

$$-\frac{\partial p}{\partial R} = 0, \quad \frac{1}{R} \frac{\partial p}{\partial \theta} = 0 \tag{5.62}$$

$$+\frac{1}{R} \frac{\partial}{\partial R} \left(R\mu \frac{\partial v}{\partial R} \right) - \frac{\partial p}{\partial z} = 0 \tag{5.63}$$

BCs: $v(D/2) = 0$ and $v(0) \neq \infty$

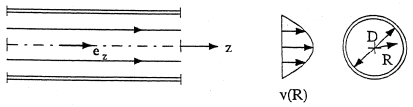

Figure 5.8: Laminar pipe flow

Velocity field for laminar pipe flow. Parabolic velocity field:

$$v = v_0 \left(1 - \left(\frac{2R}{d} \right)^2 \right) \tag{5.64}$$

$$v_0 = \frac{d^2}{16\mu} c \tag{5.65}$$

$$c = -\frac{\partial p}{\partial z} \tag{5.66}$$

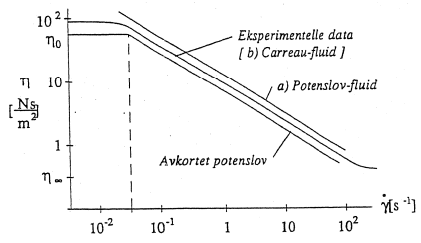

Figure 5.9: The viscosity function for experiments and for a Carrau-model and the power-law model .

5.5 Generalized Newtonian model

Generalized Newtonian fluid (GNF) model for incompressible non-Newtonian fluids.

$$\boldsymbol{T} = -p\mathbf{1} + 2\eta\boldsymbol{D} = -p\mathbf{1} + \boldsymbol{\tau} \tag{5.67}$$

Stress deviator

$$\boldsymbol{\tau} = 2\eta\boldsymbol{D} \tag{5.68}$$

Viscosity function η

$$\eta = \eta(\dot{\gamma}) \tag{5.69}$$

Shear measure $\dot{\gamma}$

$$\dot{\gamma} = \sqrt{2D_{ij}D_{ij}} = 2\sqrt{-II_D} \tag{5.70}$$

Shear measure reduce to the strain rate for simple shear flow

$$\dot{\gamma} = \frac{\partial v_1}{\partial x_2} \tag{5.71}$$

Power-law fluid. Viscosity function

$$\eta = K\dot{\gamma}^{n-1} \tag{5.72}$$

Power-law index n. Consistency parameter

$$K = K_0 \exp(-A\,(\theta - \theta_0)) \tag{5.73}$$

Pros and cons for the power-law model: cannot fit η for extremal values of $\dot{\gamma}$, however it is convenient for analytical solutions.

Most real fluids are shear thinning ($n < 1$), where $\eta \downarrow$ as $\dot{\gamma} \uparrow$.

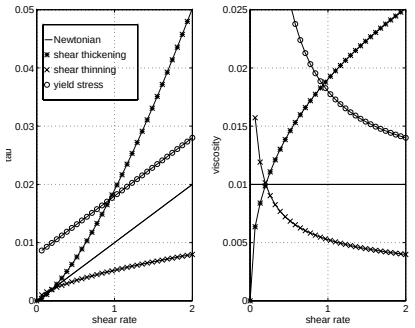

Figure 5.10: Shear stress as a function of shear rate (left) and the viscosity function as a function of the shear rate (right) .

Carreau-Yasuda model

$$\frac{\eta - \eta_\infty}{\eta_0 - \eta_\infty} = (1 + (\lambda\dot{\gamma})^2)^{n-1} \tag{5.74}$$

Some GNFs which fits experiments well. Casson

$$\tau^{\frac{1}{m}} = \tau_0^{\frac{1}{m}} + (\eta_\infty \dot{\gamma})^{\frac{1}{m}} \tag{5.75}$$

$$\eta = \eta_\infty \left[1 + \left(\frac{\tau_0}{\eta_\infty \dot{\gamma}} \right)^{\frac{1}{m}} \right]^m \tag{5.76}$$

Viscoplastic model. Bingham: $m = 1$, Casson: $m = 2$ The Casson-model was originally suggested for pigment/oil mixtures, but it has alos been used for blood for small $\dot{\gamma}$. The Casson-model has Newtonian behavior as $\dot{\gamma} \quad \uparrow$.

Cauchy equations for GNFs. Generalized Newtonian fluids

$$\boldsymbol{T} = -p\mathbf{1} + \boldsymbol{\tau} \tag{5.77}$$

Cauchy's equations

$$\rho \frac{\partial \boldsymbol{v}}{\partial t} + \rho(\boldsymbol{v} \cdot \nabla)\boldsymbol{v} = \nabla \cdot \boldsymbol{T} + \rho \boldsymbol{b} \tag{5.78}$$

Cauchy equations for generalized Newtonian fluids

$$\rho \frac{\partial \boldsymbol{v}}{\partial t} + \rho(\boldsymbol{v} \cdot \nabla)\boldsymbol{v} = -\nabla p + \nabla \cdot \boldsymbol{\tau} + \rho \boldsymbol{b} \tag{5.79}$$

Component form

$$\rho(\partial_t v_i + v_k v_{i,k}) = -p_{,i} + \tau_{ik,k} + \rho b_i \tag{5.80}$$

Cauchy equation in cylinder coordinates for GNF

$$\rho\left(\frac{\partial v_r}{\partial t}+v_r\frac{\partial v_r}{\partial r}+\frac{v_\theta}{r}\frac{\partial v_r}{\partial \theta}+v_z\frac{\partial v_r}{\partial z}-\frac{v_\theta^2}{r}\right) = -\frac{\partial p}{\partial r}+\frac{1}{r}\frac{\partial}{\partial r}(r\tau_{rr})+\frac{1}{r}\frac{\partial \tau_{r\theta}}{\partial \theta}+\frac{\partial \tau_{rz}}{\partial z}-\frac{\tau_{\theta\theta}}{r}+\rho b_r \tag{5.81}$$

$$\rho\left(\frac{\partial v_\theta}{\partial t}+v_r\frac{\partial v_\theta}{\partial r}+\frac{v_\theta}{r}\frac{\partial v_\theta}{\partial \theta}+v_z\frac{\partial v_\theta}{\partial z}+\frac{v_r v_\theta}{r}\right) = -\frac{1}{r}\frac{\partial p}{\partial \theta}+\frac{1}{r^2}\frac{\partial}{\partial r}(r^2\tau_{r\theta})+\frac{1}{r}\frac{\partial \tau_{\theta\theta}}{\partial \theta}+\frac{\partial \tau_{\theta z}}{\partial z}+\rho b_\theta \tag{5.82}$$

$$\rho\left(\frac{\partial v_z}{\partial t}+v_r\frac{\partial v_z}{\partial r}+\frac{v_\theta}{r}\frac{\partial v_z}{\partial \theta}+v_z\frac{\partial v_z}{\partial z}\right) = -\frac{\partial p}{\partial z}+\frac{1}{r}\frac{\partial}{\partial r}(r\tau_{zr})+\frac{1}{r}\frac{\partial \tau_{\theta z}}{\partial \theta}+\frac{\partial \tau_{zz}}{\partial z}+\rho b_z \tag{5.83}$$

Example 5.5.1. *Stationary pipeflow for GNF.*

Simplifications: $\boldsymbol{v}$ independent of z and θ. Deviatoric stresses are independent of z and θ.n Symmetry $\Rightarrow \tau_{rz}=\tau_{zr}$.

Cauchy's equations in cylindrical coordinates reduce to:

$$0=-\frac{\partial p}{\partial r}+\frac{1}{r}\frac{\partial}{\partial r}(r\tau_{rr})-\frac{\tau_{\theta\theta}}{r} \quad \text{and} \quad 0=-\frac{1}{r}\frac{\partial p}{\partial \theta}$$
$$0=-\frac{\partial p}{\partial z}+\frac{1}{r}\frac{\partial}{\partial r}(r\tau_{zr})$$

Constant streamwise pressure gradient (i.e., $\partial_z p = c$) due to

$$\frac{\partial^2 p}{\partial \theta \partial z}=\frac{\partial^2 p}{\partial r \partial z}=\frac{\partial^2 p}{\partial z^2}=0 \tag{5.84}$$

From simplified Cauchy equation in z-direction

$$0=-\frac{\partial p}{\partial z}+\frac{1}{r}\frac{\partial}{\partial r}(r\tau_{zr}) \tag{5.85}$$

we get

$$\frac{\partial}{\partial r}(r\tau_{zr})=r\frac{\partial p}{\partial z} \tag{5.86}$$

By integration

$$r\tau_{zr} = \frac{r^2}{2}\frac{\partial p}{\partial z} + C_1 \tag{5.87}$$

As $\tau_{rz}(r=0) = 0 \Rightarrow C_1 = 0$. Equilibrium equation for stationary pipeflow

$$\tau_{zr} = \frac{r}{2}\frac{\partial p}{\partial z} \tag{5.88}$$

May be applied to all GNFs

Example 5.5.2. *Power law for steady pipeflow.*

$$\Rightarrow \tau_{rz} = \frac{1}{2}\frac{\partial p}{\partial z} r \tag{5.89}$$

Use the power law

$$\tau_{rz} = \eta\frac{\partial v_z}{\partial r} = K|\frac{\partial v_z}{\partial r}|^{n-1}\frac{\partial v_z}{\partial r} \tag{5.90}$$

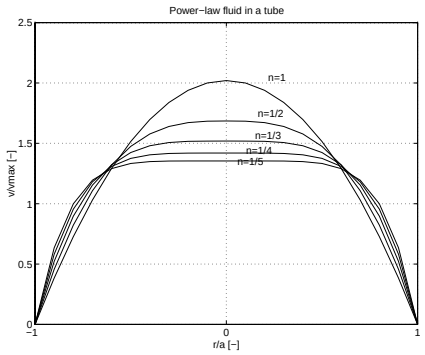

Figure 5.11: Velocity profiles for steady pipeflow of powerlaw fluids with different n.

After subst ($\partial_z p < 0$)

$$\frac{\partial v_z}{\partial r} = -\left(\frac{1}{2K}\frac{\partial p}{\partial z} r\right)^{\frac{1}{n}} \tag{5.91}$$

Integrate and impose BC

$$v_z = \left(\frac{\partial p}{\partial z}\frac{a}{2K}\right)^{\frac{1}{n}} \frac{a}{\frac{1}{n}+1}\left(\left(1-\frac{r}{a}\right)^{\frac{1}{n}+1}\right) \tag{5.92}$$

Power law and Newtonian fluid for stationary pipeflow.

Velocity profile for a power law fluid

$$v_z = \left(\frac{\partial p}{\partial z}\frac{a}{2K}\right)^{\frac{1}{n}} \frac{a}{\frac{1}{n}+1}\left(1-\left(\frac{r}{a}\right)^{\frac{1}{n}+1}\right) \tag{5.93}$$

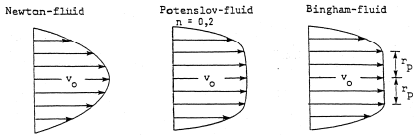

Figure 5.12: Pipe-flow velocity profiles for various model fluids.

Newtonian fluid ($K = \mu$ and $n = 1$) in $\eta = K\dot{\gamma}^{n-1}$ From power law velocity profile

$$v_z = v_0\left(1-\left(\frac{r}{a}\right)^2\right) \tag{5.94}$$

$$v_0 = -\frac{d^2}{16\mu}\frac{\partial p}{\partial z} \tag{5.95}$$

$\Rightarrow$ power law velocity profile reduces to Newtonian expression

Velocity profiles for GNFs

Velocity profiles for Bingham fluids are obtained with similar procedure Based on equilibrium relation for stationary pipeflows Velocity profiles

5.6 Pulsatile flow in straight tubes

The Navier-Stokes equations for fully developed flow in straight pipes reduce to:

$$\frac{\partial v}{\partial t} = -\frac{1}{\rho}\frac{\partial p}{\partial z} + \frac{\nu}{r}\frac{\partial}{\partial r}\left(r\frac{\partial v}{\partial r}\right) \tag{5.96}$$

By introducing characteristic scales for spatial components $r^* = r/a$ and $z^* = z/a$, and for time: $t^* = t\omega$ and velocity: $v^* = v/V$ Eq. (5.96) may be cast into a dimensionless form:

$$\left(a^2\frac{\omega}{\nu}\right)\frac{\partial v^*}{\partial t^*} = -\left(\frac{a}{\rho\nu V}\right)\frac{\partial p}{\partial z^*} + \frac{1}{r^*}\frac{\partial}{\partial r^*}\left(r^*\frac{\partial v^*}{\partial r^*}\right) \tag{5.97}$$

From Eq. (5.97) a natural scale for pressure occurs:

$$p^* = p/(\rho\nu V/a) = p/(\mu V/a) \tag{5.98}$$

which by substitution into Eq. (5.97) gives the simensionless straight tube equations

$$\alpha^2 \frac{\partial v^*}{\partial t^*} = -\frac{\partial p^*}{\partial z^*} + \frac{1}{r^*}\frac{\partial}{\partial r^*}\left(r^* \frac{\partial v^*}{\partial r^*}\right) \tag{5.99}$$

where the Womersley parameter:

$$\alpha = a\sqrt{\frac{\omega}{\nu}} \tag{5.100}$$

has been introduced.

Flows where $\alpha \to \infty$ are commonly denoted inertia dominated, as viscous forces are negligible compared to the other terms in Eq. (5.99) and the pressure gradient is used solely for acceleration of the fluid mass. Such a situation will typically occur in large vessels, at high frequency flows. In the aorta $\alpha \geq 20$.

Similarly, flows where $\alpha \to 0$ (i.e., for small vessels and/or low frequencies) are called friction dominated. In the capillaries $\alpha = 10^{-2}$.

5.6.1 Straight tube velocity profiles

For developed, transient flow in a straight tube the momentum equation reduces to:

$$\alpha^2 \frac{\partial v}{\partial t} = -\frac{\partial p}{\partial z} + \frac{1}{r}\frac{\partial}{\partial r}\left(r \frac{\partial v}{\partial r}\right) \tag{5.101}$$

As (5.101) is linear in v superposition of solutions for various harmonics is ok. To proceed further, we assume the driving force to be oscillating and represent it by:

$$\frac{\partial p}{\partial z} = \frac{\partial \hat{p}}{\partial z} e^{it} \tag{5.102}$$

Due to the harmonic form of the pressure gradient we furhter assume that the velocity may be represented in a similar manner as $v = \hat{v}e^{it}$. By substitution into momentum equation (5.101) we get:

$$i\alpha^2 \hat{v}(r) = -\frac{\partial \hat{p}}{\partial z} + \frac{1}{r}\frac{\partial}{\partial r}\left(r \frac{\partial \hat{v}}{\partial r}\right) \tag{5.103}$$

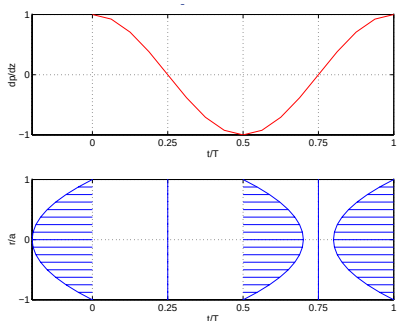

Figure 5.13: Pressure gradient (upper panel) and velocity profile (lower panel) as a function of time for friction dominated flows [40].

To approach the problem gently we first study the situation of small or vanishing Womersley parameter ($\alpha \to 0$) in (5.101), which corresponds to a situation of **friction dominated straight pipe flow**. In this situation (5.101) reduces to:

$$\frac{1}{r}\frac{\partial}{\partial r}\left(r\frac{\partial \hat{v}}{\partial r}\right) = \frac{\partial \hat{p}}{\partial z} \tag{5.104}$$

Solution

$$\hat{v} = -\frac{1}{4}\frac{\partial \hat{p}}{\partial z}\left(1 - r^2\right) \tag{5.105}$$

In the time domain

$$v(r,t) = \Re\left(-\frac{1}{4\mu}\frac{\partial p}{\partial z}(a^2 - r^2)\right) \tag{5.106}$$

To simplify the notation we remove $*$ f while noting that time is dimensionless.

The opposite extreme to friction dominated flows is **inertia dominated flows** with large Womersley parameter, corresponding to ($\alpha \to \infty$) in (5.101), corresponding to:

$$i\alpha^2 \hat{v}(r) = -\frac{\partial \hat{p}}{\partial z} \tag{5.107}$$

Solution

$$\hat{v}(r) = \frac{i}{\alpha^2}\frac{\partial \hat{p}}{\partial z} \tag{5.108}$$

In the time domain

$$v(t) = \Re\left(\frac{i}{\rho\omega}\frac{\partial p}{\partial z}\right) \tag{5.109}$$

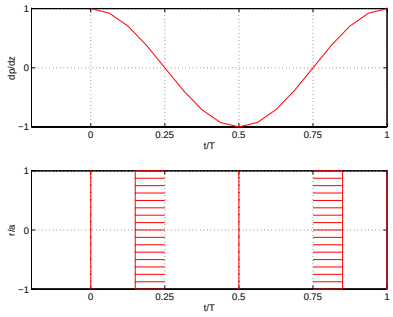

Figure 5.14: Pressure gradient (upper panel) and velocity profile (lower panel) as a function of time for inertia dominated flowscite [40].

For the case of inertia dominated flow, boundary layer analsysis may be used to characterize v [40], where the relative magnitudes of the terms are

$$\begin{aligned} \frac{\partial v}{\partial t} &= -\frac{\partial p}{\partial z} & +\frac{\nu}{r}\frac{\partial}{\partial r}\left(r\frac{\partial v}{\partial r}\right) \\ \mathcal{O}(\omega V) & & \mathcal{O}\left(\frac{\nu V}{\delta^2}\right). \end{aligned}$$

From this an instationary boundary layer thickness is estimated as

$$\mathcal{O}(V\omega) = \mathcal{O}\left(\frac{\nu V}{\delta^2}\right) \Rightarrow \delta = \mathcal{O}\left(\sqrt{\frac{\nu}{\omega}}\right) \tag{5.110}$$

which may be expressed in terms of α as

$$\delta = \mathcal{O}\left(\frac{a}{\alpha}\right), \quad \alpha > 1. \tag{5.111}$$

To derive a velocity profile for arbitrary α, condsider the momentum equation in frequency domain

$$i\omega\alpha^2\hat{v} = -\frac{\partial\hat{p}}{\partial z} + \frac{1}{r}\frac{\partial}{\partial r}\left(r\frac{\partial\hat{v}}{\partial r}\right) \ . \tag{5.112}$$

Substitute $s = i^{3/2}\alpha r$ to case the equation as an inhomogeneous Bessel equation $n = 0$

$$\frac{\partial^2\hat{v}}{\partial s^2} + \frac{1}{s}\frac{\partial\hat{v}}{\partial s} + (1 - \frac{n^2}{s^2})\, v = \frac{i}{\rho\omega}\frac{\partial\hat{p}}{\partial z}. \tag{5.113}$$

Combining the homogenous solution and a particular solution, constant v, one may show

$$\hat{v}(r) = \frac{i}{\rho\omega}\frac{\partial \hat{p}}{\partial z}\left(1 - \frac{J_0(i^{3/2}\alpha r/a)}{J_0(i^{3/2}\alpha)}\right) \tag{5.114}$$

where the boundary conditions and continuity are employed to determine the coefficients of the combiniation of independent solutions.

Thus the Womersley profiles for straight pipe flow are given by

$$v(r,t) = \Re\left(\frac{i}{\rho\omega}\frac{\partial p}{\partial z}\left(1 - \frac{J_0(i^{3/2}\alpha r/a)}{J_0(i^{3/2}\alpha)}\right)\right) \tag{5.115}$$

and shown in the following figures and movie.

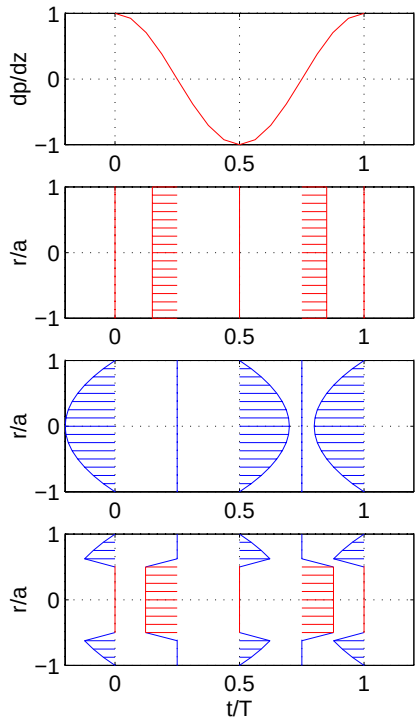

Figure 5.15: Velocity profiles for arbitrary Womersley numbers [40].

5.6.2 Wall shear stress for pulsatile flow in straight tubes

By using the property of the Bessel functions (see equation (50)):

$$\frac{\partial J_0(s)}{\partial s} = -J_1(s) \tag{5.116}$$

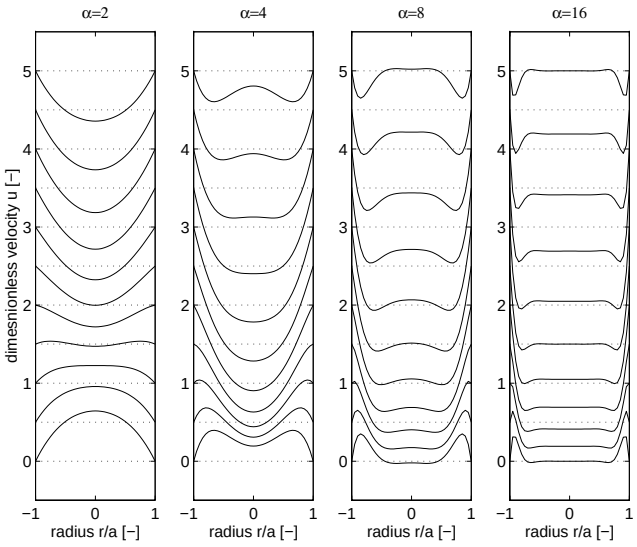

Figure 5.16: Velocity profiles for various Womersley numbers ($\alpha = 2, 4, 8, 16$) [40]. (Animation).

and introducing the Womersley function:

$$F_{10}(\alpha) = \frac{2J_1(i^{3/2}\alpha)}{\alpha i^{3/2}\, J_0(i^{3/2}\,\alpha)} \tag{5.117}$$

the wall shear stress given by:

$$\tau_w = \mu \frac{\partial v}{\partial r}|_{r=a} \tag{5.118}$$

can be found from equation (5.115) to be:

$$\tau_w = -\frac{a}{2} F_{10}(\alpha) \frac{\partial p}{\partial z} = F_{10}(\alpha)\tau_w^p \tag{5.119}$$

where τ_w^p is the wall shear stress for Poiseuille flow.

Further, the mean flow may be derived using the property (again see equation (50) for n = 1):

$$sJ_0(s)\, ds = d(sJ_1(s)) \tag{5.120}$$

together with the definition:

$$\begin{aligned} q &= \int_0^q v\, 2\pi r dr = j\frac{\pi a^2}{\rho\omega}\left(1 - F_{10}(\alpha)\right)\frac{\partial p}{\partial z} \\ &= \left(1 - F_{10}(\alpha)\right)\hat{q}_\infty \\ &= \frac{8j}{\alpha^2}\left(1 - F_{10}(\alpha)\right)\hat{q}_p \end{aligned} \tag{5.121}$$

where we have introduced limiting values for the flow: $\hat{q}_p$ and $\hat{q}_\infty$, for small and large Womersley numbers α, respectively:

$$\hat{q}_p = \frac{\pi a^4}{8\mu}\frac{\partial \hat{p}}{\partial z} \qquad \text{and} \qquad \hat{q}_\infty = \frac{j\pi a^2}{\rho\omega}\frac{\partial \hat{p}}{\partial z} \tag{5.122}$$

Finally, an expression relating the wall shear stress and the flow rate may be obtained from equation (5.119) and (5.121) in which the pressure gradient has been eliminated:

$$\tau_w = \frac{a}{2A} j\omega\rho \frac{F_{10}(\alpha)}{1 - F_{10}(\alpha)}\, q \tag{5.123}$$

where the vessel cross-sectional area is represented by $A = \pi a^2$.

5.6.3 Longitudinal impedance for pulsatile flow in straight tubes

For later use observe that the *longitudinal impedance*
defined as:

$$Z_l = -\frac{\frac{\partial p}{\partial z}}{q} \tag{5.124}$$

may be derived directly for pulsatile flow in straight pipes from (5.121):

$$Z_l = j\omega\frac{\rho}{\pi a^2}\,\frac{1}{1 - F_{10}(\alpha)} \tag{5.125}$$

For small Womersley numbers (or Poiseuille flow), the longitudinal impedance Z_p may be found by integration of equation (5.104) to be:

$$Z_p = \frac{8\mu}{\pi a^4} \tag{5.126}$$

Based on the expressions in equation (5.125) and (5.126) and expression for the the longitudinal impedance relative to the Poiseuille resitance may be derived too:

$$\frac{Z_l}{Z_p} = \frac{j\alpha^2}{8} \frac{1}{1 - F_{10}(\alpha)} \tag{5.127}$$

One may show (see illustrations in Fig. 4.7 in[40]) that for small α a good approximation is:

$$\frac{Z_l(\alpha < 3)}{Z_p} \approx 1 + \frac{j\alpha^2}{8} \tag{5.128}$$

and the viscous forces are seen to dominate and the pressure gradient is almost in phase with the flow.

For large values of α the ratio may be approximated by:

$$\frac{Z_l(\alpha > 15)}{Z_p} \approx \frac{j\alpha^2}{8} \tag{5.129}$$

The pressure gradient is consequently out of phase with the flow for inertia dominate flows.

Chapter 6

The cardiovascular system

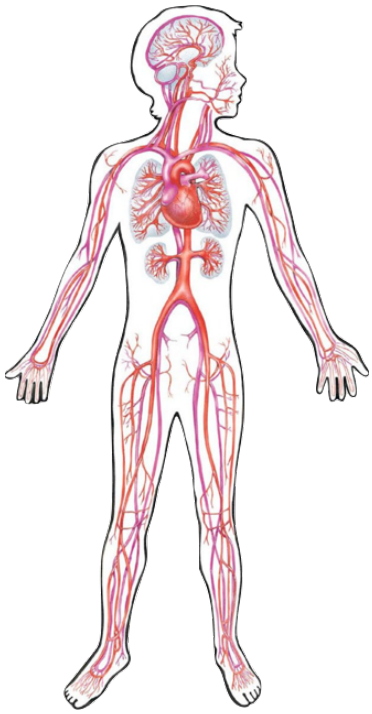

Figure 6.1: An overview of the CVS from About the circulatory system (American Heart Association).

The cardiovascular system has three main components. a) Blood is the medium of convective transport of oxygen, carbon dioxide, nutritients, and other solutes between the organs, followed by diffusive transport to the tissues at cellular level. Without this convective transport an appropriate exchange of the solutes would be impossible due to a too large diffusional resistance [40].

b) The circulatory system is the distribution system for blood and is made up of a network of blood vessels, namely the arteries which transport blood away from the heart and the veins, which the veins which transport towards the heart. c) The heart is a four-chambered pump that drives the blood flow in the circulatory system. The circulatory system may be subdivided into two systems in series, the pulmonary circulation and the systemic circulation (Figure 6.1). Blood flows from the superior and inferior vena cava in to the right atrium, then through the tricuspid valve in to the right ventricle, subsequently through the semilunar valves into the pulmonary artery, which strongly bifurcates in pulmonary arterioles transporting the blood to the lungs. Oxygenated blood is the transported through the pulmonary veins to the left atrium, and further through the mitral valve, the left ventricle, and finally thorough the aortic valve into the aorta. The peripheral circulation starts with the aorta, perfuses various organs, and returns to the right atrium. In each organ, flow begins in the arteries, perfuses the micro-circulatory bed, and finally drains into veins. The vena cava drain blood from the various organs, and return it to the heart [13].

6.1 Pressure and flow in the cardiovascular system

6.1.1 Arterial anatomy

Inspired by the presentation in [30], an overview of the of the arterial anatomy is given in this section. The aorta is the main artery with a proximal diameter of 2-3 cm in the human adult (see (6.5)). Originating from the left ventricle, the aorta is separated from the ventricle lumen during diastole,whereas there is direct communication between the left ventricle and the aorta during systole.

The aorta tapers and the distal aortic diameter is about 1 cm. Normally, three main branches are found on the top of the aortic arch, bifurcating into the arteries towards the head and the upper limbs. The descending aorta is divided into the thoracic and the abdominal part as the aorta crosses the diaphragm. In the abdomen, important aortic branches provide blood flow to the kidneys (constituting about 15% of the blood volume) and the gastro-intestinal organs. At the distal end, the aorta bifurcates into two iliac arteries, providing blood supply to the lower extremities.

Towards the head, the most important branches are the left and right common carotid arteries, which bifurcate further into the internal and external carotid arteries. These arteries are superficial, and are therefore readily accessible for non-invasive measurements of pressure and flow. The pressure

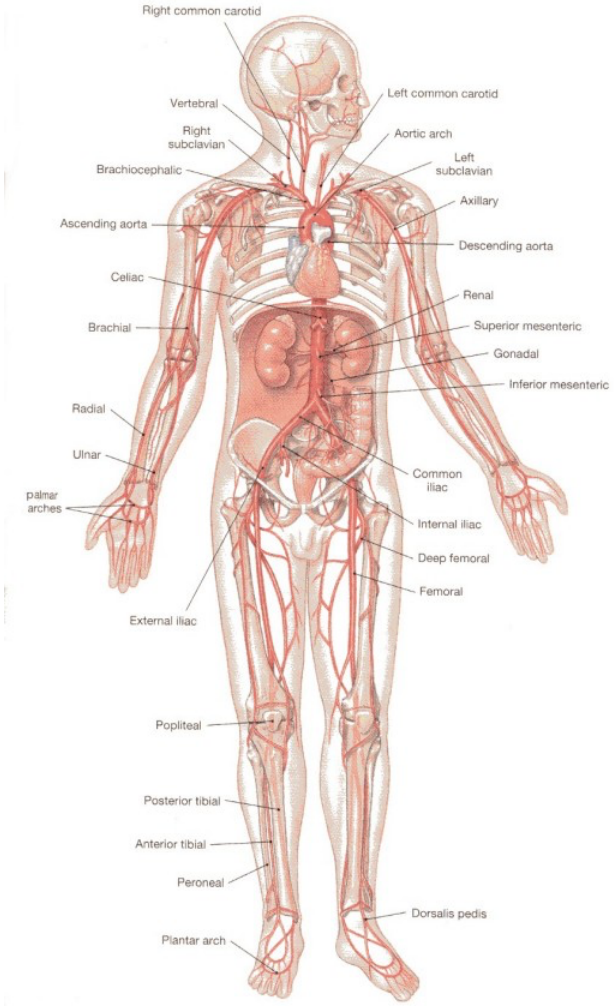

Figure 6.2: The systemic arteries

pulsation can easily be felt in then neck. Blow supply to the upper limbs are provided by the subclavian artery, which changes name to the brachial artery in the upper arm, and bifurcates at the elbow to the radial and the ulnar artery. These arteries are the most commonly used sites for non-invasive pressure recordings: the brachial for sphygmomanometric measurements; the radial and subclavian arteries for tonometric measurements.

In the abdomen, the most important branches are those which supply the gastro-intestinal organs with blood; hepatic artery to the liver; gastric artery to the stomach, splenic artery to the spleen, the superior and inferior mesenteric arteries to the intestines, and the renal arteries to the kidneys.

The renal arteries captures up to 15% of the total stroke volume, whereas all abdominal arteries receives about 40% of the total stroke volume.

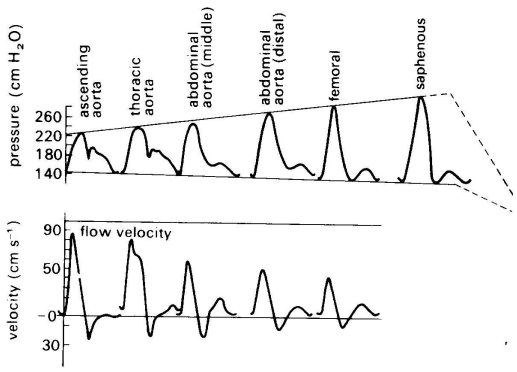

Figure 6.3: Propagation of pressure and flow waves in the systemic circulation of a dog (adopted from [25])

During systole, the ventricle ejects blood into the arteries, giving rise to pressure and flow waves traveling from the heart towards the periphery (see figure 6.3). The pressure peak is delayed with increasing distance from the heart, indicating wave propagation along the aorta with a finite pulse wave velocity or wave speed. Further, the pressure wave is characterized by a progressively increasing amplitude (systolic pressure), and a steepening of the front [24]. Only a moderate fall in the mean pressure with increasing distance is observed, indicating minor effects of viscous friction. The viscous effects are limited to only a few mmHg in the large and mid-sized arteries (e.g., radial artery).

The rise in the pressure *amplitude* on the other hand, is determined by the varying local characteristic impedance (i.e., elastic properties of the arteries and the vessel dimensions), as well as heart rate and stroke volume. As we will learn in more detail in chapter 7; any change in the characteristic impedance, which depends on the local pulse wave velocity (or compliance) and the cross-sectional area of the vessels, will give rise to wave reflections.

For now we settle for the explanation that the observed wave phenomenon in the arterial tree is a direct consequence of the locally varying distensibility or compliance (see section 6.1.2) of the arterial wall, allowing for a partial and temporary storage of the blood ejected from the heart.

In accordance with the increase in pressure amplitude, the flow wave is damped progressively due to the reflections, and to the buffering capacity (or compliance) of the arteries towards the periphery. In total, the pulsatile flow in the aorta is transformed to a quasi stationary flow at the arteriolar and capillary level.

The peak value of the pressure, measured at any location, is called the systolic pressure p_s, the minimal pressure is denoted the diastolic pressure p_d. These values are frequently measured with a sphygmomanometer at the upper arm (brachial artery).

However, it is clear from the previous paragraphs, that these values are not constant over the arterial tree. The mean arterial pressure p_m may be estimated from p_s and p_d at the brachial artery from the formula:

$$p_m = p_d + \frac{p_s - p_d}{3} = p_d + \frac{pp}{3} \tag{6.1}$$

where the pulse pressure $pp = p_s - p_d$, has been introduced.

The blood pressure is traditionally expressed in mmHg (1 mmHg = 133.3 Pa).

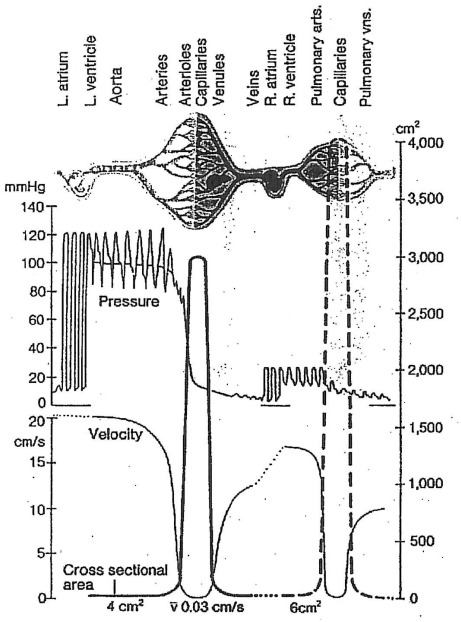

Figure 6.4: Spatial variation of pressure, mean velocity and cross sectional area for the systemic and pulmonary circulatory system (adopted from [28]).

The mean arterial pressure is mainly determined by the peripheral resistance in the smaller arteries/arterioles/capillaries, whereas the systolic and diastolic pressures result from the characteristic impedance (i.e., elastic and geometric properties) of the large arteries (wave reflection), heart rate and stroke volume.

Spatial pressure, mean velocity and cross-sectional variations in the systemic and pulmonary circulatory systems are illustrated in figure 6.4. Only a

slight pressure decrease from the aorta (at approximately 100 mmHg) to the smaller arteries. The major part of the pressure drop takes part at the arterioles and the capillaries, yielding a venous pressure of about 5 mmHg. The arterioles and capillaries are therefore commonly referred to as the *resistance vessels*, whereas the large arteries are referred to as the *conduit vessels*. The total peripheral resistance of all systemic capillaries, R is calculated from the mean arterial pressure p_m, the venous pressure p_v and the mean flow rate Q (or cardiac output CO):

$$R = \frac{p_m - p_v}{Q_m} \approx 60 \frac{p_m}{CO} \tag{6.2}$$

As an example: a typical mean pressure of $p_m = 100$ mmHg and $CO = 6$ l/min, correspond to a total peripheral resistance of R = 1 mmHg/(ml/s). Note that the right heart operates at a much lower pressure than the left heart. Consequently the wall thickness of the left ventricle will be larger than that of the right ventricle, to maintain the wall stresses in the myocardium at approximately the same levels.

Despite the bifurcating anatomy of the aorta and the progressive decrease of the volumetric flow rate at greater distance from the heart, the mean blood velocity is more or less constant, due to the geometric tapering of the aorta (see figure 6.5)

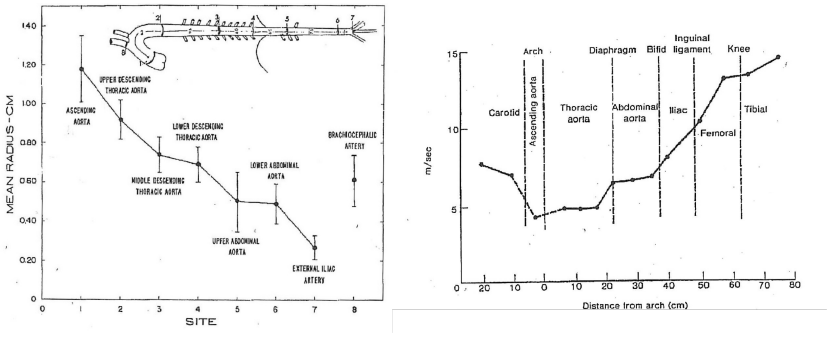

Figure 6.5: Illustration of the aortic tapering (adopted from [11]) and the progressive increase in pulse wave velocity (adopted from [26])

Apart from the geometric tapering of the aorta, the aorta also exhibits a progressive increase in the wall stiffness and accordingly, an increase in the pulse wave velocity (see figure 6.5). This property is a consequence of an increased radius/wall thickness ration and an intrinsic increase in the aortic elasticity modulus.

6.1.2 Compliance and distensibility

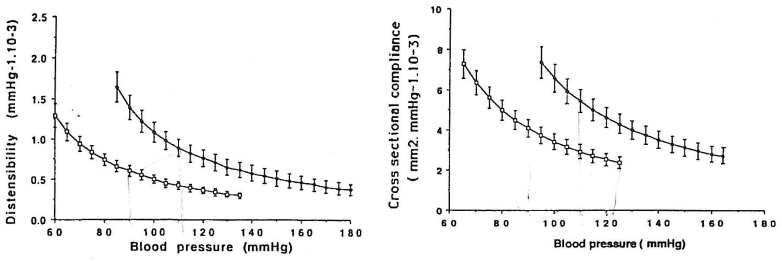

Figure 6.6: Distensibility D and compliance C in a population of normotensive (open circles) and hypertensive (filled circles). Adopted from [19].

The compliance and distensibility of a blood vessel is a local property depending on the local transmural pressure[1] and the elastic properties of the vessel wall. The relation between the cross-sectional area A and the transmural pressure p is nonlinear and can be rather complicated. Moreover, it varies from one vessel to another. Important quantities used to describe this relation are the *compliance* which is defined as:

$$C = \frac{\partial A}{\partial p} \tag{6.3}$$

and the *distensibility* D given by:

$$D = \frac{1}{A}\frac{\partial A}{\partial p} = \frac{C}{A} \tag{6.4}$$

In the sequel these quantities will be related to the material properties of the arterial wall. For thin walled vessels, with radius a, cross sectional area A, and wall thickness h one may show that (see equation (7.106)):

$$C = 2\frac{a}{h}\frac{A}{\eta} \qquad \text{and} \qquad D = 2\frac{a}{h}\frac{1}{\eta} \tag{6.5}$$

where η denotes the Youngs modulus of the vessel wall. Thus, we see that appart from the material properties of the vessel represented by η, the geometric properties (a, h) also play an important role. The value of the the radius/wall thickness ratio a/h varies strongly along the arterial tree.

[1] i.e. pressure difference over the vessel wall.

From equation (6.5) we see that the compliance C is a local property of the vessel wall, which depends both on the geometry ($\frac{a}{h}$ and A) and the mechanical property of the vessel η.

Subject to the assumption of a linear material, the distensibility D seem to be somewhat more of a mechanical property from equation (6.5), as D is not explicitly depending of cross-sectional area A. But even for this simple material law, D still depends on the radius/wall thickness ratio, and may thus not be regarded as a strict mechanical property.

Arteries are know to exhibit a nonlinear pressure-area relationship, leading to nonlinear compliance and distensibility. This should be kept in mind for the comparison of normotensive and hypertensive patients, as illustrated in figure 6.6, adopted from [19]. With respect to their own mean pressures, hypertensives (mean 90 mmHg) have lower compliance C and distensibility D than normotensives.

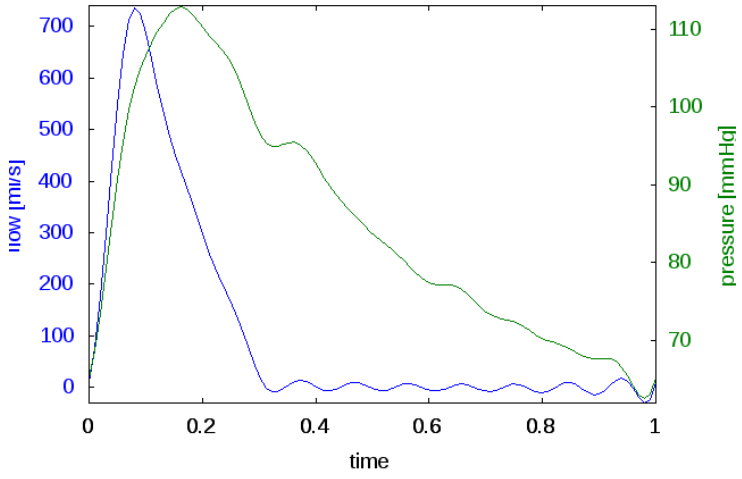

Figure 6.7: Pressure and flow in the aorta based on the data given in the table below.

6.1.3 Mathematical representation of periodic pressure and flow

The flow is driven by the pressure gradient and thus locally determined by the propagation of the pressure wave. Due to the rhythmic contractions of the heart, the pressure will have a periodic character. To describe the flow phenomena we distinguish between the steady and the unsteady part of the

pulses generated by the heart. Often it is assumed that the unsteady part may be described by linear theory, in order to introduce pressure and flow waves as superpositions of several harmonics:

$$p = \sum_{n=0}^{N} p_n \, e^{j\omega_n t} \quad \text{and} \quad q = \sum_{n=0}^{N} q_n \, e^{j\omega_n t} \tag{6.6}$$

where p_n and q_n are complex Fourier coefficients, and $\omega_n = n\,\omega_1$ and ω_1 represents the angular frequency of the fundamental harmonic of the functions (signals) p and q. Note that the functions are implicitly assumed to be periodic with the representation in equation (6.6), and that the steady parts of the pressure and flow are represented by their average values p_0 and q_0, respectively. Further, a complex notation had been used in equation (6.6) in which:

$$e^{j\omega t} = \cos(\omega t) + j \sin(\omega t) \tag{6.7}$$

with $j = \sqrt{-1}$.

n	$\lvert p\rvert$	$\angle(p)$	$\lvert Q\rvert$	$\angle(Q)$
0	110	0	85	0
1	202	-0.78	18.6	-1.67
2	156	-1.50	8.6	-2.25
3	103	-2.11	5.1	-2.61
4	62	-2.46	2.9	-3.12
5	47	-2.59	1.3	-2.91
6	42	-2.91	1.4	-2.81
7	31	2.92	1.2	2.93
8	19	2.66	0.4	-2.54
9	15	2.73	0.6	-2.87
10	15	2.43	0.6	2.87

Table: The first 10 harmonics of the pressure and flow in the aorta (adopted from [24]).

The actual pressure and flow may be obtained by taking the real part of these complex functions. Representing a function of time as the real part of a complex or exponential expression simplifies the calculations to such an extent that it is widely used in hemodynamics, though it must be remembered that it can be applied only to sinusoidal (periodic) components obtained by frequency analysis, not to natural pulsations [24]. Vascular impedance at a given frequency, for example, is defined as the ratio of complex pressure to complex flow (see section 6.1.4), the latter being complex exponential expressions whose real part are harmonics of the observed pressure and flow.

In many situations from 6 to 10 harmonics are sufficient to represent most of the features of the pressure and flow waves in the cardiovascular system. The table above is adopted from [24, 40] and represents the modulus and phase for the first 10 harmonics of pressure and flow in the aorta. The corresponding pressure and flow are given in figure 6.7.

6.1.4 Vascular impedance

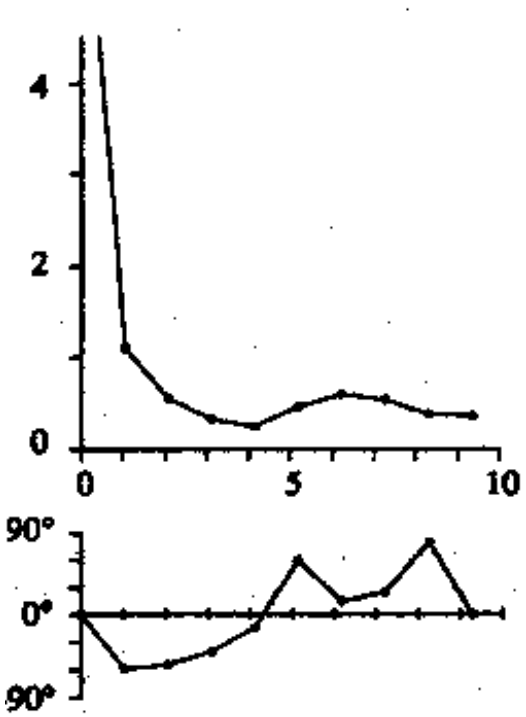

Figure 6.8: A typical Z_i for a young healthy adult (from [25]).

Based on the assumption that the relation between pressure and flow can be represented by a linear theory, as outlined in section 6.1.3,vascular impedance is introduced to represent the relation between corresponding harmonics of pressure and flow.

Thus, one may roughly think of impedance as some frequency dependent resistance. The concept of impedance is of great importance in biofluid dynamics and has many different areas of application. Therefore, four different definitions of impedance have been introduced [25].

Characteristic impedance: The characteristic impedance Z_c, and the wave speed are two important parameters characterizing the wave transmission and reflection properties in a blood vessel [47]. These two quantities can be derived from the linearized mass and momentum equations for compliant blood vessel flow (see section 7.4.2). These linearized and simplified equations are similar to those for so-called transmission-line theory, and thus the involved physics has analogies to what happens in telegraph lines, or antenna cables, for the transmission of electromagnetic waves. The characteristic impedance is defined as the ratio of the forward propagating pressure and the forward propagating flow and has (Under certain simplifying assumptions, see section 7.4.2) the representation:

$$Z_c = \frac{\rho c}{A} \tag{6.8}$$

where c represents the wave speed, ρ the fluid density, and A the vessel cross-sectional area. Note that this quantity is not influenced by wave reflections, and is thus a local characteristic property of the vessel wall.

Input impedance Z_i and terminal impedance: Z_T

The input impedance Z_i is defined in a very similar manner as the characteristic impedance, namely as the ratio of the pulsatile components of pressure and flow:

$$Z_i(\omega_n) = \frac{p_n(\omega_n)}{q_n(\omega_n)} \tag{6.9}$$

Importantly, the input impedance is *not* restricted to unidirectional waves, i.e., reflected wave components are included. Thus, Z_i is a global quantity that characterize the properties distal (downstream) to the point of measurement. The cumulative effect of all distal contributions is incorporated in the input impedance. In the aorta Z_i represents the afterload on the heart.

In Figure 6.8 the input impedance of a young healthy subject is depicted. For high frequencies the phase angles are close to zero, as high frequency components are more damped and reflections tend to cancel out. The negative phase angle for the low-frequency components correspond to that flow components lead pressure, i.e., the aorta first sees flow and the pressure.

The terminal impedance Z_T is defined in the same way as the input impedance, the only difference being that the input impedance normally alludes to the aorta, whereas the terminal impedance may be measured to represent the load anywhere in the vascular tree.

Longitudinal impedance: Z_l

It is the pressure gradient which drives the flow, and the relation of the two is expressed by the longitudinal impedance:

$$Z_l = \frac{\partial \hat{p}}{\partial z}/\hat{q} \tag{6.10}$$

The longitudinal impedance is a complex number defined by the complex pressure gradient and complex flows. It can be calculated by frequency analysis of the pressure gradient and the flow that have been measured simultaneously. Z_l plays an important role in the characterization of vascular segments. In chapter 5.6.3, Z_l is derived analytically for pulsatile rigid pipe flow using Womersley theory. For small Womersley numbers α the we get that $Z_l \approx Z_p = 8\mu/\pi a^4$, i.e., an Poiseuille resistance, whereas for large α the $Z_l \approx j\alpha^2/8$.

Transversal impedance: Z_t

The compliance of an arterial segment is characterized by the transverse impedance defined by:

$$Z_t = \hat{p}/\frac{\partial \hat{q}}{\partial z} \approx -\hat{p}/j\omega\hat{A} \tag{6.11}$$

The transverse impedance expresses the flow drop due to the storage of the vessel resulting from the radial motion of the wall [40], which in turn is caused by the pressure $\hat{p}$. From the mass conservation equation (7.14) for compliant vessels we have:

$$\frac{\partial A}{\partial t} = -\frac{\partial q}{\partial z} \tag{6.12}$$

and therefore from Fourier transformation:

$$j\omega\hat{A} = -\frac{\partial \hat{q}}{\partial z} \tag{6.13}$$

which may be substituted into the definition of Z_t in equation (6.11) to provide the given approximation.

6.2 Lumped models

Currently, the term lumped models allude to a family of mathematical models for the load to the heart, in which the physics of the entire systemic arterial tree is represented by a few, lumped parameters.

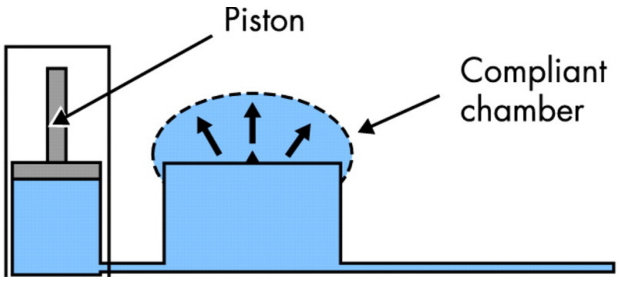

Figure 6.9: The heart ejects blood intermittently into the compliant aorta, like water pumped in to a Windkessel with a compliant air chamber (adopted from [22]).

Stephen Hales (1733) presented a basic, and conceptual model of the arterial tree, based on the observation that the blood flow in the peripheral arteries is relatively smooth, despite the pulsatile action of the heart. He envisioned that the interaction between the heart and the arteries has similarities with the working principle of a fire hose, in which the pulsatile action of the pump is damped by an air chamber (Windkessel in German). In the cardiovascular system, large arteries play the role of the air chamber of a Windkessel (fig. 6.9)

In 1899 Otto Frank formulated these ideas mathematically, by introducing the two element Windkessel which consisted of two building blocks: the peripheral resistance, R, (representing the peripheral arterioles and capillaries), and the total arterial compliance C, which accounts for the compliance (or elasticity) of the larger conduit vessels.

A more accurate description of the pressure-flow relation may be obtained by including more lumped elements in a lumped model of the cardiovascular system. For example the characteristic impedance Z_c of the aorta is added for the 3-element Windkessel model, resulting in a better description of the high frequency modes of the aortic input impedance and accordingly a better prediction of the aortic pressure pulse [44]. An overview of the most commonly used lumped models for the vascular tree is given by [39] [39]. Increasing complexity of the lumped models provides better prediction of the pressure-flow relation. However, as the number of lumped elements increase, the physical meaning and hence the determination of each individual parameter becomes less clear [30]. It has been shown that the three-element Windkessel systematically overestimates arterial compliance [34, 7]. As pointed out in [24], whenever more and more complexity must be introduced into a scientific theory to make its predictions match reality, it is usually time to look for a new hypothesis.

However, in spite of the severity of the underlying assumptions, lumped parameter models can be used for various purposes:

- Estimation of the mechanical properties of the arterial circulation.
- Representation of a part of the circulatory system (e.g., the arterioles and capillaries or the part of the vascular tree not accounted for in greater detail), for more complex models such as 1D network models accounting for wave propagation phenomena or 3D FSI-models and CFD models.
- A tool to get more insight into the physical problem.

6.2.1 The Windkessel model

Figure 6.10: The rate of change of arterial volume equals the difference between aortic inflow (Q) and outflow (Q_p) towards the periphery.

The mathematical representation of the Windkessel model attributed to Otto Frank, is obtained by the requirement of mass conservation for a model of the vascular tree as seen in figure 6.10. Let Q represent the inflow to the aorta, and Q_p the flow towards the periphery, whereas Q_a represents the stored volume per time unit in the aorta. The ordinary differential equation, representing the Windkessel model is then obtained by the requirement of mass conservation:

$$Q = Q_a + Q_p = \frac{\partial V}{\partial p}\frac{\partial p}{\partial t} + \frac{p}{R} \tag{6.14}$$

$$= C\frac{\partial p}{\partial t} + \frac{p}{R} \tag{6.15}$$

where $C = \partial V/\partial p$ is the total arterial compliance, and $Q_p = p/R$ and R is the total peripheral resistance. We may rewrite equation (6.15) on a conventional differential equation form:

Two element Windkessel model

$$\frac{\partial p}{\partial t} + \frac{1}{RC}\, p = \frac{Q(t)}{C} \tag{6.16}$$

which is the differential equation for the Windkessel model in figure 6.11. Mathematically we realize that equation (6.16) represents a first order, linear, temporally driven differential equation. The homogenous solution p_h, to equation (6.16), i.e., a vanishing right hand side of equation (6.16), is given by:

$$p_h = p_0\, e^{-\frac{(t-t_0)}{\tau}} \tag{6.17}$$

where p_0 is a constant depending on the initial conditions at time t_0 and $\tau = RC$ represents a time constant. The solution p_h is sometimes referred to as the autonomous solution, as in this case there is no driving force on the right hand side of the differential equation (6.16).

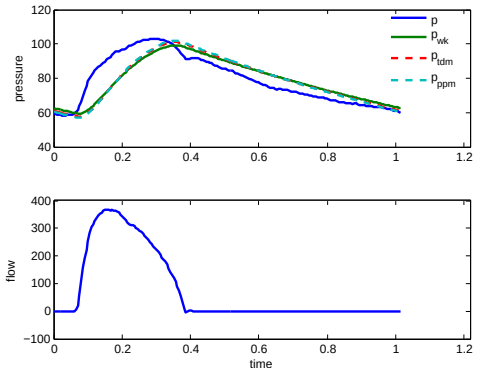

Figure 6.11: Aortic flow (lower pane) from measurements and measured and predicted aortic pressures (upper panel). The measured pressure is represented with a solid dark blue line.

The solution of equation (6.16) with a right hand side unequal to zero, normally referred to as the inhomogenous solution or the particular solution , may found by assuming that $p_0 = p_0(t)$, i.e., that p_0 is a function of time:

$$p = p_0(t)\, e^{-\frac{t}{\tau}} \tag{6.18}$$

Differentiation of equation (6.18) yields:

$$\frac{\partial p}{\partial t} = \frac{\partial p_0}{\partial t}\, e^{-\frac{t}{\tau}} - \frac{1}{\tau}\, p_0(t)\, e^{-\frac{t}{\tau}} \tag{6.19}$$

which by substitution in equation (6.16) cancels the second term and we are left with:

$$\frac{\partial p_0}{\partial t} = \frac{Q(t)}{C}\, e^{\frac{t}{\tau}} \tag{6.20}$$

Equation (6.20) may then readily be integrated to give:

$$p_0(t) = \frac{1}{C} \int_{t_0}^{t} Q(t')\, e^{\frac{t'}{\tau}}\, dt' \tag{6.21}$$

and by subsequent substitution of equation (6.21) into equation (6.18) we obtain a particular solution:

$$p_p(t) = \frac{1}{C} \int_{t_0}^{t} Q(t')\, e^{\frac{t'-t}{\tau}}\, dt' \tag{6.22}$$

Finally, we obtain the generic solution for the two-element Windkessel model, represented by equation (6.16), as the sum of the homogenous solution p_h in equation (6.17) and the particular solution p_p in equation (6.22):

Generic solution for the two-element Windkessel model.

$$p(t) = p_0\, e^{-\frac{(t-t_0)}{\tau}} + \frac{1}{C} \int_{t_0}^{t} Q(t')\, e^{\frac{t'-t}{\tau}}\, dt' \tag{6.23}$$

We observe that the flow $Q(t)$ occurs as a driving function in the second term of equation (6.23), and that this term has the form of a convolution integral. Therefore, for a given initial pressure p_0 at time t_0, and flow as a function of time $Q(t)$, on may compute the pressure $p(t)$ from equation

(6.23). The integral may readily computed numerically, e.g. with trapezoidal numerical integration, whenever an analytical solution is not tractable.

However, the numerical integration in equation (6.23) may be avoided, based on the following reasoning. Normally, pressure and flow measurements are sampled at discrete time instances $t_i = i\,\Delta t$, where Δt is the sample interval and consequently $t_1 = \Delta t$. Further, we introduce the standard notation: $p_0 = p(t_0), p_1 = p(t_1), \ldots, p_i = p(t_i)$ and similarly for samples of the flow $Q_i = Q(t_i)$. The integral in equation (6.23) may then be evaluated for $t = t_1$, i.e., the interval for the time integration is $t_1 - t_0 = \Delta t$. A fair assumption to make is that $\Delta t/\tau \ll 1$, as the sampling rate Δt, normally is small (typically $5 \cdot 10^{-3}\,s$, and τ is a relaxation scale which should be a fraction of the heart rate (approximately the period of diastole, $\tau = RC \propto 0.5\,s$). Subject to these assumptions we get from equation (6.23):

$$p(t_1) = p_0\, e^{-\frac{\Delta t}{\tau}} + \frac{1}{C}\int_{t_0}^{t_1} Q(t')\, e^{\frac{t'-t_1}{\tau}}\, dt' \tag{6.24}$$

$$= p_0\, e^{-\frac{\Delta t}{\tau}} + \frac{Q(t_1^*)}{C}\int_{t_0}^{t_1} e^{\frac{t'-t_1}{\tau}}\, dt', \qquad t_0 \le t_1^* \le t_1 \tag{6.25}$$

$$= p_0\, e^{-\frac{\Delta t}{\tau}} + \frac{Q(t_1^*)\,\tau}{C}\, e^{\frac{t'-t_1}{\tau}}\Big|_{t_0}^{t_1} = p_0\, e^{-\frac{\Delta t}{\tau}} + \frac{Q(t_1^*)\,\tau}{C}\left(1 - e^{\frac{-\Delta t}{\tau}}\right) \tag{6.26}$$

$$\approx p_0\left(1 - \frac{\Delta t}{\tau}\right) + \frac{Q(t_1^*)\,\Delta t}{C} \tag{6.27}$$

The first identity in equation (6.24) follows from the mean value theorem (33), where $Q(t_1^*)$ denote a mean value of the flow $Q(t)$ in the sampling interval $[t_0, t_1]$. The two following identities are analytical evaluations of the remaining integral. Finally, a Taylor expansion yields an approximation in the last expression in the equation (6.24). From, the estimation of the integral in equation (6.24), a generalized expression for $p(t_i)$ follows naturally:

$$p_i \approx p_{i-1}\left(1 - \frac{\Delta t}{\tau}\right) + \frac{Q(t_i^*)\,\Delta t}{C} \tag{6.28}$$

The expression in equation (6.23), works remarkably well in correlating experimental data on pressure p and flow Q, in particular during diastole (see [12, p. 23] and [23, pp. 11, 210, 423]). Otto Frank reasoned that the decay of the diastolic pressure in the ascending aorta, when flow is zero, can be expressed by and exponential curve [47, p. 122]. Observe that this observation is in agreement with the homogenous solution of equation (6.16) given by equation (6.17). The time constant $\tau = RC$, expresses the time needed for the pressure to decrease to 37% of the starting pressure. The larger the

resistance, the slower the blood will leave the compliant arteries. Conversely, the larger the compliance, the more blood is stored in the compliant arteries, and the longer time is needed for this blood to leave these vessels.

Non-invasive estimation of mean flow. The cross-sectional area compliance C_A, may be estimated if the pulse wave velocity is measured (see equation (7.78)) along with the averaged cross-sectional area [47]. Subsequently, the volume compliance C may be estimated as $C \approx C_A L_a$, if the length L_a, of the aorta is measured. The peripheral resistance may then be calculated as:

$$R = \frac{\tau}{C} \tag{6.29}$$

Finally, the mean flow $\bar{Q}$ may then be found from mean pressure $\bar{p}$ by:

$$\bar{Q} = \frac{\bar{p}}{R} \tag{6.30}$$

The assumption that all compliance is lumped in the aorta, and implicitly assuming infinite wave speed in the aorta, introduces an error. Only after pulsatile flows could be measured, and the arterial input impedance could be determined, the shortcomings of the two-element Windkessel became clear [47, chap 24].

The impedance of the two-element Windkessel. By proposing that the pressure and the flow may be expressed as Fourier series (see equation (6.6)) (and thus implicitly assume periodic solutions) the impedance for a two element Windkessel may be found by substation in equation (6.16):

Impedance of two element Windkessel.

$$Z_n^{WK} = \frac{R}{1 + j\omega_n RC} \tag{6.31}$$

which also may be conveniently represented on polar form (see [49]):

$$Z_n^{WK} = \frac{R}{\sqrt{1 + (\omega_n \tau)^2}}\, e^{j\theta} \quad \text{with} \quad \theta = -\arctan(\omega\tau) \tag{6.32}$$

where $\tau = RC$ has been introduced as a relaxation time for the Windkessel.

The impedance for the Windkessel is a complex quantity with a modulus and phase, which has been plotted for each harmonics (frequency) in figure 6.12. Observe that for the two element Windkessel, both modulus and phase decrease monotonous as a function of the frequency.

The Windkessel model as a pure resistor or a pure capacitor

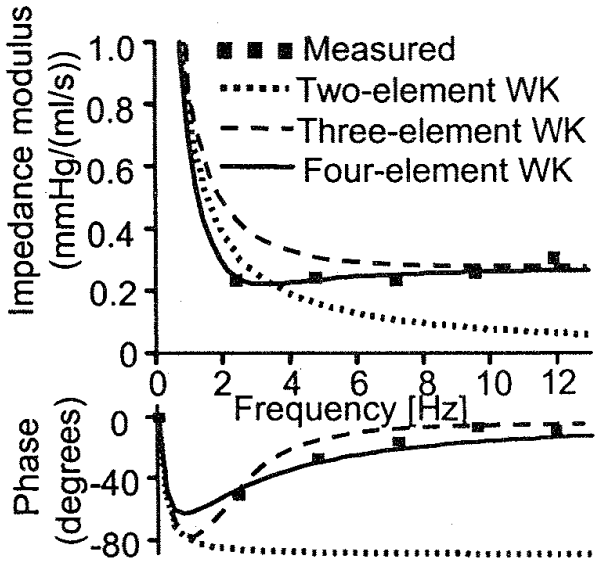

Figure 6.12: A comparison of the input impedances of the two-element, three-element and four element Windkessel models (adopted from [47]).

We observe for later use, that the impedance of the Windkessel will approach a pure resistor if:

$$Z_n^{WK} = \frac{R}{1 + j\omega_n RC} \approx R \tag{6.33}$$

which is satisfied if $RC \ll 1$, i.e., $R \ll 1/C$. At the same time we require that $R \gg C$, as the impedance is supposed to be more of a resistor type than a compliant chamber type. Consequently, for a Windkessel to approach a pure resistor we require:

$$Z_n^{WK} \approx R \quad \text{if} \quad C \ll R \ll 1/C \tag{6.34}$$

On the contrary, the Windkessel will approach a pure capacitor if:

$$Z_n^{WK} = \frac{1}{1/R + j\omega_n C} \approx \frac{1}{j\omega C} \quad \text{if} \quad C \gg 1/R \tag{6.35}$$

6.2.2 The three-element Windkessel model

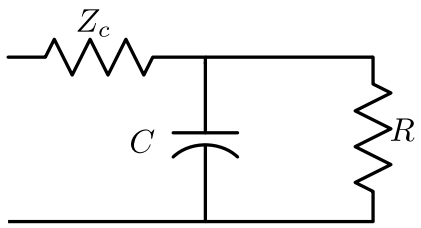

Figure 6.13: The three-element Windkessel model.

The three-element Windkessel model (see figure 6.13) is based on the two-element Windkessel model of Otto Frank, with an additional characteristic impedance Z_c [45]. The aortic characteristic impedance Z_c account for the combined effects of compliance and inertance of the very proximal aorta, and thus forms a link with the transmission line models. In order to derive the mathematical representation of the threee-element Windkessel, let p denote the pressure at the aortic root and p_d an aortic pressure at an undetermined but more distal position in the aorta (see figure 6.13). The pressure drop $p - p_d$ between these two location is then given by:

$$p - p_d = Z_c Q \tag{6.36}$$

whereas the relation between p_d and Q is given by the previously derived differential equation for the two-element Windkessel (equation (6.16)), when p_d is substituted for p. Thus,

$$\frac{\partial p_d}{\partial t} + \frac{p_d}{RC} = \frac{Q}{C} \tag{6.37}$$

The distal pressure p_d may then be eliminated by substitution of equation (6.36) into equation (6.37) which results in the following differential equation for the three-element Windkessel model:

$$\frac{\partial p}{\partial t} + \frac{p}{RC} = \frac{Q}{C}\left(1 + Z_c/R\right) + Z_c \frac{\partial Q}{\partial t} \tag{6.38}$$

The input impedance of the three-element Windkessel may be shown to be:

$$Z_i = \frac{R + Zc + j\omega R Z_c C}{1 + j\omega RC} \tag{6.39}$$

From measurements for pressure and flow, the total peripheral resistance R is calculated from the time averaged pressure p_m and flow Q_m. One the has the option to set $R = p_m/Q_m$ or $R + Z_c = p_m/Q_m$ [34]. Based on the input impedance from the measurements, the characteristic impedance may be estimated by averaging the high frequencies [18]. Leaving only one unknown model parameter, namely the compliance C.

The remaining model parameter C is finally determined by using the measured flow as input to the three-element Windkessel model and fitting the (complete) estimated pressure response to the measured pressure.

Note one can also estimate the model parameters by fitting input impedance of the model to the measured input impedance.

The procedure can be applied in a number of different ways, depending on the calculation of R and Z_c from the measurements. The various approaches have been assessed in [34] applying a non-linear 1D network-model for the vascular tree. The overall conclusion is that methods based on the three-element Windkessel model overestimate compliance (from 15-40%). Further, the calculation of the pressure response yields the best results, whereas the integral method is the inferior approach of the ones tested.

Windkessel models are frequently used to terminate more advanced models such as 1D network models and FSI/CFD-models. Such models are frequently discretize in the time-domain, and thus it is advantageous to discretize the Windkessels in the time-domain too. The discretization of the three-element Windkessel model is conveniently done by using and implicit time discretization of the differential equation (6.38):

$$\frac{p^{n+1} - p}{\Delta t} + \frac{p^{n+1}}{RC} = \frac{f(Q)}{C} \tag{6.40}$$

where we for simplicity introduce the source on the right hand side as a function of the flow:

$$f(Q) = Q\,(1 + Z_c/R) + Z_c C \frac{\partial Q}{\partial t} \tag{6.41}$$

which yields:

$$p^{n+1} = \frac{p + \Delta t/C\, f(Q)}{1 + \Delta t/\tau} \tag{6.42}$$

where $\tau = RC$. This procedure holds for both two-element and three-element Windkessel models, as the only difference the $f(Q) = Q$ in for the two-element Windkessel (see equations (6.16) and (6.38)).

6.2.3 Methods for estimation of total arterial compliance

The time decay method (TDM) for estimation of total arterial compliance

The time decay method (TDM) is based on the assumption (see fig. 6.11) that the aortic flow is approximately zero during diastole ($Q \approx 0$). From equation (6.23) we then see that for a Windkessel model the pressure reduces to:

$$p(t) = p_{t=t_d} e^{-\frac{(t-t_d)}{\tau}} \tag{6.43}$$

where t_d the time for the onset of diastole. By nature, this method is tailored to approximate the compliance of the aorta, and has thus limited applicability to other parts of the cardiovascular network due to the assumption of zero flow. To avoid high frequency disturbances, the onset of the diastole is normally not taken to be the time for the incisura in the aortic pressure (see upper panel of figure 6.11) , but rather the last $2/3^{\text{rd}}$ of the diastole.

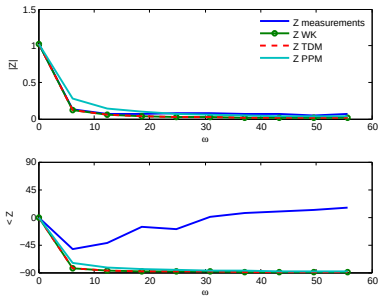

Figure 6.14: Impedance absolute value $|Z|$ and phase angle $\angle Z$ for measurements and various methods for estimation of total arterial compliance.

From the expression for the impedance of the two element Windkessel in equation (6.32) we see that:

$$Z_0^{WK} \equiv \frac{p_0}{q_0} = R \tag{6.44}$$

The TDM method requires the knowledge of some measure of the flow rate in the aorta (i.e., the mean flow rate q_0 with units $[q_0] = m^3/s$ or more commonly

the cardiac output CO which is expressed in l/min). From equation (6.44) we get:

$$R = \frac{60\ p_0}{1000\ CO} \tag{6.45}$$

i.e., the peripheral resistance R is obtained form the averaged pressure p_0 and the cardiac output CO. The only remaining unknown in the pressure given by equation (6.17) is the total arterial compliance, which may be obtained by a least square procedure (curve fitting), where the difference between the measured pressure and the predicted pressure by equation (6.17) is minimized.

Example 6.2.1. *Estimation of total arterial compliance with the TDM method.*

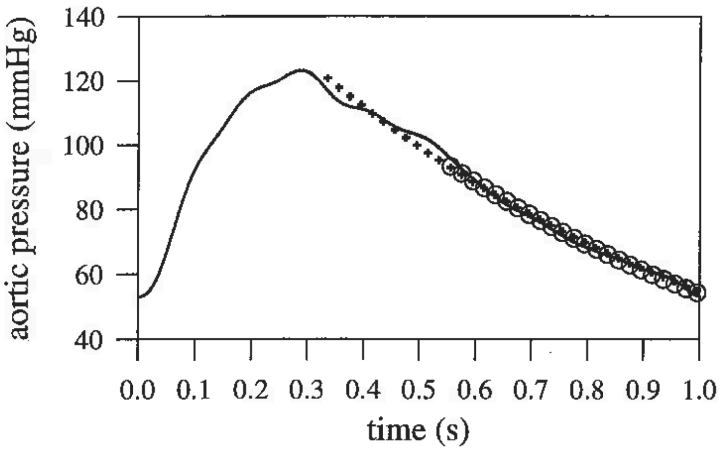

Figure 6.15: The TDM method for the complete diastole (+) and for the last $2/3^{\text{rd}}$ (o) of the diastole (taken from [30]).

To see how the TDM method may be applied, consider some synthetic pressure and flow data, simulated with a linear transmission line model [29, 30]. In the transmission line model, non-linear convective terms and viscous losses are omitted from the governing mass and momentum equations for pulsatile flow in compliant vessels (see equations (7.24) and (7.25)). Further, viscoelasticity is not accounted for in the transmission line model.

The input for the simulation is a physiological flow wave at a heart rate of 60 beats/min. The material parameters for the *model* are chosen such that the total peripheral resistance $R_{pm} = 1$ mmHg/(ml/s) and the total compliance $C_m = 0.86$ ml/mmHg. The simulated pressure resulting from the physiological flow wave input, is given by the solid line in figure 6.15.

An estimated total arterial compliance $C_e \approx 0.84$ ml/mmHg ($\pm 2.3\%$) is obtained, using the TDM on the complete diastole. When the TDM is applied on the last $2/3^{\text{rd}}$ of the diastole, the estimate of the total arterial compliance reduces to $C_e \approx 0.81$ ml/mmHg ($\pm 5.8\%$). The resulting pressures for the two TDM approaches are illustrated in figure 6.15.

The area method (AM) for estimation of total arterial compliance

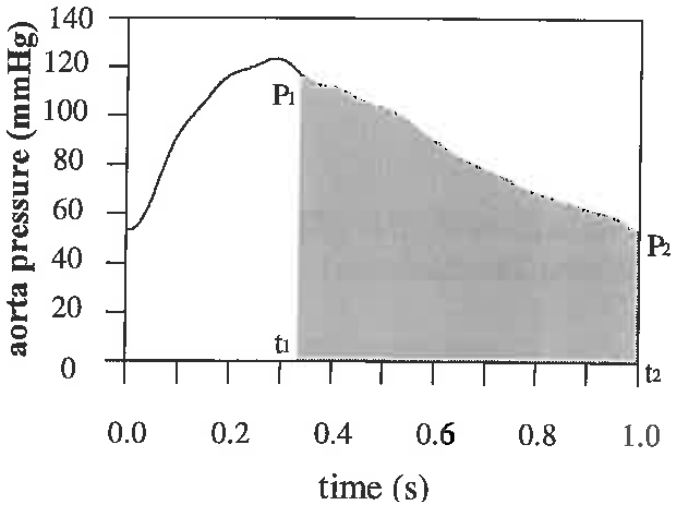

Figure 6.16: Illustration of the area method (taken from [30]).

To motivate the area method[20], let t_1 and t_2 denote two moments in time during diastole, in which we assume the flow $Q \approx 0$. From the differential equation (6.16) representing the Windkessel model we get:

$$\int_{t_1}^{t_2} \frac{\partial p}{\partial t} + \frac{1}{RC}\, p \; dt = 0 \tag{6.46}$$

which after integration and rearrangement under the assumption of constant R and C may be presented as:

$$RC = \frac{\int_{t_1}^{t_2} p \; dt}{p(t_2) - p(t_1)} \tag{6.47}$$

We observe that the integral in the numerator of equation (6.47) is the area under the pressure curve between the two moments in time t_1 and t_2,

respectively. Naturally, The name of the method is inspired from this property of the method.

As for the TDM, the peripheral resistance R is estimated from the mean pressure p_0 and the CO by equation (6.45). Thus, the total arterial compliance may be computed directly from equation (6.47). An advantage of the AM in comparison with the TDM, is that the exponentially decaying pressure curve does not have to be fitted. For the same conditions as in Example 6.2.1, the AM provides an estimate of the total arterial compliance of $C_{AM} \approx 0.87$ ml/mmHg ($\pm 1.2\%$). The method is also applicable when the pressure whenever the diastolic pressure is no true exponential function and the method can, according to the authors, be extended with a non-linear pressure volume relation. However, the compliance, obtained at mean pressure, corresponds well with the value obtained with a constant compliance [20]. Note that different diastolic time intervals may be chosen, and the resulting estimate will be sensitive to the specific interval. The authors suggest that the time interval between the dicrotic notch and the end diastole is chosen (as in figure 6.16).

The pulse pressure method (PPM) for estimation of total arterial compliance

The Pulse Pressure Method (PPM), like the previous methods in this section, provides an estimate of the total arterial compliance based on measurements of pressure and flow as a function of time at the ascending aorta.

The PPM originally suggested by [34], predicts pressure by an imposed flow from the two element Windkessel model (see e.g., equation (6.28)), where the resistance is taken as the ratio of mean pressure to mean flow (see equation (6.44)). However, the PPM differs from the other methods by the fact that it is only the *pulse pressure* (i.e., the difference between systolic(maximum pressure and diastolic pressure (minimal pressure)) which is used in the in the least square estimation procedure for estimation of the total arterial compliance. This results in a simple and stable iteration scheme, which is independent of the initial values of the parameter to be estimated. Neither does the method depend on a given time interval in the diastole. And further, the method applies for both normal and pathological cases.

Application of the PPM (approximation in the frequency domain) on synthetic data yields a total arterial compliance of 0.82 ml/mmHg, which is an underestimation of 4.2% [30].

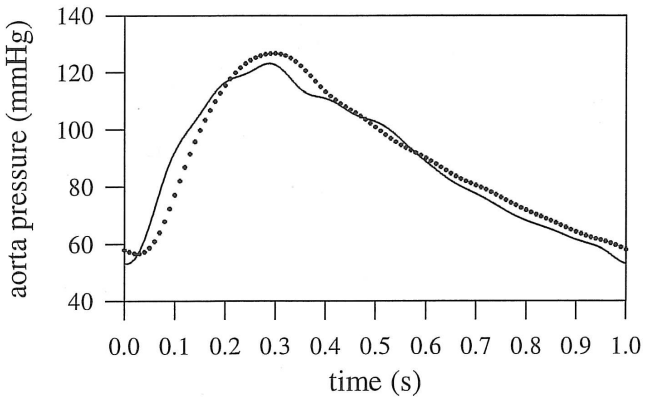

Figure 6.17: Pressure from a 2WK with a total arterial compliance from the PPM (dots), and measured pressure (solid line). Illustration of the area method (taken from [30]).

Exercise 4: Windkessel model

a) The two element Windkessel model (see (6.16)) is given by the con olution integral in (6.23). An approximated expression for the convolution integral is provided in eq:394. Show that an identical approximation may be obtained by discretizing equation (6.16) with a backward Euler scheme.

b) Outline a strategy for an evalutation of the various methods to estimate the total arterial compliance in section (6.2.1).

Chapter 7

Blood flow in compliant vessels

The arterial system is a complex network of viscoelastic vessels, with complex geometries, nonlinear elastic properties. Additionally the blood rheology is complex and the blood has generally non-Newtonian properties. Pressure and flow waves are set up by the heart and interacts with the arterial system. Thus, the arterial system will continuously modify the pressure and flow waves from the heart.

In this section the 1D governing equations for pressure and flow waves will be derived on a basis where most of the complicating factors mentioned above will be discarded.

The first section 7.1, we consider Poiseuille flow in a compliant vessel, i.e., only a simplified version of the momentum equation is included, whereas convective terms, and thus wave propagation phenomena, are not accounted for. However, an important feature for flow in compliant vessels, namely chocked flow, is illustrated with this simple model.

The following sections (7.2) and (7.3) are devoted to derivation of 1D governing equations for wave propagation in compliant vessels. In section 7.2 a flat velocity profile is assumed, whereas a velocity profile is accounted for in section (7.3).

7.1 Poiseuille flow in a compliant vessel

Simplified solution for flow in compliant vessel. In general Navier-Stokes equations for blood, Navier equations for vessel wall, must be solved simultaneously. Simplification; Poiseuille flow for the fluid, $p(A)$ relation for vessel wall.

Poiseuille flow relates pressure gradient to volume flow:

$$\frac{dp}{dx} = -\frac{8\mu}{\pi a^4}\, Q = -\frac{8\pi\mu}{A^2}\, Q \tag{7.1}$$

Compliance $C = \dfrac{\partial A}{\partial p}$

$$\frac{dp}{dx} = \frac{\partial p}{\partial A}\,\frac{dA}{dx} = \frac{1}{C}\,\frac{dA}{dx} = -\frac{8\pi\mu}{A^2}\, Q \tag{7.2}$$

$$A^2\,\frac{dA}{dx} = \frac{1}{3}\,\frac{d}{dx}\left(A^3\right) = -8\pi\mu C Q \tag{7.3}$$

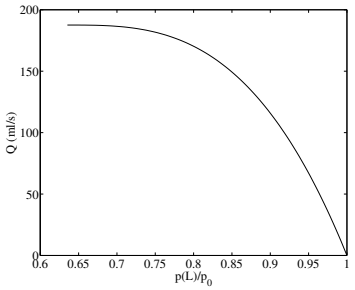

Figure 7.1: Flow versus normalized outlet pressure for Poiseuille flow in compliant pipe.

Integration

$$A(x)^3 = A(0)^3 - 24\pi\mu C Q x \tag{7.4}$$

Constitutive model: $A(p) = A_0 + C\,(p - p_0)$
Pressure and flow for stationary flow in compliant vessel

$$Q(x) = \frac{A(0)^3 - A(x)^3}{24\pi\mu C x}, \quad p(x) = p_0 + \frac{A(x) - A(0)}{C} \tag{7.5}$$

7.2 Infinitesimal derivation of the 1D governing equations for a compliant vessel

In this section the 1D governing equations for mass and momentum will be derived in a somewhat simpler way than in section (7.3). In the derivation we will first consider mass and momentum for a control volume. However,

the length of the control volume will later be reduced to zero. Thus, higher order terms may be neglected for several terms.

Some of the first scientific papers on this issue include [36, 2, 14].

7.2.1 Conservation of mass

Blood may normally be considered incompressible ($\rho = \text{constant}$) and thus conservation of mass per time unit reduces to:

$$\dot{V} = Q_i - Q_o \tag{7.6}$$

where $\dot{V}$ denotes rate of change in volume, whereas Q_i and Q_o is volume flow rate in and out of the volume, respectively (see Figure 7.2).

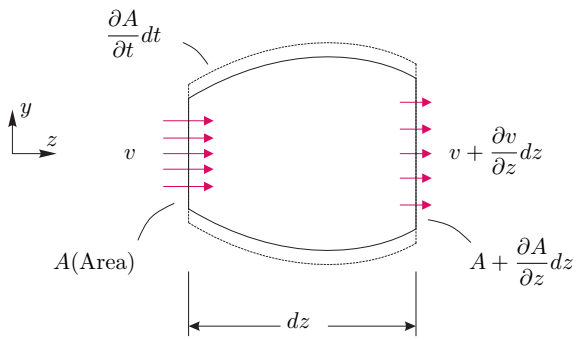

Figure 7.2: A deformable control volume with fixed endpoints.

By adopting the convention in ((7.43)) of section 7.3 the volumetric influx into the volume Q_i (Figure 7.2) may be expressed by:

$$Q_i = \int_{A_0} v_3 \, \mathrm{dA} = vA \tag{7.7}$$

For the outflux the spatial changes in the velocity in the axial direction must be accounted for:

$$Q_o = \int_A \left(v_3 + \frac{\partial v_3}{\partial z} \, dz \right) \, \mathrm{dA} \approx vA + \frac{\partial (vA)}{\partial z} \, \mathrm{dz}, \quad A_0 = A + \frac{\partial A}{\partial z} \, dz \tag{7.8}$$

The deformation of the volume is assumed to be homogeneous in the axial direction and consequently the rate of change in volume may be expressed by:

$$\dot{V} \approx \frac{\partial A}{\partial t} \, dz \tag{7.9}$$

Note, that the assumption of homogeneous deformation has no significant bearings as the length dz control volume collapse to zero in the final expression.

Finally, the equation for conservation of mass is obtained by combination of (7.6), (7.7), (7.8) and (7.9) and subsequent division by dz :

$$\frac{\partial A}{\partial t} + \frac{\partial Av}{\partial z} = 0 \tag{7.10}$$

The equation for mass conservation in (7.10) may alternatively be derived by using the Reynolds transport theorem for deformable control volumes (2.33). As for the former derivation in this section, we assume a control volume which deforms with the compliant vessels, but tether the endpoints (see Figure 7.2). The mass equation is obtained by letting the generic intensive property b be the mass density ρ:

$$\dot{m} = \frac{dm}{dt} = \frac{d}{dt} \int\limits_{V_c(t)} \rho \, dV + \int\limits_{A_c(t)} \rho \left(\boldsymbol{v} - \boldsymbol{v}_c \right) \cdot \boldsymbol{n} \, dA = 0 \tag{7.11}$$

Note, that the control volume velocity $\boldsymbol{v}_c = 0$ at the fixed endpoints z_1 and z_2 of $V_c(t)$ the control volume, whereas $\boldsymbol{v}_c = \boldsymbol{v}$ at the compliant vessel wall. Thus, the flux terms in (7.11) will only give contributions at the endpoints, as the flux at the the vessel wall be zero. Further, the time derivative of the volume integral in (7.11) may be put inside the integral sign if the axial coordinate z is iterated first:

$$\dot{m} = \int\limits_{z_1}^{z_2} \frac{\partial(\rho A)}{\partial t} \, dz + (\rho v A)_2 - (\rho v A)_1 = 0 \tag{7.12}$$

where $v = \bar{v}_z$, i.e., the cross-sectional averaged z-component of $\boldsymbol{v}$, $A = A(z)$ is the cross-sectional area at any location z. The subscripts of the flux terms refers to location z_1 and z_2, respectively. By assuming a constant density ρ of the fluid in the compliant vessel, it may be eliminated from (7.12) to yield:

$$\dot{m} = \int\limits_{z_1}^{z_2} \frac{\partial A}{\partial t} + \frac{\partial vA}{\partial z} \, dz = 0 \tag{7.13}$$

As (7.13) must be valid for any choice of $V_c(t)$, i.e., z_1 and z_2, the integrand must vanish, and thus the differential form of the mass conservation equation given in (7.10) is obtained. As $vA = Q$ an equivalent equation for mass conservation is:

$$\frac{\partial A}{\partial t} + \frac{\partial Q}{\partial z} = 0 \tag{7.14}$$

7.2.2 The momentum equation

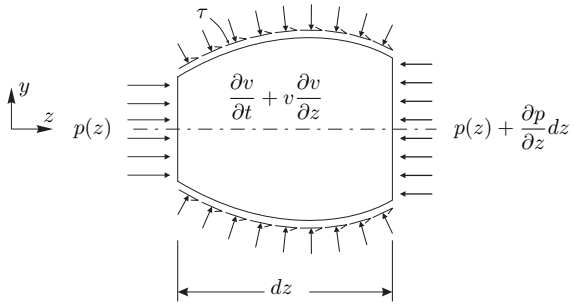

Figure 7.3: Outline of control volume with pressure and velocity.

The derivation of the momentum equation is based on Euler's first axiom which states that the rate of linear momentum is balanced balanced by the net force. In this section we will express the various contributions to the net force and subsequently present an expression for the rate of linear momentum, which will lead us to a momentum equation.

The first force contribution we will consider is that of pressure. As can be seen from Figure 7.3, pressure will contribute on all surfaces of our control volume. The pressure force acting on the left hand side will be:

$$F_{p_i} = pA \tag{7.15}$$

On the right hand side the expression for the pressure contribution is somewhat more complicated:

$$F_{p_o} = -\left(p + \frac{\partial p}{\partial z}\,dz\right)\left(A + \frac{\partial A}{\partial z}dz\right) \tag{7.16}$$

The pressure acting on the surface A will also have an axial contribution which may be shown to be:

$$F_{p_A} = p\frac{\partial A}{\partial z}\,dz \tag{7.17}$$

Wall friction may be accounted for by introducing the wall shear stress τ, which will be a function of the cross-wise velocity profile (see (7.70)). In order to derive the momentum equation it will suffice to present the viscous force contribution as:

$$F_\tau = \tau\pi D\,dz \tag{7.18}$$

Finally, the net force is found by summation of (7.15), (7.16), (7.17), and (7.18):

$$F_{\text{net}} = -A\frac{\partial p}{\partial z}\,dz + \tau\pi D\,dz \tag{7.19}$$

Further, we need an expression for the rate of change of linear momentum $\boldsymbol{P}$ (see (2.6)) in the z-direction, and employ the Reynolds transport theorem for deformable control volumes, in the same manner as for the derivation of the mass conservation equation.

$$\dot{P}_z = \frac{d}{dt}\int\limits_{V_c(t)} \rho v_z\,dV + \int\limits_{A_c(t)} \rho v_z\,(\boldsymbol{v}-\boldsymbol{v}_c)\cdot\boldsymbol{n}\,dA \tag{7.20}$$

which, by arguing in the same manner as for the mass conservation derivation, may be simplified to:

$$\dot{P}_z = \int\limits_{z_1}^{z_2} \frac{\partial \rho\overline{v_z}A}{\partial t}\,dz + (\rho\overline{v_z^2}A)_2 - (\rho\overline{v_z^2}A)_1 \tag{7.21}$$

By assuming a flat velocity profile we have $\overline{v_z^2} = \bar{v}_z^2$ and by further simplification of the notation by $v = \bar{v}_z$ we get:

Finally, a momentum equation may be formed by assembling the rate of change of linear momentum in equation (7.21) and the net force in equation (7.19):

$$\frac{\partial v}{\partial t} + v\frac{\partial v}{\partial z} = -\frac{1}{\rho}\frac{\partial p}{\partial z} + \frac{\pi D}{\rho A}\,\tau \tag{7.22}$$

Note, that conceptually we have a problem with (7.22) as the left hand side is derived for invicid flow, whereas the right hand side has a viscous friction term. However, in this section (7.22) will serve as an approximation to the more elaborated expression derived in (7.70). The friction term depends on the local, time-dependent velocity profile and must be estimated in some appropriate way.

Together, mass conservation equation (7.10) and balance of linear momentum (7.22) form a system of partial differential equations:

$$\frac{\partial v}{\partial t} + v\frac{\partial v}{\partial z} = -\frac{1}{\rho}\frac{\partial p}{\partial z} + \frac{\pi D}{\rho A}\,\tau \tag{7.23}$$

which are the governing equations for wave propagation in blood vessels.

It can be shown, by using the mass conservation equation, that an alternative formulation of the governing equations, with volume flow Q rather that mean velocity v as the primary variable, satisfy:

$$\frac{\partial A}{\partial t} + \frac{\partial Q}{\partial z} = 0 \tag{7.24}$$

$$\frac{\partial Q}{\partial t} + \frac{\partial}{\partial z}\left(\frac{Q^2}{A}\right) = -\frac{A}{\rho}\frac{\partial p}{\partial z} + \frac{\pi D}{\rho}\tau \tag{7.25}$$

Regardless of the chosen formulation, the governing equations constitute two differential equations, with three primary variables (either p, v, and A or p, Q, and A). Consequently a constitutive equation, i.e., a relation between pressure and area, is needed to close the system of equations. An example of a simple linear constitutive model is:

$$A(p) = A_0 + C\,(p - p_0), \quad C = \frac{\partial A}{\partial p} \tag{7.26}$$

where the subindex of zero refers to a given state of reference. From (7.26) and the chain rule for derivation we get:

$$\frac{\partial A}{\partial t} = \frac{\partial A}{\partial p}\frac{\partial p}{\partial t} = C\frac{\partial p}{\partial t} \tag{7.27}$$

7.3 Integral derivation of the 1D governing equations for a compliant vessel

7.3.1 1D transport equation

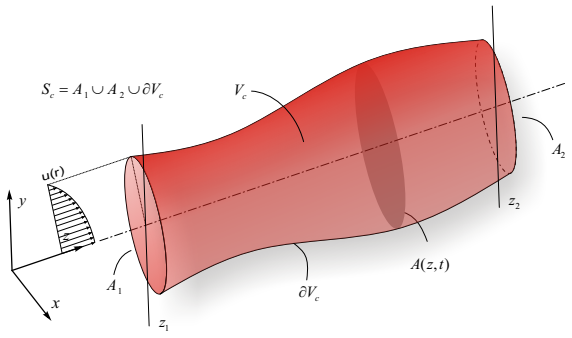

Figure 7.4: A compliant vessel with axial coordinate z and surface area $A(z,t)$

A fluid with constant mass density ρ is flowing through a compliant vessel of volume V_c. The volume is bounded by two *fixed* spatial planes in the xy-plane, denoted A_1 and A_2, with corresponding coordinates z_1 and z_2. Vector

components with respect to a fixed spatial coordinate system are denoted with subscripts 1, 2, 3, corresponding to respective spatial directions x, y, z, e.g., v_1, v_2, v_3 are the components of the velocity vector $\boldsymbol{v}$. The lateral surface (luminary boundary) A of the vessel is allowed to move. However, note that it does not necessarily have to be a material surface with respect to the fluid, as fluid may be allowed to pass through the vessel wall [14]. Thus, the vessel volume V_c, which we will consider as our control volume, has a surface $S_c = A_1 \cup A_2 \cup A_3$.

The Reynolds transport theorem for a moving control volume (2.33) with a generic density β takes the form:

$$\dot{B} = \frac{d}{dt} \int\limits_{V(t)} \beta \, dV = \frac{d}{dt} \int\limits_{V_c(t)} \beta \, dV + \int\limits_{S_c(t)} \beta \, (\boldsymbol{v} - \boldsymbol{v}_c) \cdot \boldsymbol{n} \, dA \tag{7.28}$$

where $\boldsymbol{v}_c$ denotes the velocity vector of the moving control volume $V_c(t)$. In order to derive a 1D transport equation for a generic specific property, we will assume a particular controle volume V_c, which is fixed in the axial direction (z-direction in figure 7.4), but follows the walls of the compliant vessel in the directions orthogonal to the chosen spatial direction (i.e., x- and y-directions in figure 7.4). By adopting the conventions of equation (2.26) a the more compact represenation of the RTT is obtained:

$$\frac{dB}{dt} = \frac{dB_c}{dt} + \int_{S_c(t)} \beta(\boldsymbol{v} - \boldsymbol{v}_c) \cdot \boldsymbol{n} \, dA \tag{7.29}$$

The surface integrals may be simplified and split as $S_c = A_1 \cup A_2 \cup A_3$ and $\boldsymbol{v}_c = 0$ for all $\boldsymbol{v}_c \in \{A_1, A_2\}$. By focusing on the first term of equation (7.29), we get from *Leibniz's rule* for 3D integrals (see equation (45)) or equation (2.32) for dB_c/dt:

$$\frac{dB_c}{dt} = \int_{V_c(t)} \frac{\partial \beta}{\partial t} \, dV + \int_{A_3} \beta \, \boldsymbol{v}_c \cdot \boldsymbol{n} \, dA \tag{7.30}$$

To simplify the integral in equation (7.30), we define an iterated them first in the direction which we want to express the spatial dependency and then in the orthogonal directions over which we will average:

$$\int\limits_{V_c} (\cdot) \, dV = \int\limits_{z_1}^{z_2} \left\{ \int\limits_{A(x,t)} (\cdot), dA \right\} dz \quad \text{and} \quad \int\limits_{A_3} (\cdot) \, dA = \int\limits_{z_1}^{z_2} \left\{ \oint\limits_{C(x,t)} (\cdot) \, dl \right\} dz \tag{7.31}$$

where C is the closed curve bounding A_3 orthogonal to the streamwise z-direction, and dl is the corresponding differential line element. Now, both integrals of equation (7.30) may be integrated along the z-axis:

$$\frac{dB_c}{dt} = \int_{z_1}^{z_2} \left(\int_{A_c} \frac{\partial \beta}{\partial t}\, dA + \oint_C \beta\, \boldsymbol{v}_c \cdot \boldsymbol{n}\, dl \right) dz \tag{7.32}$$

Further, the cross-sectional mean value $\bar{\beta}$ is defined conventionally as:

$$\bar{\beta} = \frac{1}{A} \int_A \beta\, dA \tag{7.33}$$

and for convenience we define B_s:

$$B_s \equiv A\bar{\beta} = \int_{A(t)} \beta dA \tag{7.34}$$

Based on the definitions in equation (7.34) we get from Leibniz's rule for 2D integrals (see equation (41)):

$$\frac{dB_s}{dt} = \int_{A(t)} \frac{\partial \beta}{\partial t}\, dA + \oint_C \boldsymbol{v}_c \cdot \boldsymbol{n}\, dl = \frac{d}{dt}\left(A\bar{\beta}\right) = \frac{\partial A\bar{\beta}}{\partial t} \tag{7.35}$$

The latter identity follows as this integral is valid for a fixed z only. This result in equation (7.35) may be substituted into equation (7.32) to yield:

$$\frac{dB_c}{dt} = \int_{z_1}^{z_2} \frac{\partial A\bar{\beta}}{\partial t}\, dz \tag{7.36}$$

To proceed further, the surface integral of equation (7.29) may be split in the following manner:

$$\int_{S_c(t)} \beta\,(\boldsymbol{v}-\boldsymbol{v}_c)\cdot\boldsymbol{n}\, dA = \int_{A_1} \beta\,(\boldsymbol{v}-\boldsymbol{v}_c)\cdot\boldsymbol{n}\, dA + \int_{A_2} \beta\,(\boldsymbol{v}-\boldsymbol{v}_c)\cdot\boldsymbol{n}\, dA + \int_{A_3(t)} \beta\,(\boldsymbol{v}-\boldsymbol{v}_c)\cdot\boldsymbol{n}\, dA \tag{7.37}$$

At the inlet where $z = z_1$, we have $\boldsymbol{n}_1 = [0, 0, -1]$, whereas at the outlet where $z = z_2$, the normal vector points in positive z-direction $\boldsymbol{n}_2 = [0, 0, 1]$. Further, $\boldsymbol{v}_c = 0$ at both z_1 and z_2. Thus, the first and second surface integrals of (7.37) may be simplified to:

$$\int_{A_1} \beta\,(\boldsymbol{v}-\boldsymbol{v}_c)\cdot\boldsymbol{n}\, dA + \int_{A_2} \beta\,(\boldsymbol{v}-\boldsymbol{v}_c)\cdot\boldsymbol{n}\, dA = \int_{A_2} \beta\, v_3\, dA - \int_{A_1} \beta\, v_3\, dA = \int_{z_1}^{z_2} \frac{\partial}{\partial z}\left(A(\overline{\beta v_3})\right) dz \tag{7.38}$$

Furthermore, a leakage may be allowed for by introducing the normal component of the relative velocity $v_n = (\boldsymbol{v} - \boldsymbol{v}_c) \cdot \boldsymbol{n}$, and thus the last integral in equation (7.37) may be represented:

$$\int\limits_{A_3(t)} \beta \, (\boldsymbol{v} - \boldsymbol{v}_c) \cdot \boldsymbol{n} \, dA = \int_{z_1}^{z_2} \oint_{C(t)} \beta v_n \, dl \, dz \tag{7.39}$$

Now, by substitution of equations (7.39) and (7.38) into equation (7.37), which again may be substituted into equation (7.29) together with equation (7.36), we obtain the:

1D transport equation for a generic density

$$\frac{dB}{dt} = \int_{z_1}^{z_2} \frac{\partial}{\partial t} \left(A\bar{\beta}\right) + \frac{\partial}{\partial z} \left(A(\overline{\beta v_3})\right) + \oint_C \beta v_n \, dl \, dz \tag{7.40}$$

Equation (7.40) represent a 1D transport equation for a generic specific property in a compliant vessel, which we will use in the derivation of the mass and momentum equations below.

7.3.2 Mass conservation

The differential equation for mass conservation is obtained from (7.40), simply by setting $\beta = 1$. Obviously the right hand side of (7.40), vanishes for a constant β and we get:

$$\frac{\partial A}{\partial t} + \frac{\partial A\overline{v_3}}{\partial z} + \oint_C v_n \, dl = 0 \tag{7.41}$$

Further, we define volumetric outflow per unit length and time as:

$$\psi = \oint_C v_n \, dl \tag{7.42}$$

As the equation is 1D we drop the subscripts and the bar for averaged vector components in the streamwise direction:

$$v = \bar{v}_3 = \frac{1}{A} \int\limits_A v_3 \, dA \tag{7.43}$$

and thus (7.41) becomes:

$$\frac{\partial A}{\partial t} + \frac{\partial Av}{\partial z} + \psi = 0 \tag{7.44}$$

However, in most application the volumetric source term is neglected and the mass conservation equation takes the form:

$$\frac{\partial A}{\partial t} + \frac{\partial Av}{\partial z} = \frac{\partial A}{\partial t} + \frac{\partial Q}{\partial z} = 0 \tag{7.45}$$

where the flow rate $Q = Av$ has been introduced as the flow variable in the second expression in equation (7.45).

7.3.3 Momentum equation

By letting the specific property be $\beta = v_3$ (i.e., linear momentum per unit mass in the streamwise direction) in (7.40) we get:

$$\frac{\partial}{\partial t}(Av) + \frac{\partial}{\partial z}\left(A\overline{v_3^2}\right) + \oint_C v_3 v_n \, dl = \int_A \dot{v}_3 \, dA \tag{7.46}$$

By repeated use of the chain rule, introduction of the mass equation (7.44), and the mathematical identity $\partial v^2/\partial z = 2v\partial v/\partial z$ (7.46) may be reformulated:

$$\frac{\partial v}{\partial t} + v\frac{\partial v}{\partial z} + \frac{1}{A}\frac{\partial}{\partial z}\left(A(\overline{v_3^2} - v^2)\right) = \frac{1}{A}\int_A \dot{v}_3 \, dA + \frac{v}{A}\psi - \frac{1}{A}\oint_C v_3 v_n \, dl \tag{7.47}$$

For 1D flows it is natural to define a material derivative:

$$\dot{v} = \frac{\partial v}{\partial t} + v\frac{\partial v}{\partial z} \tag{7.48}$$

Then, by substitution of (7.48) and (7.42) into (7.47), we get:

$$\dot{v} + \frac{1}{A}\frac{\partial}{\partial z}\left(A(\overline{v_3^2} - v^2)\right) = \frac{1}{A}\int_A \dot{v}_3 \, dA + \frac{1}{A}\oint_C (v - v_3) v_n \, dl \tag{7.49}$$

Notice that both v and v_3 intentionally, appear in (7.49). The aim in the following is to derive a momentum equation formulated by means of cross-sectionally averaged quantities only.

To evaluate $\dot{v}_3$ on the right hand side of (7.49) we step back to Cauchy's equations for balance of linear momentum:

$$\dot{\boldsymbol{v}} = \frac{1}{\rho}\nabla \cdot \boldsymbol{T} + \boldsymbol{b} \tag{7.50}$$

where $\boldsymbol{T}$ is the stress tensor and $\boldsymbol{b}$ is the body force vector. For a Newtonian fluid the constitutive equation is given by:

$$\boldsymbol{T} = -p\,\boldsymbol{I} + 2\mu\,\boldsymbol{D} \tag{7.51}$$

where $\boldsymbol{I}$ is the identity tensor, μ is the dynamic viscosity and $\boldsymbol{D}$ is the rate of deformation tensor. Substitution of (7.51) into (7.50) yields the Navier-Stokes equations:

$$\dot{\boldsymbol{v}} = -\frac{1}{\rho}\nabla p + \nu\nabla^2\boldsymbol{v} + \boldsymbol{b} \tag{7.52}$$

Here the kinematic viscosity is denoted by $\nu = \mu/\rho$. On component form (7.52) reads

$$\dot{v}_i = -\frac{1}{\rho}p_{,i} + \nu v_{i,kk} + b_i \tag{7.53}$$

Here, we use the standard Einstein convention of summation of repeated indexes and comma for partial differentiation. Motivated by the arguments [14], we define appropriate velocity scales:

$$V = \max(v_3), \qquad U = \max(v_2, v_3) \tag{7.54}$$

and assume that:

$$\epsilon = \frac{U}{V} \ll 1 \tag{7.55}$$

i.e., that mean transverse velocities are small compared to mean axial velocities. Further, as spatial scale we define a mean "radius" to be $R = (A_0/\pi)^{\frac{1}{2}}$, where A_0 is the mean cross sectional vessel area over a cycle. Based on these scales we define the following nondimensional primed numbers:

$$\begin{aligned} x_3 &= \frac{R}{\epsilon}\,x_3', & x_\alpha &= R\,x_\alpha' \\ v_3 &= V\,v_3', & v_\alpha &= U\,v_\alpha' \\ t &= \frac{R}{U}\,t', & p &= \rho V^2\,p' \\ b_3 &= \frac{UV}{R}\,b_3', & b_\alpha &= \frac{U^2}{R}\,b_\alpha' \end{aligned}$$

where α takes the values $1, 2$. By introduction of the scales in above into (7.53), and letting $\epsilon \to 0$, and the resulting dimensional equations become:

$$\dot{v}_3 = -\frac{1}{\rho}\frac{\partial p}{\partial z} + \frac{\partial}{\partial x_\alpha}\left(\nu\frac{\partial v_3}{\partial x_\alpha}\right) + b_3 \tag{7.56}$$

$$\frac{\partial p}{\partial x_\alpha} = 0 \tag{7.57}$$

Note that through this scaling, the streamwise derivative has disappeared ($\partial^2 v_3/\partial x^2 \propto \epsilon$) in the streamwise momentum equation (7.56) (as α only takes the values $1, 2$). Further, (7.57) means that the pressure is approximately constant (i.e., $p(z,t) = \bar{p}(z,t)$) in the crosswise directions.

Now we may integrate (7.56) over the vessel cross section, and use the Gauss theorem to obtain:

$$\int_A \dot{v}_3\, dA = -\frac{A}{\rho}\frac{\partial p}{\partial z} + \oint_C \nu\frac{\partial v_3}{\partial x_\alpha}\, n_\alpha\, dl + Ab \tag{7.58}$$

where $\boldsymbol{n} = [n_1, n_2]$ is the outward unit vector but on C in the xy-plane and $b = 1/A\int b_3\, dA$. (We could have used three dimensions for both the normal vector and the velocity gradient, here as well, but we use α-notation to stress that the streamwise derivative has been discarded.)

A 1D equation for balance of linear momentum for pulsatile flow in a compliant vessel is then obtained by substitution of the expression for $\int_A \dot{v}_3\, dA$ in (7.58) (7.49):

$$\dot{v} + \frac{1}{A}\frac{\partial}{\partial z}\left(A(\overline{v_3^2} - v^2)\right) = -\frac{1}{\rho}\frac{\partial p}{\partial z} + b + \frac{1}{A}\oint_C \nu\frac{\partial v_3}{\partial x_\alpha}\, n_\alpha + (v - v_3)v_n\, dl \tag{7.59}$$

The equation still contains both v and v_3 and in order to proceed further, assumptions have to be made for the velocity profile of v_3.

Example 7.3.1. *Momentum equations for invicid flow.*

A simple zeroth order approximation is to abandon the no-slip boundary condition by assuming $v_3 = v$ which:

$$\dot{v} = -\frac{1}{\rho}\frac{\partial p}{\partial z} + b \tag{7.60}$$

which is nothing but the inviscid Navier-Stokes equations in 1D.

Example 7.3.2. *Momentum equations for polynomial velocity profiles.*

In order to account for viscous losses and thus provide estimates of local wall shear stresses, a crosswise velocity profile must be introduced for v_3 in some way. In [14] is simply assumed

$$v_3 = \phi v \tag{7.61}$$

the profile function must satisfy the conditions:

$$\phi|_C = 0 \tag{7.62}$$

$$\overline{v_3^2} - v^2 = \delta v^2 \tag{7.63}$$

where a nonlinear correction factor has been introduced to simplify the expressions in (7.59). The correction factor is given by:

$$\delta = \frac{1}{A}\int_A (\phi^2 - 1)\, dA \tag{7.64}$$

For axisymmetric case one might postulate a polynomial velocity profile on the form:

$$\phi = C_1(1 - (\frac{r}{R})^n) = C_1(1 - \tilde{r}^n) \tag{7.65}$$

where R is the radius of the vessel, whereas $\tilde{r} = r/R$ is a nondimensional radius, and C_1 is an arbitrary constant to be determined below. For $n = 2$ (7.65) correspond to a parabolic profile, while the profile becomes blunter for higher values of n and approaches a flat profile as $n \to \infty$. For this polynomial velocity profile the correction factor integral (7.64) has an analytical solution:

$$\begin{aligned}
\delta &= \frac{1}{\pi R^2}\int_0^R (\phi^2 - 1)\, 2\pi r\, dr = 2\int_0^1 (\phi^2 - 1)\, \tilde{r}\, d\tilde{r} \\
&= 2C_1^2 \int_o^1 (1 - C_1^{-2})\tilde{r} - 2\tilde{r}^{n+1} + \tilde{r}^{2n+1}\, d\tilde{r} \qquad (7.66) \\
&= 2C_1^2 \left[\frac{1 - C_1^{-2}}{2}\tilde{r}^2 - \frac{2}{n+2}\tilde{r}^{n+2} + \frac{1}{2(n+1)}\tilde{r}^{2(n+1)}\right]_0^1 \\
&= \frac{C_1^2 n^2 - (n+2)(n+1)}{(n+2)(n+1)} \qquad (7.67)
\end{aligned}$$

Now, by inspection of (7.66) we see that if C_1 is chosen to be:

$$C_1 = \frac{n+2}{n} \Rightarrow \phi = \frac{n+2}{n}(1 - \tilde{r}^n) \tag{7.68}$$

the expression for the correction factor in (7.66) reduces to:

$$\delta = \frac{1}{n+1} \tag{7.69}$$

Thus, $\delta = 1/3$ for Poiseuille flow (n=2) while $\delta \to 0$ as the profile becomes blunter (i.e., $n \to \infty$). Substitution of (7.63) into (7.59) and assumption of zero outflow $w_n = 0$ yields:

$$\dot{v} + \frac{\delta}{A}\frac{\partial}{\partial z}\left(Av^2\right)\Big) = -\frac{1}{\rho}\frac{\partial p}{\partial z} + b + \frac{v}{A}\oint_C \nu \frac{\partial \phi}{\partial x_\alpha} n_\alpha \, dl \tag{7.70}$$

This is the simplest form of momentum balance accounting for viscous forces based on a velocity profile function. Note that (7.70) is valid as long as (7.61) and (7.63) are satisfied, i.e., no assumption of a polynomial, axisymmetric, velocity profile is mandatory.

By multiplying (7.70) with A we get:

$$A\frac{\partial v}{\partial t} + Av\frac{\partial v}{\partial z} + \delta\frac{\partial}{\partial z}\left(Av^2\right) = -\frac{A}{\rho}\frac{\partial p}{\partial z} + Ab + v\oint_C \nu \frac{\partial \phi}{\partial x_\alpha} n_\alpha \, dl \tag{7.71}$$

which by using the chain rule may be re-written as:

$$\frac{\partial Q}{\partial t} - v\frac{\partial A}{\partial t} - v\frac{\partial Q}{\partial z} + \frac{\partial}{\partial z}\left(\frac{Q^2}{A}\right) + \delta\frac{\partial}{\partial z}\left(Av^2\right) = -\frac{A}{\rho}\frac{\partial p}{\partial z} + Ab + v\oint_C \nu \frac{\partial \phi}{\partial x_\alpha} n_\alpha \, dl \tag{7.72}$$

The second and third term vanish due to conservation of mass (7.45), which has the same mathematical representation regardless of whether the velocity profile is accounted for or not. Thus, a conservative formulation of (7.70) is:

$$\frac{\partial Q}{\partial t} + (1+\delta)\frac{\partial}{\partial z}\left(\frac{Q^2}{A}\right) = -\frac{A}{\rho}\frac{\partial p}{\partial z} + Ab + v\oint_C \nu \frac{\partial \phi}{\partial x_\alpha} n_\alpha \, dl \tag{7.73}$$

7.4 The wave nature of the pressure and flow equations

7.4.1 Linearized and inviscid wave equations

By introducing (7.27) into the linearized and inviscid form of (7.24) and (7.25), the derivative of the cross-sectional area is eliminated and we get:

$$C\,\frac{\partial p}{\partial t}+\frac{\partial Q}{\partial z}=0 \tag{7.74}$$

$$\frac{\partial Q}{\partial t}=-\frac{A}{\rho}\frac{\partial p}{\partial z} \tag{7.75}$$

By cross-derivation and subtraction of (7.74) and (7.75) the following differential equations are obtained:

$$\frac{\partial^2 p}{\partial t^2}-c_0^2\,\frac{\partial^2 p}{\partial z^2}=0 \tag{7.76}$$

$$\frac{\partial^2 Q}{\partial t^2}-c_0^2\,\frac{\partial^2 Q}{\partial z^2}=0 \tag{7.77}$$

where we have introduced the *pulse wave velocity* for inviscid flows:

$$c_0^2=\frac{\partial p}{\partial A}\,\frac{A}{\rho}=\frac{1}{C}\,\frac{A}{\rho} \tag{7.78}$$

Thus, (7.76) and (7.77) have both the form of a classical wave equation and one may show that they together have the general solutions:

$$p=p_0\;f(z-c_0\,t)+p_0^*\;g(z+c_0\,t) \tag{7.79}$$

$$Q=Q_0\;f(z-c_0\,t)+Q_0^*\;g(z+c_0\,t) \tag{7.80}$$

where f and g represents waves traveling with wave speed c forward and backward, respectively. By using the velcity as the primary variable in the momentum equation (7.23) one may show, by proceeding in a similar manner as above that the cross-sectional mean velocity v has the solution:

$$v=v_0\;f(z-c_0\,t)+v_0^*\;g(z+c_0\,t) \tag{7.81}$$

7.4.2 Characteristic impedance

By introducing (7.79) and (7.80) into (7.75) one obtains:

$$-Q_0\,c\,f'+Q_0^*\,c\,g'=-\frac{A}{\rho}\,(p_o f'+p_0^* g')$$

$$f'\left(p_0\frac{A}{\rho}-Q_0 c\right)+g'\left(p_0^*\frac{A}{\rho}+Q_0^* c\right)=0 \tag{7.82}$$

As (7.82) must hold for arbitrarily chosen f and g, an expression for the *characteristic impedance* Z_c is obtained:

$$Z_c \equiv \frac{p_0}{Q_0} = \frac{\rho\, c}{A} = -\frac{p_0^*}{Q_0^*} \tag{7.83}$$

From the expression above characteristic impedance is seen to be the ratio of the pulsatile pressure and flow components in the case of a unidirectional wave, i.e., in absence of reflections. The Z_c can also be shown to express the ratio of local inertance (ρ/A) to compliance capacity (C) as:

$$c = \sqrt{\frac{A}{\rho}\frac{1}{C}}, \quad C = \frac{\partial A}{\partial p} \tag{7.84}$$

which by substitution into (7.83) yields:

$$Z_c = \sqrt{\frac{\rho}{A}\frac{1}{C}} \tag{7.85}$$

Thus, the characteristic impedance is a quantity that relates to both geometry and the elastic properties of the vessel.

By proceeding in a similar manner one may also show that:

$$\frac{p_0}{v_0} = \rho c \tag{7.86}$$

7.4.3 Progressive waves superimposed on steady flow

Note that the derivations on the wave nature of the governing equations in the previous section 7.4.1, based on the assumption that the convective and inviscid terms in the governing equations ((7.24) and (7.25)), may be neglected. Typically, this assumption is valid valid for a straight, cylindrical tube filled with a liquid which is not flowing. The reason for the latter assumption of zero flow, is that a non-zero flow requires a driving pressure gradient and consequently a gradually decreasing pressure in the flow direction of the tube. The decrease in pressure will cause the tube to taper due to the compliant tube. Additionally, the compliance and the associated wave speed will vary in the flow direction as these properties are pressure dependent.

However as outlined in [12, chap. 3.9], if the resulting taper and variation in compliance/wave speed are negligible, the linearized equations (7.74) and (7.75) are valid for a compliant tube with a steady flow, provided that we adopt a coordinate system that follows the steady flow and c as the wave speed relative to the undisturbed flow. We show this in the following.

Let V denote the velocity of the undisturbed flow, and v a small velocity perturbation superposed on it. Similarily, we introduce and undisturbed area A_0 and an area perutbation A. Treating v and A as first order, infinitesimal perturbations and $Q = (A_0 + A)(V + v)$, we may linearize the govering equations (7.24) and (7.23) to:

$$\frac{\partial A}{\partial t} + A_0 \frac{\partial v}{\partial z} = 0 \tag{7.87}$$

$$\frac{\partial v}{\partial t} + V \frac{\partial v}{\partial z} = -\frac{1}{\rho} \frac{\partial p}{\partial x} \tag{7.88}$$

We may now introduce a Lagrangian coordinate $(x', t)'$ system, travelling with the undisturbed steady flow velocity V such that:

$$z' = z - Vt, \qquad \text{and} \qquad t' = t \tag{7.89}$$

from these definitions it follows:

$$\frac{\partial t'}{\partial t} = 1 \qquad \text{and} \qquad \frac{\partial z'}{\partial z} = 1 \qquad \text{and} \qquad \frac{\partial z'}{\partial t} = -V \tag{7.90}$$

and further the differential oprators in the Eulerian coordinate system (z, t) and the Lagrangian coordinate system $(z', t)'$ are related by:

$$\begin{aligned} \frac{\partial(\cdot)}{\partial t} &= \frac{\partial(\cdot)}{\partial t'} \frac{\partial t'}{\partial t} + \frac{\partial(\cdot)}{\partial z'} \frac{\partial z'}{\partial t} = \frac{\partial(\cdot)}{\partial t'} - V \frac{\partial(\cdot)}{\partial z'} \\ \frac{\partial(\cdot)}{\partial z} &= \frac{\partial(\cdot)}{\partial t'} \frac{\partial t'}{\partial z} + \frac{\partial(\cdot)}{\partial z'} \frac{\partial z'}{\partial z} = \frac{\partial(\cdot)}{\partial z'} \end{aligned} \tag{7.91}$$

Then, by transforming equations (7.87) and (7.88) in to the Lagrangian coordinate system given by equation (7.91) we get':

$$\frac{\partial A}{\partial t'} + A_0 \frac{\partial v}{\partial z'} = 0 \tag{7.92}$$

$$\frac{\partial v}{\partial t'} + \frac{1}{\rho} \frac{\partial p}{\partial z'} = 0 \tag{7.93}$$

Now, by proceeding in the same manner as for the linearized, invisicd case, the area A may be eliminated from equations (7.92) and (7.93) by substitution of (7.27). Further, by cross-derivation and subtraction we obtain the wave equations:

$$\frac{\partial^2 p}{\partial t'^2} - c_0^2 \frac{\partial^2 p}{\partial z'^2} = 0 \tag{7.94}$$

$$\frac{\partial^2 v}{\partial t^2} - c_0^2 \frac{\partial^2 v}{\partial z'^2} = 0 \tag{7.95}$$

where the wave speed has been introduced as:

$$c_0^2 = \frac{1}{C}\frac{A_0}{\rho} \tag{7.96}$$

the the solutions are given in the Lagrangian coordinate frame as:

$$p = p_0\, f(z' - c_0\, t') + p_0^*\, g(z' + c_0\, t') \tag{7.97}$$

$$v = v_0\, f(z' - c\, t') + Q_0^*\, g(z' + c\, t') \tag{7.98}$$

which may be transformed back into the original Eulerian frame of reference by equation (7.89):

$$\begin{aligned} p &= p_0\, f(z - (c_0 + V)\, t) + p_0^*\, g(z + (c_0 - V)\, t) \\ &= p_0\, f(z - c_f\, t) + p_0^*\, g(z + c_b\, t) \\ v &= v_0\, f(z - c_f\, t) + v_0^*\, g(z + c_b\, t) \end{aligned}$$

From the equations above we realize that for a wave superimposed on a steady flow with velocity V the forward propagating velocity (which propagates in the same positive direction as the steady flow) will propagate with a wave speed c_f given by:

$$c_f = c_0 + V \tag{7.99}$$

whereas the wave propagating upstream will have the wave speed c_b:

$$c_b = c_0 - V \tag{7.100}$$

7.4.4 The Moens-Korteweg formula for pulse wave velocity

To obtain the Moens-Korteweg formula for pulse wave velocity the circumferential stress and strain are assumed to satisfy Hooke's law:

$$\Delta\sigma_\theta = \eta\, \varepsilon_\theta = \eta\, \frac{da}{a} \tag{7.101}$$

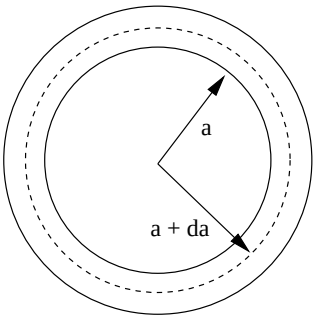

Figure 7.5: Thin walled cylinder with inner radius a and a small change in the radius of $a + da$.

as the circumferential strain ε_θ is given by:

$$\varepsilon_\theta = \frac{2\pi(a + da) - 2\pi a}{2\pi a} = \frac{da}{a} \tag{7.102}$$

Under the assumption of small deformations, the circumferential stresses before and after deformation ($\sigma_{\theta 1}$ and $\sigma_{\theta 2}$) are given by:

$$\sigma_{\theta 1} = \frac{pa}{h}, \qquad \sigma_{\theta 2} \approx \frac{(p + dp)a}{h} \tag{7.103}$$

which yields:

$$\Delta\sigma_\theta = \sigma_{\theta 2} - \sigma_{\theta 1} \approx \frac{dp\ a}{h} \tag{7.104}$$

Then by combination of (7.101) and (7.104):

$$\eta\frac{da}{a} = \eta\frac{dA}{2\,A} = \frac{dp\ a}{h} \tag{7.105}$$

which yields the expression:

$$\frac{dp}{dA} = \frac{\eta h}{2Aa} = \frac{1}{C} \tag{7.106}$$

This is an expression for the inverse compliance which may be substituted into the general expression for the pulse wave velocity in (7.78), to give the Moens-Korteweg formula for pulse wave velocity:

$$c_0^2 = \frac{1}{C}\frac{A}{\rho} = \frac{\eta h}{2\rho a} \tag{7.107}$$

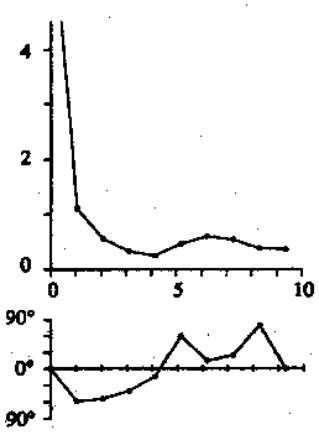

Figure 7.6: The input impedance of a young healthy subject (Adapted from O'Rourke 1992).

7.5 Input impedance

The input impedance Z_{in} is defined in a very similar manner as the characteristic impedance, namely as the ratio of the pulsatile components of pressure and flow:

$$Z_{in}(\omega) = \frac{P(\omega)}{Q(\omega)} \tag{7.108}$$

where uppercase denotes the Fourier-component of the corresponding lowercase primary variable for a given angular frequency ω. However, the input impedance is *not* restricted to unidirectional waves, i.e., reflected wave components are included. Thus, Z_{in} is a global quantity that characterize the properties distal (downstream) to the measuring point. The cumulative effect of all distal contributions is incorporated in the input impedance. In the aorta Z_{in} represents the afterload on the heart.

In Figure 7.6 the input impedance of a young healthy subject is depicted. For high frequencies the phase angles are close to zero, as high frequency components are more damped and reflections tend to cancel out. The negative phase angle for the low-frequency components correspond to that flow components lead pressure, i.e., the aorta first sees flow and the pressure.

7.6 Wave reflections

So far we have discussed propagation of pressure and flow waves in an infinitely long, straight, cylindrical, elastic vessel filled with an incompressible inviscid fluid. However, for real blood vessels we have:

- short, curved, tapered, bifurcating vessels
- the vessel walls exhibit nonlinear viscoelastic properties
- the blood is viscous

It turns out that the effect of nonlinear viscoelasticity is not so severe, as the Womersley number often is sufficiently large. However, the "infinitely long" assumption must be removed. When pressure and flow reach an end they must conform to the end conditions. Consequently, the waves will be modified and reflections will occur. The concept of wave reflection is easily understood for a single pulse which travels to the end of the vessel and is reflected. However, for a train of pulses or continuous oscillations, the reflected waves will interfere with the original pulse. In this case, the only evidence of reflections is spatial variations in amplitude of the waves. Reflections occur wherever there is a change in the characteristic impedance (mismatch in impedance).

The reflection factor: Let p_f denote the oscillatory pressure associated with the forward propagating wave and p_b associated with the reflected, backward propagating wave. Further, let the flow wave be split into forward and backward components in the same manner. These components superimpose to form the actual values:

$$p = p_f + p_b \tag{7.109}$$

The reflection factor Γ is then defined as:

$$\Gamma \equiv \frac{p_b}{p_f} = -\frac{Q_b}{Q_f} \tag{7.110}$$

The reflection factor may also be expressed in terms of the input impedance $Z_{in} = p/Q$ and the characteristic impedance $Z_c = p_f/Q_f = -p_b/Q_b$:

$$Q = \frac{p}{Z_{in}} = \frac{p_f}{Z_c} - \frac{p_b}{Z_c} \tag{7.111}$$

$$\frac{Z_{in}}{Z_c} = \frac{p_f + p_b}{p_f - p_b} = \frac{1+\Gamma}{1-\Gamma} \tag{7.112}$$

And thus:

$$\Gamma = \frac{Z_{in} - Z_c}{Z_{in} + Z_c} \tag{7.113}$$

Figure 7.7: An elastic vessel terminated with Z_T

The quarter wavelength formula. To illustrate the effect of reflections on the input impedance, let us consider a frictionless vessel with a total reflective impedance at the end, i.e., $\Gamma = 1$ (see Figure 7.7). Let the forward waves at the inlet of the vessel take the form:

$$p_f = p_0\, e^{j\omega t}, \quad Q_f = \frac{p_0}{Z_c}\, e^{j\omega t} \tag{7.114}$$

These waves travel the length L with pulse wave velocity c, are totally reflected, and must then travel the same distance back. Thus, the expressions for the reflected waves are:

$$p_b = p_0\, e^{j\omega(t-2L/c)}, \quad Q_b = -\frac{p_0}{Z_c}\, e^{j\omega(t-2L/c)} \tag{7.115}$$

And the input impedance at the inlet of the vessel is:

$$Z_{in} = \frac{p_f + p_b}{Q_f + Q_b} = Z_c\, \frac{e^{j\omega t} + e^{j\omega(t-2L/c)}}{e^{j\omega t} - e^{j\omega(t-2L/c)}} \tag{7.116}$$

From (7.116) we see that $Z_{in} = 0$ whenever:

$$\frac{2\omega L}{c} = \pi \tag{7.117}$$

As $\omega = 2\pi f$ and $\lambda = c/f$ *the quarter wave length formula* is obtained:

$$L = \frac{\lambda}{4} \tag{7.118}$$

Thus, from the first minimum of Z_{in} an indication of "the effective length" to the major reflection site of the arterial system may be obtained.

For example if the first minimum of $|Z_{in}|$ is found at 3.8 Hz, an estimate of $L \approx 0.33$ m may be obtained by assuming a typical pulse wave velocity of $c \approx 5$ m/s.

7.7 General equations with reflection and friction

For the linearized, frictionless case obtained previously in (7.79):

$$p = p_0\, f(z - ct) + p_0^*\, g(z - ct) = p_f + p_b$$

and for a frictionless vessel the forward component was conveniently expressed as:

$$p_f = p_0\, f(z - ct) = P_0\, e^{j\omega(t - x/c)}$$

Viscous friction may conveniently be incorporated by the introduction of a complex *propagation coefficient*:

$$\gamma = \frac{j\omega}{\hat{c}} = a + jb \tag{7.119}$$

where a is the *attenuation constant*, b the *phase constant*, and $\hat{c}$ a complex pulse wave velocity. An expression a may be obtained from the equation for the shear stress (7.18), however this is discarded here for brevity. The phase constant b is related to the pulse wave velocity by: $c = \omega/b$. Having adopted this convention, the forward propagating waves incorporating viscous friction may be expressed:

$$p_f = p_0\, e^{j\omega t}\, e^{-\gamma z}, \quad Q_f = Q_0\, e^{j\omega t}\, e^{-\gamma z}$$

And further, by assuming that the waves propagates in a vessel depicted in Figure 7.7, one may obtain expressions for the backward propagating components also:

$$\begin{aligned} p_f(L) &= p_f(0) e^{-\gamma L}, \qquad p_f(0) = p_0 e^{j\omega t} \\ p_b(L) &= \Gamma\, p_f(L) = \Gamma\, p_f(0)\, e^{-\gamma L} \\ p_b(0) &= p_b(L)\, e^{-\gamma L} = \Gamma\, p_f(0)\, e^{-2\gamma L} \end{aligned}$$

The forward and backward components at the inlet of the vessel may subsequently be superimposed to form the resulting pressure:

$$p(0) = p_f(0) + p_b(0) = p_f(0)\, (1 + \Gamma e^{-2\gamma L}) \tag{7.120}$$

This solution incorporates both viscous friction and reflections.

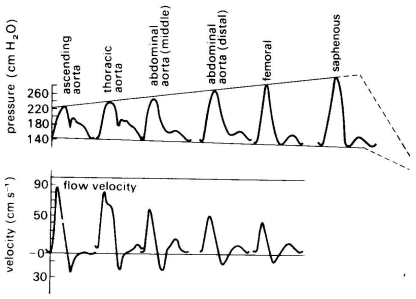

Figure 7.8: Spatial variation in pressure and velocity in the arterial tree (McDonald, 1974)

By taking into account that the reflected flow wave opposes the forward wave, an expression for the total flow at the inlet may be obtained in the same manner:

$$
\begin{aligned}
Q_f(L) &= Q_f(0)e^{-\gamma L}, \qquad Q_f(0) = Q_0 e^{j\omega t} \\
Q_b(L) &= -\Gamma\, Q_f(L) = -\Gamma\, Q_f(0)\, e^{-\gamma L} \\
Q_b(0) &= Q_b(L)\, e^{-\gamma L} = -\Gamma\, Q_f(0)\, e^{-2\gamma L}
\end{aligned}
$$

which yields:

$$
Q(0) = Q_f(0) + Q_b(0) = Q_f(0)\,(1 - \Gamma e^{-2\gamma L}) \tag{7.121}
$$

Further, from (7.120) and (7.121) an expression for the input impedance may also be found:

$$
Z_{in} = Z_c\, \frac{1 + \Gamma\, e^{-2\gamma L}}{1 - \Gamma\, e^{-2\gamma L}}, \quad Z_c = \frac{p_f(0)}{Q_f(0)} \tag{7.122}
$$

or alternatively:

$$
Z_{in} = Z_c\, \frac{Z_T + Z_c\, \tanh(\gamma L)}{Z_c + Z_T\, \tanh(\gamma L)} \tag{7.123}
$$

where:

$$
\Gamma = \frac{Z_T - Z_c}{Z_T + Z_c}, \qquad Z_T = \frac{p(L)}{Q(L)}
$$

From (7.120) and (7.121) it is clearly seen that a positive reflection factor Γ will cause an *amplification in pressure*, whereas the flow will be reduced. Thus, the presence of reflections will cause the pressure and flow waves to

have different forms. Such reflections are believed to explain the streamwise increase in pressure amplitude in the arterial tree (Figure 7.8).

7.8 Wave separation

Several methods have been suggested to separate measured pressure and flow into forward and backward traveling components. This has been motivated by the notion that waves traveling from the heart toward the periphery contain information related to the heart, while the reflected waves contain information related to the periphery. The simplest method, which is still the method of choice for most applications, was suggested in [46]. This method is based on the linearized and inviscid form of the governing equations.

$$p = p_f + p_b, \quad Q = Q_f + Q_b = \frac{p_f}{Z_c} - \frac{p_b}{Z_c} \tag{7.124}$$

which by simple algebraic elimination yield:

$$p_f = \frac{p + Z_c Q}{2}, \qquad p_b = \frac{p - Z_c Q}{2} \tag{7.125}$$

$$Q_f = \frac{Z_c Q + p}{2Z_c}, \qquad Q_b = \frac{Z_c Q - p}{2Z_c} \tag{7.126}$$

In a normal healthy subject the reflections in the aorta come in the diastole after the aortic valve has closed. Thus, they are believed of enhance coronary perfusion. However, for elderly subjects with "stiffer" vessels the reflections may arrive in the systole. Thus, the reflections will increase the aortic systolic pressure and thereby increase the heart load. Such an condition may lead to hypertrophy.

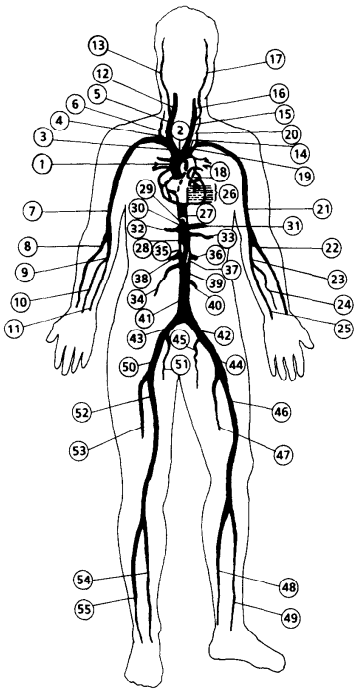

Figure 7.9: A model of the human arterial system (from [35]).

7.9 Wave travel and reflection

7.10 Networks 1D compliant vessels

The propagation of pressure and flow waves in the arterial system and how they influence stenotic regions, aneurysms and other vascular diseases, has been the subject of many studies [15, 43, 42, 31, 8, 10, 27, 35].

Recently there have also been a renewed interest for such 1D network models, as they both may provide valuable physiological insight in patient specific modalities (morphometric rendering of the arterial network) in addition to that they may provide better boundary conditions for 3D FSI models [6, 5, 3, 32, 33, 41].

Network models have also been used for various segments of the arterial tree. To provide better understanding of the genesis of ischemia that develops in the gastrointestinal system, a model for the mesenteric arterial system have been developed to simulated realistic blood flow during normal conditions [21].

One of the early papers on this topic was on the blood flow in the human arm [4]. It used FEM to discretize the equations and a modified Windkessel model for the distal boundary conditions.

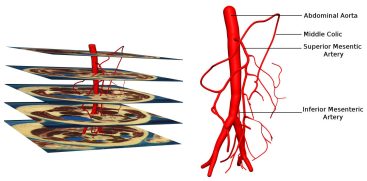

Figure 7.10: Anterior view of a subset of five images from the Visible Human dataset showing how the mesenteric arteries were created (from [21]).

A hybrid on-dimensional/Womersley model of pulsatile blood flow in the entire coronary arterial tree have also been developed recently[15].

Blood flow in the circle of Willis (CoW) has been modeled using the 1D equations of pressure and flow wave propagation in compliant vessels [1]. The model starts at the left ventricle and includes the largest arteries that supply the CoW. Based on published physiological data, it is able to capture the main features of pulse wave propagation along the aorta, at the brachiocephalic bifurcation and throughout the cerebral arteries.

7.10.1 Numerical solution of the 1D equations for compliant vessels and boundary conditions

When the governing 1D equations for compliant vessels (see e.g., equation (7.45) and (7.73)) are to be solved numerically, it is beneficial to recast them in the following generic form:

$$\frac{\partial \boldsymbol{u}}{\partial t} + \boldsymbol{M}\frac{\partial \boldsymbol{u}}{\partial x} = 0 \tag{7.127}$$

In particular, the formulation equation (7.127) and what follows this section is important for the implementation of the boundary conditions. For the internal domain, any kind of numerical discretization may be employed.

By choosing the state vector as $\boldsymbol{u} = [p, Q]^T$, the equations may be cast into the canonical given in equation (7.127) with:

$$\boldsymbol{M} = \begin{bmatrix} 0 & \dfrac{1}{C} \\ \dfrac{A}{\rho} - (1+\delta)\, v^2 C & 2(1+\delta)\, v \end{bmatrix} \tag{7.128}$$

The off diagonal elements in $\boldsymbol{M}$ represent a coupling in time and space between the components in the state vector, in this case the pressure p and the flow rate Q.

In the following we will transform the equation system represented by equation (7.127), to a form where the rows of the equation system are independent. In order to do this we introduce the the diagonal eigenvalue-matrix of $\boldsymbol{M}$:

$$\boldsymbol{\Lambda} = \begin{bmatrix} \lambda_1 & 0 \\ 0 & \lambda_2 \end{bmatrix} \tag{7.129}$$

the relation between $\boldsymbol{M}$ and it's eigenvalues and corresponding eigenvectors may be written:

$$\boldsymbol{M}\,\boldsymbol{R} = \boldsymbol{R}\,\boldsymbol{\Lambda} \tag{7.130}$$

The right eigenmatrix $\boldsymbol{R}$ is composed of the right eigenvectors as *columns*. From basic linear algebra one may prove that the left eigenmatrix is $\boldsymbol{L}$ related to the right eigenmatrix by $\boldsymbol{L} = \boldsymbol{R}^{-1}$. The i-th *row* of $\boldsymbol{L}$, denoted $\boldsymbol{l}_i$, is the left eigenvector of $\boldsymbol{M}$ corresponding to the i-th eigenvalue λ_i. From equation (7.130) we see that $\boldsymbol{M} = \boldsymbol{R}\boldsymbol{\Lambda}\boldsymbol{L}$ and thus by premultiplication of $\boldsymbol{L}$ in equation (7.127), we obtain:

$$\boldsymbol{L}\frac{\partial \boldsymbol{u}}{\partial t} + \boldsymbol{\Lambda}\boldsymbol{L}\frac{\partial \boldsymbol{u}}{\partial x} = 0 \tag{7.131}$$

Further, we may introduce a change of variables such that

$$\frac{\partial \boldsymbol{\omega}}{\partial \boldsymbol{u}} = \boldsymbol{L} \tag{7.132}$$

where $\boldsymbol{\omega} = [\omega_1, \omega_2]^T$ is the vector of characteristic variables, also commonly denoted Riemann invariants, which in general satisfy:

$$\boldsymbol{\omega} = \int_{\boldsymbol{u}_0}^{\boldsymbol{u}} \frac{\partial \boldsymbol{\omega}}{\partial \boldsymbol{u}}\, d\boldsymbol{u} = \int_{\boldsymbol{u}_0}^{\boldsymbol{u}} \boldsymbol{L}\; d\boldsymbol{u} \approx \boldsymbol{L}(\boldsymbol{u}_\epsilon)\, \Delta \boldsymbol{u}, \qquad \text{and} \quad \Delta \boldsymbol{u} = \boldsymbol{u} - \boldsymbol{u}_0 \tag{7.133}$$

The latter approximation follows from the mean value theorem (33) and is valid for some $\boldsymbol{u}_0 \leq \boldsymbol{u}_\epsilon \leq \boldsymbol{u}$. In particular, the approximation is good if the change in the state variable vector from $\boldsymbol{u}_0$ to $\boldsymbol{u}$ is small. This will typically be the case for an explicit numerical scheme where $\boldsymbol{u}_0$ refers to the state vector at the previous timestep and the timestep is small due to the CFL-limitation.

With this change of variables and use of the chain rule equation (7.131) transforms to a decoupled system of canonical wave equations:

$$\frac{\partial \boldsymbol{\omega}}{\partial t} + \boldsymbol{\Lambda}\frac{\partial \boldsymbol{\omega}}{\partial x} = 0 \tag{7.134}$$

which on component form reads:

$$\frac{\partial \omega_1}{\partial t} + \lambda_1\frac{\partial \omega_1}{\partial x} = 0 \tag{7.135}$$

$$\frac{\partial \omega_2}{\partial t} + \lambda_2\frac{\partial \omega_2}{\partial x} = 0 \tag{7.136}$$

For real eigenvalues λ_1 and λ_2, the Riemann invariants ω_1 and ω_2 are scalars which will propagate as waves, with wavespeeds λ_1 and λ_2, respectively. That is they have solutions:

$$\omega_1 = \hat{\omega}_1\, f(x - \lambda_1 t) \tag{7.137}$$

$$\omega_2 = \hat{\omega}_2\, g(x - \lambda_2 t) \tag{7.138}$$

Note that when λ_1 and λ_2 have different signs, the waves will travel in opposite directions.

For our particular case in equation (7.128) on may find that the eigenvalues are:

$$\begin{aligned}\lambda_{1,2} &= (1+\delta)v \pm \sqrt{(1+\delta)^2 v^2 + c^2 - (1+\delta)v^2} \\ &= \delta' v \pm c^*\end{aligned} \tag{7.139}$$

where we have introduced for simplicity:

$$\delta' = (1+\delta), \qquad c^* = c\sqrt{1 + \delta'(\delta'-1)\mathcal{M}^2} \qquad \text{and} \qquad \mathcal{M} = v/c \tag{7.140}$$

Here, c denote the invisicid pulse wave velocity as defined in equation (7.78). The δ' is simply a modified correction factor, whereas c^* is the modified wave speed due to the velocity field, and $\mathcal{M}$ is a Mach number. Note that a flat

velocity profile corresponds to $\delta = 0$, and consequently $\delta' = 1$ and $c^* = c$. Normally, $v \ll c^*$ and therefore we see from equation (7.139) that $\lambda_1 > 0$ and $\lambda_2 < 0$, and therefore ω_1 will travel to the right (or in the positive coordinate direction) whereas ω_2 will travel to the left (or in the negative coordinate direction) according to equation (7.135) and (7.136).

The corresponding left eigenmatrix may be taken as:

$$\boldsymbol{L} = \begin{bmatrix} 1 & -1/\lambda_2 C \\ 1 & -1/\lambda_1 C \end{bmatrix} = \begin{bmatrix} 1 & Z_c^b \\ 1 & -Z_c^f \end{bmatrix} \approx \begin{bmatrix} 1 & Z_c \\ 1 & -Z_c \end{bmatrix} \tag{7.141}$$

where we have introduced the modified characteristic impedances for the forward and backward traveling waves as Z_c^f and Z_c^b, respectively.

From equations (7.133) and (7.141) we get:

$$\boldsymbol{\omega} = [\omega_1, \omega_2]^T = \boldsymbol{L}(\boldsymbol{u}_\epsilon)\, \Delta \boldsymbol{u} = [\Delta p + Z_c^b \Delta Q, \quad \Delta p - Z_c^f \Delta Q]^T \tag{7.142}$$

Note, that the $Z_c^f = Z_c^f(p, Q)$ and $Z_c^b = Z_c^b(p, Q)$, and are to be evalued in the given range $\boldsymbol{u}_0 \leq \boldsymbol{u}_\epsilon \leq \boldsymbol{u}$. Normally, the value at the previous timestep may be used.

The Riemann invariants $\boldsymbol{\omega}$ are conventionally found from the internal field and from the boundary conditions. Subsequently the updated values of the primary variables are found at the boundary by:

$$\Delta \boldsymbol{u} = \boldsymbol{L}(\boldsymbol{u}_\epsilon)^{-1} \boldsymbol{\omega} = \boldsymbol{R}(\boldsymbol{u}_\epsilon) \boldsymbol{\omega} \tag{7.143}$$

where:

$$\boldsymbol{R} = \frac{1}{Z_c^f + Z_c^b} \begin{bmatrix} Z_c^f & Z_c^b \\ 1 & -1 \end{bmatrix} \approx \frac{1}{2\, Z_c} \begin{bmatrix} Z_c & Z_c \\ 1 & -1 \end{bmatrix} \tag{7.144}$$

The increments in the primary variables may also be expressed by means of the Riemann invariants by rearrangements of the expressions in equation (7.142):

$$\Delta Q = \frac{\omega_1 - \omega_2}{Z_c^f + Z_c^b}, \qquad \Delta p = \frac{Z_c^f \omega_1 + Z_c^b \omega_2}{Z_c^f + Z_c^b} \tag{7.145}$$

Note that for waves superimposed on a quiescent fluid fluid, i.e., for $v = 0$ in equation (7.139), then $\lambda_1 = -\lambda_2$ and $Z_c^f = Z_c^b = Z_c$, and consequently equation (7.145) simplifies to:

$$\Delta Q = \frac{\omega_1 - \omega_2}{2 Z_c}, \qquad \Delta p = \frac{\omega_1 + \omega_2}{2} \tag{7.146}$$

now we may define:

$$\Delta Q_f = \frac{\omega_1}{Z_c^f + Z_c^b}, \qquad \Delta Q_b = \frac{-\omega_2}{Z_c^f + Z_c^b} \tag{7.147}$$

$$\Delta p_f = \frac{Z_c^f\,\omega_1}{Z_c^f + Z_c^b}, \qquad \Delta p_b = \frac{Z_c^b\,\omega_2}{Z_c^f + Z_c^b} \tag{7.148}$$

which by substitution into equation (7.145) yields:

$$\Delta Q = \Delta Q_f + \Delta Q_b \tag{7.149}$$

$$\Delta p = \Delta p_f + \Delta p_b \tag{7.150}$$

Inlet boundary conditions. A prescribed flow at the inlet boundary may be imposed in such a way that the wave approaching this boundary from the interior field is also handled in a way which respects the physics or the differential equations for the problem. Clearly, as flow is imposed we know the value of Q_{in}, the pressure, however, has to be computed and will be a function both of the flow at the inlet and of waves coming from the interior. The mathematical consequence of this outset is that two conditions need to be fulfilled, namely that the flow Q_{in} may be taken as a time varying function $Q_{in} = Q(t)$, whereas the outgoing wave will be accounted for by imposing $\boldsymbol{l_2 \cdot u_{in}} = \omega_2$. Note we assume here that the inlet is taken at the left boundary, i.e., where the x-coordinate is at minimum.

Now, to compute the resulting pressure from the imposed flow Q_{in} and the (potential) wave ω_2 from the interior, we construct an equation system similar to equation (7.133). As we need to respect the physics from the interior we keep the second row of $\boldsymbol{L}$, corresponding to the wave from the interior ω_2, but modify the first row to ensure that the flow is imposed:

$$\boldsymbol{L}_{in}\boldsymbol{u}_{in} = \boldsymbol{\omega}_{in} \tag{7.151}$$

where:

$$\boldsymbol{L}_{in} = \begin{bmatrix} 0 & 1 \\ 1 & -Z_c^f \end{bmatrix} \quad \text{and} \quad \boldsymbol{\omega}_{in} = \begin{bmatrix} Q(t) \\ \omega_2 \end{bmatrix} \tag{7.152}$$

By inspecting equations (7.151) and (7.152), we see that the above mentioned conditions are satisfied. The inverse of $\boldsymbol{L}_{in}$ may be computed as:

$$\boldsymbol{L}_{in}^{-1} = \begin{bmatrix} Z_c^f & 1 \\ 1 & 0 \end{bmatrix} \tag{7.153}$$

and the resulting pressure p_{in} (and flow) from the imposed flow may be computed as:

Imposed flow

$$\boldsymbol{u}_{in} = \begin{bmatrix} p_{in} \\ Q_{in} \end{bmatrix} = \boldsymbol{L}_{in}^{-1} \cdot \boldsymbol{\omega}_{in} = \begin{bmatrix} Z_c^f Q(t) + \omega_2 \\ Q(t) \end{bmatrix} \tag{7.154}$$

and we clearly see from equation (7.154), that the pressure has contributions from both the imposed flow and the wave from the interior ω_2. Observe also that with no reflected wave present (i.e., $\omega_2 = 0$, pressure and flow are related with the characteristic impedane Z_c^f, as expected.

A similar strategy may be taken for an imposed time varying pressure $p_i = p(t)$:

$$\boldsymbol{L}_{in} = \begin{bmatrix} 1 & 0 \\ 1 & -Z_c^f \end{bmatrix} \quad \text{and} \quad \boldsymbol{L}_{in}^{-1} = \begin{bmatrix} 1 & 0 \\ -1/Z_c^f & 1/Z_c^f \end{bmatrix} \quad \text{and} \quad \boldsymbol{\omega}_{in} = \begin{bmatrix} p(t) \\ \omega_2 \end{bmatrix} \tag{7.155}$$

which yields the following equations for the inlet:

Imposed pressure

$$\boldsymbol{u}_{in} = \begin{bmatrix} p_{in} \\ Q_{in} \end{bmatrix} = \begin{bmatrix} p(t) \\ \dfrac{\omega_2 - p(t)}{Z_c^f} \end{bmatrix} \tag{7.156}$$

We observe from equation (7.156) that the inlet flow Q_{in} has contributions both from the imposed pressure $p(t)$ and from the interior wave ω_2. In the absence of a reflected wave ω_2, pressure and flow are related with the characteristic impdeance Z_c^f as expected for unidirectional waves.

Impose forward flow/pressure. Impose $\Delta Q_f = Q_0$. From equation (7.147) ω_1 may be computed as:

$$\omega_1 = (Z_c^f + Z_c^b)\Delta Q_f = (Z_c^f + Z_c^b)\Delta Q_0 \tag{7.157}$$

Extrapolation from interior field:

$$\omega_2 = w_2(t^n, \lambda_2 \Delta t) \tag{7.158}$$

and compute values at the inlet by:

$$\boldsymbol{\Delta u}_{in} = \mathbf{R}\boldsymbol{\omega} \tag{7.159}$$

The expressions in equation (7.157) may be simplified whenever $v \ll c$ and concequently $Z_c^f \approx Z_c^b = Z_c$ and thus:

$$\omega_1 = 2\, Z_c \Delta Q_0 \tag{7.160}$$

and the imposed primary variables then become:

Imposed forward flow

$$\mathbf{\Delta u}_{in} = \begin{bmatrix} p_{in} \\ Q_{in} \end{bmatrix} = \mathbf{R\omega} = \begin{bmatrix} Z_c\, Q_f + \omega_2/2 \\ Q_f - \omega_2/2\, Z_c \end{bmatrix} \tag{7.161}$$

Outlet boundary conditions. In the numerical scheme for the governing equations (7.45) and (7.73), a values for ω_1 are ω_2 are needed in order to prescribe the pressure/flow at the outlet in a way which repsects both the wave ω_1 coming from the inside of the vessel and the wave entering the vessel ω_2. This amounts to solving equation (7.143) at the boundary.

For the outlet (i.e., for $x = L$) the outgoing Riemann invariant may be extrapolated from the interior field from the previous timestep. Whenever source terms are negligible in equation (7.135), the outgoing Riemann invariant at the outlet is constant along the characteristic curve $dx/dt = \lambda_1$, and thus we can approximate:

$$\omega_1^{n+1} = \omega_1(t_n, L - \lambda_1^n \Delta t) \tag{7.162}$$

The question now is how one may obtain a value for ω_2, which represents the incoming wave due to the two element Windkessel. Terminal vessels are often modeled with lumped models Windkessel model, which is represented by the differential equation (6.15). On incremental form the two element Windkessel mode has the corresponding differential equation:

$$\Delta Q = C\frac{\partial \Delta p}{\partial t} + \frac{\Delta p}{R} \tag{7.163}$$

Now, by substiution of equation (7.146), which expresses the primary variables p, and Q by means of the Riemann invariants, into the differential equation (7.163) which models the physics of the exterior, a differential equation for ω_2 is obtained:

$$Z_c^b C\,\frac{d\omega_2}{dt} + \omega_2\left(1 + \frac{Z_c^b}{R}\right) = Z_c^f C\,\frac{d\omega_1}{dt} + \omega_1\left(1 - \frac{Z_c^f}{R}\right) \tag{7.164}$$

As the right hand side of equation (7.164) is known from previous values of ω_1 and from the extrapolated current value given by equation (7.162), an

updated value for ω_2 may readily be obtained by an appropriate discretization of equation (7.164), e.g., backward Euler.

7.10.2 Lumped heart model: varying elastance model

The varying elastance model, is a phenemenological model of the left ventricular function, originally proposed [38, 37]

$$E(t) = \frac{p_v(t)}{V(t) - V_0} \tag{7.165}$$

Modified version

$$E(t) = \frac{p_v(t)}{(V(t) - V_0)\,(1 + KQ_v(t))} \tag{7.166}$$

with K as a resistance in the left ventricle. Normally, K is rather small, and therefore a first approximation is to assume it to be zero as in equation (7.165).

As $V(t)$ is the instantaneous left ventricular volume, the flow rate $Q_v(t)$ ejected by the left ventricle is given by $Q_v(t) = -dV/dt$. From the varying elastance model in equation (7.165) we get:

$$Q_v(t) = -\frac{dV}{dt} = \frac{dE}{dt}\left(\frac{1}{E^2}\right) p_v - \frac{1}{E}\frac{dp_v}{dt} \tag{7.167}$$

from the representation we see that $1/E$ plays the role of a compliance and:

$$\frac{d}{dt}\left(\frac{1}{E}\right) \tag{7.168}$$

the role of a resistance [9].

The varying elastance model may be used as an inlet condition, subject to the assumption that $Q = Q_v$ and $p = p_v$ at the inlet. As we now are at the inlet, we may extraplate the outgoing Riemann invariant ω_2 in the same manner as in equation (7.162):

$$\omega_2^{n+1} = \omega_2(t_n, \lambda_2^n \Delta t) \tag{7.169}$$

Further, the differential equation for ω_1 may be obtained by substitution of equation (7.145) into the differential equation (7.167) for the varying elastance model:

$$\frac{Z_c^f}{E}\frac{d\omega_1}{dt} + \omega_1\left(1 - \frac{Z_c^f}{E^2}\frac{dE}{dt}\right) = -\frac{Z_c^b}{E}\frac{d\omega_2}{dt} + \omega_2\left(1 + \frac{Z_c^b}{E^2}\frac{dE}{dt}\right) \tag{7.170}$$

Thus, an updated value at time level $n+1$ may be obtained for (ω_1^{n+1}) by e.g., a backward Euler dicretization of equation (7.170).

When, modelling the interaction of the heart and the cardiovacular system, one obviously have to account for the presence of the aortic valve and the fact that it is closed during diastole. The closure of the aortic valve is normally attributed to a negative pressure difference between the left ventricle and the aorta.

From equations (7.165) and (7.167) on may estimate an updated left ventricular pressure at the next time level:

$$p_v^{n+1} = E(t)\left(V_n - Q_n\Delta t - V_0\right) \tag{7.171}$$

The negative pressure difference criterion for valve closure will therefore be $p_v < p^{n+1}$.

Whenever the valve is closed, there is no outflow from the heart which corresponds $Q_v = 0$ in equation (7.167). Note that despite a closed aortic valve, waves may still arrive from the periphery $\omega_2 \neq 0$, and such waves will be reflected at the closed valve. A complete reflection ($\Gamma = 1$), is a first approximation which corresponds to $\omega_1 = \omega_2$).

The pressure criteria for valve closure together with the varying elastance model as inlet condition may therefore be summarized to:

$$\omega_1 = \begin{cases} (refeq : 425b) & \text{if } p_v > p \\ \omega_2 & \text{if } p_v \leq p \end{cases} \tag{7.172}$$

7.10.3 Nonlinear wave separation

Expressions for nonlinear wave separation follow readily from equation (7.145) as ω_1 is a forward propagating Riemann invariant and ω_2 is a backward propagating Riemann invariant. The forward/backward propagating pressures and flows are found simply by setting $\omega_2 = 0$ and $\omega_1 = 0$, respectively, in equation (7.146):

$$\begin{aligned} \Delta Q_f &= \frac{\omega_1}{Z_c^f + Z_c^b}, \quad \Delta Q_b = \frac{-\omega_2}{Z_c^f + Z_c^b} \\ \Delta p_f &= \frac{Z_c^f \omega_1}{Z_c^f + Z_c^b}, \quad \Delta p_b = \frac{Z_c^b \omega_2}{Z_c^f + Z_c^b} \end{aligned} \tag{7.173}$$

Naturally, for the more simpler case of a quiescent fluid fluid, the previously derived expressions for linear wave separation (see equation (7.125) and (7.126)) in section 7.8) may be obtained from equation (7.146).

7.11 Fluid structure interaction for small deformations in Hookean vessel

7.11.1 The governing equations for the Hookean vessel

The averaged Cauchy equations. The Cauchy equations were derived in section 2.4 in cylindrical coordinates (see equations (2.111)-(2.113). We will in this section average the equations for the z-direction and r-direction over the vessel wall, assuming azimuthal symmetry (i.e., all $\partial(\cdot)/\partial\theta -$ terms $= 0$). Based on this assumption the Cauchy equation (2.113) in the z-direction may be integrated over the vessel wall to yield:

$$\int_{A_w} \rho_w a_z \ \mathrm{dA} = \int_{A_w} \left(\frac{1}{r} \frac{\partial}{\partial r} \left(r \tau_{zr} \right) + \frac{\partial \sigma_z}{\partial z} + \rho_w b_z \right) \ \mathrm{dA} \tag{7.174}$$

where ρ_w denotes the density of the vessel wall, which is assumed to be constant the following derivation.

By introducing the common notation that a bar-ed quantity denote the cross-sectional averaged of the same quantity without a bar, i.e., $\bar{(\cdot)} = \int_A (\cdot) \ \mathrm{dA}/A$, the first term of equation (7.174) may be reformulated to:

$$\int_{A_w} \rho_w a_z \ \mathrm{dA} = \rho_w \bar{a}_z A_w \approx \rho_w \bar{a}_z 2\pi r_i h \tag{7.175}$$

where A_w is the vessel wall area, i.e., $A_w = \pi(r_o^2 - r_i^2)$, and r_i and r_o denote inner and outer radius, respectively and h the wall thickness. For a thin walled vessels $h/r_i \ll 1$:

$$A_w = \pi(r_o^2 - r_i^2) = \pi(2r_i h + h^2) \approx 2\pi r_i h \tag{7.176}$$

and thus the approximation in equation (7.175) is valid for thin walled structures.

By expanding $dA = r\,dr d\theta$, the first term in the rhs of equation (7.174) take the form:

$$\int_0^{2\pi}\int_{r_i}^{r_o} \frac{1}{r}\frac{\partial}{\partial r}\left(r\tau_{zr}\right)\; r\,dr d\theta = 2\pi r\tau_{rz}|_{r_i}^{r_o} = 2\pi r_i \tau_w \tag{7.177}$$

where we have assumed $\tau_{rz}|_{r=r_o} = 0$ and $\tau_{rz}|_{r=r_i} = -\tau_w$.

The second term on the rhs of equation (7.174) may similarly be written:

$$\int \frac{\partial \sigma_z}{\partial z}\,\mathrm{dA} = \overline{\frac{\partial \sigma_z}{\partial z}}\,A_w \approx \overline{\frac{\partial \sigma_z}{\partial z}}\,2\pi r_i h \tag{7.178}$$

The last term of equation (7.174) may be treated in exactly the same manner as the lhs. Thus, by substitution of equations (7.175), (7.177), and (7.178) into equation (7.174) we get:

$$\rho_w \bar{a}_z A_w = 2\pi r_i \tau_w + \overline{\frac{\partial \sigma_z}{\partial z}}\,A_w + \rho_w \bar{b}_z A_w \tag{7.179}$$

which by neglection of body forces and assumption of a thin walled structure reduces to:

$$\rho_w \bar{a}_z\, h = \overline{\frac{\partial \sigma_z}{\partial z}}\,h + \tau_w \tag{7.180}$$

Thus, equations (7.179) and (7.180) represent cross-sectional averaged Cauchy equations in the axial direction.

In order to derive the cross-sectional averaged Cauchy equations in the radial, we proceed in the same way as above, for the Cauchy equation (2.111) in the radial direction:

$$\int \rho a_r\;\mathrm{dA} = \int \left(\frac{\partial \sigma_r}{\partial r} + \frac{\sigma_r - \sigma_\theta}{r} + \frac{\partial \tau_{rz}}{\partial z} + \rho b_r\right)\;\mathrm{dA} \tag{7.181}$$

For the first and last terms of equation (7.181) we proceed in the same manner as for the axial Cauchy equation, whereas for the first term of the rhs we get:

$$\int \frac{\partial \sigma_r}{\partial r}\; r\,dr\,d\theta = 2\pi\sigma_r r|_{r_i}^{r_o} - \int \sigma_r\,dr\,d\theta \tag{7.182}$$

To evaluate the expression we need boundary conditions and assume $\sigma_r|_{r=r_i} = -p$ and $\sigma_r|_{r=r_o} = 0$. Further, we introduce the hat-symbol for another averaging procedure:

$$\hat{\sigma}_r = \frac{1}{2\pi h} = \int_0^{2\pi}\int_{r_i}^{r_o} \sigma_r\;dr\,d\theta \tag{7.183}$$

which by substitution into equation (7.182) yields:

$$\int \frac{\partial \sigma_r}{\partial r}\, r\, dr\, d\theta = 2\pi p r_i - \hat{\sigma}_r\, 2\pi h \tag{7.184}$$

By using the hat-convention for the second term of equation (7.181) we get:

$$\int \frac{\sigma_r - \sigma_\theta}{r}\, r\, dr\, d\theta = \hat{\sigma}_r\, 2\pi h - \hat{\sigma}_\theta\, 2\pi h \tag{7.185}$$

while the third term of equation (7.181) may be expressed as:

$$\int \frac{\partial \tau_{rz}}{\partial z}\ \mathrm{dA} = \overline{\frac{\partial \tau_{rz}}{\partial z}}\ A_w \approx \overline{\frac{\partial \tau_{rz}}{\partial z}}\ 2\pi r_i h \tag{7.186}$$

Finally, we may substitute equations (7.184), (7.185), and (7.186) into (7.181) to get:

$$\rho_w \bar{a}_r A_w = 2\pi r_i p - \hat{\sigma}_\theta\, 2\pi h + \overline{\frac{\partial \tau_{rz}}{\partial z}}\ A_w + \rho_w \bar{b}_r A_w \tag{7.187}$$

which represents a cross-sectionally averaged Cauchy equation in the radial direction. For a thin-walled structure without body forces, equation (7.187) reduce to:

$$\rho_w \bar{a}_r h = p - \frac{\hat{\sigma}_\theta\, h}{r_i} + \overline{\frac{\partial \tau_{rz}}{\partial z}}\, h \tag{7.188}$$

The constitutive equation for plane stress. In general the constitutive equations for a Hookean material in a plane stress situation have been provided previously in equation (4.36). For cylindrical coordinates (r, θ, z) we have also derived previously equation (save for some notation) that the circumferential strain $E_{\theta\theta} = u_r/r$, when u_r denote radial displacement. Thus, in engineering notation the constitutive equation for a thin walled vessel of a Hookean material, takes the form in cylindrical coordinates:

$$\sigma_z = \frac{\eta}{1-\nu_p^2}\left(\frac{\partial u_z}{\partial z} + \nu_p \frac{u_r}{r}\right) \quad \text{and} \quad \sigma_\theta = \frac{\eta}{1-\nu_p^2}\left(\frac{u_r}{r} + \nu_p \frac{\partial u_z}{\partial z}\right) \tag{7.189}$$

In the following we drop the symbols for averaging, and substitute equation (7.189) in the averaged Cauchy equations ((7.180) and (7.188)):

$$\rho_w a_z \, h = \frac{\eta \, h}{1-\nu_p^2}\left(\frac{\partial^2 u_z}{\partial z^2} + \frac{\nu_p}{r}\frac{\partial u_r}{\partial z}\right) + \tau_w \tag{7.190}$$

$$\rho_w a_r h = p - \frac{\eta \, h}{(1-\nu_p^2)\, r_i}\left(\frac{u_r}{r} + \nu_p \frac{\partial u_z}{\partial z}\right) \tag{7.191}$$

while assuming equation (7.189) to be a valid constitutive equation also for averaged stress/strain relations (the term $\overline{\frac{\partial \tau_{rz}}{\partial z}}$ was discarded as ???). Assume further, that $a_z = \partial^2 u_z/\partial t^2$ and $a_r = \partial^2 u_r/\partial t^2$, i.e., neglect convective terms, to obtain the averaged governing equations for the thin walled vessel:

$$\frac{\partial^2 u_z}{\partial t^2} = \frac{\eta}{(1-\nu_p^2)\rho_w}\left(\frac{\partial^2 u_z}{\partial z^2} + \frac{\nu_p}{r}\frac{\partial u_r}{\partial z}\right) + \frac{\tau_w}{\rho_w \, h} \tag{7.192}$$

$$\frac{\partial^2 u_r}{\partial t^2} = \frac{p}{\rho_w \, h} - \frac{\eta}{(1-\nu_p^2)\,\rho_w}\left(\frac{u_r}{r^2} + \frac{\nu_p}{r}\frac{\partial u_z}{\partial z}\right) \tag{7.193}$$

where we implicitly assume that $r \approx r_i$.

7.11.2 The governing equations for the fluid

The momentum equations without convective terms:

$$\frac{\partial v_z}{\partial t} = -\frac{1}{\rho}\frac{\partial p}{\partial z} + \nu\left(\frac{\partial^2 v_z}{\partial r^2} + \frac{1}{r}\frac{\partial v_z}{\partial r}\right) \tag{7.194}$$

$$\frac{\partial v_r}{\partial t} = -\frac{1}{\rho}\frac{\partial p}{\partial r} + \nu\left(\frac{1}{r}\frac{\partial}{\partial r}\left(r\frac{\partial v_r}{\partial r}\right)\right) \tag{7.195}$$

The equation for conservation of mass takes the form in cylindrical coordinates:

$$\frac{\partial v_r}{\partial r} + \frac{v_r}{r} + \frac{\partial v_z}{\partial z} = 0 \tag{7.196}$$

The momentum equations. Assume solutions on the form:

$$p = \hat{p}e^{i\omega\,(t-z/c)}, \quad v_z = \hat{v}_z e^{i\omega\,(t-z/c)}, \quad v_r = \hat{v}_r e^{i\omega\,(t-z/c)} \tag{7.197}$$

which by substitution into equation (7.194) yields:

$$i\omega\ \hat{v}_z = -\frac{1}{\rho}\left(\frac{-i\omega}{c}\right)\ \hat{p} + \frac{\nu}{r_i^2}\left(\frac{\partial^2 \hat{v}_z}{\partial y^2} + \frac{1}{y}\frac{\partial \hat{v}_z}{\partial y}\right) \tag{7.198}$$

where we have introduced the nondimensional scale $y = r/r_i$ and the Womersley parameter, previously introduced in equation (5.100),

$$\alpha = r_i\sqrt{\frac{\omega}{\nu}} \tag{7.199}$$

Rearrangement of equation (7.198) yields:

$$\frac{\partial^2 \hat{v}_z}{\partial y^2} + \frac{1}{y}\frac{\partial v_z}{\partial y} + i^3\alpha^2\hat{v}_z = \frac{i^3\alpha^2}{\rho c}\ \hat{p} \tag{7.200}$$

Now, by introducing another scale:

$$s = i^{3/2}\alpha y = i^{3/2}\alpha r/r_i \tag{7.201}$$

equation (7.200) may be transformed to an inhomogeneous Bessel equation of order zero (see equation (5.113)):

$$\frac{\partial^2 \hat{v}_z}{\partial s^2} + \frac{1}{s}\frac{\partial v_z}{\partial s} + \hat{v}_z = \frac{1}{\rho c}\ \hat{p} \tag{7.202}$$

By proceeding in the same manner for equation (7.195) we get:

$$i\omega\hat{v}_r = -\frac{1}{\rho r_i}\frac{\partial \hat{p}}{\partial y} + \frac{\nu}{r_i^2}\left(\frac{\partial^2 \hat{v}_r}{\partial y^2} + \frac{1}{y}\frac{\partial \hat{v}_r}{\partial y} - \frac{\hat{v}_r}{y^2}\right) \tag{7.203}$$

which by rearrangement may be presented:

$$\frac{\partial^2 \hat{v}_r}{\partial y^2} + \frac{1}{y}\frac{\partial \hat{v}_r}{\partial y} + i^3\alpha^2\hat{v}_r - \frac{\hat{v}_r}{y^2} = \frac{r_i}{\mu}\frac{\partial \hat{p}}{\partial y} \tag{7.204}$$

which also may be transformed to a Bessel equation by introducing the scale in equation (7.201), albeit of order one:

$$\frac{\partial^2 \hat{v}_r}{\partial s^2} + \frac{1}{s}\frac{\partial \hat{v}_r}{\partial s} + \left(1 - \frac{1}{s^2}\right)\hat{v}_r = \frac{ir_i}{\mu\alpha^2}\frac{\partial \hat{p}}{\partial y} = \frac{r_i}{\mu i^{3/2}\alpha}\frac{\partial \hat{p}}{\partial s} \tag{7.205}$$

For the continuity equation (7.196) we get:

$$\frac{\partial \hat{v}_r}{\partial r} + \frac{1}{r}\hat{v}_r - \frac{i\omega}{c}\hat{v}_z = 0 \tag{7.206}$$

which by introduction of the scale in equation (7.201) is transformed to:

$$\frac{1}{s}\frac{\partial}{\partial s}\left(s\hat{v}_r\right) = -\frac{i^{3/2}\sqrt{\nu\omega}}{c}\hat{v}_z \tag{7.207}$$

or alternatively:

$$\frac{1}{y}\frac{\partial}{\partial y}\left(y\hat{v}_r\right) = -\frac{ir_i\omega}{c}\hat{v}_z \tag{7.208}$$

The solutions of homogeneous Bessel equations of order zero and one, like equations (7.202) and (7.205), are given by their corresponding Bessel functions of order zero and one. Thus for general solutions of equations (7.202) and (7.205) we must provide particular solutions. Assume that a particular solution $\hat{v}_z^p$ of equation (7.202) is given by:

$$\hat{v}_z^p = B_1 J_o(ks) \quad \text{with} \quad \hat{p} = AJ_0(ks) \tag{7.209}$$

where k is to be determined. Substitution into equation (7.202) gives:

$$\frac{\partial^2 \hat{v}_z}{\partial s^2} + \frac{1}{s}\frac{\partial v_z}{\partial s} + \hat{v}_z = \frac{1}{\rho c}\,\hat{p}B_1k^2\frac{d^2}{dt^2}J_0(t) + \frac{B_1k}{s}\frac{d}{dt}J_0(t) + B_1J_0(ks) = \frac{A}{\rho c}J_0(ks) \tag{7.210}$$

where $t = ks$. From the useful properties of the Bessel functions given in (49) and (50) we may deduce:

$$\frac{d}{dt}J_0(t) = -J_1(t) \tag{7.211}$$

$$\frac{d}{dt}\left(tJ_1(t)\right) = tJ_0(t) = J_1(t) + t\frac{d}{dt}J_1(t) \tag{7.212}$$

$$\frac{d^2}{dt^2}J_0(t) = -\frac{d}{dt}J_1(t) = \frac{J_1(t)}{t} - J_0(t) \tag{7.213}$$

Equations (7.211) and (7.213) may subsequently be substituted into equation (7.210) to yield:

$$B_1 k^2 \left(\frac{J_1(ks)}{ks} - J_0(ks) \right) - \frac{B_1 k}{s} J_1(ks) + B_1 J_0(ks) \\ = B_1(1-k^2) J_0(ks) = \frac{A}{\rho c} J_0(ks) \tag{7.214}$$

Thus, equation $\hat{v}_z^p$ in (7.209) is a valid particular solution provided that:

$$B_1 = \frac{A}{(1-k^2)\rho c} \tag{7.215}$$

and a general solution of equation (7.202) is given by:

$$\hat{v}_z = \hat{v}_z^h + \hat{v}_z^p = \frac{C_1}{J_0(i^{3/2}\alpha)} J_0(s) + \frac{A}{\rho c\,(1-k^2)} J_0(ks) \tag{7.216}$$

where C_1 and k are constants to be determined (C_1 is scaled with $J_0(i^{3/2}\alpha)$ for analogy with rigid pipe solution).

Similarly, we propose a particular solution for equation (7.205) of the form:

$$\hat{v}_r^p = B_2 J_1(ks) \tag{7.217}$$

and we deduce from equation (7.211) and (7.213):

$$\frac{d^2}{dt^2} J_1 = \frac{d}{dt} J_0 - \frac{d}{dt}\left(\frac{J_1}{t}\right) = \left(\frac{1}{t^2} - 1\right) J_1 - \frac{1}{t}\frac{d}{dt} J_1 \tag{7.218}$$

Substitution of equations (7.217) and (7.218) into equation (7.205) yields:

$$B_2 k^2 \left(\frac{1}{(sk)^2} - 1 \right) J_1 - \frac{B_2 k^2}{sk}\frac{dJ_1}{dt} + \frac{B_2 k}{s}\frac{dJ_1}{dt} + \left(1 - \frac{1}{s^2}\right) B_2 J_1 \\ = B_2\,(1-k^2) J_1(ks) = \frac{r_i A}{\mu i^{3/2}\alpha}\frac{\partial \hat{p}}{\partial s} = \frac{-r_i A k}{\mu i^{3/2}\alpha}\, J_1(ks) \tag{7.219}$$

where we have used:

$$\frac{\partial \hat{p}}{\partial s} = -Ak\ J_1(ks) \tag{7.220}$$

From equation (7.219) we get that $\hat{v}_r^p$ in equation (7.217) is a particular provided that:

$$B_2 = \frac{r_i Ak}{\mu i^{3/2}\alpha(k^2-1)} \tag{7.221}$$

And consequently, a general solution of equation (7.205) is:

$$\hat{v}_r = \hat{v}_r^h + \hat{v}_r^p = \frac{C_2}{J_0(i^{3/2}\alpha)}\ J_1(s) + \frac{r_i A}{\mu i^{3/2}\alpha}\ \frac{k}{k^2-1}\ J_1(ks) \tag{7.222}$$

Fulfillment of the continuity equation. The two general solutions given by equations (7.216) and (7.222) must also satisfy the continuity equation (7.207). Observe first that:

$$\begin{aligned} \frac{1}{s}\left(\frac{d}{ds}(\hat{v}_r s)\right) &= \frac{1}{s}\left(\frac{d}{ds}(\hat{v}_r^h s) + \frac{d}{ds}(\hat{v}_r^p s)\right) \\ &= \frac{1}{s}\frac{d}{ds}(\hat{v}_r^h s) + \frac{1}{s}\frac{d}{dt}(\hat{v}_r^p(t)t) \end{aligned} \tag{7.223}$$

From equation (7.222) we get:

$$\frac{1}{s}\frac{d}{ds}(\hat{v}_r^h s) = \frac{C_2}{J_0(i^{3/2}\alpha)}J_0(s) \tag{7.224}$$

by the use of equation (7.212) and similarly:

$$\hat{v}_r^p(t)t = \frac{r_i Ak}{\mu i^{3/2}\alpha(k^2-1)}\ J_1(t)t \tag{7.225}$$

and thus:

$$\begin{aligned} \frac{1}{s}\frac{d}{dt}(\hat{v}_r^p(t)t) &= \frac{r_i Ak}{\mu i^{3/2}\alpha(k^2-1)}\ \frac{sk}{s}J_0(sk) \\ &= \frac{r_i Ak^2}{\mu i^{3/2}\alpha(k^2-1)}J_0(sk) \end{aligned} \tag{7.226}$$

Substitution of equation (7.224) and (7.226) in equation (7.222) results in the following expression:

$$\frac{1}{s}\left(\frac{d}{ds}(\hat{v}_r s)\right) = \frac{C_2}{J_0(i^{3/2}\alpha)}J_0(s) + \frac{r_i A k^2}{\mu i^{3/2}\alpha(k^2-1)}J_0(ks) \tag{7.227}$$

which is the left hand side of the continuity equation (7.207). For the right hand side of the continuity equation we get by substitution of equation (7.216):

$$\begin{aligned} -\frac{i^{3/2}\sqrt{\nu\omega}}{c}\hat{v}_z &= \frac{ir_i\omega}{i^{3/2}\alpha c}\hat{v}_z \\ &= \frac{ir_i\omega}{i^{3/2}\alpha c J_0(i^{3/2}\alpha)}\, C_1\, J_0(s) + \frac{ir_i\omega}{i^{3/2}\alpha c}\,\frac{A}{\rho c\,(1-k^2)}\, J_0(ks) \end{aligned} \tag{7.228}$$

By comparing equation (7.227) and equation (7.228) we find that the ratio of C_2 and C_1 must satisfy:

$$\frac{C_2}{C_1} = \frac{ir_i\omega}{i^{3/2}\alpha c} \tag{7.229}$$

and k must fulfill the condition:

$$\frac{k^2}{\mu} = \frac{i^3\omega}{\rho c^2} \quad \Rightarrow \quad k = \pm\frac{i^{3/2}\sqrt{\nu\omega}}{c} = \pm\frac{i^{3/2}r_i\omega}{\alpha c} \tag{7.230}$$

Thus, one may argue that for physiological values of ν, ω, and c we will have $|k| \ll 1$. Further, by introducing the definition of the scale in equation (7.201) we get:

$$ks = \pm\frac{i^{3/2}r_i\omega}{\alpha c}i^{3/2}\alpha y = \mp\frac{ir_i\omega}{c}y = \mp\frac{i\omega}{c}r \tag{7.231}$$

For terms involving $J_0(ks)$ and $J_1(ks)$ one may approximate:

$$J_0(ks) = I_0(\mp\frac{r_i\omega}{c}\, y) \approx 1 \quad \text{and} \quad J_1(ks) = I_1(\mp\frac{r_i\omega}{c}\, y) \approx \mp\frac{ir_i\omega}{2c}\, y \tag{7.232}$$

where I_n denotes the modified Bessel function of order n (see equation (54) in section .5). From equation (7.230) and (7.232) we get:

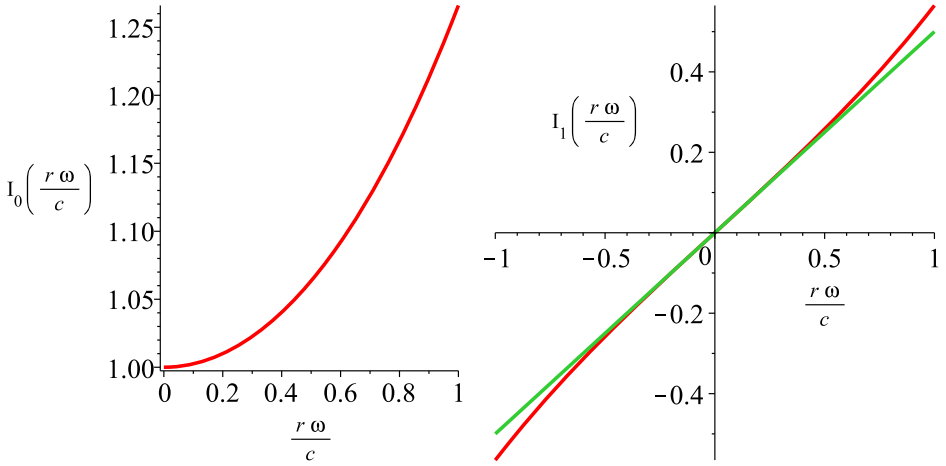

Figure 7.11: Plots of modified Bessel functions of order zero (left) and one (right): I_0 and I_1.

$$kJ_1(ks) \approx \pm\frac{i^{3/2}r_i\omega}{\alpha c} \mp \frac{ir_i\omega}{2c}\, y = -\frac{i^{3/2}r_i\omega}{\alpha c}\frac{ir_i\omega}{2c}\, y \tag{7.233}$$

The solution in the radial direction in equation (7.222) may now be simplified by first using $|k| \ll 1|$:

$$\hat{v}_r \approx \frac{C_2}{J_0(i^{3/2}\alpha)}\, J_1(s) - \frac{r_i A}{\mu i^{3/2}\alpha}\, k\, J_1(ks) \tag{7.234}$$

and then using the results in equation (7.229) and (7.233) which results in:

$$\hat{v}_r \approx \frac{ir_i\omega}{2c}\left(\frac{2C}{\alpha i^{3/2} J_0(i^{3/2}\alpha)}\, J_1(i^{3/2}\alpha\, y) + \frac{A}{\rho c} y\right) \tag{7.235}$$

The solution in the axial direction $\hat{v}_z$ in equation (7.216) may be simplified, by taking the approximations in equation (7.232) and $|k| \ll 1$ into account, to yield:

$$\hat{v}_z \approx \frac{C}{J_0(i^{3/2}\alpha)}\, J_0(i^{3/2}\alpha\, y) + \frac{A}{\rho c} \tag{7.236}$$

where we have dropped the subscript of C for convenience, *i.e.* $C = C_1$.

Boundary conditions. In order to provide boundary conditions for the structural equations given in section 7.11.1 we must evaluate the solutions in the axial and radial directions at the inner surface of the vessel:

$$\hat{v}_z(y=1) = C + \frac{A}{\rho c} \tag{7.237}$$

$$\hat{v}_r(y=1) = \frac{ir_i\omega}{2c}\left(CF_{10}(\alpha) + \frac{A}{\rho c}\right) \tag{7.238}$$

where we have introduced the Womersley function F_{10}:

$$F_{10}(\alpha) = \frac{2J_1(i^{3/2}\alpha)}{\alpha i^{3/2}\, J_0(i^{3/2}\,\alpha)} \tag{7.239}$$

An expression for $\partial\hat{v}_z/\partial y$ must be provided to estimate the wall shear stress at the vessel wall, which is needed in equation (7.180). By differentiation of equation (7.216) we get by introducing equation (7.231):

$$\begin{aligned}\frac{\partial\hat{v}_z}{\partial y} &\approx \frac{C}{J_0(i^{3/2}\alpha)}\,\frac{d}{dy}J_0(i^{3/2}\alpha\, y) + \frac{A}{\rho c}\,\frac{d}{dy}J_0\left(\mp\frac{ir_i\omega}{c}y\right) \\ &= -\frac{Ci^{3/2}\alpha}{J_0(i^{3/2}\alpha)}\,J_1(i^{3/2}\alpha\, y) - \frac{A}{\rho c}\left(\mp\frac{ir_i\omega}{c}\right)\,J_1\left(\mp\frac{ir_i\omega}{c}y\right)\end{aligned} \tag{7.240}$$

and then from equation (7.239), (7.231) and (7.240) we get:

$$\frac{\partial\hat{v}_z}{\partial y}(y=1) = -\frac{C}{2}i^3\alpha^2F_{10}(\alpha) + \frac{1}{2}\left(\frac{\omega r_i}{c}\right)^2\,\frac{A}{\rho c} \tag{7.241}$$

7.11.3 Coupling of structure and fluid

Assume solutions of the governing equations equation (7.192) and (7.193) for the vessel wall on the form:

$$u_r = De^{i\omega(t-z/c)} \quad \text{and} \quad u_z = Ee^{i\omega(t-z/c)} \tag{7.242}$$

The condition that the fluid velocity and the structural velocity must be equal at the inner vessel wall, *i.e.* $y = 1$, is normally referred to as the kinematic condition. The mathematical representation of the kinematic condition by means of axial displacement is:

$$\frac{\partial u_z}{\partial t} = \hat{v}_z(y=1)e^{i\omega(t-z/c)} \tag{7.243}$$

which by using equation (7.237) and (7.242) is equivalent to:

$$i\omega E = C + \frac{A}{\rho c} \tag{7.244}$$

An identical approach in the radial direction yields:

$$i\omega D = \frac{ir_i\omega}{2c}\left(CF_{10}(\alpha) + \frac{A}{\rho c}\right) \tag{7.245}$$

Further, substitution of equation (7.242) into the governing equations (7.192) and (7.193) for the vessel wall yields:

$$-\omega^2 D = \frac{A}{\rho_w h} - \frac{\eta}{(1-\nu_p^2)\rho_w}\left(\frac{D}{r^2} - \frac{i\omega\nu_p}{rc}E\right) \tag{7.246}$$

$$-\omega^2 E = \frac{\eta}{(1-\nu_p^2)\rho_w}\left(-\frac{\omega^2}{c^2}E - \frac{i\omega\nu_p}{rc}D\right) + \frac{\tau_w}{\rho_w h} \tag{7.247}$$

One may argue that the wall shear stress, which in general is given by:

$$\tau_w = \mu\left(\frac{\partial v_z}{\partial r} + \frac{\partial v_r}{\partial z}\right)\Big|_{r=r_i} \approx \mu\frac{\partial v_z}{\partial r}\Big|_{r=r_i} \tag{7.248}$$

as $\partial v_r/\partial z \ll \partial v_z/\partial r$ and thus:

$$\frac{\hat{\tau}_w}{\rho_w h} = \frac{\mu}{r_i}\frac{\partial \hat{v}_z}{\partial y}\Big|_{y=1} = \frac{\rho}{\rho_w}\frac{\nu}{2r_i h}\left(-Ci\alpha^2 F_{10}(\alpha) + \left(\frac{\omega r_i}{c}\right)^2 \frac{A}{\rho c}\right) \tag{7.249}$$

which by substitution into equation (7.247) yields:

$$-\omega^2 E = \frac{\eta}{(1-\nu_p^2)\rho_w}\left(-\frac{\omega^2}{c^2}E - \frac{i\omega\nu_p}{rc}D\right) + \frac{\rho}{\rho_w}\frac{\nu}{2r_i h}\left(-Ci\alpha^2 F_{10}(\alpha) + \left(\frac{\omega r_i}{c}\right)^2 \frac{A}{\rho c}\right) \tag{7.250}$$

The four equations (7.244), (7.245), (7.246), and (7.250) constitute a homogeneous algebraic equation system in the arbitrary constants A, C, D, and E, which has the matrix representation:

$$\begin{bmatrix} \frac{1}{\rho\, c} & 1 & 0 & -i\omega \\ \frac{i\omega\, r_i}{2\rho\, c^2} & \frac{i\omega\, r_i}{2c} F_{10} & -i\omega & 0 \\ \frac{1}{\rho_w h} & 0 & \omega^2 - \frac{B}{\rho_w {r_i}^2} & \frac{iB\omega\, \nu_p}{\rho_w r_i c} \\ \frac{\rho}{\rho_w}\frac{\nu}{2r_i h}\left(\frac{\omega r_i}{c}\right)^2 \frac{1}{\rho c} & -\frac{i\rho\,\omega\, r_i F_{10}}{2\rho_w h} & \frac{-iB\omega\, \nu_p}{\rho_w r_i c} & \omega^2\left(1 - \frac{B}{\rho_w c^2}\right) \end{bmatrix} \begin{bmatrix} A \\ C \\ D \\ E \end{bmatrix} = 0 \tag{7.251}$$

where we for convenience have introduced the constant:

$$B = \frac{\eta}{1 - \nu_p^2} \tag{7.252}$$

Further, let $\boldsymbol{M}$ denote the matrix in equation (7.251) and M_{ij} the element on row i and column j. The Womersley number: $\nu\alpha^2 = \omega r_i^2$ may then be used to simplify element M_{42}:

$$M_{42} = \frac{\rho}{\rho_w}\frac{\nu}{2r_i h} i\alpha^2 F_{10}(\alpha) = \frac{i\rho\,\omega\, r_i F_{10}}{2\rho_w h} \tag{7.253}$$

Further, one may argue that:

$$M_{32} = \omega^2 - \frac{B}{\rho_w r_i^2} \approx -\frac{B}{\rho_w r_i}^2 \tag{7.254}$$

as B/ρ_w is proportional to the transverse wave speed in the structure (see equation (4.139)), which is assumed to be greater than the wave-speed in the coupled problem, *i.e.* $B/\rho_w c^2 > 1$, whereas $(\omega r_i/c)^2 \ll 1$ for physiological values.

From basic linear algebra, we know that for a non-trivial solution (*i.e.* unequal to zero) to exist of equation (7.251), the determinant of the matrix must be zero. Further, multiplication of the columns and rows of a matrix $\boldsymbol{M}$ by constants will not the change the solutions to the equation $\det(\boldsymbol{M}) = 0$. Thus, in the pursuit of a simple and convenient expression for the determinant of the matrix in equation (7.251), we will make all terms non-dimensional by the following recipe:

- Multiply c1 with ρc.

- Multiply r2 with $c/i\omega r_i$
- Multiply c3 with r_i/c
- Multiply r3 with r_i/c
- Multiply c4 with $-1/i\omega$
- Multiply r4 with $1/i\omega$

Element M_{41} will be of the order $(\omega r_i/c\alpha)^2$ and may thus be discarded. These operations leave the following expression:

$$\det(\boldsymbol{M}) = \begin{vmatrix} 1 & 1 & 0 & 1 \\ 1/2 & 1/2\,F_{10} & -1 & 0 \\ \dfrac{\rho\, r_i}{\rho_w h} & 0 & -\dfrac{B}{\rho_w c^2} & -\dfrac{B\nu_p}{\rho_w c^2} \\ 0 & -\dfrac{\rho\, r_i F_{10}}{2\rho_w h} & -\dfrac{B\nu_p}{\rho_w c^2} & 1-\dfrac{B}{\rho_w c^2} \end{vmatrix} \tag{7.255}$$

to proceed further we introduce:

$$k = \rho_w h/\rho\, r_i \quad \text{and} \quad x/k = B/\rho_w c^2 \tag{7.256}$$

and multiply row 3 and four with k:

$$\det(\boldsymbol{M}) = \begin{vmatrix} 1 & 1 & 0 & 1 \\ 1/2 & 1/2\,F_{10} & -1 & 0 \\ 1 & 0 & -x & -\nu_p x \\ 0 & -1/2\,F_{10} & -\nu_p x & k-x \end{vmatrix} \tag{7.257}$$

to eliminate the first elements in row 2 and row 3 we perform some linear combinations of the rows. First, we replace row 2 by row 1 - 2× row 2, second row 3 is replaced by row 1 - row 3. This will simplify the expression for the determinant by Laplacian expansion:

$$\det(\boldsymbol{M}) = \begin{vmatrix} 1 & 1 & 0 & 1 \\ 0 & 1-F_{10} & 2 & 1 \\ 0 & 1 & x & \nu_p x+1 \\ 0 & -1/2\,F_{10} & -\nu_p x & k-x \end{vmatrix} = \begin{vmatrix} 1-F_{10} & 2 & 1 \\ 1 & x & \nu_p x+1 \\ -1/2\,F_{10} & -\nu_p x & k-x \end{vmatrix} \tag{7.258}$$

which may be evaluated to:

$$\det(\boldsymbol{M}) = (1-F_{10})(1-\nu_p^2)\, x^2-(k(1-F_{10})+F_{10}\,(1/2-2\nu_p)+2)\;\; x+F_{10}+2k = 0 \tag{7.259}$$

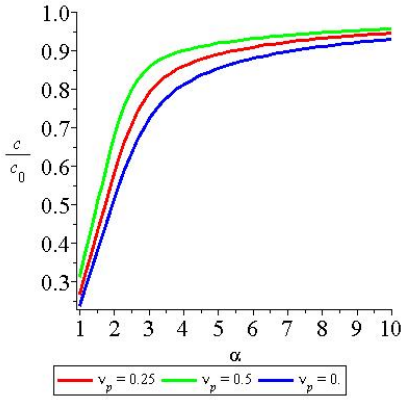

Figure 7.12: Plots of $\gamma_r = \Re(c/c_0)$ as function of α and ν_p for $k = 0.1$.

This is a simple second order algebraic equation in x which is easy to solve. The complex solutions of equation (7.259) will be functions of ν_p, k, and α, i.e., $x = x(\nu_p k, \alpha)$, which may readily be found with e.g., Maple. From equation (7.256) one may deduce:

$$x = k\frac{\eta}{1-\nu_p^2}\frac{1}{\rho_w}\frac{1}{c^2} = \frac{h}{\rho r_i}\frac{\eta}{1-\nu_p^2}\frac{1}{c^2} \tag{7.260}$$

The Moens-Korteweg formula for the wave speed c_0 under inviscid conditions is given by equation (7.107), which by substitution and rearrangement in equation (7.260) results in:

$$\gamma = \frac{c}{c_0} = \left(\frac{(1-\nu_p^2)\, x}{2}\right)^{-1/2} \tag{7.261}$$

The symbol γ has been introduced for the ratio of the wave speed c for the coupled problem to c_0. As x is complex, so will γ be, and we write $\gamma = \gamma_r + i\gamma_i$ for the real and complex parts. Thus, having found the solutions of equation (7.259), we may plot γ_r as a function of ν_p, k, and α (see figure 7.12).

The dependence of k and ν_p may also be illustrated in 3D, albeit some less quantitative accuracy (see figure 7.13).

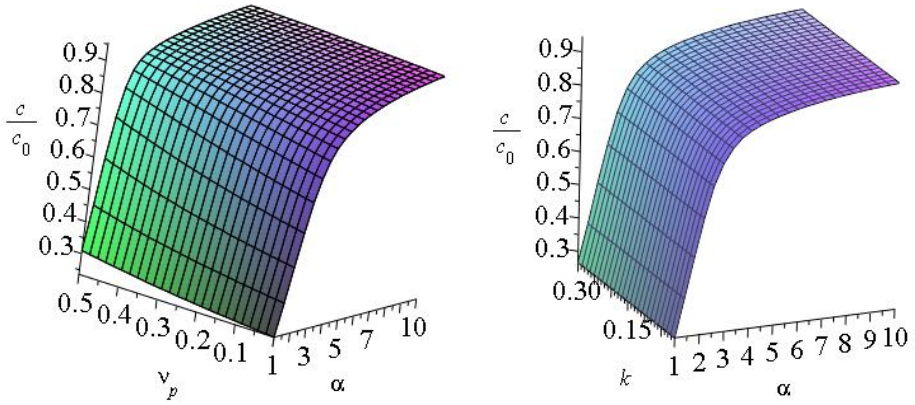

Figure 7.13: $\gamma_r = \Re(c/c_0)$ as function of α and ν_p for $k = 0.1$ (left) and k for $\nu_p = 0.25$ (right).

Chapter 8

Appendix

.1 Trigonometric relations

$$\sin 2\phi = 2\sin\phi\cos\phi, \qquad \cos 2\phi = \cos^2\phi - \sin^2\phi \tag{1}$$

$$\cos^2\phi = \frac{1}{2}\left(1+\cos 2\phi\right), \qquad \sin^2\phi = \frac{1}{2}\left(1-\cos 2\phi\right) \tag{2}$$

.2 Vectors

A vector is a coordinate invariant quantity, uniquely defined by a magnitude and a direction in space, and that obeys the parallelogram law by addition.

The magnitude of a vector $\mathbf{a}$ is denoted:

$$|\mathbf{a}| \equiv a \tag{3}$$

A vector $\mathbf{a}$ may be decomposed into *scalar vector components* or for short *components*, a_i, parallel to the coordinate axes, i.e., parallel to the base vectors $\mathbf{e}_i$, and then be presented in various, equivalent ways:

$$\mathbf{a} = a_1\mathbf{e}_1 + a_2\mathbf{e}_2 + a_3\mathbf{e}_3 \equiv a_i\mathbf{e}_i \equiv (a_1, a_2, a_3) \equiv [a_i] \equiv \begin{bmatrix} a_1 \\ a_2 \\ a_3 \end{bmatrix} \tag{4}$$

Addition and subtraction of vectors are defined according to the geometric parallelogram law [17, see section 2.2], but the geometrical definition is transformed to the component form given by:

$$\mathbf{a} + \mathbf{b} = \mathbf{c} \Leftrightarrow a_i + b_i = c_i \tag{5}$$

The *scalar product* (or dot product) of two vectors **a** and **b** is defined by:

$$\mathbf{a} \cdot \mathbf{b} = |\mathbf{a}||\mathbf{b}| \cos(\mathbf{a}, \mathbf{b}) \tag{6}$$

where $(\mathbf{a}, \mathbf{b})$ is the angle between the two vectors. The operation is commutative and distributive. For orthogonal base vectors in a coordinate system Ox we get:

$$\mathbf{e}_i \cdot \mathbf{e}_j = \delta_{ij} \tag{7}$$

where δ_{ij} is the *Kronecker delta* defined as:

$$\delta_{ij} = \begin{cases} 1 & \text{when } i = j \\ 0 & \text{when } i \neq j \end{cases} \tag{8}$$

From these fundamental definitions and properties one may show[17, see section 2.2]:

$$\mathbf{a} \cdot \mathbf{b} = a_i b_i \tag{9}$$

The *vector product*or *cross product* is defined by:

$$\mathbf{a} \times \mathbf{b} = \mathbf{c} \equiv |\mathbf{a}||\mathbf{b}| \sin((\mathbf{a}, \mathbf{b})\, \mathbf{e} \tag{10}$$

where $(\mathbf{a}, \mathbf{b})$ is the smallest angle between the two vectors **a** and **b**, and **e** is a unit vector orthogonal to the plane defined by **a** and **b**. By introducing the *permutation symbol*:

$$e_{ijk} = \begin{cases} 0 & \text{when two or three indices are equal} \\ 1 & \text{when the indices are cyclic permutations of 123} \\ -1 & \text{when the indices are cyclic permutations of 321} \end{cases} \tag{11}$$

one may also conveniently express the vector product by:

$$\mathbf{a} \times \mathbf{b} = \mathbf{c} \qquad \Leftrightarrow \qquad e_{ijk}\, a_i b_j = c_k \tag{12}$$

.3 Orthogonal Coordinates

In a general orthogonal coordinate system we denote the coordinates by y_i. The position $\boldsymbol{r}$ is then a function of y_i and time t which we denoted by $\boldsymbol{r} = \boldsymbol{r}(y_i, t)$. A one-to-one correspondence between the general orthogonal coordinates y_i and the Cartesian coordinates x_i. For convenience we denote the the general orthogonal coordinate system for the y-system.

The base vectors $\boldsymbol{g}_i$ (not unit vectors) of the y-system, are tangent vectors to the coordinate lines of the y-coordinates:

$$\boldsymbol{g}_i = \frac{\partial \boldsymbol{r}}{\partial y_i} = \frac{\partial \boldsymbol{r}}{\partial x_k}\frac{\partial x_k}{\partial y_i} = \boldsymbol{e}_k \frac{\partial x_k}{\partial y_i} \quad \Leftrightarrow \quad \boldsymbol{e}_k = \frac{\partial y_i}{\partial x_k}\boldsymbol{g}_i \tag{13}$$

with corresponding magnitude:

$$h_i = \sqrt{\boldsymbol{g}_i \cdot \boldsymbol{g}_i} = \sqrt{\frac{\partial x_k}{\partial y_i}\frac{\partial x_k}{\partial y_i}}, \quad \text{no sum over i} \tag{14}$$

Further, due to orthogonality of the coordinate lines:

$$\boldsymbol{g}_i \cdot \boldsymbol{g}_j = 0 \quad \text{for} \quad i \neq j \quad \Rightarrow \frac{\partial x_k}{\partial y_i}\frac{\partial x_k}{\partial y_j} = 0 \quad \text{for} \quad i \neq j \tag{15}$$

From equation (14) and (15) we get the following relation:

$$\frac{\partial x_k}{\partial y_i}\frac{\partial x_k}{\partial y_j} = h_i^2\, \delta_{ij} \tag{16}$$

From the fundamental properties of the general orthogonal coordinate system we have:

$$\frac{\partial y_i}{\partial y_j} = \frac{\partial y_i}{\partial x_k}\frac{\partial x_k}{\partial y_j} = \delta_{ij} \tag{17}$$

Thus, the components in the sum in equation (17) may be interpreted as the product of two matrices with the components:

$$\left[\frac{\partial y_i}{\partial x_k}\right] = \left[\frac{\partial x_k}{\partial y_i}\right]^{-1} \tag{18}$$

Then from equation (16) and (18) we get:

$$\left(\frac{\partial y_i}{\partial x_k}\frac{\partial y_j}{\partial x_k}\right) = \left(\frac{\partial x_k}{\partial y_i}\frac{\partial x_k}{\partial y_j}\right)^{-1} = \frac{1}{h_i^2}\,\delta_{ij} \tag{19}$$

The del-operator is normally defined as follows in a Cartesian coordinate system:

$$\nabla() = \boldsymbol{e}_k \frac{\partial()}{\partial x_k} \tag{20}$$

A representation of the del-operator in a general orthogonal coordinate system may then be found by substitution of equation (13) and (19) into equation (20):

$$\nabla() = \left(\frac{\partial y_i}{\partial x_k}\,\boldsymbol{g}_i\right)\left(\frac{\partial()}{\partial y_j}\frac{\partial y_j}{\partial x_k}\right) = \sum_i \left(\frac{1}{h_i^2}\delta_{ij}\right)\boldsymbol{g}_i\frac{\partial()}{\partial y_j} = \sum_i \frac{1}{h_i^2}\boldsymbol{g}_i\frac{\partial()}{\partial y_i} \tag{21}$$

By introducing a unit base vector in the y-system:

$$\boldsymbol{e}_i^y = \frac{\boldsymbol{g}_i}{h_i} \tag{22}$$

the expression for the del-operator take the form:

$$\nabla() = \sum_i \frac{1}{h_i}\boldsymbol{e}_i^y\frac{\partial()}{\partial y_i} \tag{23}$$

.3.1 Gradient, divergence and rotation in general orthogonal coordinates

The physical components of a vector $\boldsymbol{a}$ and a second order tensor $\boldsymbol{A}$ are defined in the following manner:

$$\boldsymbol{a} = a_k^y\boldsymbol{e}_k^y, \qquad \boldsymbol{A} = A_{kl}^y\,\boldsymbol{e}_k^y\otimes\boldsymbol{e}_l^y \tag{24}$$

From the expression in equation (21) we get for a scalar α:

$$\nabla\alpha = \sum_i \frac{1}{h_i}\boldsymbol{e}_i^y\frac{\partial\alpha}{\partial y_i} \tag{25}$$

and for the divergence of a vector $\boldsymbol{a}$:

$$\nabla\cdot\boldsymbol{a} = \sum_i \frac{1}{h_i}\boldsymbol{e}_i^y\frac{\partial(a_k^y\boldsymbol{e}_k^y)}{\partial y_i} \tag{26}$$

rotation of a vector $\boldsymbol{a}$:

$$\nabla\times\boldsymbol{a} = \sum_i \frac{1}{h_i}\boldsymbol{e}_i^y\times\frac{\partial(a_k^y\boldsymbol{e}_k^y)}{\partial y_i} \tag{27}$$

The divergence of a second order tensor $\boldsymbol{A}$ is:

$$\mathrm{div}\boldsymbol{A} = \boldsymbol{A}\cdot\overleftarrow{\nabla} = \sum_i \frac{1}{h_i}\frac{\partial\left(A_{kl}^y\boldsymbol{e}_k^y\otimes\boldsymbol{e}_l^y\right)}{\partial y_i}\cdot\boldsymbol{e}_i^y \tag{28}$$

This expression for the div$\boldsymbol{A}$ in equation (28) may be expanded by using the chain rule and taking into account $(\boldsymbol{a}\otimes\boldsymbol{b})\cdot\boldsymbol{c} = \boldsymbol{a}\,(\boldsymbol{b}\cdot\boldsymbol{c})$ and the orthogonality of the y-system (i.e., $\boldsymbol{e}_l^y \cdot \boldsymbol{e}_i^y = \delta_{li}$):

$$\mathrm{div}\boldsymbol{A} = \sum_i \frac{1}{h_i}\frac{\partial A_{ki}^y}{\partial y_i}\boldsymbol{e}_k^y + \frac{1}{h_i}A_{ki}^y\frac{\partial \boldsymbol{e}_k^y}{\partial y_i} + \frac{1}{h_i}A_{ki}^y\boldsymbol{e}_k \otimes \frac{\partial \boldsymbol{e}_l^y}{\partial y_i}\cdot\boldsymbol{e}_i^y \tag{29}$$

.4 Integral Theorems

Theorem .4.1. Gauss' Integral Theorem

Let V be a volume with surface A and $\mathbf{n}$ an outward unit vector on A. The for any field $f(x)$:

$$\int_V f_{,k}\, dV = \int_A f\, n_k\, dA \tag{30}$$

For a proof see e.g. [17, C.3].

Theorem .4.2. The Divergence Theorem

By replacing the function $f(x)$ in by the vector components $a_i(x)$ of a vector field $\mathbf{a}(x)$ we get:

$$\int_V a_{k,k}\, dV = \int_A a_k\, n_k\, dA \tag{31}$$

$$\int_V \nabla\cdot\mathbf{a}\, dV = \int_A \mathbf{a}\cdot\mathbf{n}\, dA \tag{32}$$

It is trivial that Eq. (31) holds when no summation involved, by just replacing f with a_k in Eq. (30). However, as the integral operator is linear, it will also hold when Einstein's summation convention is employed. Consequently, Eq. (31) is valid when using the summation convention too, and then Eq. (32) follows as the vector representation of Eq. (31).

Theorem .4.3. The First Mean Value Theorem

Let $f(\mathbf{x})$ and $g(\mathbf{x})$ represent continuous field functions, such that $f, g : \mathbb{R}^3 \to \mathbb{R}$. Further, let V represent a contiguous volume, i.e., $V \in \mathbb{R}^3$. Then there exists a $\bar{\mathbf{x}} \in V$ such that:

$$\int_V f(\mathbf{x})\, g(\mathbf{x})\, dV = f(\bar{\mathbf{x}}) \int_V g(\mathbf{x})\, dV \tag{33}$$

In particular, if $g(\mathbf{x}) = 1$ for all $\mathbf{x} \in V$

$$\int_V f(\mathbf{x})\, dV = f(\bar{\mathbf{x}})\, V \tag{34}$$

Thus, $f(\bar{\mathbf{x}})$ is the mean value of $f(\mathbf{x})$ in V.
For proofs see [50] and [17, C.3].

Theorem .4.4. Leibniz's rule for 1D integrals
Let

$$F(t) = \int_{a(t)}^{b(t)} f(x,t)\,dx \tag{35}$$

then

$$\frac{dF(t)}{dt} = \int_{a(t)}^{b(t)} \frac{\partial f(x,t)}{\partial t}\,dx + f(x,t)\frac{\partial b(t)}{\partial t} - f(x,t)\frac{\partial a(t)}{\partial t} \tag{36}$$

Theorem .4.5. Leibniz's rule for 2D integrals
Let us consider the integral $F(t)$ obtained by integration of the function $f(x,y,t)$ over the domain in 2D space $\{x,y\} \in A(t)$ where $A(t)$ is a function of t:

$$F(t) = \int_{A(t)} f(x,y,t)\,dA \tag{37}$$

then:

$$\frac{dF(t)}{dt} = \int_{A(t)} \frac{\partial f(x,y,t)}{\partial t}\,dA + \left[f(x,y,t)\frac{dA}{dt}\right]_{C(t)} = \int_{A(t)} \frac{\partial f(x,y,t)}{\partial t}\,dA + \oint_{C(t)} f\frac{dn}{dt}\,dc \tag{38}$$

where dA at the boundary (or contour) is expressed as $dA = dn\,dc$. Hence, (n,c) is the local coordinate, where dc is tangential and dn is orthogonal to $C(t)$.

If $\boldsymbol{v}$ is the velocity on $C(t)$, the velocity component of $\boldsymbol{v}$ in the outward normal direction $\boldsymbol{n}$ to $C(t)$ is:

$$v_n = \boldsymbol{v}\cdot\boldsymbol{n} = \frac{dn}{dt} \tag{39}$$

and thus:

$$\frac{dn}{dt}\,dc = v_n\,dc = \boldsymbol{v}\cdot\boldsymbol{n}\,dc \tag{40}$$

and consequently:

$$\frac{dF(t)}{dt} = \int_{A(t)} \frac{\partial f(x,y,t)}{\partial t}\,dA + \oint_{C(t)} f\,\boldsymbol{v}\cdot\boldsymbol{n}\,dc \tag{41}$$

Theorem .4.6. Leibniz's rule for 3D integrals

Let us consider the integral $F(t)$ obtained by integration of the function $f(x, y, z, t)$ over the domain in 3D space $\{x, y, z\} \in V(t)$ where $V(t)$ is a function of t:

$$F(t) = \int_{V(t)} f(x, y, z, t)\, dV \tag{42}$$

The, volume $V(t)$ has the surface $A(t)$.

$$\frac{dF(t)}{dt} = \int_{V(t)} \frac{\partial f(x, y, t)}{\partial t}\, dV + \left[f(x, y, t) \frac{dV}{dt} \right]_{A(t)} = \int_{V(t)} \frac{\partial f(x, y, t)}{\partial t}\, dV + \int_{A(t)} f \frac{dn}{dt}\, dA \tag{43}$$

where $dV = dn\, dA$ is the area increment and dn is the increment in the direction of the outward normal to A. Note that:

$$\frac{dV}{dt} = \frac{dn}{dt}\, dA = v_n\, dA = \boldsymbol{v} \cdot \boldsymbol{n}\, dA \tag{44}$$

and consequently:

$$\frac{dF(t)}{dt} = \int_{V(t)} \frac{\partial f(x, y, t)}{\partial t}\, dV + \int_{A(t)} f\, \boldsymbol{v} \cdot \boldsymbol{n}\, dA \tag{45}$$

.5 Properties of Bessel functions

The presentation of the Bessel functions are based on a articles in [48, 51]. The Bessel functions are solutions $y(x)$:

$$y(x) = c_1 J_n(x) + c_2 Y_n(x) \tag{46}$$

of Bessel's differential equation[1]:

$$\frac{d^2 y}{dx^2} + \frac{1}{x}\frac{dy}{dx} + \left(1 - \frac{n^2}{x^2}\right) y = 0 \tag{47}$$

Bessel functions are also known as cylinder functions or cylindrical harmonics because they are found in the solution to Laplace's equation in cylindrical coordinates. Bessel functions of the first kind, denoted as $J_n(x)$, are solutions of Bessel's differential equation that are finite at the origin (x = 0) for non-negative integer n, and diverge as x approaches zero for negative non-integer n. The solution type (e.g. integer or non-integer) and normalization of $J_n(x)$

[1]Note that n may in general be a complex number. Here we assume n to be an integer.

are defined by its properties below. It is possible to define the function by its Taylor series expansion around x = 0:

$$J_n(x) = \sum_{m=0}^{\infty} \frac{(-1)^m}{m!\Gamma(m+n+1)} (\frac{x}{2})^{2m+n} \tag{48}$$

where $\Gamma(z)$ is the gamma function, a generalization of the factorial function to non-integer values.

The Bessel functions of the second kind, denoted by $Y_n(x)$, are also solutions of the Bessel differential equation. However, they are singular (infinite) at the origin (x = 0). Such solutions are not relevant for the applications in the this presentation, and thus we consider $c_2 = 0$ in equation (46).

Some useful properties of the Bessel functions of first kind are:

$$J_{-n}(x) = (-1)^n J_n(x) \tag{49}$$

$$\frac{d}{dx}\left(x^n J_n(x)\right) = x^n J_{n-1}(x) \tag{50}$$

The modified Bessel equation is very similar to equation (47) and may be presented:

$$\frac{d^2y}{dx^2} + \frac{1}{x}\frac{dy}{dx} - \left(1 - \frac{n^2}{x^2}\right) y = 0 \tag{51}$$

The solutions are the modified Bessel functions of the first and second kinds, and can be written:

$$y = a_1 J_n(-ix) + a_2 Y_n(-ix) \tag{52}$$

$$= c_1 I_n(x) + c_2 K_n(x) \tag{53}$$

where $I_n(x)$ are $K_n(x)$ modified Bessel functions of order n of the first and second kind, respectively.

The modified Bessel function of order n of first kind may be defined by the relation:

$$I_n(x) = i^{-n} J_n(ix) \tag{54}$$

Bibliography

[1] J. Alastruey, K.H. Parker, J. Peiro, S.M. Byrd, and S.J. Sherwin. Modelling the circle of willis to assess the effects of anatomical variations and occlusions on cerebral flows. *journal of Biomechanics*, 40(8):1794–1805, 2007.

[2] Max Anliker, Robert L. Rockwell, and Eric Ogden. Nonlinear analysis of flow pulses and shock waves in arteries part i: Derivation and properties of mathematical model. *Zeitschrift für Angewandte Mathematik und Physik (ZAMP)*, 22(2):217–246, March 1971. Birkhäuser Basel.

[3] Karim Azer and Charles S. Peskin. A one-dimensional model of blood flow in arteries with friction and convection based on the womersley velocity profile. *Cardiovascular Engineering*, 7(2):51–73, 2007.

[4] SD Balar, TR Rogge, and Young DF. Computer simulation of blood flow in the human arm. *J. Biomech.*, 22(6-7):691–7, 1989.

[5] David Bessems. On the propagation of pressure and flow waves through the patient specific arterial system, September 2007.

[6] David Bessems, Marcel Rutten, and Frans van de Vosse. A wave propagation model of blood flow in large vessels using an approximate velocity profile function. *J Fluid Mech*, 580:145–168, 2007.

[7] B. Deswysen, A. Charlier, and M. Gevers. Quantitative evaluation of the proximal aorta determined in the time and frequency domain: a comparison. *Med Biol Eng Comput*, 18:153–166, 1981.

[8] Luca Formaggia, Daniele Lamponi, and Alfino Quarteroni. One-dimensional models for blood flow in arteries. *journal of Engineering Mathematics*, 47:251–276, 2003.

[9] Luca Formaggia, Daniele Lamponi, Massimiliano Tuveri, and Alessandro Veneziani. Numerical modeling of 1d arterial networks coupled with a

lumped parameters description of the heart. *Comput. Meth. Biomech. Biomed. Eng.*, 9(5):273–288, Oct 2006.

[10] Luca Formaggia, F. Nobile, Alfino Quarteroni, and A. Veneziani. Multiscale modelling of the circulatory system: a preliminary analysis. *Comput. Vis. Sci.*, pages 75–83, 1999.

[11] D. Fry, D. Griggs, and J. Greenfield. In vivo studies of pulsatile blood flow: the relationship of the pressure gradient to the blood velocity. In EO Attinger, editor, *Pulsatile blood flow*. McGraw Hill, 1964.

[12] Y.C. Fung. *Biodynamics. Circulation*. Springer, 1984.

[13] Y.C. Fung. *Biomechanics. Motion, Flow, Stress and Growth*. Springer, 1990.

[14] Thomas J. R. Hughes and J. Lubliner. On the one-dimensional theory of blood flow in the larger vessels. *Mathematical Biosciences*, 18:161–170, 1973.

[15] Yunlong Huo and Ghassan S. Kassab. A hybrid one-dimensional/womersley model of pulsatile blood flow in the entire coronary arterial tree. *Am J Physiol Heart Circ Physiol*, 292(6):H2623–2633, 2007.

[16] Fridtjov Irgens. *Continuum Mechanics*, volume I. Dept Structural Engineering, NTNU, Trondheim, Norway, 2005.

[17] Fridtjov Irgens. *Continuum Mechanics*. Springer, Berlin Heidelberg, 2008.

[18] W. Laskey, H. Parker, V. Ferrari, W. Kussmaul, and A. Noordergraaf. Estimation of total systemic arterial compliance in humans. *J Appl Physiol*, 1990.

[19] S. Laurent, D. Hayoz, S. Trazi, P. Boutouyrie, B. Waeber, S. Omboni, G. Mancia, and M. Safar. Isobaric compliance of the radial artery in increased in patients with essential hypertension. *Hypertension*, pages 89–98, 1993.

[20] Z. Liu, K. P. Brin, and F. C. Yin. Estimation of total arterial compliance: an improved method and evaluation of current methods. *Am J Physiol*, 251(3 Pt 2):H588–600, Sep 1986.

[21] Thusitha Mabotuwana, Leo Cheng, and Andrew Pullan. A model of blood flow in the mesenteric arterial system. *BioMedical Engineering OnLine*, 6(1):17, 2007.

[22] Jamil Mayet and Alun Hughes. Cardiac and vascular pathophysiology in hypertension. *Heart*, 89(9):1104–1109, 2003.

[23] Donald A. McDonald. *Blood Flow in Arteries.* The Camelot Press, second edition, 1973.

[24] William R. Milnor. *Hemodynamics.* Williams & Wilkins, Maryland, USA, second edition, 1989.

[25] W. Nichols and O'Rourke M. *McDonalds's Blood Flow in Arteries. Theoretical, Experimental and Clinical Principles.* Edward Arnold, 3rd edition, 1990.

[26] WW Nichols and DA McDonald. Wave velocity in the proximal aorta. *Med Biol Eng Comput*, 10:327–335, 1972.

[27] MS Olufsen. Structured tree outflow condition for blood flow in larger systemic arteries. *Am J Physiol*, 45(1):H257–H268, 1999.

[28] R. Schmidt and G. Thews. *Human Physiology.* Springer, 1989.

[29] P. Segers, N. Stergiopulos, P. Verdonck, and R. Verhoeven. Assessment of distributed arterial network models. *Med Biol Eng Comput*, 35(6):729–736, 1997.

[30] Patrick Segers and Pascal Verdonck. *Non-Invasive Estimation of Total Arterial Compliance.* Institute Biomedical Technology, University of Gent, Belgium, ????

[31] SJ Sherwin, V. Franke, J. Peiró, and K. Parker. One-dimensional modelling of vascular network in space-time variables. *journal of Engineering Mathematics*, 47:217–250, 2003.

[32] RL Spilker, JA Feinstein, DW Parker, VM Reddy, and CA Taylor. Morphometry-based impedance boundary conditions for patient-specific modeling of blood flow in pulmonary arteries. *Ann. Biomed. Eng.*, 35(4):546–559, Apr 2007.

[33] Brooke N. Steele, Mette S. Olufsen, and Charles A. Taylor. Fractal network model for simulating abdominal and lower extremity blood flow during resting and exercise conditions. *Computer Methods in Biomechanics and Biomedical Engineering*, 10(1):39–51, Feb 2007.

[34] N. Stergiopulos, J. J. Meister, and N. Westerhof. Evaluation of methods for estimation of total arterial compliance. *Am J Physiol*, 4(2):H1540–8, 1995.

[35] N. Stergiopulos, D.F. Young, and T.R. Rogge. Computer simulation of arterial flow with applications to arterial and aortic stenoses. *J. Biomech.*, 25(12):1477–1488, 1992.

[36] Victor L. Streeter, W. Ford Keitzer, and David F. Bohr. Pulsatile pressure and flow through distensible vessels. *Circ Res*, 13:3–20, 1963.

[37] H. Suga and K. Sagawa. Instantaneous pressure-volume relationships and their ratio in excised, supported canine left-ventricle. *Circulation Research*, 35(1):117–134, 1974.

[38] H. Suga, K. Sagawa, and Aa. Shoukas. Load independence of instantaneous pressure-volume ratio of canine left ventricle and effects of epinephrine and heart-rate on ratio. *Circulation Research*, 32(3):314–322, 1973.

[39] S. Toy, J. Melbin, and A. Noordergraf. Reduced models of arterial systems. *IEEE Trans. Biomed. Eng.*, 32:174–176, 1985.

[40] Frans N. van de Vosse and M.E.H van Dongen. *Cardiovascular Fluid Mechanics*. Eindhoven university, 1998. Lecture notes.

[41] I. Vignon and C.A. Taylor. Outflow boundary conditions for one-dimensional finite element modeling of blood flow and pressure waves in arteries. *Wave motion*, 39:361–374, 2004.

[42] J. Wan, B. Steele, SA Spicer, S. Strohband, GR Feijóo, TJ Hughes, and CA Taylor. A one-dimensional finite element method for simulation-based medical planning for cardiovascular disease. *Comput. Meth. Biomech. Biomed. Eng.*, 5(3):195–206, Jun 2002.

[43] J.J. Wang and K.H. Parker. Wave propagation in a model of the arterial circulation. *journal of Biomechanics*, 37(4):457–470, 2004.

[44] N. Westerhof, F. Bosman, C. De Vries, and A. Noordergraaf. Analog studies of the human systemic arterial tree. *J. Biomech.*, 2:121–143, 1969.

[45] N. Westerhof, G. Elzinga, and P. Sipkema. An artificial system for pumping hearts. *J Appl Physiol*, 31:776–781, 1971.

[46] N. Westerhof, P. Sipkema, C.G. Van den Bos, and G. Elzinga. Forward and backward waves in the arterial system. *Cardiovasc Res*, 6:648–656a, 1972.

[47] Nico Westerhof, Nikos Stergiopulos, and Mark I.M. Noble. *Snapshots of Hemodynamics. an Aid for Clinical Research and Graduate Education.* Springer, 2005.

[48] Bessel function. http://en.wikipedia.org/wiki/Bessel_function, 2009.

[49] Wikipedia. Complex number - wikipedia, the free encyclopedia, 2011. [Online; accessed 26-August-2011].

[50] Wikipedia. Mean value theorem - wikipedia, the free encyclopedia, 2012. [Online; accessed 9-May-2012].

[51] Bessel function of the first kind. http://mathworld.wolfram.com/BesselFunctionoftheFirstKind.html, 2009.

Index